

HIGH REYNOLDS NUMBER WAVE FORCE INVESTIGATION
IN A WAVE FLUME, VOLUME I

FINAL REPORT

to

Naval Civil Engineering Laboratory
ATTENTION: Jerry Dummer
Port Hueneme, CA 93043

Minerals Management Service
Department of Interior
ATTN: Charles Smith
Reston, VA

Contract No. N62474-82-C08295

by

Robert T. Hudspeth

and

John H. Nath

Ocean Engineering Program
Civil Engineering Department
Oregon State University
Corvallis, OR 97331

February 1984

TABLE OF CONTENTS

	<u>Page</u>
1.0 ABSTRACT	1
2.0 INTRODUCTION	3
2.1 Background	3
2.2 Purposes of Test Program	5
2.3 Scope	6
3.0 EXPERIMENT SETUP AND PROCEDURES	9
3.1 Wave Research Laboratory	9
3.2 Experimental and Data Acquisition Equipment	9
3.2.1 Test Cylinder	9
3.2.2 Force Beam Gauging	12
3.2.3 Data Acquisition	15
3.3 Test Procedures	16
3.3.1 Calibrations	16
3.3.2 Test Plan	19
4.0 DATA ANALYSIS	21
4.1 Record Format and Filtering	22
4.2 Data Processing	29
4.2.1 PROGRAM WAVE8	30
4.2.2 PROGRAM FDATAR5/FD5A	32
4.2.3 PROGRAM LABT4	33
4.3 Random Waves	39
4.3.1 PROGRAM WAVER	40
4.3.2 PROGRAM FDATAR	40
4.3.3 PROGRAM LABT4	41
5.0 SUMMARY OF RESULTS	43
6.0 CONCLUSIONS	45
7.0 REFERENCES	49
8.0 ACKNOWLEDGEMENTS	51
9.0 TABLES	53
10.0 FIGURES	93
11.0 APPENDIX	
11.1 Druck Pressure Transducer Specifications	A3
11.2 Parametric Dependency of Force Coefficients on Dean Number	A9
11.3 FDATAR	A13

1.0 ABSTRACT

A 12.75-inch diameter vertical cylinder was subjected to large laboratory waves with Keulegan-Carpenter number up to 17 at the local force transducer (20 at the still water surface) and Reynolds numbers up to 2.7×10^5 (3.2×10^5 at the still water surface). Local force, local pressures, total force, and the elements for determining the overturning moments were measured. The purpose was to produce a high quality data set in the wave regime where both the velocity and the acceleration-dependent components of the wave forces are important. It was found that the forces were more acceleration-dependent than originally anticipated.

The local forces were predicted quite well with the two-term Morison equation using the kinematics from the measurements, the linear, and the stream function wave theories. The best predictions used the measured kinematics.

2.0 INTRODUCTION

2.1 Background

On 27 September 1982 a contract was established between the Naval Civil Engineering Laboratory (NCEL), Port Hueneme, California, and Oregon State University (OSU), to conduct an experiment pertaining to wave forces on a 12.5-inch diameter vertical cylinder. The design work for the equipment began in October 1982, and the equipment was delivered on site in February 1983. The laboratory tests were performed in the period from 12-26 April 1983 and data analyses were completed during the Fall 1983. These final data analyses were made possible by a modification to the original NCEL contract with funding from the Minerals Management Service (MMS) through NCEL.

The Morison equation relating wave forces on vertical cylinders is given in the following equation. The force per unit of cylinder length, f , is expressed by

$$F = C_d \frac{D\rho}{2} u(t) |u(t)| + C_m \frac{\pi D^2}{4} \rho \dot{u}(t) \quad (2.1-1)$$

where C_d and C_m are the empirically determined drag and inertia coefficients, respectively ($C_m = 1 + C_a$, where C_a is the added mass coefficient), D is the cylinder diameter, ρ is the mass density of the surrounding water, $u(t)$ is the horizontal water particle velocity, and $\dot{u}(t)$ is the local fluid acceleration au/at .

Many data have been generated from experiments by many investigators to determine the drag and inertia coefficients as functions of the Keulegan-Carpenter number, K ($= U_m T/D$, where U_m is the maximum water particle speed and T is the wave period), and the Reynolds

number, R ($= U_m d / \nu$, where ν is the kinematic viscosity of the water). However, many reportings have been questioned for one reason or another and only a few have very reliable values for these force transfer coefficients. One reliable source is from planar oscillatory flow laboratory experiments. However, they are limited because the flow is not truly that of waves. Other data sources have their own limitations. For example, field experiments rely heavily on current measurements that are made at some distance from the force transducer and wave theory is ultimately used to extend the measurement to the force transducer location. To our knowledge, no set of well-documented, thoroughly instrumented measurements have been made in a truly controlled wave condition and reported on in the open literature.

Even the data from planar oscillatory flow have **some** scatter and indicate that Eq. 1 may be improved to reproduce well the forces acting on a cylinder within certain ranges of K . Therefore, Sarpkaya (1981) suggested the use of a so-called four-term Morison equation, wherein two terms are added to Eq. 1 to take into account energies in the force spectrum that occur at the 3rd and 5th harmonics of the fundamental wave frequency. The coefficients for the added two terms can be determined, essentially, from the drag and inertia coefficients as determined from the two-term equation.

The form of the four-term MOJS equation used for this work is

$$\begin{aligned}
F = C_d \frac{D\rho}{2} u(t) |u(t)| + C_m \frac{\pi D^2}{4} \rho \dot{u}(t) + \frac{\rho D U_m^2}{2\lambda^{1/2}} [A_{c3} + B_{c3} \exp(C_{c3}\alpha)] \\
\cos\{3\omega t - \lambda^{-1/2} [A_{\phi 3} + B_{\phi 3} \exp(C_{\phi 3}\alpha)]\} + \frac{\rho D U_m^2}{2\lambda^{1/2}} [A_{c5} + B_{c5} \exp(C_{c5}\alpha)] \\
\cdot \cos\{5\omega t - \lambda^{-1/2} [A_{\phi 5} + B_{\phi 5} \exp(C_{\phi 5}\alpha)]\} \quad (2.1-2)
\end{aligned}$$

where $\alpha = (K - 12.5)^2$, $\omega = 2\pi/T$, $K = U_m T/D$, $\lambda = (C_m^* - C_m)/KC_d$ (C_m^* is the potential flow value--for a cylinder, $C_m^* = 2.9$), and

$A_{c3} = 0.01$	$B_{c3} = 0.10$	$C_{c3} = -0.08$
$A_{\phi 3} = -0.05$	$B_{\phi 3} = -0.35$	$C_{\phi 3} = -0.04$
$A_{c5} = 0.0025$	$B_{c5} = 0.053$	$C_{c5} = -0.06$
$A_{\phi 5} = 0.25$	$B_{\phi 5} = 0.60$	$C_{\phi 5} = -0.02$

Only two terms were added to the Morison equation because the spectrum analyses of the residues from the U-tube experiments (Sarpkaya, 1981) showed appreciable energy from only these two higher ordered terms.

2.2 Purposes of Test Program

The major purpose of this program was to provide a high quality set of data of force measurements and pressure measurements for a vertical smooth cylinder of appreciable size (12.75-inch diameter) in real waves with a reasonable range of Keulegan-Carpenter and Reynolds numbers so that different methods of analyses can be examined (for this and future efforts). Also required were comparisons of the force transfer coefficients from different methods of analysis and comparisons of forces, using the differently derived coefficients.

2.3 Scope

The work entailed constructing a 12.75-inch diameter test cylinder equipment, conducting the laboratory model tests, recording and analyzing the data, and production of the reports. The test cylinder equipment was of all new construction. Local forces, total forces, and the elements for determining the overturning moments were measured. In addition, eight pressure transducers measured peripheral time-dependent pressures around the center of the local force transducer. Wave water particle velocities were measured opposite the center of the local force transducer, in line with the wave axis (crests). The water surface profile was measured in line with the wave axis and the center of the cylinder.

A minimum of 26 runs were required to satisfy the requirements of the statement of work (SOW). However, a total of 47 runs were made since testing time did permit them. Data from 26 runs were analyzed as required in the SOW. Ten waves in a sequence were recorded from which eight were later extracted for the analysis. The eight wave periods, beginning at any time in the sequence, allowed for seven complete peak-to-peak waves to be defined.

The force transfer coefficients, C_d and C_m , were derived with least square methods, using linear and stream function wave theories and the measured kinematics. In addition, C_d and C_m were determined from the Wave Project II data, where C_m is constant and C_d varies with time through the wave cycle (Hudspeth, et. al. 1974), and from Sarpkaya's U-tube results (Sarpkaya, 1981). The predicted forces were then compared against the measured forces, wherein the predicted forces included calculations using Eqs. 2.1-1 and 2.

In summary, the analysis included 12 combinations of time-dependent force determinations. Using the kinematics from each of the linear wave theory, the stream function wave theory, and the measured kinematics, the time-dependent forces were determined for both the 2-term and the 4-term Morison equations, using C_d and C_m determined from the least squares method, Wave Project II data, and the U-tube data.

3.0 EXPERIMENT SETUP AND PROCEDURES

3.1 Wave Research Laboratory

The experimental work was done in the O.H. Hinsdale Wave Research Laboratory at Oregon State University (WRL). The overall length of the wave flume is 340 ft., of which 129 ft. constitute the length in which tests can be performed well beyond the evanescent modes of the wave board and in front of the toe of the beach. The location of the test cylinder in the WRL is shown in Fig. 3-1. Good, repeatable waves can be produced ranging from a high frequency of 1.0 Hz to a low of about 0.12 Hz. For these tests, the wave frequency range was from 0.5 Hz to 0.12 Hz. Up to 16 channels of information were recorded digitally in real time on a PDP 11 computer. Other channels of information were recorded on an analogue tape recorder and then digitized at a later time.

3.2 Experimental and Data Acquisition Equipment

3.2.1 Test Cylinder

The design of the test cylinder required that it be stiff for the applied loads so that the natural frequency of the lowest mode would be relatively high with respect to the forcing frequencies. From impulse response tests, where the cylinder was hit with a rubber hammer and the time response was measured by strip chart recorder, the local force transducer demonstrated a natural frequency of 8.2 Hz when submerged. The highest wave frequency in this test was 0.5 Hz. On some runs, a distinct transverse force was experienced, due to vortex shedding, that had frequencies higher

than the wave frequency by up to approximately three times. In addition, other turbulences may cause transverse forces. The amplitude spectra for transverse forces in Vol. II were examined for maximum significant frequencies. An approximate value of 1.5 Hz was determined as a conservatively high estimate, even though the amplitudes therefrom were fairly small. Some other very small energies exist at 5.0 Hz and at 8.0 Hz for the center force, east direction (probably due to the vibration of the local force transducer from near-impact loads in steep waves). Thus, the largest ratio of importance of excitation frequency to transducer frequency was about $1.5/8 = 0.19$. The largest ratio of fundamental wave frequency to transducer frequency was $.5/8 = .062$. Therefore, vibrations of the local force transducer had a negligible effect on the measurements as can be seen in any reference on dynamics for the response curve of a one-degree-of-freedom vibrator. The signals were also filtered with a two-pole Butterworth filter with a cutoff frequency of 8 Hz. However, the signals were recorded filtered and unfiltered in case future reference is to be made to the unfiltered signals.

Another design criterion was to size the test cylinder so that the component parts could be handled relatively easily at the wave flume. It was decided to provide a stiff inner core structure with a removable shell surrounding it.

Figure 3-2 gives the general concept of the test cylinder. Figures 3-3 and 4 are photos of it during installation, where Fig. 3-4 has only one-half of the lower skin in place. Figure 3-5 shows the strain gauges on the bottom support; Fig. 3-6 shows the bolt-

down arrangement at the bottom; and Fig. 3-7 shows how the bottom skin covered the supporting core.

The upper support consisted of a 1.5-inch round stainless steel rod, 30 inches long, inserted into roller bearings and supported at its upper end with a U-joint identical to the one at the bottom support, as shown in Fig. 3-2. Thus, the structure was completely statically determinate and no longitudinal forces could be applied to the structure from temperature variations or other longitudinal stresses from construction because of the upper roller support.

It was necessary to design the local force transducer for much smaller forces than would be measured at the top and bottom transducers and to make it individually statically determinate and free from the small deflections of the central structure. Details of the local force transducer (LFT) are shown in Figs. 3-8 and 9. Photos of the strain bar supports and the interior of the LFT are given in Figs 3-10 and 11.

The test cylinder was supported at the upper end by an 8x12 steel tube that spanned the 12 ft. clear distance between the wave flume walls, to which it was securely bolted. The wave profiler was mounted in this beam with the center of the profiler in line with the center of the test cylinder, perpendicular to the wall. It was mounted 3 ft. from the east wall, mid-way between the wall and the cylinder center line. A Marsh-McBirney current meter was mounted with the sensing elements directly under the wave profiler at a level of 3.7 ft. below the still water surface--the same level as the center of the local force transducer. A second Marsh-McBirney

current meter was mounted directly in line with the first one, but on the opposite (west) wall. The sensors of the second meter were about 1.2 ft. from the face of the west wall.

The test cylinder was carefully assembled so that the center line was vertical. The local force transducer was separated only 1/16-inch from the rest of the cylinder, but the surface was slightly out of alignment with the smooth cylinder skins. Figures 3-12 and 13 show the best and worst alignments. Several measurements were made of the misalignments and they are summarized in Table 3-1. The table shows the LFI was slightly larger in diameter than the adjoining test cylinder by 0.7 mm, which had a negligible influence on the resulting measurements.

After the Druck pressure transducers were installed and the LFT was mounted, the surface around the pressure transducers was filled with a paint-like substance and sanded smooth with the surrounding cylinder surface.

3.2.2 Force Beam Gauging

Forces were measured with strain gauge force dynamometers. Metal foil strain gauges were used of 120 ohms each. The gauging stations are referred to as the top gauge, the local force transducer, and the bottom gauge. The top and bottom gauges were wired as shown in Fig. 3-14.

The local force transducer was wired as shown in Fig. 3-15. Each of the four 5/16-inch square support beams had four gauges, intending to have two complete circuits for each of the in-line and transverse directions. However, small torsional loads from the

calibration string gave inconsistent results so the two in-line and two transverse circuits were added together. This action nullified any influence on the readings from torsional loads. All strain gauge bridging was conditioned with Vishay signal conditioners.

The Vishay strain gauge conditioner contains two sections. The first is a precision adjustable voltage regulator. The output of the regulator is used as the excitation for the strain gauges. For this work it was adjusted for 10.00 volts. The exact value is not critical if the instrument to which the gauges are attached is calibrated at that voltage, whatever it is. The second section includes several stages of amplification to the very small voltage changes coming from the strain gauge bridge. The first stage is a differential-type amplifier which will detect and amplify only voltage potentials which exist between the two return leads from the bridge. Any potential between ground and one lead or in common with both will not be amplified. This last stage then provides isolation from many noise problems. The other stage of the amplifier section provides further adjustable gain which can be set to obtain a usable voltage output within a desired range from the conditioner box.

Auxiliary circuits in the conditioner provide bridge balancing circuitry to nullify any static offset so that a maximum gain may be used for very small bridge outputs. Circuitry for different types of bridges and amplifier adjustments for best output are included. Outputs from the conditioners were input to the Rockland 8.0 Hz low pass double pole filters.

Selected outputs were then passed into summing-type inverting operational amplifiers with a gain of very nearly -1.0. The exact value, again, does not matter if the instrument is calibrated using the output of the last piece of electronic equipment. The summing amplifier has a very large bandpass from DC to several thousand hertz and therefore will cause no measurable phase shift at our frequencies.

Some of the characteristics of the general operation amplifier are that it has a very high input impedance and low input current (useful to prevent loading of the preceding instrument). Because of this very high input impedance, the current drawn by the 'op amp' is negligible and therefore point 'A' (see Figure 3-16) is very nearly at ground potential, or zero volts. Because of this, the current drawn through the input resistor R_1 and R_2 , I_i , is equal to the current through R_f , the feedback resistor. Upon solving for these relations (without including every step here), we find that $V_o/V_{in} = -R_f/R_u$. Our R_f/R_i is set to be 1.0.

In the more specific case of the summing op amp, the current I_i is the sum of the currents I_{r1} and I_{r2} and so we arrive at the relation (again without showing all the intermediate steps):

$$-V_o/R_f = V_1/R_1 + V_2/R_2 \quad (3.2.2-1)$$

In our case $R_1/R_f = 1.0$ and $R_2/R_f = 1.0$ and so we have as a final output the sum of the inputs:

$$-V_o = V_1 + V_2 \quad (3.2.2-2)$$

This being the last instrument we have our final output voltage corrected for torsion and other unwanted bending moments and with very reduced noise ready to be digitized by the computer.

In summary, Fig. 3-17 shows the test cylinder with only one of the four cylinder skins attached to the core beam. Figure 3-18 shows three of the four skins bolted on. Figure 3-19 shows the completed assembly just prior to testing. The west wall Marsh-McBirney current meter is shown on the left side and east wall installation is shown on the right side of the photograph.

3.2.3 Data Acquisition

The signals were routed as shown in Fig. 3-20. A maximum of 16 channels of information can be digitized simultaneously with the PDP-11 computer. The remaining channels were recorded on analogue tape for digitizing at a later time. The analogue tape introduced additional high frequency noise so the signals therefrom were again filtered prior to digitizing.

The analogue filter is a two-pole Butterworth filter manufactured by Rockwell. The digital recording was done with a PDP-11 minicomputer. The analogue tape recorder was a Bell and Howell model CPR-4010. The digital information was stored on an 11-track mag tape and a copy of all data recorded were provided to NCEL.

In order to help synchronize all channels in real time, a 5-volt step function signal was generated by the computer and recorded on one channel. This 5-volt "switch" was activated at the start of digital recording. This signal was also recorded on the analogue tape. The data analysis used this "switching" technique to help phase all information.

3.3 Test Procedures

3.3.1 Calibrations

The completed cylinder was calibrated in four force directions corresponding to the four points of the compass. In addition, one horizontal diagonal calibration was made to illustrate independence between the N-S and E-W force measurements. Two ranges of forces were used for the top and bottom force transducers in order to check their linearity. One range had a maximum load of 201.44 pounds and the other was 16.56 pounds, as shown in Table 3-2. Force calibrations were made at one or more of the five elevations as shown in Fig. 3-21. One measurement was made with the forces applied simultaneously at locations 2, 3, and 4. These were compared with force calibrations at position 3 alone. The purpose of this was to determine if distributed loads, which create bending in the overall structure, would influence the force measurements at position 3 alone. When the forces were applied simultaneously to positions 2, 3, and 4, it is designated as the XXX test. In that case, the light calibration was applied at position 3 while the heavy calibration loads were applied to positions 2 and 4 with approximately the steps indicated in Table 3-2. (This loading at positions 2 and 4 could be approximate since it was only intended to provide a significant general bending of the core beam to see if it influenced the calibrations of the LFT.) When the force was applied to position 3 only, it is designated as the OXO calibration. It was found that force measurements from the local force transducer were independent of the general loading on the cylinder. Of course, during tests the

sensors for the local force transducer and the bottom force transducer were submerged. They were therefore calibrated in the submerged condition.

The XXX calibration arrangement is shown in Fig. 3-22. Figure 3-23 shows a calibration in progress at position 5 (submerged). When calibrating at position 3 in the north or south directions, it was necessary to provide a horizontal truss at the correct level to take the horizontal and vertical thrust from the calibration loads. It is shown in Fig. 3-23.

Linear regression analysis was used to obtain the calibration coefficients. The measured calibration data values, f_i , were approximated by a linear relation to the measured voltage, x_i , according to

$$f_i = m x_i + b; \quad i = 1, 2, \dots, N \quad (3.3.1-1)$$

where the slope, m , and the intercept, b , were determined by a best least squares analysis. The correlation coefficient, R was computed by

$$R^2 = \frac{[\sum_i f_i x_i - \sum_i f_i \sum x_i / N]^2}{[\sum_i f_i^2 - (\sum f_i)^2 / N] [\sum_i x_i^2 - (\sum x_i)^2 / N]} \quad (3.3.1-2)$$

and is a measure of the goodness-of-fit of the two regression coefficients since $0.0 < R^2 < 1.0$. If R were identically equal to 1.0, the data would be perfectly linear.

The results of the force calibrations are shown in Tables 3-3 through 3-10.

The low range of calibrations are consistently steeper than the high range of calibrations, but they only differ by less than 3.3% for the instruments used in the analysis. The calibrations were quite linear and consistent. In summary, the force calibrations were consistent, linear, and very repeatable between the beginning of the tests and the end of the tests for all of the data channels used in the NCEL data analyses. Table 3-4 shows that TE1 Ch #3 was not consistent and should not be used in future data analyses of the transverse force and moments.

The cylinder was also calibrated at location 5 with the cylinder in torsion. That is, the forces were applied to the edge of the cylinder as shown in Fig. 3-24. This was done in both the clockwise and counterclockwise directions. It was found that torsional loads had very little effect on the output from the force transducers. Therefore, if any torsional loads were applied to the cylinder (and they could only have been so from uneven boundary layer development between the east and west sides of the cylinder) they would not influence the force measurements.

One calibration result for a pressure meter is shown in Fig. 3-25. All of the amplified individual calibrations are available upon request. They were all very linear except for P6 (the 240° azimuth). Figure 3-26 is typical of the linear calibrations and Fig. 3-27 shows P6. The calibration was made when the wave flume was being filled or emptied. Some pressure meters had a considerably larger calibration constant than others, but the calibration values remained constant and the pressure measurements were consis-

tent and reasonable for the measurements in waves. The pressure calibrations are summarized in Tables 3-11 and 12.

The east current meter had been previously calibrated by Dibble in (1980) at 20.77 fps/V, and after this testing by Kim in June 1983 at 20.47 fps/V (a 1.5% difference). A value of 20.6 fps/V was used in the NCEL data analysis. This meter was more consistent than the West meter and was the one used in the data analysis.

3.3.2 Test Plan

The test cylinder was designed and constructed in the Fall and early Spring of 1982-83. Prior to assembly in the WRL, the force dynamometers were bench tested to ascertain their workability. The equipment was then completely assembled. Calibrations of force transducers were made. The primary current meter (East side) had been previously calibrated. The pressure transducers were calibrated as the wave flume was filled and emptied. The cylinder was then subjected to 31 periodic waves to satisfy all requirements of the SOW, plus a few extra waves. Then four random wave sequences were generated according to the SOW. Some time remained in that work day so 10 more periodic wave runs were made at three wave periods--to fall in between the wave periods previously tested. (However, only 26 periodic wave runs were processed, according to the SOW).

The flume was then pumped down and calibrations were made for the force transducers for comparison with the calibrations prior to testing. The log of runs, Table 3-13, is self-explanatory, completing the description of the test plan.

Some photos of the cylinder subjected to the waves are given in
Figs. 3-28, 29 and 30.

4.0 DATA ANALYSIS

Periodic wave data were collected on 22 April 1983 and the random wave data on 25 April 1983. A total of 21 channels of electronic data signals were recorded during the NCEL tests. Table 4-1 identifies these 21 data signal channels and their method of recording during both calibration and wave measurements. Only 16 channels of analogue-to-digital (A/D) were available on the PDP-11/E10 used at the WRL. These 16 channels are identified in the column titled "A/D Run Ch. #" in Table 4-1. The remaining five channels of data recorded during wave tests were recorded on a Bell and Howell CPR-4010 analogue tape deck and are identified in the column titled "Analogue Tape Ch.#" in Table 4-1.

The local force transducers 9 and 10 were combined to A/D Calibration Channel #9 as a single signal for both digital (A/D Run channels #5 and #7) and in analogue (analogue channel #1) format (see Fig. 3-20). A five-volt step signal was used to reference the analogue time series to the discrete digital time sequence. This five-volt step signal was sent by the PDP-11/E10 to the Bell and Howell CPR-4010 analogue tape recorder at the instant digital recording began. The local wave force transducer signal was recorded simultaneously on two A/D channels in order to determine if there was any significant phase shift introduced by the 8 Hz Rockland filters. The A/D Run channel #5 was filtered by the Rockland filter while A/D Run channel #7 was not (see Table 4-1).

The data recorded on analogue tape were passed through the Rockland two-pole Butterworth filters before recording. These

analogue data signals were again passed through the Rockland filters before being digitized in order to filter out undesirable high frequency noise introduced by the analogue tape recorder. The water surface profiler was not filtered by the Rockland filter because of signal distortions which are introduced into the record due to "drop-outs" in the data. These distortions are characteristic of all sonic sensors. The question of phase-locking the data properly to the water surface then becomes important. All the data records were filtered to produce the proper signal amplitudes and phase angles with respect to the water surface. The theory behind these filters is presented below.

Six channels of data were also recorded for immediate observations by a stripchart recorder. A sample record is shown in Fig. 4-1.

4.1 Record Format and Filtering

Figure 4-2 demonstrates schematically the data recording procedure for the horizontal current meter measurement.

A recorded measurement, $m(t)$, can be expressed as a linear sum of cosines and sines by

$$m(t) = a_{mo} + \sum_{n=1}^N (a_{mn} \cos 2\pi f_n t + b_{mn} \sin 2\pi f_n t) \quad (4.1-1a)$$

$$= \sum_{n=-N}^N H_m(f_n) \exp(i 2\pi f_n t) \quad (4.1-1b)$$

where $m(t)$ is the raw (unfiltered) recorded value of the horizontal current measurement, $u(t)$, and $a_{m0} = \langle m \rangle$, the average value of $m(t)$ during the recording interval. The Fourier transform of $m(t)$ is given by

$$H_m(f) = \int_{-\infty}^{\infty} m(t) \exp(-i2\pi ft) dt \quad (4.1-2)$$

where the complex-valued Fourier coefficient, $H_m(f)$, is defined as

$$H_m(f) = R_m(f) + iI_m(f) \quad (4.1-3a)$$

$$\text{or } H_m(f) = |H_m(f)| \exp\{i\theta(f)\} \quad (4.1-3b)$$

where the amplitude (modulus) is defined as

$$|H_m(f)| = (R_m^2 + I_m^2)^{1/2} \quad (4.1-4a)$$

and the phase by

$$\theta_m = \tan^{-1} \left\{ \frac{I_m(f)}{R_m(f)} \right\}. \quad (4.1-4b)$$

Substituting Eq. 4.1-3b into Eq. 4.1-1b demonstrates that

$$a_m = R_m(f), \quad b_m = I_m(f). \quad (4.1-5)$$

For example, high frequency noise can be filtered from a measured signal, if desired, by setting $a_{mn} = b_{mn} = 0$ for $f > f_c$ where f_c is the "cutoff frequency." This type of digital filtering will be termed the "FFT filter." High frequency FFT filtering was done to many of the NCEL data records. For example, the high fre-

quency noise above 1.5 Hz was filtered from the horizontal current and force measurements (see Fig. 4-10). That particular cutoff frequency is specified on graphic plots when it was used. It was selected arbitrarily to be low enough to sufficiently smooth the signals, but high enough so that most influences from vortex shedding would not be filtered.

When an operation is made on a signal from a filter, the Fourier transforms of the signal and filter are multiplied in the frequency domain in order to determine the Fourier transform of the output from the filter. If the signal is passed through two filters, as shown in Fig. 4-2, there are two multiplications. Thus, the Fourier transform of the recording can be found from

$$\begin{aligned} H_m(f) &= |H_u(f)| \exp\{i\theta_u(f)\} |H_M(f)| \exp\{i\theta_M(f)\} |H_R(f)| \exp\{i\theta_R(f)\} \\ &= |H_m(f)| \exp\{i\theta_m(f)\} \end{aligned} \quad (4.1-6)$$

where H_u is the transform of u , with phase θ_u (both quantities are now sought); H_M is the transform of the meter, which introduces the phase shift, θ_M ; and H_R is the transform of the Rockland filter, which introduces the phase shift, θ_R . To simplify the following discussion, it is assumed that $|H_R(f)| = 1.0$ and $\theta_R(f) = 0$. Later the actual values can be considered and multiplied by the product of the other two. Substituting Eqs. 4.1-3a and 4.1-3b into Eq. 4.1-6 gives

$$H_m(f) = R_m(f) + i I_m(f) \quad (4.1-7a)$$

$$= H_u(f) [R_M(f) + i I_M(f)] \quad (4.1-7b)$$

from which

$$H_u(f) = \frac{R_m R_M + I_m I_M}{R_M^2 + I_M^2} + i \frac{I_m R_M - I_M R_m}{R_M^2 + I_M^2} \quad (4.1-8)$$

The FFT filtered horizontal current $u(t)$ is determined from the inverse transform according to

$$u(t) = \int_{-\infty}^{\infty} H_u(f) \exp(i2\pi ft) df \quad (4.1-9)$$

Marsh-McBirney Filter

The single-pole filter characteristics of the Marsh-McBirney current meter are

$$H_M(f) = \frac{1}{1 + i2\pi\tau f} \quad (4.1-10a)$$

$$= [1 + (2\pi f\tau)^2]^{-1} \cdot [1 - i2\pi f\tau] \quad (4.1-10b)$$

where τ is the time constant of the current meter and f is the cyclic frequency of the signal in Hz.

The complex-valued FFT filtered signal, $H_u(f)$, may be computed from

$$|H_u| \exp(i\theta_u) = |H_u| \exp(i\theta_u) |H_M| \exp(i\theta_M) \quad (4.1-11)$$

which may be used to compute the amplitude of the current from

$$|H_u| = \frac{|H_u|}{|H_M|} \quad (4.1-12a)$$

and the phase from

$$\theta_u = \theta_m - \theta_M \quad (4.1-12b)$$

The value of the time constant τ is selectable on the Marsh-McBirney current meters. One experimentally determined value for the east meter was $\tau = 0.159$ sec. (see Fig. 3 and Table 4-1 in Dibble, 1980). From Eq. 4.1-10b the modulus of the Marsh-McBirney filter is

$$|H_M| = [1 + (2\pi\tau f)^2]^{-1/2} \quad (4.1-13a)$$

$$\text{and } \theta_M = \tan^{-1}\{-2\pi\tau f\}. \quad (4.1-13b)$$

Table 4-2 summarizes the amplitude attenuation and phase shift introduced by the Marsh-McBirney single pole filter in the NCEL data.

The current meters used have time constants, τ , with three or four selections. For the NCEL tests, they were set on 0.2. Small differences in phase can make appreciable differences in C_d or C_m , depending on whether the wave is drag or inertia dominant. The time constants used for the NCEL data reduction were $\tau = 0.159$ sec. for the east meter and $\tau = 0.20$ for the west meter.

Since the amplitudes in the frequency domain are proportional to the amplitudes in the time domain, Eq. 4-13a also expresses the division correction factor for the amplitudes of each frequency component of the water velocity signal. Likewise, the phase angle properly defines the phase of each signal. A problem was encountered with the horizontal signal from the west current meter. The source of this problem has not been determined. However, the east current meter (the same one calibrated by Dibble, 1980) gave excellent results and is the one that was used for the NCEL data analyses.

Rockland Filter

The Rockland filter is a two-pole Butterworth filter. The filter function is given by

$$H_R(f) = \frac{f_0^2}{(if)^2 + 2\beta_1 f_0 if + f_0^2} \cdot \frac{f_0^2}{(if)^2 + 2\beta_2 f_0 if + f_0^2} \quad (4.1-14)$$

where f_0 is the cutoff frequency, f is the signal frequency in Hz, $\beta_1 = 0.924$, and $\beta_2 = 0.700$ for the flat decay response. Introducing a dimensionless frequency ratio, $\epsilon = f/f_0$, reduces Eq. 4-14 to

$$H_R(\epsilon) = \frac{1}{(1-\epsilon^2)^2 + i 1.848\epsilon} \cdot \frac{1}{(1-\epsilon^2)^2 + i 1.4\epsilon} \quad (4.1-15a)$$

$$H_R(\epsilon) = \frac{(1-4.5872 \epsilon^2 + \epsilon^4) - i 3.248 \epsilon (1-\epsilon^2)}{(1-4.5872 \epsilon^2 + \epsilon^4) + 10.55 \epsilon^2 (1-2\epsilon^2 + \epsilon^4)} \quad (4.1-15b)$$

The amplitude division factor, $|H_R|$, is

$$|H_R| = [(1+1.415 \epsilon^2 + \epsilon^4)(1-.04 \epsilon^2 + \epsilon^4)]^{-1/2} \quad (4.1-16a)$$

and the phase angle, θ_R , is

$$\theta_R = \tan^{-1} \left\{ -\frac{3.248 \epsilon (1-\epsilon^2)}{(1-4.5872 \epsilon^2 + \epsilon^4)} \right\} \quad (4.1-16b)$$

Table 4-3 summarizes the amplitude attenuation and the phase shift introduced by the Rockland filters in the NCEL data.

Digital Formatting

Exactly ten periods of data were recorded for each of the 21 channels of data measured during the periodic wave tests. These data were reduced to exactly eight waves and were digitized at a

sampling interval determined by the deterministic wave period, T, and the FFT base $2^{11} = 2048$ according to

$$\Delta t = 8T/2048 = T/256 \quad (4.1-17)$$

Each single periodic wave in the eight-wave sequence thus contained 256 data values. This data digitization scheme was required in order to insure that the data could be FFT filtered as previously described using an FFT algorithm of base 2. The FFT algorithm was taken from Bloomfield (1976). Only seven of the eight waves were actually used in the final data analyses.

The sonic profiler used to record the instantaneous water elevation occasionally suffers from data "drop-outs" or "over-ranges." These data are identified as "bad-points" and are removed numerically by linearly interpolating between the good data values. On rare occasions, these intervals of bad-points are excessively long and result in forming a fictitious wave (see Wave #4 in Run #5 in Fig. 4-5). These data have been ignored in the data analyses because there were only two "bad point" waves in the total of 182 waves recorded. These 256 data points per wave were reduced to 33 data values (32 time increments) for each individual periodic wave in the final data analyses for the force coefficients. The total number of discrete data values digitized for the eight waves in the 41 periodic runs that are identified in Table 3-13 was

$$\begin{aligned} \text{NPTS} &= (41) \text{ runs} \cdot (21) \frac{\text{channels}}{\text{runs}} \cdot (8) \frac{\text{waves}}{\text{channel}} \cdot (256) \frac{\text{pts}}{\text{wave}} \\ &= 1,763,328 \text{ pts} \end{aligned}$$

These data were FFT filtered to produce the records that were used in the force coefficient analysis. The total number of discrete data values used in the final force coefficient analyses was

$$\begin{aligned} \text{NPTS} &= (26) \text{ runs} (21) \frac{\text{channels}}{\text{run}} (7) \frac{\text{waves}}{\text{channel}} (33) \frac{\text{pts}}{\text{wave}} \\ &= 126,126 \text{ pts.} \end{aligned}$$

For the four random wave tests listed in Table 3-13, a total of 8192 data values were recorded during each test. The total number of data values recorded during these random tests was

$$\begin{aligned} \text{NPTS} &= (4) \text{ runs} (21) \frac{\text{channels}}{\text{run}} (8192) \frac{\text{pts}}{\text{channels}} \\ &= 688,128 \text{ pts.} \end{aligned}$$

4.2 Data Processing

The 16 channels of digitally recorded data and the 5 channels of analogue recorded data were all copied in digital format as integer values (0-4095) on magnetic tape by the PDP 11/E10 at the WRL. This data tape was then read by the CDC CYBER 73 main frame computer at Oregon State University for subsequent data processing by a suite of three FORTRAN-coded algorithms. Figure 4-3 illustrates schematically the flow chart for the data processing.

4.2.1 PROGRAM WAVE8

The integer data obtained from the PDP 11/E10 digitizing process at the WRL was converted into physical units using the appropriate calibration constants listed in Chapter 3. Figure 4-4 illustrates the calibration constants entered into the program for run #5. Figure 4-5 illustrates a sample wave profile for run #5 in integer (uncalibrated) values; and Fig. 4-6 illustrates the same wave profile record following conversion from integer values to physical units. Note the "bad point" values in the individual waves #3 and #4. Figure 4-6 is also inverted compared to Fig. 4-5 because larger integers (i.e., higher voltages) indicate wave trough values, so a negative calibration constant is required (see Fig. 4-4, Column #1: "WAVE PROFILE" = -.5333).

Following calibration, the "bad points" were removed numerically by linear interpolation. On some rare occasions, the time interval of "bad point" values was so long that these data were interpreted by the numerical algorithm as an "inverted wave" and were not removed by the subroutine. This rare event is illustrated in Figs. 4-5 and 4-6 where the "bad points" in waves #3 and #4 have not been removed; but have, instead, been converted to waves. This rare event only occurred in the NCEL data during Runs #5 and #24. Figure 4-7 illustrates the "bad point wave" in Run #24.

Figures 4-8 to 4-10 show the more typical results obtained from the "bad points" removed algorithm for Run #12. All of the wave profiles recorded during the NCEL tests may be seen in Vol. II.

Next, all data channels were Fourier analyzed by a FFT algorithm with base 2. The FFT algorithm was written by Bloomfield (1976). One-sided amplitude spectra were computed and visually inspected for high frequency phenomena. The force amplitude spectra were displayed graphically out to 10 Hz. Figure 4-11 illustrates a transverse force amplitude spectra from the local force transducer for Run #30. In order to obtain better visual resolution of the spectral amplitudes at low frequency, all spectra were plotted out to only 4 Hz. Figure 4-12 illustrates a sample horizontal current amplitude spectrum for Run #5 at this expanded scale out to only 4 Hz. A digital, low-pass FFT filter was then applied to the amplitude spectra in the frequency domain to remove high frequency noise. Inversion of the FFT algorithm synthesized the filtered time series for later analyses. Figure 4-13 illustrates a filtered time series of the horizontal current for Run #5 with a cutoff frequency, $f_c = 1.5$ Hz. Figures 4-14 and 4-15 illustrate the effect of the low-pass FFT filter on the bottom transverse force for Run #5.

Horizontal water particle accelerations required for the Morison equation were computed from the measured horizontal current by differentiation. This differentiation was computed in the frequency domain. Figure 4-16 illustrates a typical horizontal acceleration amplitude spectrum computed from the measured data for Run #5. Although the horizontal current amplitude spectrum had been FFT filtered at 1.5 Hz, Fig. 4-16 illustrates the problem of amplification of high frequency spectral amplitudes that is common in numerical differentiation algorithms. In order to avoid this high

frequency amplification, only the fundamental and the first harmonic were used to synthesize the horizontal acceleration time series. Figure 4-17 illustrates the horizontal acceleration amplitude spectrum used to synthesize a horizontal acceleration time series from the measured horizontal current. Note that only the amplitudes at the fundamental and the first harmonic have been retained and that ALL of the other amplitudes have been set equal to zero. Figure 4-18 illustrates the horizontal acceleration time series synthesized from the amplitude spectrum shown in Fig. 4-17.

4.2.2 PROGRAM FDATA5/FD5A

The FFT filtered data from PROGRAM WAVE8 were read into PROGRAM FDATA5 or FD5A for the selection of seven individual periodic waves from the continuous eight wave sequence.

PROGRAM FD5A automatically selects the first seven waves in the sequence beginning with the first crest as shown in Fig. 4-19. The period of each individual wave in the seven-wave sequence is determined by first establishing a time at a wave crest, e.g. crest number; secondly by adding one wave period to (as set into the function generator that drives the wave board) that time. This accounts for the small variability in wave periods found in the data analyses tables in Section 5. However, the small error involved averages to zero. The wave heights are computed by averaging the leading and trailing crest elevations and then subtracting the trough value in-between the crests.

PROGRAM FDATA5 allows for the manual selection of the individual waves shown in Fig. 4-20. Cross-hair cursors on the TEKTRONIX

4010 screen are positioned at the individual wave crests and troughs to define the seven individual waves. The wave heights and periods are then computed the same as in FD5A. Figure 4-21 illustrates the manual determination of the individual waves by PROGRAM FDATA5 for Run #5. Only Runs #5 & #24 were processed by PROGRAM FDATA5 in order to manually override the automatic selection of the fictitious "bad point waves" that would have occurred had PROGRAM FD5A been used.

Finally, both programs reduce the number of data values in an individual wave from approximately 256 values (= 2048/8) to 33 points per wave (32 time increments). This reduces the CPU time required to compute the force coefficients, C_d and C_m , by Fourier analysis without loss of accuracy.

4.2.3 PROGRAM LABT4

PROGRAM LABT4 computes force coefficients, C_d and C_m , from the two-term MOJS equation by least-squares analysis. Each of the seven individual waves selected either automatically from PROGRAM FD5A or manually from PROGRAM FDATA5 is analyzed separately. First, an average velocity is computed from the measured horizontal current profile. Then the drag, C_d , and inertia, C_m coefficients are computed by least-squares analysis according to Sarpkaya and Isaacson (1981). The predicted 2-term Morison equation force is given by

$$F_p(\theta) = 1/2 C_d \rho D [u(\theta) + \langle u \rangle] |u(\theta) + \langle u \rangle| + 1/4 C_m \rho \pi D^2 \dot{u}(\theta) \quad (4.2-1)$$

where $F_p(\theta)$ is the instantaneous predicted local in-line force per unit of the vertical cylinder and $\langle u \rangle$ is the average velocity. A mean-square error between the instantaneous measured force per unit length, $F_m(\theta)$, and the force predicted by the 2-term Morison equation in Eq. 4.2-1 may be defined by

$$\epsilon^2 = \frac{1}{2\pi} \int_0^{2\pi} [F_m(\theta) - F_p(\theta)]^2 d\theta \quad (4.2-2)$$

The drag, C_d , and inertia, C_m , coefficients may be estimated from 4.2-2 in a best least-squares sense according to

$$\frac{\partial \epsilon^2}{\partial C_d} = 0; \quad \frac{\partial \epsilon^2}{\partial C_m} = 0 \quad (4.2-3)$$

By Cramer's rule, the estimates for the two force coefficients are given by

$$C_m = \frac{B_1 A_4 - B_2 A_2}{1/4 \rho \pi D \text{DET}\{C_m, C_d\}} \quad (4.2-3a)$$

$$C_d = \frac{B_2 A_1 - B_1 A_2}{1/2 \rho D \text{DET}\{C_m, C_d\}} \quad (4.2-3b)$$

where

$$\begin{aligned} A_1 &= \int_0^{2\pi} \dot{u}^2(\theta) d\theta \\ A_2 &= \int_0^{2\pi} \dot{u}(\theta) [u(\theta) + \langle u \rangle] |u(\theta) + \langle u \rangle| d\theta \\ A_4 &= \int_0^{2\pi} [u(\theta) + \langle u \rangle]^4 d\theta \\ B_1 &= \int_0^{2\pi} F_m(\theta) \dot{u}(\theta) d\theta \end{aligned}$$

$$B_2 = \int_0^{2\pi} F_m(\theta) [u(\theta) + \langle u \rangle] |u(\theta) + \langle u \rangle| d\theta$$

$$\text{DET}\{C_m, C_d\} = A_1 A_4 - A_2^2 \quad (4.2-4)$$

The integrals in Eqs. 4.2-4 were evaluated numerically using Simpson's rule (Crandall, p. 161, 1956).

The horizontal water particle kinematics required in the integrals in Eqs. 4.2-4 were computed by three different means: 1) by the measured kinematics from the east current meter; 2) by the linear wave theory plus the average measured velocity; and 3) by the nonlinear Dean stream function wave theory plus the average measured velocity. In addition to the three sets of water particle kinematics used to obtain the force coefficients, two additional sets of existing force coefficients were employed in the analysis: 1) Wave Project II coefficients; and 2) U-tube coefficients. Both the root-mean-square and the maximum errors between the measured and predicted forces were computed for each of the 7 waves analyzed for each Run.

The Wave Project II force coefficients were computed by

$$C_m = 1.33 \quad (4.2-5a)$$

$$C_d(\theta) = \begin{cases} 1.20 & ; R < 2.0 \times 10^5 \\ 10^E & ; 2.0 \times 10^5 < R < 5.5 \times 10^6 \\ 0.55 & ; R > 5.5 \times 10^6 \end{cases} \quad (4.2-5b)$$

where

$$E = 3.59197 - 1.0227 \log_{10}(R) + 0.0673774 [\log_{10}(R)]^2$$

$$R = |u(\theta) + \langle u \rangle| D/v$$

and where R is the instantaneous Reynolds number and v = kinematic viscosity of the fluid ($= 1.41 \times 10^{-5}$ ft 2 /sec.). Since C_d varies with R (and time, or θ), there is no single value to show for a particular run. The maximum Reynolds number possible during any run is 3×10^5 . Therefore, according to Eq. 4.2-5b, the drag coefficient will vary as $1.03 < C_d < 1.20$.

The U-tube coefficients published by Sarpkaya and Isaacson (1981) do not extend to either the Reynolds numbers or the Beta values measured for the NCEL data. Since U-tube tests have never been extended to the Reynolds numbers or to the Beta values obtained in large wave tank experiments, it is questionable that the U-tube values can be reliably extended to in-service design of prototype structures. Nevertheless, an effort was made to extrapolate graphically the data reported for U-tube tests. The results obtained by these graphical extrapolation methods are not unique and should not be interpreted as recommendations for the use of U-tube coefficients for computing wave forces. They were done for interest only in accordance with the SOW.

The U-tube inertia coefficients were estimated from

$$C_m = \begin{cases} 2.00 & ; K < 2.0 \\ 0.001336K^3 - 0.029881K^2 + 0.17002K + 1.71668 & ; 2.0 < K < 11.0 \\ 1.75 & ; K > 11.0 . \end{cases} \quad (4.2-6)$$

The U-tube drag coefficients were estimated from

$R < 1.0 \times 10^5$:

$$C_d = 0.000476K^3 - 0.017877K^2 + 0.185404K + 0.244354 \quad (4.2-7)$$

$R > 1.0 \times 10^5$:

$$C_d = \begin{cases} 0.5 & ; K < 2.5 \\ 0.00124K^3 - 0.3636K^2 + 0.280324K - 0.000779 & ; 2.5 \leq K \leq 8.0 \\ 0.55 & ; K > 8.0 \end{cases} \quad (4.2-8)$$

Measured Kinematics. Figure 4-22 illustrates the measured horizontal water particle kinematics and the numerically computed horizontal water particle acceleration for wave #3 in Run #5. The measured horizontal water particle velocity includes the average current, $\langle u \rangle$. The units of the vertical axis in Fig. 4-22 are ft. for the water surface elevation, ft/sec for the velocity and ft/sec² for the acceleration. Figures 4-23 to 4-25 compare both the measured forces and the forces predicted by the 2-term MOJS equation using the measured horizontal water particle kinematics and each of the three sets of force coefficients.

Linear Wave Theory Kinematics. Figure 4-26 illustrates the horizontal water particle velocity and acceleration computed from linear wave theory for wave #3 in Run #5. Figures 4-27 to 4-29 compare both the measured forces and the forces predicted by the 2-term MOJS equation using the linear wave theory kinematics and each of the three sets of coefficients for wave #3 in Run #5.

Table 4-4 summarizes the three sets of force coefficients (C_d and C_m) that were used individually with each of the three different

wave field kinematics. This resulted in nine different analyses for each of the seven individual waves in each of the deterministic runs listed in Table 3-1 that were analyzed by the 2-term MOJS equation. (In addition, the 4-term MOJS equation was used with the three sets of kinematics, yielding a total of 12 different analyses.)

Stream Function Theory Kinematics. Figure 4-30 illustrates the horizontal water particle kinematics computed by the stream function wave theory for wave #3 in Run #5. Figures 4-31 to 4-33 compare with the measured forces and the forces predicted by the 2-term MOJS equation using the stream function theory kinematics and each of the three sets of coefficients for wave #3 in Run #5.

Four-Term MOJS Equation. The 4-term MOJS equation developed by Sarpkaya (1981) introduced two additional time-dependent terms having **universal coefficients** that could be used with the Fourier coefficients obtained from the 2-term MOJS equation (Sarpkaya, 1981, p. 59). Since these **universal coefficients** were developed by Sarpkaya (1981) specifically for the use with the Fourier coefficients obtained from the 2-term MOJS equation, it was not realistic to use either the Wave Project II or the U-tube force coefficients in the 4-term MOJS equation since they were not obtained by Fourier analysis from the NCEL data. Consequently, only the least-squares coefficients were used for each of the three sets of wave field kinematics in the analysis by the 4-term MOJS equation. Sarpkaya and Isaacson (1981) have shown that the inertia coefficients are identical between the Fourier and least-squares regression analyses

and that the drag coefficients differ only slightly (Sarpkaya and Isaacson, 1981, p. 90). Therefore, the **least-squares** force coefficients were used with the **universal constants** in the 4-term MOJS equation in the NCEL data analyses.

Only the least-squares coefficients were used to compute the predicted forces by the 4-term MOJS equation using each of the three sets of kinematics. Because some of the inertia coefficients computed by Eq. 4.2-3a were greater than 2.0 and some of the drag coefficients computed by Eq. 4.2-3b were negative, the lambda term in Eq 2.1-2 sometimes becomes negative. When this occurred the two additional terms in the 4-term MOJS equation were not used. However, if the inertia coefficient was greater than 2.0 and the drag coefficient was less than zero, then lambda was positive and all four terms were computed.

Figures 4-34 to 4-36 compare the measured and predicted forces computed by the 4-term MOJS equation for each of the three sets of kinematics using only the least-squares coefficients for wave #3 in Run #5.

4.3 Random Waves

Four random wave runs were recorded during the NCEL tests. Two of these four random wave runs were analyzed and 10 individual periodic waves were selected for analyses based on comparisons with wave heights and periods in Table 3-13. A suite of three computer programs was developed to analyze the 10 individual periodic waves that are listed in Table 4-5.

4.3.1 PROGRAM WAVER

PROGRAM WAVER calibrated the integer data from the random wave runs similar to PROGRAM WAVE8 for the deterministic wave runs. A block of data containing 512 values was considered as a sequence of periodic waves. The fundamental wave period was then determined from $T = 0.06*512 = 30.72$ sec., where $\Delta t = 0.06$ sec. This single block of data was then FFT filtered to remove the high frequency noise. The time series for the horizontal water particle acceleration was computed numerically as before for the deterministic wave data in the frequency domain. However, there seemed to be a little more high frequency noise in the velocity spectra for the random waves. Thus, the high frequency noise problem in the acceleration spectra were exacerbated due to the transfer function approach that was taken. In order to obtain relatively smooth and useful accelerations, the acceleration spectra were generally filtered at 0.5 Hz instead of 1.5 Hz, which was the general case for the velocity spectra. There was one exception for Run 32, wave #2, where the horizontal acceleration was filtered at 0.4 Hz.

4.3.2 PROGRAM FDATAR

The FFT filtered data from PROGRAM WAVER were then visually inspected on the TEKTRONIX 4010 CRT screen one block at a time. From the hard copy output, the individual waves were selected on the basis of wave height and wave period. Figure 4-37 illustrates a single block of 512 values of the wave profile from random wave #32. The individual wave #6 was selected for analysis as an individual periodic wave. The number of data values in the individual

periodic wave selected was reduced to 33 values for that period by FFT methods (see Appendix 3). The individual waves were thus defined from crest-to-crest from the water profile record.

4.3.3 PROGRAM LABT4

The individual random wave was analyzed as a single periodic wave. Figures 4-38 to 4-52 illustrate the results from the individual wave #6 and from block #7 in random wave #32. Note that in Fig. 4-38 the wave profile is asymmetric and that both the sine and cosine components were retained from the FFI coefficients. The resulting wave profile is not a periodic cosine. Figure 4-38 also shows that the velocity profile, as measured, was not perfectly in phase with the water profile as measured (which was from crest-to-crest). It should be remembered that the wave period was defined in terms of the times from crest-to-crest of the water surface profile. Because of current measurement error the measured horizontal velocities should not necessarily be in phase with the surface profile, which is, in fact, the case for Fig. 4-38.

It should also be kept in mind that the return flow (\bar{u}) is superimposed on the water particle kinematics when a periodic wave theory is imposed on an individual wave from the random wave record. Therefore, because of the nonlinear drag term in the Morison equation, the predicted force will not yield a symmetrical plot, which is the case, for example, in Fig. 4-43.

Three plots of the comparison of wave kinematics appear in Figs. 4-53, 54, and 55. Similar plots can be constructed if desired for all the runs from the results shown in Vol. II.

5.0 SUMMARY OF RESULTS

Table 5-1 summarizes the average force coefficients from the 26 periodic runs. Table 5-2 summarizes the force coefficients from the seven individual waves for each of the 26 periodic wave runs and then the random waves. Each of the seven individual waves were represented by 33 data points from the original 256 data points. The two "bad points" waves in Runs #5 and #24 are identified by asterisks.

Figures 5-1 to 5-3 illustrate the parametric dependency of the average inertia force coefficient, C_m , on the Keulegan-Carpenter number, K , for the 26 periodic waves. Figures 5-4 to 5-6 illustrate the parametric dependency of the average drag force coefficient, C_d , on the Keulegan-Carpenter number. Note that negative drag coefficients are not plotted. Also shown in Figs. 5-1 to 5-6 are the maximum β values obtained from published U-tube tests (Sarpkaya and Isaacson, 1981) and the β values for these tests.

Figures 5-7 to 5-9 illustrate the inertia force coefficients for the 10 individual waves selected from the two random wave runs. Figures 5-10 to 5-12 illustrate the drag force coefficients for the 10 individual waves selected from the two random wave runs. Again, negative values of C_d were not plotted.

Table 5-3 summarizes the RMS error and the absolute value of the maximum error for both the 26 periodic wave runs and the 10 individual waves from the two random wave runs. The RMS errors were calculated from the differences between the predicted force and the measured force (as functions of time). In each case the predicted

force was based on the choice of kinematics and coefficients as so indicated. For example, under the stream function theory and WPII columns, the stream function kinematics, in conjunction with the force transfer coefficients as obtained from the WPII data, were used.

Table 5-4 summarizes the RMS error as a percentage of the maximum force for the 26 periodic wave runs and the 10 individual waves from the two random wave runs. Also tabulated is the percentage of energy in the two-harmonic acceleration spectrum compared to the unfiltered acceleration spectrum. This measure indicates the loss of energy in the acceleration spectrum due to filtering the non-harmonic components in the spectrum. Figures 5-13 to 5-21 display the RMS error as a percentage of the maximum force for the range of Keulegan-Carpenter numbers measured. These results were obtained from the 2-term MOJS equation.

Figures 5-22 to 5-24 display the RMS errors as a percentage of the maximum force for the range of Keulagan-Carpenter numbers measured for the 4-term MOJS equation. Table 5-5 summarizes the RMS errors for the analyses dealing with the 4-term MOJS equation.

6.0 CONCLUSIONS

1. Data of high quality were obtained on measured forces and wave conditions for a 12.75-inch diameter vertical cylinder. Drag and inertia coefficients were obtained therefrom for wave conditions with a Keulegan-Carpenter number up to 16 at the local force transducer and 20 at the still water surface. According to the open literature, this environment should have produced conditions that were drag dominant (although the inertia effects should still be significant). However, the results indicate the conditions were inertia dominant (and the drag effects were still significant).

The assumption that drag-dominated wave forces exist at Keulegan-Carpenter numbers near approximately 20 is not correct. This assumption arises from U-tube results which demonstrate that there is no parametric dependency of the force coefficients for $K > 20$. In contrast, the Dean number, E , (see Appendix 11.2) demonstrates that wave data do not become independent of K until $E > 4.0$, and $E \approx .088 K$, from which $K \approx 45$. As a consequence, most laboratory data determined herein are dependent on both C_d and C_m . For the data with $K \approx 6$ we found that the center forces were completely inertia dominated.

2. The wave forces as functions of time were calculated using measured kinematics and theoretical kinematics from linear and stream function theory, using least square coefficients, Wave Project II coefficients, and U-tube coefficients--all for the

2-term MOJS equation; and for the 4-term MOJS equation using least square coefficients. The β values were much higher than normally seen for laboratory testing. In fact, they were only moderately smaller than for conditions at sea. The C_m values for measured kinematics were slightly larger than for the linear and stream function kinematics. The C_d values for the measured kinematics had less scatter than for the two theoretical kinematic models. In addition, the values of C_d in the range of K where they were relatively reliable ($K > 10$) were approximately one-half those reported by Sarpkaya (1981) for oscillatory flow U-tube experiments with β values up to 8370.

3. Plots of the RMS errors vs. K indicate that the most accurate analysis methods used herein were the measured kinematics and the coefficients derived from a least square analysis.
4. The published U-tube coefficients do not extend to high enough Reynolds numbers or beta parameters to be used for the OSU laboratory wave analyses. Since the Reynolds numbers and beta parameters in the NCEL-OSU laboratory wave tests are still lower than in-service ocean designed values, U-tube coefficients, should be viewed with caution for wave force design.
5. The 2-term MOJS equation gave lower RMS and maximum errors than did the 4-term MOJS equation. The universal coefficients in the 4-term MOJS equation were not valid for these laboratory wave data.

6. The 2-term MOJS equation used with measured kinematics and measured coefficients gave lower RMS and maximum errors compared to either linear wave or stream function wave theory kinematics or the Wave Project II or U-tube coefficients.
7. Linear wave theory and stream function wave theory kinematics should be corrected for wave tank circulation currents in wave force analyses.
8. Although interesting observations have been made from the several types of calculations required by the SOW, many other analyses wait to be made on the data. Some of these are:
 - a) Phase shift vs. K plots for water surface vs. total force.
 - b) Maximum force coefficient vs. K plots.
 - c) In conjunction with a and b, new C_d 's and C_m 's can be derived.
 - d) Total forces and overturning moments can be examined.
 - e) Transverse forces should be examined regarding maximum lift coefficients.
 - f) More analyses should be directed to the random wave runs. Much more extensive transfer function and wave-by-wave analyses can be made to shed light on proper methods and techniques that differentiate analyses in random waves from those for periodic waves.

- g) For both periodic waves and random waves a cross-correlation analysis may produce more insight to the phase shift model.
- 9. The phase shift and maximum force coefficients analysis referred to above has innate advantages. First, both the phase shift and maximum force coefficient are more stable, displaying little scatter for all values of K. Secondly, the relative importance of the drag or inertia term is immediately evident in the phase plot. Thirdly, the maximum force is much more accurately predicted than in any of the methods utilized in this work. It should be added that this proposed technique has only recently revealed itself. In fact, the ideas encompassing the new methods were stimulated by this research. They should be further explored because of the promise of a major improvement in available methods of determining C_d and C_m from laboratory experimentation and projecting the results to prototype conditions.

7.0 REFERENCES

- Bloomfield, P. (1976), Fourier Analysis of Time Series: An Introduction, Wiley-Interscience, New York, NY, pp 75-76.
- Crandall, S.H. (1956), Engineering Analysis, McGraw-Hill Book Co., NY.
- Dean, R.G. and P.M. Aagaard (1970), "Wave Forces: Data Analysis of Engineering Calculation Method," Journal Petroleum Technology, March, pp 368-375.
- Dibble, T.L. (1980), "Frequency Response Characterization of Current Meters," thesis submitted in partial fulfillment of the requirements for M.S.C.E., Oregon State University, Corvallis, OR.
- Hudspeth, R.T., R.A. Dalrymple and G. Dean (1974), "Comparison of Wave Forces Computed by Linear and Stream Function Methods," Proceedings Sixth Offshore Technology Conference, OTC Paper 2037, Vol. II, pp 17-32.
- Sarpkaya, T. (1981), "Morison's Equation and the Wave Forces on Offshore Structures," Naval Civil Engineering Laboratory Report CR82.008.
- Sarpkaya, T. and M. Isaacson (1981), Mechanics of Wave Forces on Offshore Structures, Van Nostrand Reinhold Co., NY.

8.0 ACKNOWLEDGEMENTS

The authors wish to thank Mr. Jerry Dummer of the Naval Civil Engineering Laboratory for his support and encouragement during this project. In addition, Mr. Charles Smith of Minerals Management Service provided additional support that allowed for a more complete analysis. The computer programs, data acquisition, and analyses were helped greatly by the efforts of Mr. David Standley and Mr. Ming-Kuang Hsu. The laboratory work was conducted by Mr. Larry Crawford.

9.0 TABLES

Table 3-1 Measurements of LFT surface alignment. OUT from the cylinder
 surface = +, IN = -. Bearing means 0° = North (downwave)
 180° = South (upwave) and 90° = East. Measurements in mm.

Bearing (degree)	Bottom Alignment	Top Alignment	Longitudinal Spacing From Cylinder	
			Top	Bottom
0	0.0	+ .8	1.4	1.5
30	+ .3	+ 1.1		
60	+ .4	+ .8		
90	+ .5	+ .4	1.5	1.9
120	+ .5	+ .2		
150	+ .3	0.0		
180	+ .7	0.0	1.5	1.3
210	+ 1.0	+ 1.0		
240	+ .8	+ .9		
270	+ .5	+ .3	1.5	1.0
300	- .6	- .5		
330	- 1.1	- .5		
Average	+ .3	+ .4	1.5	1.4
σ	.6	.6		

Table 3-2 Light and heavy calibration weights

Step	Calibration Weight (lbs)	
	Light	Heavy
1	0	0
2	.74	3.22
3	2.66	14.35
4	4.59	28.07
5	6.54	43.45
6	8.50	63.92
7	10.47	84.46
8	12.47	108.33
9	14.51	132.64
10	16.56	157.08
11		181.61
12		201.44

Table 3-3 NCEL VERTICAL CYLINDER CALIBRATION SUMMARY

INSTRUMENT	CALIB	UP	DOWN	$\frac{U_D}{U}(\%)$	AVE	$\frac{PR-PO}{PR}(\%)$	AVE	$\frac{H-L}{H}(\%)$	ANALYSES	DIGITAL MAG TAPE CHANNEL
TOP N#1	PRE	41.57 (1.0000)	41.42 (1.0000)	0.36 (1.0000)	41.47 (1.0000)	0.60	41.345		41.345 (0.60%)	#1
TN 1 CH #1 HEAVY	POST	41.20 (1.0000)	41.30 (1.0000)	-0.24 (0.9999)	41.22 (0.9999)			-3.31		
TOP N#1	PRE	43.79 (0.9988)	42.04 (0.9999)	4.00 (0.9999)	42.83 (0.9923)	0.54	42.715			
TN 1 CH #1 LIGHT	POST	42.28 (0.9997)	42.81 (0.9997)	-1.25 (0.9997)	42.60 (0.9992)					
TOP N#2	PRE	44.40 (1.0000)	44.24 (1.0000)	0.36 (1.0000)	44.30 (0.9999)	0.68	44.15			
TN 2 CH #2 HEAVY	POST	43.96 (1.0000)	44.08 (1.0000)	-0.27 (0.9999)	44.00 (0.9999)			-2.58		
TOP N#2	PRE	46.33 (0.9878)	44.63 (0.9998)	3.67 (0.9917)	45.37 (0.9917)	0.35	45.29			
TN 2 CH #2 LIGHT	POST	44.98 (0.9999)	45.46 (0.9999)	-1.07 (0.9996)	45.21 (0.9996)					

UNITS: lbs/volt
 (.) = correlation coefficient

Table 3-4 NCEL VERTICAL CYLINDER CALIBRATION SUMMARY

INSTRUMENT	CALIB	UP	DOWN	U-D U (%)		PR-PO PR (%)	AVE	$\frac{H-L}{H} (%)$	ANALYSES	DIGITAL MAG TAPE CHANNEL
				AVE	AVE					
TOP E #1 TE1 CH #3 HEAVY	PRE	48.30 (0.9996)	48.35 (0.9999)	-0.10	48.38 (0.9997)	13.83	45.035			
	POST	41.73 (1.0000)	41.71 (0.9999)	0.05	41.69 (0.9999)			3.58		
TOP E #1 TE1 CH #3 LIGHT	PRE	44.87 (0.9998)	44.53 (0.9997)	0.76	44.60 (0.9997)	5.27	43.425			
	POST	42.18 (1.0000)	42.41 (0.9999)	-0.55	42.25 (0.9999)					
TOP E #2 TE2 CH #4 HEAVY	PRE	44.28 (1.0000)	44.09 (0.9999)	0.43	44.15 (0.9999)	0.25	44.095			
	POST	44.04 (1.0000)	44.09 (0.9999)	-0.11	44.04 (0.9999)			-1.01		
TOP E #2 TE 2 CH #4 LIGHT	PRE	44.58 (0.9998)	44.31 (0.9997)	0.61	44.40 (0.9996)					
	POST	44.77 (1.0000)	44.61 (0.9999)	0.36	44.68 (0.9999)					

UNITS: lbs/volt
 (.) = correlation coefficient

Table 3-5 NCEL VERTICAL CYLINDER CALIBRATION SUMMARY

INSTRUMENT	CALIB	UP	DOWN	$\frac{U-D}{U}(\%)$	AVE	$\frac{PR-PO}{PR}(\%)$	AVE	$\frac{H-L}{H}(\%)$	ANALYSES	DIGITAL MAG TAPE CHANNEL
Bottom N#1 BN1 CH #5 HEAVY	PRE	40.69 (1.0000) N5WET.027	40.44 (0.9998)	0.61	40.48 (0.9998)	-3.71	41.23		41.1675	#3
	POST	42.26 (1.0000) N5WH.072	41.79 (0.9996)	1.11	41.98 (0.9996)			-0.63	(N+5) (HEAVY) (0.30%)	
Bottom N#1 BN1 CH #5 LIGHT	PRE	41.78 (0.9987) N5WET.028	41.59 (0.9994)	0.45	41.6673 (0.9983)	0.86	41.49			
	POST	41.60 (0.998) N5WL.071	41.11 (0.9998)	1.18	41.31 (0.9996)					
Bottom S#1 BS1 CH #5 HEAVY	PRE	-40.57 (1.0000) S5WL.071	-40.31 (0.9999)	0.64	-40.40 (0.9999)	-3.49	-41.105			
	POST	-42.21 (1.0000) S5WH.075	-41.48 (1.0000)	1.73	-41.81 (0.9997)					
Bottom S#1 BS1 CH #5 LIGHT	PRE	-41.61 (0.9991) S5WL.031	-41.04 (0.9993)	1.37	-41.21 (0.99983)					
	POST									

UNITS: lbs/volt
(.) = correlation coefficient

Table 3-6 NCEL VERTICAL CYLINDER CALIBRATION SUMMARY

INSTRUMENT	CALIB			$\frac{U-D}{U}(\%)$	AVE	$\frac{PR-PO}{PR}(\%)$	AVE	$\frac{H-L}{H}(\%)$	ANALYSES	DIGITAL MAG TAPE CHANNEL
		UP	DOWN							
Bottom N#2 BN2 CH #6 HEAVY	PRE	44.04 (1.0000)	43.75 (0.9998)	0.66	43.81 (0.9998)	-1.19	44.07			
	POST	44.48 (1.0000)	44.25 (0.9996)	0.52	44.33 (0.9997)			-1.38		
			N5NH.072							
Bottom N#2 BN2 CH #6 LIGHT	PRE	44.77 (0.9995)	44.70 (0.9996)	0.16	44.71 (0.9990)	0.13	44.68			
	POST	44.85 (0.9993)	44.39 (0.9998)	1.03	44.64 (0.9993)					
			N5NL.071							
Bottom S#2 BS2 CH #6 HEAVY	PRE	-43.92 (1.0000)	-43.65 (0.9999)	0.61	-43.74 (0.9998)	-0.69	-43.89			
	POST	-44.27 (1.0000)	-43.85 (1.0000)	0.95	-44.04 (0.9999)			-1.62		
			S5NH.075							
Bottom S#2 BS2 CH #6 LIGHT	PRE	-45.06 (0.9991)	-44.46 (0.9990)	1.33	-44.60 (0.9984)			-44.60		
	POST									

UNITS: lbs/volt
 (.) = correlation coefficient

Table 3-7 NCEL VERTICAL CYLINDER CALIBRATION SUMMARY

INSTRUMENT	CALIB			$\frac{U-D}{U}(\%)$	AVE	$\frac{PR-PO}{PR}(\%)$	AVE	$\frac{H-L}{H}(\%)$	ANALYSES	DIGITAL MAG TAPE CHANNEL
		UP	DOWN							
Bottom E#1 BE1 CH #7 HEAVY	PRE	41.37 (1.0000)	41.11 (0.9998)	0.63	41.17 (0.9993)	-0.51	41.275		41.27	4
	POST	41.59 (1.0000)	41.26 (0.9999)	0.79	41.38 (0.9999)					
			E5WH.034	E5WH.067				-2.15		
Bottom E#1 BE1 CH #7 LIGHT	PRE	42.05 (0.9996)	42.17 (0.9996)	0.29	42.09 (0.9991)					-
	POST	42.10 (0.9989)	42.31 (0.9996)	-0.50	42.24 (0.9991)					
			E5WL.033	E5WL.070						
Bottom W#1 BW1 CH #7 HEAVY	PRE	-41.29 (1.0000)	-41.20 (0.9997)	0.218	-41.16 (0.9997)					-
	POST	-41.57 (1.0000)	-41.29 (0.9999)	0.67	-41.38 (0.9999)					
			W5WH.038	W5WH.066						
PRE										
	POST									

UNITS: lbs/volt
 (.) = correlation coefficient

Table 3-8 NCEL VERTICAL CYLINDER CALIBRATION SUMMARY

INSTRUMENT	CALIB	$\frac{U-D}{U}(\%)$			$\frac{PR-PO}{PR}(\%)$	AVE	$\frac{H-L}{H}(\%)$	ANALYSES	DIGITAL MAG TAPE CHANNEL
		UP	DOWN	AVE					
LOCAL N 1 + 2 LN 1 + 2 CH #9 LIGHT	PRE	-4.89 (0.9999)	-4.86 (0.9999)	0.61 (0.9999)	-4.87 (0.9999)	0.00	-4.87		
	POST	-4.88 (0.9999)	-4.87 (0.9999)	0.21 (0.9999)	-4.87 (0.9999)			0.21	#5 (filtered)
	PRE	4.88 (0.9999)	4.86 (0.9999)	0.41 (0.9999)	4.87 (0.9998)	0.82	4.85		#7 (unfiltered)
	POST	4.83 (1.0000)	4.83 (0.9999)	0.00 (0.9999)	4.83 (0.9999)				
LOCAL S 1 + 2 LS 1 + 2 CH #9 LIGHT	PRE	-4.86 (0.9997)	-4.82 (0.9999)	0.82 (0.9999)	-4.84 (0.9997)				
	POST	-4.89 (0.9998)	-4.89 (0.9999)	0.00 (0.9999)	-4.89 (0.9998)	-1.03	-4.865		
	PRE	4.83 (0.9999)	4.84 (0.9999)	0.41 (0.9999)	4.835 (0.9999)			0.36	#6
	POST	4.88 (0.9998)	4.84 (0.9999)	0.82 (0.9999)	4.86 (0.9999)			-4.856	
LOCAL W 1 + 2 LW 1 + 2 CH #10 LIGHT	PRE	4.83 (0.9999)	4.84 (0.9999)	-0.21 (0.9999)	4.835 (0.9999)	-0.52	4.8475		
	POST	4.88 (0.9999)	4.84 (0.9999)	0.82 (0.9999)	4.86 (0.9999)				

UNITS: lbs/volts
 (\cdot) = correlation coefficient

Table 3-9 NCEL VERTICAL CYLINDER CALIBRATION SUMMARY

INSTRUMENT	CALIB			$\frac{U-D}{U}(\%)$	AVE	$\frac{PR-PO}{PR}(\%)$	AVE	$\frac{H-L}{H}(\%)$	ANALYSES	DIGITAL MAG TAPE CHANNEL
		UP	DOWN							
Bottom E#2 BE2 CH #8 HEAVY	PRE	43.81 (1.0000)	43.71 (0.9998)	0.23	43.69 (0.9995)					
	POST									
	PRE	43.71 (0.9895)	45.87 E5NL .033	-4.94	44.33 (0.9878)					
	POST									
Bottom E#2 BE2 CH #8 LIGHT	PRE									
	POST									
	PRE									
	POST									
Bottom W#2 BW2 CH #8 HEAVY	PRE	-44.14 (0.9996)	-44.06 (0.9990)	0.20	-43.85 (0.9991)					
	POST									
	PRE									
	POST									

UNIT: lbs/volt
 (.) = correlation coefficient

Table 3-10 NCEL VERTICAL CYLINDER CALIBRATION SUMMARY

INSTRUMENT	CALIB	UP		DOWN		$\frac{U-D}{U}(\%)$	AVE	$\frac{PR-PO}{PR}(\%)$	AVE	$\frac{H-L}{H}(\%)$	ANALYSES	DIGITAL MAG TAPE CHANNEL
		LOCAL	N	LOCAL	LIGHT							
LOCAL N CH #9	0X0	-4.86 (1.0000)	-4.86 (1.0000)	0.00 N300X0.024	0.00 (1.0000)	-4.35 (1.0000)						
LIGHT	XXX	-4.86 (0.9999)	-4.87 (1.0000)	-0.21	-4.86 (0.999)							
LOCAL E CH #10	0X0	-4.77 (1.0000)	-4.76 E300X0.015	0.21	-4.77 (1.0000)							
LIGHT	XXX	-4.74 (0.9999)	-4.74 E3XXX.016	0.00	-4.79 (0.9999)							
LOCAL NE	#9	-6.08 (0.9999)	-6.08 NE300X0.026	0.00	-6.08 (0.9999)							
LIGHT	#10	-8.12 (0.9999)	-8.10 NE300X0.026	0.25	-8.12	$\times \sin 54^\circ = -4.92$						
	PRE											
	POST											

Table 3-11 NCCL VERTICAL CYLINDER CALIBRATION SUMMARY
for the pressure transducers

INSTRUMENT	CALIB	UP		DOWN		$\frac{U-D}{U}(%)$	AVE	$\frac{PR-P0}{PR}(%)$	AVE	$\frac{H-L}{H}(%)$	ANALYSES	DIGITAL MAG TAPE CHANNEL
		PRE	POST	PRE	POST							
PRESSURE P1 000 CH #1	PRE	1.00557 (0.9998)	1.09210 (0.9976)	-8.61								
	POST	1.01703 (0.9991)	1.02744 (0.9994)	-1.02	1.04884	2.54	1.03554					
PRESSURE P2 060° CH #2	PRE	0.97212 (0.9998)	0.94238 (0.9976)	3.06		0.95724	1.40	0.95056				
	POST	0.94433 (0.9993)	0.94341 (0.9996)	0.10	0.94387							
PRESSURE P3 090° CH #3	PRE	0.98343 (0.9998)	0.96698 (0.9977)	1.67	0.97521							
	POST	0.99571 (0.992)	0.99340 (0.9995)	0.23	0.99456							
PRESSURE P4 120° CH #4	PRE	1.00890 (0.9998)	0.98441 (0.9978)	2.43	0.99666							
	POST	1.01872 (0.9992)	1.01501 (0.9995)	0.36	1.01687							

UNITS: psi/v
(.) =correlation coefficient

Table 3-12 NCEL VERTICAL CYLINDER CALIBRATION SUMMARY
for the pressure transducers

INSTRUMENT	CALIB	UP		DOWN		$\frac{U-D}{U}(x)$	AVE	$\frac{P_r-P_0}{P_r}(x)$	AVE	$\frac{H-L}{H}(x)$	ANALYSES	DIGITAL MAG TAPE CHANNEL
		UP	DOWN	UP	DOWN							
PRESSURE P5 180° CH #5	PRE	0.98742 (0.9998)	0.51972 (0.9005)	4/22/83	4/26/83	47.66	0.75357 (0.98742)*	-2.15	0.99804			
	POST	1.00824 (0.9989)	1.00908 (0.9994)			-0.08	1.00866					
		4/27/83	4/27/83									
PRESSURE P6 240° CH #6	PRE	0.96663 (0.9998)	0.48196 (0.9793)			50.14	0.72430 (0.966663)*	-0.18	0.96752			
	POST	0.98724 (0.9830)	0.94957 (0.9828)	4/22/83	4/26/83	3.82	0.96841					
		4/27/83	4/27/83									
PRESSURE P7 270° CH #7	PRE	0.92667 (0.9998)	0.90831 (0.9977)			1.92	0.91719					
	POST	0.94453 (0.9993)	0.94309 (0.9995)	4/22/83	4/26/83	0.15	0.94381					
		4/27/83	4/27/83									
PRESSURE P8 300° CH #8	PRE	0.98904 (0.9998)	0.99906 (0.9966)			-1.01	0.99405					
	POST	1.01568 (0.9993)	1.01407 (0.9995)	4/22/83	4/26/83	0.16	1.01488					
		4/27/83	4/27/83									

UNITS: psi/v
 (\cdot) =correlation coefficient
 (\cdot) *=value from UP-PRE used in average

Table 3-13 Log of runs

Run No.	Wave Frequency (Hz)	T (s)	Span (waveboard)	Target H (ft)	Analog Counter Start	Analog Counter Stop	Remarks
1	.500	2	95	1.0	35	51	
2	.500	2	32	0.4	51	65	
3	.400	2.5	110	1.1	66	83	X 10 A/D = 2
4	.400	2.5	205	2.0	83	101	X 10 - 2
5	.400	2.5	375	3.7	101	119	X 10
6	.270	3.7	175	1.0	119	140	X 10 -
7	.270	3.7	444	2.5	140	163	X 10
8	.270	3.7	780	4.4	163	185	(voltage out of r
9	.217	4.6	147	0.7	185	209	X 10
10	.217	4.6	336	1.6	209	233	X 10
11	.217	4.6	827	3.1	233	257	X 10 - #2
12	.217	4.6	1000	4.3	257	281	X 1 - #2
13	.189	5.3	202	0.9	281	308	X 10
14	.189	5.3	338	1.5	308	334	X 10
15	.189	5.3	693	2.6	334	359	X 10
16	.189	5.3	933	3.5	359	386	X 1
17	.189	5.3	1000	3.9	386	412	X 1
18	.167	6.0	665	1.9	412	445	X 10 4/25/83
19	.167	6.0	800	2.6	445	477	X 10
20	.167	6.0	950	3.3	477	510	X 1
21	.238	4.2	1000	5.2	510	537	X 1
22	.189	5.3	1000	3.9	537	568	X 1
23	.217	4.6	1000	4.3	568	597	X 1
24	.270	3.7	780	4.4	597	622	X 1
25	.400	2.5	375	3.7	622	645	X 1
26	.167	6.0	950	3.3	645	676	X 1
27	.5	2	95	1.0	676	698	X 10 Copy of R1
28	.270	3.7	780	4.4	698	723	X 1 Copy of R8
29	.217	4.6	827	3.1	723	751	X 1 Copy of R11
30	.167	6.0	665	1.9	751	784	X 1 Copy of R18
31	.167	6.0	800	2.6	784	816	X 1 Copy of R19
32	Random JONSWAP $\hat{T} = 3.7 \times H_{1/3} = 2.9$				816	990	X 1
33	Random JONSWAP $\hat{T} = 3.7 \times H_{1/3} = 2.9$				990	1160	X 1
34	Random JONSWAP $\hat{T} = 3.7 \times H_{1/3} = 2.9$				1160	1330	Different
35	Random JONSWAP $\hat{T} = 3.7 \times H_{1/3} = 2.9$				1330	1498	X 1
36	.333	3.0	140	1.0	1498	1519	X 1
37	.333	3.0	320	2.5	1519	1539	X 1
38	.333	3.0	850	5.0	1539	1564	X 1
39	.250	4.0	180	1.0	1564	1587	X 1
40	.250	4.0	450	2.5	1587	1610	X 1
41	.250	4.0	900	5.0	1610	1633	X 1
42	.200	5.0	200	1.0	1633	1660	X 1
43	.200	5.0	700	2.5	1660	1684	X 1
44	.200	5.0	1000	5.0	1684	1710	X 1
45	.333	3.0	650	5.0	1710	1731	X 1

NOTES: Water Temperature = 50°F (4/22 & 4/23)
 Water Depth = 11.5 ft.

Table 4-1 Signal routing and recording

Transducer Name	Transducer	A/D Cal. Ch. #	Run Ch. #	Analog Tape Ch. #	8 Hz Rockland Filter Yes	Rockland Filter No	Analog Tape Yes	Final Digital Tape Ch. #
Top North 1	1	1	1	1	X			1
North 2	2	2	NR					
East 1	3	3	NR					
East 2	4	4	2		X			2
Bottom North 1	5	5	3		X			3
North 2	6	6	NR					
East 1	7	7	4		X			4
East 2	8	8	NR					
Center North 1	9 combined = 9		5,7	1	X(5)	X(7)	X(7)	17,7,5
North 2	10 -		NR					
East 1	11 -		NR		X			
East 2	12 -		6					6
East Vertical	mm#1 X		8		X			8
East Horizontal	mm#2 Y		9		X			9
West Vertical	mm#3 X		10		X			10
West Horizontal	mm#4 Y		11		X			11
Pressure	0° P1	1		3	X			18
	60° P2	2		12	X			12
	90° P3	3		13	X			13
	120° P4	4		14	X			14
	180° P5	5		15	X			15
	240° P6	6		RL	4	X		19
	270° P7	7		RL	5	X		20
	300° P8	8		RL	9	X		21
Wave Sensor	Sonic #1						X	16

NOTE: NR = Not Recorded, RL = Recorded Later (digitally)

Table 4-2 Summary of amplitude attenuation and phase shifts introduced by the Marsh-McBirney current meters
 $(\tau = 0.159 \text{ sec.})$

f (Hz)	$ H_M $	θ_M (radians)	θ_M (degrees)
0.0	1.000	0.0	0.0
0.2	0.981	-0.197	-11.3
0.4	0.927	-0.380	-21.8
0.5*	0.895	-0.463	-26.5
1.0	0.707	-0.785	-45.0
1.5	0.555	-0.982	-56.3

*denotes highest wave frequency tested during periodic wave runs.

Table 4-3 Summary of amplitude attenuation and phase shifts introduced by the Rockland filters
 $(f_0 = 8 \text{ Hz})$

f (Hz)	ϵ (f/f_0)	$ H_R $	θ_R (radians)	θ_R (degrees)
0.0	0.0	1.0	0.0	0.0
0.2	0.025	0.9996	-0.080	-4.6
0.4	0.05	0.998	-0.162	-9.3
0.5	0.0625	0.997	-0.202	-11.6
1.0	0.125	0.989	-0.407	-23.3
1.5	0.1875	0.976	-0.610	-35.0

Table 4-4 Summary of combinations of force coefficients and wave kinematics for 2-term MOJS equation analyses

Force Coefficients (C_d and C_m)	1. Least-Squares 2. Wave Project II 3. U-Tube
Wave Kinematics	1. Measured 2. Linear Wave Theory 3. Stream Function Wave Theory

Table 4-5 Individual periodic waves selected from random wave runs

Run No.	Wave No.	Block No.	Individual Wave No.	T (sec)	H (ft)
32	1	5	4	4.68	1.95
	2	7	6	3.78	3.50
	3	9	2	2.52	2.97
	4	13	2	4.74	2.99
	5	19	6	2.52	2.89
34	1	7	4	4.26	1.96
	2	11	2	4.08	2.34
	3	15	3	3.84	2.65
	4	15	5	3.66	2.89
	5	19	3	4.98	1.61

Table 5-1 Summary of the average force coefficients from the 26 periodic wave runs

Run No.	T (sec)	Linear Wave Theory						Stream Function Theory						Measured Kinematics									
		\bar{K} ($\times 10^{-5}$)	\bar{C}_d	σC_d	\bar{C}_m	σC_m	RMS	\bar{R} ($\times 10^{-5}$)	\bar{C}_d	σC_d	\bar{C}_m	σC_m	RMS	\bar{R} ($\times 10^{-5}$)	\bar{C}_d	σC_d	\bar{C}_m	σC_m	RMS				
1	2.00	1.07	0.46	1.15	0.61	1.48	2.03	0.03	0.026	0.46	1.15	0.62	1.48	2.02	0.03	0.027	0.47	1.19	-0.30	0.36	2.35	0.09	0.073
2	2.00	0.35	0.15	0.37	-0.09	2.37	2.05	0.01	0.010	0.15	0.37	-0.09	2.38	2.05	0.02	0.010	0.15	0.39	2.76	1.89	2.66	0.04	0.084
3	2.50	1.01	0.51	1.60	-0.12	0.58	2.07	0.01	0.015	0.51	1.59	-0.12	0.59	2.07	0.01	0.014	0.52	1.62	-0.86	0.50	2.32	0.03	0.049
4	2.50	1.88	0.91	2.85	0.23	0.22	2.01	0.03	0.021	0.90	2.81	0.24	0.23	2.03	0.03	0.018	0.89	2.77	-0.39	0.34	2.28	0.02	0.014
5	3.70	2.29	1.71	5.35	0.45	0.40	1.85	0.05	0.065	1.60	4.99	0.49	0.44	1.94	0.04	0.054	1.54	4.80	0.12	0.09	2.30	0.03	0.070
6	3.70	0.94	0.55	2.55	-0.01	0.42	2.08	0.03	0.050	0.54	2.50	0.00	0.43	2.09	0.03	0.031	0.54	2.50	-0.02	0.20	2.22	0.02	0.032
7	3.70	2.52	1.47	6.81	0.48	0.20	1.81	0.12	0.124	1.41	6.50	0.49	0.22	1.87	0.11	0.071	1.36	6.28	0.20	0.07	2.10	0.04	0.057
28(8)	3.70	4.40	2.64	12.19	0.13	0.11	1.61	0.04	0.204	2.36	10.92	0.15	0.14	1.80	0.04	0.086	2.32	10.74	0.44	0.20	1.92	0.04	0.113
9	4.60	0.63	0.38	2.19	-0.14	2.16	1.77	0.21	0.052	0.38	2.15	-0.15	2.18	1.77	0.21	0.061	0.42	2.41	0.57	0.31	2.29	0.13	0.087
10	4.60	1.41	0.85	4.88	0.42	0.26	1.82	0.11	0.055	0.84	4.82	0.42	0.26	1.82	0.12	0.086	0.80	4.59	0.15	0.17	2.13	0.09	0.048
29(11)	4.60	3.53	2.17	12.46	0.55	0.20	1.70	0.08	0.103	2.13	12.23	0.62	0.22	1.68	0.09	0.223	2.05	11.81	0.48	0.11	1.95	0.03	0.114
12	4.60	4.17	2.69	15.43	0.13	0.15	1.77	0.07	0.166	2.40	13.76	0.15	0.20	1.83	0.07	0.178	2.43	13.97	0.48	0.10	1.89	0.06	0.130
13	5.30	0.76	0.46	3.04	-0.20	0.34	1.73	0.13	0.098	0.47	3.14	-0.19	0.35	1.74	0.13	0.060	0.40	2.61	-0.06	0.75	2.36	0.05	0.066
14	5.30	1.22	0.74	4.89	0.27	0.18	1.78	0.07	0.125	0.78	5.18	0.29	0.19	1.81	0.08	0.060	0.79	5.21	0.196	0.38	2.11	0.04	0.060
15	5.30	2.57	1.55	10.27	0.33	0.16	1.56	0.08	0.218	1.69	11.20	0.36	0.17	1.69	0.09	0.093	1.56	10.35	0.25	0.15	1.99	0.02	0.078
16	5.30	3.42	2.16	14.28	0.26	0.06	1.54	0.05	0.268	2.16	14.30	0.28	0.06	1.76	0.07	0.107	2.11	13.95	0.36	0.07	1.91	0.08	0.069
17	5.30	3.66	2.31	15.29	0.29	0.05	1.49	0.08	0.289	2.32	15.34	0.31	0.08	1.75	0.08	0.123	2.29	15.12	0.41	0.07	1.88	0.04	0.073
30(18)	6.00	1.90	1.16	8.73	0.47	0.24	1.92	0.13	0.166	1.28	9.57	0.46	0.26	1.98	0.12	0.073	1.42	10.66	0.37	0.17	1.97	0.05	0.072
31(19)	6.00	2.28	1.40	10.48	0.44	0.16	1.87	0.07	0.213	1.55	11.61	0.45	0.17	1.99	0.08	0.076	1.68	12.61	0.40	0.18	1.92	0.02	0.060
20	6.00	2.81	1.79	13.40	0.34	0.05	1.66	0.09	0.265	1.86	13.95	0.36	0.08	1.85	0.09	0.115	2.01	15.06	0.37	0.09	1.81	0.09	0.067
21	4.20	4.90	3.09	16.34	0.61	0.06	1.49	0.05	0.159	2.68	14.14	0.75	0.09	0.65	0.06	0.137	2.69	14.13	0.53	0.06	1.83	0.03	0.093
22	5.30	3.71	2.32	15.26	0.25	0.05	1.47	0.08	0.278	2.39	15.74	0.27	0.07	1.69	0.08	0.108	2.46	16.25	0.37	0.08	1.75	0.04	0.080
23	4.60	4.16	2.58	14.80	0.11	0.19	1.73	0.07	0.158	2.48	14.26	0.09	0.23	1.81	0.07	0.163	2.49	14.31	0.47	0.08	1.87	0.04	0.117
24	3.70	4.41	2.64	12.21	0.09	0.06	1.65	0.05	0.192	2.37	10.95	0.10	0.08	1.82	0.06	0.090	2.38	11.00	0.43	0.13	1.89	0.06	0.124
25	2.50	3.38	1.77	5.52	0.53	0.10	1.80	0.04	0.069	1.64	5.12	0.59	0.12	1.90	0.04	0.045	1.63	5.10	0.06	0.13	2.09	0.01	0.052
26	6.00	2.79	1.74	13.04	0.38	0.14	1.68	0.11	0.253	1.87	14.01	0.38	0.18	1.85	0.14	0.112	1.534	15.34	0.33	0.12	1.78	0.05	0.081

$$\text{NOTE: } \text{RMS} = \frac{1}{7} \sum_{j=1}^7 \left\{ \frac{1}{33} \sum_{i=1}^{33} [F_m^{(i)} - F_p^{(i)}]^2 \right\}^{1/2} / F_m^{(\text{max})}$$

Table 5-2 Summary of force coefficients for each of the seven individual waves in the 26 periodic wave runs and the 10 individual random waves (*denotes "bad points" wave omitted from analyses) (RMS err = 100x%)

Run	Wave No.	T _{meas} (sec)	H _{meas} (ft)	Linear Wave Theory			Stream Function Wave Theory			Measured Kinematics									
				R (x10 ⁻⁵)	K	C _d	RMS err	R (x10 ⁻⁵)	K	C _d	RMS err	R (x10 ⁻⁵)							
1	1	2.00	1.18	0.51	1.27	-2.55	0.51	1.27	-2.54	1.96	0.059	0.52	1.29	-0.02	2.56	0.050	-0.07		
	2	1.04	0.45	1.13	2.14	2.02	0.028	0.45	1.13	2.14	2.02	0.027	0.46	1.15	-0.65	2.29	0.089	-0.07	
	3	1.04	0.45	1.12	0.78	2.06	0.018	0.45	1.12	0.78	2.05	0.019	0.48	1.21	0.18	2.31	0.073	-0.07	
	4	1.06	0.46	1.15	1.31	2.03	0.023	0.46	1.15	1.31	2.03	0.024	0.46	1.14	0.04	2.33	0.074	-0.07	
	5	1.06	0.45	1.13	0.76	2.03	0.016	0.45	1.13	0.76	2.02	0.017	0.47	1.18	-0.46	2.32	0.077	-0.06	
	6	1.06	0.45	1.13	0.72	2.04	0.019	0.45	1.13	0.72	2.03	0.021	0.47	1.19	-0.48	2.33	0.071	-0.06	
	7	1.05	0.44	1.09	1.14	2.05	0.018	0.44	1.09	1.14	2.05	0.019	0.46	1.15	-0.69	2.32	0.075	-0.05	
2	1	2.00	0.36	0.15	0.38	1.79	2.06	0.018	0.15	0.38	1.80	2.06	0.018	0.15	0.38	4.05	2.73	0.081	-0.02
	2	0.36	0.15	0.38	3.09	2.03	0.011	0.15	0.38	3.10	2.03	0.011	0.17	0.43	3.82	2.65	0.082	-0.02	
	3	0.35	0.15	0.36	-0.70	2.04	0.005	0.14	0.36	-0.70	2.04	0.005	0.13	0.33	5.55	2.61	0.091	-0.01	
	4	0.36	0.15	0.37	-4.52	2.03	0.022	0.15	0.37	-4.53	2.03	0.022	0.15	0.37	3.25	2.68	0.078	-0.01	
	5	0.35	0.15	0.39	0.12	2.05	0.004	0.15	0.38	0.12	2.06	0.004	0.18	0.45	0.82	2.65	0.089	-0.02	
	6	0.35	0.15	0.36	-0.12	2.05	0.008	0.15	0.36	-0.12	2.06	0.008	0.14	0.36	0.75	2.63	0.083	-0.01	
	7	0.35	0.15	0.37	-0.28	2.06	0.005	0.15	0.37	-0.28	2.06	0.005	0.16	0.40	1.08	2.64	0.084	-0.02	
3	1	2.50	1.04	0.52	1.64	0.10	2.06	0.025	0.52	1.63	0.10	2.06	0.025	0.54	1.70	-0.58	2.38	0.043	-0.04
	2	0.99	0.51	1.58	-0.84	2.06	0.013	0.50	1.57	-0.84	2.07	0.012	0.49	1.55	-0.48	2.29	0.045	-0.04	
	3	1.01	0.52	1.61	0.11	2.06	0.011	0.51	1.60	0.12	2.07	0.013	0.53	1.64	-0.16	2.32	0.048	-0.05	
	4	1.01	0.52	1.63	0.57	2.05	0.018	0.52	1.62	0.58	2.06	0.016	0.55	1.72	-0.80	2.30	0.052	-0.06	
	5	1.00	0.52	1.61	-1.02	2.07	0.013	0.51	1.60	-1.03	2.08	0.013	0.51	1.58	-1.07	2.32	0.048	-0.05	
	6	0.99	0.50	1.55	0.24	2.09	0.011	0.50	1.55	0.25	2.10	0.010	0.50	1.55	-1.37	2.31	0.054	-0.03	
	7	1.01	0.51	1.59	-0.02	2.07	0.011	0.51	1.58	-0.02	2.08	0.009	0.51	1.60	-1.56	2.31	0.056	-0.04	
4	1	2.50	1.88	0.92	2.88	0.06	1.99	0.025	0.91	2.83	0.06	2.01	0.018	0.90	2.82	-0.18	2.26	0.016	-0.04
	2	1.88	0.90	2.82	0.26	1.98	0.020	0.90	2.81	0.26	2.01	0.015	0.86	2.69	0.04	2.26	0.012	0.01	
	3	1.87	0.92	2.88	0.39	2.05	0.021	0.90	2.82	0.40	2.07	0.026	0.86	2.69	-0.28	2.31	0.020	-0.04	
	4	1.84	0.92	2.86	0.62	2.06	0.021	0.90	2.81	0.64	2.08	0.023	0.96	2.99	-0.22	2.29	0.017	-0.05	
	5	1.88	0.91	2.84	0.01	2.01	0.018	0.84	2.78	0.01	2.03	0.013	0.93	2.90	-0.44	2.28	0.010	-0.02	
	6	1.89	0.92	2.86	0.03	2.00	1.019	0.90	2.80	0.03	2.02	0.015	0.85	2.65	-0.71	2.28	0.011	-0.02	
	7	1.89	0.90	2.82	0.26	2.00	0.21	0.90	2.81	0.27	2.02	0.018	0.86	2.68	-0.95	2.29	0.015	0.00	
5	1	2.50	3.24	1.71	5.34	0.15	1.89	0.049	1.60	5.00	0.16	1.98	0.040	1.55	4.83	0.06	2.29	0.056	-0.23
	2	3.26	1.73	5.41	0.08	1.92	0.055	1.62	5.06	0.08	2.00	0.055	1.59	4.97	0.10	2.34	0.063	-0.24	
	3	3.37	1.79	5.58	0.17	1.83	0.064	1.66	5.19	0.18	1.93	0.060	1.57	4.90	0.23	2.32	0.072	-0.24	
	4	3.12	1.61	5.03	1.14	1.89	0.076	1.52	4.73	1.24	1.97	0.058	1.68	5.25	0.13	2.28	0.077	-0.17	
	5	3.34	1.75	5.47	0.22	1.71	0.074	1.63	5.08	0.24	1.90	0.059	1.48	4.61	0.22	2.26	0.083	-0.21	
	6	3.37	1.73	5.40	0.66	1.80	0.069	1.60	5.00	0.73	1.90	0.054	1.49	4.67	0.11	2.30	0.075	-0.17	
	7	3.32	1.68	5.25	0.90	1.82	0.069	1.56	4.88	0.77	1.91	0.054	1.54	4.80	-0.01	2.29	0.073	-0.14	

$$\text{NOTE: RMS err} = \left\{ \frac{1}{N} \sum_{i=1}^N [F_m(i) - F_p(i)]^2 \right\}^{1/2} / F_m(\max)$$

Table 5-2 (continued)

Run	Wave No.	T _{meas} (sec)	H _{meas} (ft)	Linear Wave Theory						Stream Function Wave Theory						Measured Kinematics					
				R	K	C _d	C _m	RMS	err	(x10 ⁻⁵)	R	K	C _d	C _m	RMS	R	K	C _d	C _m	RMS	err
6	1	3.70	0.93	0.53	2.43	0.60	2.09	0.037	0.52	2.42	0.61	2.10	0.017	0.53	2.46	-0.34	2.20	0.049	-0.01		
	2	0.94	0.61	2.81	-0.02	2.11	0.017	0.60	2.75	-0.02	2.12	0.023	0.61	2.80	-0.10	2.24	0.068	-0.11			
	3	0.95	0.55	2.55	0.13	2.07	0.035	0.54	2.50	0.13	2.07	0.013	0.51	2.37	-0.01	2.22	0.045	-0.03			
	4	0.94	0.55	2.53	-0.64	2.06	0.061	0.54	2.47	-0.64	2.07	0.035	0.55	2.53	-0.12	2.21	0.016	-0.03			
	5	0.94	0.54	2.51	-0.18	2.12	0.71	0.53	2.45	-0.17	2.13	0.049	0.54	2.47	-0.10	2.26	0.019	-0.02			
	6	0.95	0.55	2.53	-0.32	2.06	0.070	0.54	2.47	-0.31	2.08	0.045	0.54	2.52	0.21	2.24	0.011	-0.02			
	7	0.95	0.55	2.52	0.39	2.02	0.062	0.54	2.47	0.40	2.04	0.038	0.51	2.36	0.26	2.20	0.015	-0.01			
7	1	3.70	2.39	1.42	6.58	0.70	1.93	0.095	1.32	6.11	0.74	1.98	0.045	1.36	6.27	0.17	2.13	0.035	-0.11		
	2	2.44	1.43	6.61	0.29	1.93	-0.108	1.35	6.24	0.30	1.98	0.044	1.37	6.32	0.10	2.15	0.035	-0.08			
	3	2.45	1.46	6.76	0.47	1.86	0.128	1.35	6.26	0.49	1.92	0.069	1.36	6.27	0.22	2.11	0.053	-0.12			
	4	2.45	1.46	6.72	0.78	1.83	0.138	1.35	6.22	0.82	1.90	0.081	1.34	6.20	0.21	2.11	0.061	-0.11			
	5	2.76	1.58	7.31	0.46	1.64	0.123	0.57	7.24	0.47	1.70	0.074	1.36	6.30	0.24	2.10	0.061	-0.04			
	6	2.48	1.43	6.63	0.46	1.80	0.138	1.40	6.45	0.45	1.86	0.096	1.39	6.42	0.30	2.06	0.079	-0.05			
	7	2.67	1.53	7.09	0.21	1.67	0.139	1.51	6.96	0.19	1.73	0.090	1.33	6.17	0.15	2.04	0.072	-0.05			
28	1	3.70	4.33	2.66	12.28	0.31	1.67	0.173	2.26	10.46	0.37	1.83	0.070	2.15	9.95	0.74	9.95	0.110	-0.30		
	2	4.42	2.69	12.44	0.25	1.59	0.190	2.32	10.74	0.30	1.75	0.087	2.23	10.32	0.67	1.87	0.113	-0.28			
	3	4.50	2.70	12.46	0.13	1.57	0.200	2.41	11.16	0.15	1.76	0.079	2.21	10.19	0.54	1.90	0.106	-0.22			
	4	4.42	2.56	11.82	0.02	1.59	0.217	2.46	11.38	0.02	1.78	0.081	2.40	11.11	0.34	1.92	0.095	-0.10			
	5	4.33	2.61	12.05	0.02	1.67	0.216	2.32	10.71	0.01	1.86	0.090	2.51	11.59	0.26	1.97	0.102	-0.23			
	6	4.42	2.65	12.25	0.13	1.57	0.216	2.37	10.95	0.13	1.77	0.093	2.33	10.79	0.31	1.87	0.129	-0.22			
	7	4.40	2.60	12.02	0.08	1.63	0.216	2.39	11.05	0.06	1.83	0.103	2.44	11.29	0.25	1.93	0.139	-0.18			
9	1	4.60	0.60	0.37	2.10	-0.65	1.98	0.061	0.36	2.04	-0.67	1.99	0.042	0.43	2.44	0.69	2.38	0.121	-0.02		
	2	0.62	0.38	2.18	0.18	1.95	0.061	0.37	2.12	0.15	1.95	0.061	0.46	2.63	0.80	2.41	0.098	-0.02			
	3	0.60	0.36	2.08	2.98	1.91	0.048	0.35	2.03	3.00	1.91	0.058	0.47	2.70	0.68	2.40	0.066	-0.01			
	4	0.60	0.36	2.06	-2.93	1.87	0.050	0.35	2.01	-2.96	1.87	0.063	0.42	2.43	0.71	2.34	0.073	-0.01			
	5	0.66	0.39	2.24	-2.49	1.60	0.036	0.39	2.22	-2.51	1.60	0.067	0.42	2.44	-0.01	2.21	0.068	-0.01			
	6	0.67	0.41	2.36	-0.10	1.63	0.049	0.40	2.29	-0.11	1.64	0.059	0.39	2.26	0.28	2.19	0.097	-0.03			
	7	0.69	0.41	2.33	2.03	1.44	0.061	0.42	2.37	2.04	1.44	0.074	0.35	2.00	0.84	2.08	0.088	0.00			
	8	4.60	1.41	0.84	4.84	0.46	1.92	0.030	0.85	4.87	0.46	1.92	0.080	0.81	4.64	-0.04	2.24	0.028	-0.02		
10	1	1.38	0.84	4.82	0.24	1.95	0.038	0.82	4.69	0.22	1.95	0.073	0.83	4.75	0.07	2.22	0.31	-0.04			
	2	1.36	0.84	4.85	-0.04	1.95	0.048	0.79	4.56	-0.06	1.96	0.067	0.84	4.82	0.13	2.19	0.041	-0.06			
	3	1.43	0.86	4.94	0.61	1.75	0.062	0.86	4.94	1.60	1.75	0.093	0.79	4.52	0.08	2.09	0.047	-0.03			
	4	1.44	0.88	5.05	0.46	1.71	0.064	0.85	4.86	0.47	1.91	0.075	0.77	4.45	0.03	2.04	0.049	-0.05			
	5	1.43	0.84	4.82	0.74	1.72	0.079	0.88	5.04	0.72	1.71	0.114	0.77	4.42	0.37	2.06	0.072	0.00			
	6	1.40	0.85	4.86	0.50	1.76	0.063	0.84	4.81	0.50	1.76	0.103	0.79	4.53	0.38	2.05	0.066	-0.03			
	7																				

Table 5-2 (continued)

Run	Wave No.	T _{meas} (sec)	Linear Wave Theory				Stream Function Wave Theory				Measured Kinematics				U _{*k}				
			R (x10 ⁻⁵)	K	C _d	C _m	RMS err	R (x10 ⁻⁵)	K	C _d	C _m	RMS err	R (x10 ⁻⁵)	K	C _d	C _m	RMS err		
29	1	4.60	3.56	2.23	12.82	0.53	1.74	0.089	2.10	12.11	0.57	1.74	0.205	2.04	11.73	0.58	1.95	0.151	-0.19
	2	3.57	2.23	12.79	0.31	1.80	0.065	2.12	12.20	0.35	1.81	0.175	2.04	11.76	0.45	2.00	0.101	-0.18	
	3	3.65	2.16	12.42	0.33	1.70	0.076	2.28	13.11	0.36	1.67	0.219	2.04	11.75	0.35	1.94	0.115	-0.03	
	4	3.51	2.13	12.24	0.48	1.76	0.111	2.14	12.30	0.54	1.74	0.236	2.04	11.73	0.35	1.98	0.115	-0.10	
	5	3.48	2.11	12.14	0.73	1.66	0.124	2.13	12.21	0.82	1.63	0.244	2.08	11.94	0.48	1.94	0.111	-0.10	
	6	3.45	2.18	12.52	0.77	1.56	0.160	2.02	11.59	0.90	1.53	0.244	2.15	12.36	0.50	1.90	0.116	-0.20	
	7	3.49	2.14	12.30	0.70	1.66	0.098	2.11	12.11	1.78	1.62	0.236	1.99	11.43	0.66	1.93	0.089	-0.14	
12	1	4.60	4.30	2.84	16.32	0.36	1.78	0.106	2.39	13.71	0.46	1.77	0.249	2.60	14.94	0.44	1.98	0.147	-0.43
	2	4.22	2.77	15.92	0.13	1.83	0.158	2.36	13.58	0.17	1.91	0.159	2.65	15.22	0.50	1.94	0.093	-0.40	
	3	4.29	2.67	15.34	0.10	1.74	0.172	2.55	14.63	0.15	1.82	0.162	2.40	13.76	0.34	1.93	0.105	-0.21	
	4	4.25	2.73	15.67	-0.12	1.64	0.210	2.45	14.07	-0.18	1.73	0.176	2.30	13.24	0.40	1.82	0.143	-0.31	
	5	4.06	2.60	14.95	0.24	1.83	0.142	2.34	13.43	0.27	1.89	0.171	2.35	13.48	0.49	1.88	0.145	-0.30	
	6	3.96	2.63	15.10	0.14	1.77	0.228	2.20	12.63	0.16	1.87	0.168	2.36	13.55	0.60	1.84	0.134	-0.40	
	7	4.14	2.56	14.70	0.06	1.78	0.146	2.48	14.24	0.04	1.84	0.161	2.37	13.62	0.62	1.84	0.143	-0.18	
13	1	5.30	0.70	0.42	2.81	-0.32	1.92	0.099	0.44	2.90	-0.33	1.94	0.054	0.44	2.90	1.04	2.42	0.064	0.01
	2	0.72	0.43	2.86	0.23	1.87	0.083	0.44	2.90	0.23	1.89	0.049	0.41	2.74	0.89	2.40	0.067	-0.01	
	3	0.74	0.45	2.95	-0.52	1.79	0.069	0.46	3.06	-0.51	1.80	0.030	0.40	2.65	-0.12	2.39	0.041	0.00	
	4	0.77	0.47	3.08	-0.73	1.64	0.110	0.48	3.20	-0.74	1.66	0.057	0.38	2.50	-0.43	2.29	0.071	0.01	
	5	0.77	0.47	3.12	0.03	1.64	0.089	0.49	3.24	0.04	1.65	0.044	0.38	2.50	-0.87	2.28	0.051	0.02	
	6	0.80	0.48	3.20	0.02	1.61	0.136	0.50	3.34	0.06	1.62	0.104	0.40	2.63	-0.70	2.34	0.076	0.01	
	7	0.82	0.49	3.26	-0.10	1.63	0.101	0.50	3.33	-0.10	1.64	0.079	0.36	2.38	-0.23	2.38	0.093	-0.01	
14	1	5.30	1.17	0.70	4.62	0.18	1.86	0.122	0.74	4.89	0.17	1.89	0.048	0.77	5.08	0.68	2.10	0.061	0.00
	2	1.18	0.71	4.69	0.38	1.83	0.112	0.75	4.84	0.38	1.86	0.034	0.77	5.11	0.61	2.10	0.056	0.00	
	3	1.18	0.72	4.73	0.43	1.86	0.122	0.76	5.00	0.45	1.89	0.058	0.81	5.35	0.43	2.12	0.062	0.01	
	4	1.23	0.75	4.95	0.40	1.78	0.120	0.79	5.24	0.42	1.81	0.060	0.78	5.15	0.13	2.12	0.055	0.02	
	5	1.25	0.76	5.04	-0.08	1.76	0.140	0.80	5.34	-0.05	1.79	0.076	0.85	5.60	-0.27	2.13	0.046	0.02	
	6	1.26	0.79	5.21	0.21	1.66	0.105	0.83	5.52	0.22	1.68	0.053	0.74	4.92	-0.10	2.02	0.069	0.04	
	7	1.26	0.76	5.00	0.39	1.74	0.152	0.80	5.30	0.41	1.78	0.088	0.79	5.23	-0.15	2.16	0.074	0.00	
15	1	5.30	2.54	1.54	10.19	0.06	1.67	0.219	1.65	10.93	0.09	1.79	0.081	1.53	10.13	0.54	2.03	0.094	-0.03
	2	2.48	1.50	9.95	0.28	1.64	0.209	1.60	10.62	0.27	1.77	0.075	1.56	10.34	0.37	1.98	0.076	-0.03	
	3	2.49	1.52	10.03	0.28	1.62	0.208	1.67	11.03	0.31	1.74	0.096	1.62	10.70	0.16	1.98	0.072	0.03	
	4	2.58	1.54	10.20	0.28	1.56	0.228	1.69	11.21	0.32	1.68	0.096	1.58	10.45	0.17	1.99	0.054	0.00	
	5	2.65	1.60	10.59	0.55	1.45	0.193	1.77	11.68	0.59	1.55	0.096	1.53	10.15	0.24	1.95	0.089	0.02	
	6	2.62	1.58	10.45	0.35	1.50	0.239	1.71	11.35	0.40	1.65	0.104	1.56	10.35	0.12	1.95	0.077	-0.02	
	7	2.62	1.59	10.51	0.48	1.49	0.227	1.75	11.59	0.52	1.62	0.112	1.56	10.31	0.17	2.00	0.084	0.03	

Table 5-2 (continued)

Run	Wave No.	T_{meas} (sec)	H_{meas} (ft)	Linear Wave Theory						Stream Function Wave Theory						Measured Kinematics					
				R (x10 ⁻⁵)	K	C_d	C_m	RMS err	R (x10 ⁻⁵)	K	C_d	C_m	RMS err	R (x10 ⁻⁵)	K	C_d	C_m	RMS err	\bar{u}^{**}		
16	1	5.30	3.47	2.23	14.73	0.25	1.47	0.222	2.16	14.29	0.28	1.64	0.061	2.04	13.48	0.50	1.77	0.072	-0.20		
	2	3.38	2.08	13.78	0.22	1.62	0.249	2.18	14.46	0.25	1.84	0.097	2.10	13.93	0.41	1.96	0.058	-0.09			
	3	3.40	2.14	14.14	0.25	1.59	0.283	2.16	14.29	0.27	1.84	0.117	2.12	14.07	0.31	2.00	0.064	-0.14			
	4	3.45	2.14	14.20	0.36	1.53	0.281	2.22	14.69	0.40	1.78	0.124	2.18	14.42	0.31	1.98	0.084	-0.11			
	5	3.46	2.23	14.74	0.25	1.48	0.284	2.14	14.18	0.27	1.72	0.125	2.18	14.42	0.35	1.90	0.073	-0.21			
	6	3.44	2.17	14.36	0.20	1.53	0.281	2.17	14.38	0.20	1.75	0.103	2.12	14.03	0.31	1.90	0.053	-0.16			
	7	3.32	2.12	14.01	0.30	1.53	0.274	2.08	13.78	0.32	1.77	0.123	2.01	13.30	0.31	1.88	0.081	-0.18			
17	1	5.30	3.75	2.42	16.00	0.29	1.49	0.252	2.33	15.42	0.32	1.72	0.066	2.17	14.34	0.54	1.86	0.069	-0.23		
	2	3.62	2.20	14.55	0.25	1.53	0.276	2.37	15.70	0.28	1.81	0.120	2.31	15.32	0.38	1.90	0.066	-0.06			
	3	3.56	2.25	14.88	0.26	1.62	0.287	2.25	14.87	0.22	1.88	0.144	2.38	15.77	0.39	1.95	0.086	-0.17			
	4	3.71	2.32	15.36	0.31	1.44	0.308	2.37	15.70	0.33	1.71	0.128	2.41	15.93	0.34	1.86	0.073	-0.14			
	5	3.84	2.47	16.35	0.31	1.36	0.325	2.38	15.77	0.36	1.67	0.142	2.21	14.62	0.45	1.91	0.084	-0.24			
	6	3.69	2.28	15.10	0.21	1.46	0.280	2.39	15.81	0.20	1.71	0.127	2.27	15.00	0.37	1.83	0.070	-0.10			
	7	3.46	2.23	14.79	0.37	1.54	0.298	2.13	14.13	0.44	1.84	0.132	2.25	14.88	0.37	1.87	0.064	-0.23			
30	1	6.00	2.02	1.25	9.34	0.66	1.68	0.175	1.33	10.00	0.69	1.75	0.060	1.46	10.93	0.56	1.89	0.086	-0.04		
	2	1.89	1.15	8.64	0.47	1.90	0.189	1.27	9.50	0.47	1.99	0.056	1.34	10.01	0.56	1.97	0.058	-0.01			
	3	1.80	1.10	8.26	0.86	1.99	0.163	1.22	9.15	0.88	2.04	0.085	1.50	11.26	0.47	1.99	0.054	0.02			
	4	1.84	1.14	8.53	0.13	1.99	0.141	1.26	9.45	0.11	2.02	0.067	1.36	10.17	0.28	1.92	0.049	0.04			
	5	1.83	1.12	8.38	0.35	2.08	0.134	1.21	9.10	0.33	2.12	0.065	1.42	10.65	0.36	1.99	0.065	-0.02			
	6	1.83	1.17	8.77	0.47	1.95	0.177	1.31	9.78	0.43	2.02	0.082	1.48	11.06	0.24	2.02	0.093	0.01			
	7	2.00	1.22	9.16	0.34	1.88	0.183	1.33	9.99	0.32	1.95	0.095	1.40	10.52	0.10	2.02	0.097	-0.02			
31	1	6.00	2.37	1.47	11.05	0.37	1.80	0.196	1.58	11.84	0.39	1.90	0.048	1.71	12.78	0.58	1.92	0.061	-0.06		
	2	2.35	1.44	10.80	0.58	1.75	0.199	1.58	11.84	0.61	1.85	0.068	1.63	12.19	0.59	1.88	0.052	-0.03			
	3	2.21	1.36	10.20	0.58	1.90	0.208	1.53	11.47	0.57	2.02	0.095	1.67	12.51	0.53	1.93	0.064	0.03			
	4	2.22	1.38	10.31	0.14	1.91	0.234	1.55	11.58	0.12	2.05	0.089	1.76	13.21	0.30	1.92	0.043	0.04			
	5	2.25	1.37	10.23	0.45	1.86	0.226	1.54	11.53	0.46	2.00	0.069	1.72	12.89	0.34	1.92	0.044	0.01			
	6	2.23	1.35	10.13	0.55	1.92	0.219	1.52	11.40	0.55	2.05	0.080	1.69	12.63	0.35	1.95	0.065	0.00			
	7	2.31	1.42	10.67	0.44	1.96	0.206	1.55	11.58	0.44	2.07	0.082	1.61	12.03	0.11	2.03	0.088	-0.04			
20	1	6.00	3.00	1.93	14.50	0.39	1.53	0.227	1.97	14.73	0.39	1.68	0.084	2.07	15.48	0.44	1.72	0.080	-0.16		
	2	2.78	1.75	13.11	0.41	1.69	0.252	1.85	13.86	0.47	1.86	0.102	2.09	15.63	0.43	1.79	0.048	-0.09			
	3	2.78	1.72	12.89	0.30	1.72	0.261	1.88	14.09	0.25	1.88	0.130	2.09	14.83	0.46	1.78	0.072	-0.05			
	4	2.85	1.75	13.12	0.28	1.60	0.284	1.95	14.60	0.26	1.81	0.130	2.09	15.65	0.38	1.76	0.063	-0.04			
	5	2.81	1.82	13.65	0.34	1.62	0.309	1.83	13.68	0.39	1.85	0.114	2.12	15.88	0.36	1.79	0.046	-0.16			
	6	2.79	1.78	13.35	0.36	1.66	0.283	1.83	13.73	0.40	1.87	0.128	2.12	14.20	0.35	1.80	0.066	-0.13			
	7	2.69	1.76	13.15	0.33	1.82	0.237	1.73	12.95	0.34	1.98	0.114	1.84	13.77	0.19	1.80	0.094	-0.17			

Table 5-2 (continued)

Run No.	Wave No.	H_{meas} (ft)	T_{meas} (sec)	Linear Wave Theory				Stream Function Wave Theory				Measured Kinematics							
				R	K	C_d	C_m	RMS err	R	K	C_d	C_m	RMS err	R	K	C_d	C_m	RMS err	\bar{u}^{**}
				(x10 ⁻⁵)	(x10 ⁻⁵)				(x10 ⁻⁵)				(x10 ⁻⁵)						
21	1	4.20	4.84	3.10	16.41	0.55	1.54	0.161	2.59	13.70	0.68	1.72	0.104	2.57	13.47	0.57	1.83	0.097	-0.43
	2	4.92	3.12	16.51	0.72	1.40	0.151	2.66	14.06	0.92	1.54	0.142	2.75	14.40	0.61	1.83	0.090	-0.39	
	3	4.93	3.02	15.97	0.64	1.45	0.169	2.78	14.68	0.76	1.62	0.148	2.56	13.43	0.58	1.81	0.103	-0.25	
	4	4.93	3.10	16.39	0.53	1.48	0.160	2.70	14.27	0.65	1.64	0.118	2.66	13.93	0.45	1.78	0.076	-0.35	
	5	4.91	3.06	16.16	0.62	1.50	0.153	2.72	14.36	0.74	1.65	0.146	2.70	14.18	0.50	1.82	0.082	-0.31	
	6	4.92	3.13	16.57	0.59	1.51	0.157	2.65	13.99	0.71	1.67	0.152	2.80	14.71	0.45	1.85	0.108	-0.41	
	7	4.88	3.10	16.37	0.62	1.55	0.161	2.64	13.95	0.76	1.71	0.147	2.82	14.82	0.53	1.86	0.098	-0.39	
22	1	5.30	3.71	2.39	15.73	0.29	1.43	0.250	2.32	15.29	0.36	1.63	0.069	2.37	15.66	0.48	1.70	0.063	-0.22
	2	3.75	2.38	15.67	0.27	1.45	0.227	2.37	15.64	0.31	1.62	0.052	2.36	15.64	0.46	1.69	0.064	-0.18	
	3	3.61	2.17	14.32	0.22	1.52	0.265	2.41	15.86	0.23	1.73	0.113	2.53	16.73	0.33	1.74	0.069	-0.02	
	4	3.56	2.28	15.02	0.33	1.63	0.275	2.23	14.68	0.31	1.85	0.131	2.59	17.13	0.37	1.81	0.111	-0.20	
	5	3.74	2.31	15.20	0.21	1.44	0.304	2.44	16.07	0.22	1.69	0.125	2.54	16.80	0.26	1.76	0.080	-0.09	
	6	3.82	2.38	15.72	0.26	1.41	0.316	2.46	16.19	0.27	1.68	0.126	2.44	16.17	0.39	1.79	0.086	-0.13	
	7	3.78	2.30	15.16	0.17	1.41	0.311	2.50	16.45	0.16	1.66	0.142	2.36	15.60	0.30	1.75	0.090	-0.05	
23	1	4.60	4.34	2.72	15.65	0.43	1.68	0.111	2.56	14.69	0.49	1.72	0.201	2.38	13.69	0.58	1.91	0.121	-0.24
	2	4.21	2.60	14.94	0.07	1.76	0.142	2.52	14.47	0.05	1.82	0.173	2.39	13.74	0.47	1.87	0.116	-0.18	
	3	4.21	2.55	14.62	0.08	1.65	0.210	2.57	14.79	0.08	1.79	0.112	2.42	13.93	0.36	1.85	0.139	-0.11	
	4	4.12	2.51	14.45	-0.00	1.80	0.123	2.50	14.38	-0.03	1.85	0.177	2.60	14.91	0.40	1.89	0.107	-0.13	
	5	4.01	2.52	14.45	0.14	1.82	0.180	2.37	13.63	0.13	1.91	0.168	2.61	15.02	0.42	1.89	0.133	-0.21	
	6	4.11	2.62	15.08	0.21	1.77	0.161	2.38	13.67	0.20	1.86	0.139	2.72	15.64	0.56	1.89	0.098	-0.29	
	7	4.09	2.51	14.43	-0.18	1.66	0.182	2.47	14.18	-0.27	1.73	0.171	2.31	13.26	0.51	1.78	0.105	-0.15	
24	1	3.70	4.40	2.69	12.43	0.13	1.66	0.164	2.31	10.69	0.16	1.80	0.095	2.28	10.54	0.60	1.89	0.110	-0.29
	2	4.38	2.66	12.27	0.01	1.69	0.203	2.32	10.74	0.00	1.87	0.088	2.34	10.79	0.57	1.94	0.110	-0.26	
	3	4.45	2.57	11.89	0.02	1.57	0.197	2.48	11.47	-0.00	1.74	0.091	2.38	10.98	0.41	1.80	0.141	-0.10	
	4	4.42	2.64	12.22	0.14	1.69	0.205	2.38	10.99	0.16	1.88	0.093	2.34	10.82	0.33	1.97	0.125	-0.21	
	5	4.44	2.69	12.42	0.14	1.65	0.191	2.35	10.85	0.15	1.83	0.084	2.45	11.34	0.37	1.89	0.136	-0.26	
	6	4.37	2.60	12.01	0.09	1.61	0.193	2.37	10.94	0.11	1.77	0.089	2.50	11.54	0.27	1.84	0.120	-0.19	
	7	*																	
25	1	2.50	3.32	1.74	5.42	0.44	1.85	0.063	1.62	5.04	0.48	1.94	0.050	1.62	5.07	0.14	2.09	0.048	-0.21
	2	3.30	1.77	5.53	0.45	1.86	0.063	1.65	5.16	0.50	1.96	0.048	1.78	5.56	0.13	2.10	0.049	-0.27	
	3	3.36	1.78	5.55	0.42	1.81	0.071	1.65	5.16	0.46	1.91	0.050	1.65	5.15	0.15	2.08	0.052	-0.23	
	4	3.45	1.85	5.76	0.59	1.77	0.068	1.71	5.33	0.66	1.87	0.050	1.60	5.00	0.20	2.09	0.052	-0.27	
	5	3.39	1.77	5.52	0.71	1.78	0.068	1.64	5.12	0.79	1.88	0.051	1.62	5.06	0.05	2.08	0.049	-0.21	
	6	3.42	1.77	5.53	0.53	1.77	0.078	1.64	5.11	0.59	1.87	0.053	1.62	5.06	-0.07	2.07	0.056	-0.19	
	7	3.39	1.70	5.31	0.58	1.79	0.070	1.57	4.71	0.64	1.89	0.062	1.61	5.02	-0.16	2.09	0.057	-0.12	

Table 5-2 (continued)

Run	Wave No.	T _{meas} (sec)	H _{meas} (ft)	Linear Wave Theory				Stream Function Wave Theory				Measured Kinematics				Random Waves				
				R (x10 ⁻⁵)	K (x10 ⁻⁵)	C _d	C _m	RMS err	R (x10 ⁻⁵)	K (x10 ⁻⁵)	C _d	C _m	RMS err	R (x10 ⁻⁵)	K (x10 ⁻⁵)	C _d	C _m	RMS err	\bar{u}^{**}	
26	1	6.00	3.01	1.92	14.36	0.57	1.54	0.201	1.99	14.91	0.66	1.64	0.055	1.96	14.66	0.46	1.76	0.109	-0.13	
	2		2.86	1.78	13.31	0.49	1.60	0.225	1.93	14.47	0.51	1.73	0.091	1.90	14.26	0.47	1.73	0.084	-0.07	
	3		2.78	1.69	12.68	0.53	1.62	1.255	1.92	14.36	0.52	1.79	0.131	2.16	16.19	0.41	1.76	0.083	-0.01	
	4		2.80	1.69	12.69	0.28	1.69	0.279	1.94	14.51	0.23	1.87	0.128	2.09	15.67	0.31	1.80	0.072	0.00	
	5		2.68	1.68	12.62	0.26	1.76	0.288	1.78	13.36	0.20	1.96	0.147	2.06	15.43	0.29	1.80	0.077	-0.09	
	6		2.67	1.67	12.50	0.24	1.72	0.267	1.8	13.35	0.22	1.90	0.122	2.12	15.88	0.19	1.74	0.071	-0.08	
	7		2.70	1.75	13.12	0.29	1.85	0.256	1.75	13.08	0.30	2.03	0.108	2.04	15.28	0.16	1.87	0.072	-0.16	
32	1	4.68	1.95	1.40	8.18	0.10	1.64	0.262	1.47	8.59	0.01	1.71	0.235	1.43	8.36	0.36	1.84	0.084	0.34	B 1 W 0 a c v k e
	2	3.78	3.50	2.21	10.44	1.24	1.65	0.194	1.94	9.16	1.34	1.74	0.206	2.49	11.75	0.83	2.04	0.196	0.31	7 6
	3	2.52	2.97	1.65	5.20	-1.72	1.16	0.313	1.57	4.94	-1.88	1.22	0.295	1.60	5.04	0.51	1.76	0.196	-0.31	9 2
	4	4.74	2.99	1.79	10.62	1.69	0.26	0.473	1.87	11.05	1.59	0.01	0.522	1.66	9.85	0.71	1.95	0.113	-0.05	13 2
	5	2.52	2.89	2.62	3.43	-0.55	0.83	0.201	2.50	3.28	-0.60	0.86	0.183	2.64	3.46	0.24	0.89	0.118	-0.41	19 6
	1	4.26	1.96	1.24	6.62	-0.22	1.62	0.225	1.30	6.90	-0.31	1.64	0.221	1.34	7.14	0.03	2.16	0.218	0.14	7 4
	2	4.08	2.34	1.49	7.61	-0.02	1.79	1.37	6.99	-0.04	1.87	0.117	1.27	6.45	0.39	2.23	0.093	-0.20	11 2	
	3	3.84	2.64	1.66	7.98	-0.10	1.57	0.248	1.72	8.24	-0.08	1.69	0.186	1.81	8.69	0.73	2.18	0.169	0.22	15 3
34	4	3.66	2.89	1.77	8.07	0.31	1.74	0.202	1.61	7.36	0.33	1.85	0.136	1.50	6.88	0.60	2.13	0.196	-0.20	15 5
	5	4.98	1.61	1.08	6.72	-1.17	1.08	0.619	1.14	7.10	-1.22	1.25	0.541	1.39	8.62	0.02	1.73	0.375	0.17	19 3

** \bar{u} is the average value of the measured horizontal velocity during a particular wave. Note that it is mostly negative, indicating a flow from the beach toward the wave board.

Table 5-3 Summary of Maximum and RMS Errors for 26 periodic waves and 10 individual random waves
 (See Table 5-4 for F_{\max} measured, Tables 5-1 and 5-2 for Reynolds numbers)

Run No.	Wave No.	T (sec)	H (ft)	β	α	Measured Kinematics						Linear Wave Theory						Stream Function Theory								
						LSQ			WPTI			U-Tube			LSQ			WPTI			U-Tube					
						K	RMS (lbs)	MAX (lbs)	RMS (lbs)	MAX (lbs)	RMS (lbs)	K	RMS (lbs)	MAX (lbs)	RMS (lbs)	MAX (lbs)	K	RMS (lbs)	MAX (lbs)	RMS (lbs)	MAX (lbs)	K	RMS (lbs)	MAX (lbs)		
1	1	1.18	1.06	1.3	0.32	0.85	2.21	3.17	1.04	1.63	1.3	0.36	0.69	1.74	2.60	0.81	1.35	1.3	0.37	0.72	1.74	2.62	0.82	0.38		
	2	1.04	1.01	1.2	0.51	0.91	1.79	2.63	0.74	1.35	1.1	0.14	0.25	1.40	2.07	0.37	0.62	1.1	0.14	0.25	1.40	2.07	0.37	0.62		
	3	1.04	0.95	1.2	0.42	0.71	1.80	2.75	0.70	1.31	1.1	0.10	0.21	0.45	2.12	0.17	0.35	1.1	0.10	0.23	1.45	2.12	0.17	0.36		
	4	2.0	1.06	4.0032	1.05	1.1	0.44	0.76	1.82	0.73	1.41	1.2	0.14	0.29	0.61	2.11	0.22	0.37	1.2	0.14	0.31	1.42	2.09	0.22	0.38	
	5	1.06	1.00	1.2	0.45	0.73	1.81	2.72	0.73	1.27	1.1	0.10	0.16	1.41	2.09	0.14	0.26	1.1	0.10	0.18	1.41	2.08	0.14	0.26		
	6	1.06	0.94	1.2	0.45	0.69	1.84	2.77	0.75	1.29	1.1	0.10	0.24	1.43	2.12	0.14	0.31	1.1	0.10	0.25	1.43	2.12	0.14	0.31		
	7	1.05	1.04	1.2	0.45	0.69	1.84	2.77	0.75	1.29	1.1	0.10	0.22	1.45	2.18	0.20	0.40	1.1	0.10	0.23	1.45	2.18	0.20	0.41		
2	1	0.36	1.10	0.4	0.17	0.28	0.75	1.12	0.41	0.66	0.4	0.00	0.07	0.51	0.79	0.00	0.13	0.4	0.00	0.07	0.51	0.79	0.00	0.13		
	2	0.36	1.02	0.4	0.17	0.29	0.70	1.04	0.37	0.62	0.4	0.00	0.05	0.48	0.71	0.00	0.09	0.4	0.00	0.05	0.48	0.71	0.00	0.09		
	3	0.35	1.47	0.3	0.17	0.33	0.69	1.05	0.36	0.64	0.4	0.00	0.02	0.50	0.70	0.00	0.05	0.4	0.00	0.02	0.50	0.70	0.00	0.06		
	4	2.0	0.36	4.0032	1.10	0.4	0.17	0.29	0.73	1.09	0.40	0.66	0.4	0.00	0.09	0.50	0.74	0.10	0.21	0.4	0.00	0.09	0.50	0.75	0.10	0.21
	5	0.35	1.09	0.5	0.17	0.29	0.71	1.05	0.37	0.61	0.4	0.00	0.02	0.49	0.72	0.00	0.07	0.4	0.00	0.02	0.49	0.72	0.00	0.07		
	6	0.35	1.27	0.4	0.17	0.26	0.70	1.03	0.36	0.59	0.4	0.00	0.03	0.49	0.72	0.00	0.07	0.4	0.00	0.03	0.49	0.72	0.00	0.07		
	7	0.35	1.02	0.4	0.17	0.28	0.71	1.05	0.37	0.62	0.4	0.00	0.02	0.49	0.72	0.00	0.07	0.4	0.00	0.02	0.49	0.72	0.00	0.07		
3	1	1.04	0.91	1.7	0.24	0.41	1.89	2.79	0.76	1.26	1.6	0.14	0.29	1.48	2.33	0.20	0.42	1.6	0.14	0.29	1.49	2.34	0.22	0.44		
	2	0.99	1.02	1.6	0.24	0.38	1.69	2.45	0.59	0.92	1.6	0.10	0.16	1.48	2.12	0.36	0.60	1.6	0.00	0.14	1.49	2.12	0.37	0.60		
	3	1.01	0.93	1.6	0.28	0.45	1.75	2.67	0.63	1.15	1.6	0.00	0.12	1.44	2.11	0.17	0.27	1.6	0.10	0.15	1.45	2.12	0.17	0.28		
	4	2.5	1.01	32025	0.91	1.7	0.28	0.48	1.75	2.52	0.68	1.12	1.6	0.10	0.18	1.40	2.09	0.14	0.24	1.6	0.10	0.16	1.40	2.10	0.14	0.27
	5	1.00	0.92	1.6	0.28	0.42	1.77	2.59	0.70	1.08	1.6	0.10	0.16	1.54	2.16	0.42	0.70	1.6	0.10	0.14	1.54	2.16	0.42	0.70		
	6	0.99	1.04	1.6	0.30	0.51	1.77	2.56	0.73	1.17	1.6	0.00	0.11	1.46	2.12	0.20	0.31	1.6	0.00	0.10	1.47	2.13	0.20	0.32		
	7	1.01	0.96	1.6	0.32	0.56	1.81	2.56	0.78	1.27	1.6	0.00	0.13	1.46	2.13	0.20	0.29	1.6	0.00	0.10	1.46	2.14	0.20	0.31		
4	1	1.88	0.88	2.8	0.17	0.41	4.26	3.18	1.09	1.73	2.9	0.24	0.49	2.58	3.48	0.59	1.20	2.8	0.17	0.38	2.61	3.55	0.55	1.16		
	2	1.88	0.91	2.7	0.10	0.22	3.08	4.27	0.95	1.27	2.8	0.20	0.45	2.51	3.48	0.41	0.77	2.8	0.14	0.29	2.55	3.55	0.37	0.75		
	3	1.87	0.94	2.7	0.20	0.39	3.29	4.68	1.20	1.67	2.9	0.22	0.41	2.66	3.94	0.36	0.70	2.8	0.26	0.54	2.70	4.02	0.41	0.79		
	4	2.5	1.84	32025	0.91	3.0	0.17	0.42	3.31	4.41	1.22	1.63	2.9	0.22	0.37	2.61	3.78	0.30	0.62	2.8	0.24	0.43	2.66	3.88	0.36	0.78
	5	1.88	0.85	2.9	0.10	0.18	3.30	4.46	1.27	1.76	2.8	0.17	0.40	2.67	3.68	0.61	1.10	2.8	0.14	0.27	2.70	3.75	0.59	1.03		
	6	1.89	0.88	2.7	0.10	0.21	3.24	4.47	1.29	1.70	2.9	0.20	0.42	2.63	3.65	0.59	1.17	2.8	0.14	0.31	2.65	3.72	0.57	1.08		
	7	1.89	0.91	2.7	0.14	0.33	3.31	4.52	1.40	2.01	2.8	0.22	0.50	2.57	3.67	0.41	0.81	2.8	0.17	0.40	2.61	3.74	0.38	0.77		
5	1	3.24	0.85	4.8	0.95	2.01	5.56	7.48	2.19	3.79	5.3	0.82	1.63	4.65	6.46	1.79	3.14	5.0	0.68	1.45	4.73	6.29	0.68	1.45		
	2	3.26	0.88	5.0	1.08	2.24	5.77	7.86	2.37	4.09	5.4	0.95	1.93	4.95	6.99	1.99	3.82	5.1	0.94	1.90	5.04	6.71	1.79	3.73		
	3	3.37	0.85	4.9	1.27	2.61	5.67	8.18	2.29	4.05	5.6	1.13	2.32	4.69	6.93	2.18	4.00	5.2	1.04	2.25	4.76	6.46	1.77	3.89		
	4	3.12	32025	0.91	5.3	1.33	2.55	5.27	8.21	2.16	4.22	5.0	1.32	2.83	3.59	6.66	1.90	3.68	4.7	1.03	1.99	3.81	5.65	1.69	3.64	
	5	3.34	0.86	4.6	1.44	2.91	5.44	8.09	2.20	4.35	5.5	1.29	2.44	4.42	7.13	2.22	3.63	5.1	1.03	2.08	4.47	6.61	1.67	3.54		
	6	3.37	0.89	4.7	1.31	2.69	5.57	8.18	2.20	4.52	5.4	1.21	2.33	3.64	5.65	1.75	3.44	5.0	0.95	1.67	3.81	5.84	1.49	2.41		
	7	3.32	0.84	4.8	1.26	2.52	5.61	8.09	2.43	4.82	5.3	1.20	2.31	3.62	5.73	1.65	3.40	4.9	0.93	1.75	3.80	5.91	1.10	2.17		

NOTE: LSQ = Least Squares
 WPTI = Wave Project II (Hudspeth, et al., 1974)
 U-Tube (Sapphaya and Isaacson, 1981)

Table 5-3 (continued)

Run No.	Wave No.	T (sec)	H (ft)	β	α	Measured Kinematics						Linear Wave Theory						Stream Function Theory								
						WPII			U-Tube			LSQ			WPII			U-Tube			LSQ					
						K	RMS	MAX	(lbs)	(lbs)	(lbs)	K	RMS	MAX	(lbs)	(lbs)	(lbs)	K	RMS	MAX	(lbs)	(lbs)	(lbs)			
6	1	0.93	0.62	2.5	0.20	0.37	1.26	1.78	0.44	0.76	2.4	0.14	0.25	1.09	1.55	0.20	0.36	2.5	0.00	0.18	1.09	1.54	0.14	0.23		
	2	0.94	0.67	2.8	0.30	0.48	1.41	2.75	0.55	1.16	2.8	0.10	0.16	1.19	1.72	0.28	0.39	3.0	0.10	0.18	1.20	1.79	0.30	0.51		
	3	0.95	0.69	2.4	0.20	0.31	1.24	1.77	0.59	0.65	2.6	0.14	0.27	1.12	1.56	0.22	0.41	2.5	0.00	0.12	1.12	0.51	0.20	0.35		
	4	3.7	0.94	21639	0.71	2.5	0.00	0.11	1.23	1.76	0.36	0.48	2.5	0.24	0.43	1.22	1.92	0.48	0.83	2.6	0.14	0.28	1.21	1.82	0.42	0.72
	5	0.94	0.66	6.6	2.5	0.10	0.13	1.29	1.82	0.41	0.60	2.5	0.30	0.53	1.24	1.97	0.41	0.69	2.6	0.20	0.39	1.22	1.83	0.36	0.62	
	6	0.95	0.63	2.5	0.00	0.08	1.26	1.84	0.35	0.50	2.5	0.28	0.49	1.20	1.97	0.42	0.78	2.6	0.17	0.32	1.19	1.87	0.36	0.62		
	7	0.95	0.69	2.4	0.00	0.13	1.19	1.75	0.28	0.42	2.5	0.26	0.38	1.07	1.76	0.26	0.45	2.5	0.14	0.25	1.06	1.70	0.17	0.32		
(28)	1	2.39	0.65	6.3	0.36	0.71	3.35	4.43	1.17	2.08	6.6	1.00	1.89	2.61	3.77	1.00	2.03	6.4	0.47	0.77	2.53	3.48	0.51	1.07		
	2	2.44	0.64	6.3	0.37	0.75	3.50	4.97	1.33	2.35	6.6	1.14	2.11	3.17	5.07	1.36	2.26	6.5	0.47	0.93	3.06	4.62	0.87	1.84		
	3	2.45	0.62	6.3	0.58	1.14	3.26	5.01	1.15	2.44	6.8	1.42	2.58	2.92	4.74	1.48	2.25	6.5	0.77	1.40	2.76	4.33	0.85	1.77		
	4	3.7	0.67	6.2	0.71	1.25	3.36	5.59	1.26	2.88	6.7	1.60	3.05	2.62	4.72	1.66	3.15	6.4	0.94	1.87	2.41	4.28	1.01	1.97		
	5	2.76	0.65	6.3	0.69	1.40	3.32	5.02	1.18	2.75	7.3	1.41	2.51	2.83	5.11	1.79	2.90	6.6	0.84	1.69	2.63	5.32	1.20	2.10		
	6	2.48	0.67	6.4	0.88	1.64	3.17	5.63	1.20	2.87	6.6	1.53	2.47	2.89	5.53	1.65	2.68	6.6	1.06	2.78	5.15	1.18	2.50	3.29		
	7	2.67	0.72	6.2	0.80	1.40	3.13	5.03	1.25	3.07	7.1	1.54	2.47	2.89	5.53	1.65	2.78	6.6	1.06	2.78	5.15	1.18	2.50	3.29		
9	1	4.33	0.59	10.0	1.87	3.47	4.83	8.42	2.23	4.35	12.3	2.93	4.80	6.68	11.92	3.42	7.42	10.3	1.18	2.30	5.65	10.29	1.69	4.07		
	2	4.42	0.54	10.3	1.82	3.87	4.56	9.97	1.97	3.90	12.4	3.06	5.00	7.09	12.63	3.89	8.17	10.7	1.40	2.54	5.92	10.91	2.08	4.45		
	3	4.50	0.53	10.2	1.93	3.35	5.15	10.94	2.10	4.08	12.5	3.62	5.88	8.26	14.93	4.94	10.06	10.6	1.42	2.66	6.90	13.14	2.92	6.24		
	4	3.7	4.42	21639	0.51	11.1	1.65	3.16	5.88	11.89	2.30	5.45	11.8	3.74	6.43	8.73	15.72	3.78	5.92	11.6	1.39	3.23	7.45	13.59	3.47	6.77
	5	4.33	0.42	11.6	1.78	5.43	12.13	1.32	2.76	6.56	12.1	3.77	6.20	8.72	15.28	3.78	5.28	11.29	1.57	3.19	7.52	13.71	3.56	7.06		
	6	4.42	0.46	10.8	2.28	4.84	5.97	11.89	2.75	5.68	12.3	3.83	6.77	8.17	14.74	5.02	11.10	11.3	1.65	3.55	6.84	12.91	2.98	6.07		
	7	4.40	0.51	11.3	2.59	6.34	6.51	12.36	3.29	5.96	12.0	4.02	7.79	8.60	15.59	4.32	11.65	11.6	4.42	7.43	13.76	3.54	6.86	6.86		
10	1	0.60	0.56	2.4	0.28	0.51	0.72	1.25	1.37	0.78	2.1	0.14	0.21	0.58	0.87	0.22	0.43	2.5	0.10	0.16	0.57	0.85	0.20	0.43		
	2	0.62	2.6	0.22	0.45	0.72	1.21	0.35	0.65	2.2	0.14	0.23	0.53	0.87	0.17	0.30	2.7	0.14	0.22	0.53	0.90	0.17	0.27			
	3	0.60	0.62	2.7	0.14	0.29	0.69	1.09	0.30	0.57	2.1	0.10	0.22	0.52	0.84	0.36	0.55	2.8	0.14	0.29	0.52	0.81	0.36	0.55		
	4	4.6	0.60	17405	0.50	2.4	0.14	0.30	0.66	0.99	0.26	0.47	2.1	0.10	0.19	0.71	1.01	0.50	0.78	2.6	0.14	0.28	0.71	1.07	0.51	0.84
	5	0.66	0.61	2.4	0.14	0.29	0.58	0.86	0.20	0.39	2.2	0.10	0.13	0.66	1.06	0.62	0.99	2.5	0.14	0.20	0.67	1.08	0.62	1.08		
	6	0.67	0.66	2.3	0.20	0.39	0.58	0.89	0.22	0.39	2.4	0.10	0.21	0.36	0.60	0.98	0.35	0.58	2.4	0.10	0.23	0.36	0.60	0.35	0.61	
	7	0.69	0.55	2.0	0.17	0.34	0.51	0.83	0.17	0.40	2.3	0.10	0.21	0.30	0.60	0.97	0.35	0.58	2.1	0.14	0.28	0.32	0.49	0.57	1.01	

Table 5-3 (continued)

Run No.	Wave No.	H (ft)	T (sec)	β	Ω	Measured Kinematics						Linear Wave Theory						Stream Function Theory									
						LSQ			WPII			U-Tube			LSQ			WPII			U-Tube						
						K	RMS	MAX	(lbs)	(lbs)	(lbs)	RMS	MAX	(lbs)	RMS	MAX	(lbs)	RMS	MAX	(lbs)	RMS	MAX	(lbs)	RMS	MAX	(lbs)	
(29) 11	1	3.56	0.58	11.7	1.72	3.48	4.07	7.60	1.89	3.26	12.8	1.02	1.68	3.92	1.03	1.75	12.1	2.34	4.00	4.09	7.16	2.34	3.96	4.09	3.96		
	2	3.57	0.53	11.8	1.17	2.30	4.41	6.66	1.63	3.20	12.8	0.76	1.71	4.90	1.45	2.41	12.2	2.04	3.28	4.78	7.88	2.27	3.93	4.86	3.93		
	3	3.65	0.48	11.8	1.32	2.65	4.43	8.18	1.75	3.88	12.4	0.87	2.03	4.77	1.47	2.74	13.1	2.49	4.77	4.86	8.79	2.71	4.68	4.86	4.68		
	4	4.6	17405	0.48	11.7	1.28	2.66	4.60	8.01	1.82	3.81	12.2	1.22	2.65	4.08	6.65	1.27	2.64	12.3	2.62	5.58	4.25	6.83	2.62	5.51	5.58	
	5	3.48	0.50	11.9	1.20	2.93	3.94	6.98	1.45	3.07	12.1	1.35	3.44	2.93	5.32	1.64	2.96	12.2	2.65	5.61	3.37	6.43	2.89	5.57	5.57		
	6	3.45	0.50	12.4	1.21	2.69	3.91	6.34	1.38	2.57	12.5	1.67	3.22	2.68	5.90	2.13	3.92	11.6	2.56	5.34	2.99	5.54	3.05	5.66	5.66		
	7	3.49	0.56	11.4	0.95	2.28	3.46	5.47	1.25	2.42	12.3	1.05	2.69	2.94	4.51	1.32	2.20	12.1	2.53	4.98	3.35	5.59	2.74	4.87	4.87		
12	1	4.30	0.52	14.9	1.96	3.92	5.71	9.73	2.37	4.59	16.3	1.41	3.00	6.19	11.01	1.99	3.98	13.7	3.32	6.50	5.86	9.78	3.38	6.20	6.20		
	2	4.22	0.46	15.2	1.26	2.32	5.70	8.74	1.62	3.02	15.9	2.14	4.35	7.87	13.73	3.76	6.74	13.6	2.15	4.06	6.94	10.20	3.28	5.11	5.11		
	3	4.29	0.49	13.8	1.45	2.74	5.59	9.07	2.10	3.63	15.3	1.91	4.85	7.93	13.56	3.95	6.93	14.6	2.24	5.42	6.94	9.99	3.31	5.92	5.92		
	4	4.25	17405	0.53	13.2	1.76	3.21	4.76	10.48	2.04	4.19	15.7	2.58	5.64	9.47	15.77	5.53	9.88	14.1	2.17	4.85	8.56	14.75	4.94	8.19	8.19	
	5	4.06	0.47	13.5	1.83	3.82	5.06	8.97	2.09	1.99	3.07	15.0	1.80	3.63	6.63	10.25	2.73	4.97	13.4	2.17	3.84	6.06	9.84	2.74	5.18	5.18	
	6	3.96	0.41	13.6	1.45	3.11	4.46	9.37	1.53	3.09	15.1	2.49	5.08	7.17	11.63	3.61	6.82	12.6	1.83	3.44	6.28	10.10	2.82	5.22	5.22		
	7	4.14	0.51	13.6	1.96	3.98	4.41	8.05	2.03	4.07	14.7	1.99	3.75	7.82	12.12	3.85	6.17	14.2	2.20	4.44	7.25	3.50	3.59	6.38	6.38		
13	1	0.70	0.38	2.9	0.14	0.28	0.71	1.17	0.30	0.63	2.8	0.22	0.35	0.60	1.07	0.30	0.53	2.9	0.14	0.19	0.57	0.96	0.22	0.46	0.46		
	2	0.72	0.40	2.7	0.14	0.30	0.70	1.15	0.30	0.63	2.9	0.20	0.41	0.52	0.82	0.22	0.44	2.9	0.10	0.24	0.50	0.74	0.17	0.32	0.32		
	3	0.74	0.50	2.7	0.10	0.19	0.69	0.99	0.28	0.41	3.0	0.14	0.30	0.57	0.90	0.35	0.63	3.1	0.00	0.13	0.56	0.79	0.32	0.54	0.54		
	4	5.3	0.77	15106	0.53	2.5	0.14	0.27	0.66	1.02	0.28	0.56	3.1	0.22	0.45	0.59	1.14	0.51	0.78	3.2	0.10	0.25	0.57	1.06	0.47	0.57	0.57
	5	0.77	0.56	2.5	0.10	0.22	0.64	0.97	0.26	0.53	3.1	0.17	0.33	0.42	0.83	0.39	0.66	3.2	0.10	0.25	0.41	0.71	0.35	0.57	0.57		
	6	0.80	0.50	2.6	0.17	0.32	0.69	1.01	0.32	0.47	3.2	0.28	0.58	0.49	0.84	0.49	0.77	3.3	0.22	0.45	0.46	0.83	0.44	0.88	0.88		
	7	0.82	0.60	2.4	0.20	0.37	0.71	1.09	0.33	0.56	3.3	0.22	0.45	0.50	0.94	0.46	0.77	3.3	0.17	0.30	0.49	0.85	0.44	0.73	0.73		
14	1	1.17	0.43	5.1	0.24	0.43	1.01	1.69	0.28	0.58	4.6	0.48	0.83	1.02	1.73	0.61	1.08	4.9	0.20	0.39	0.95	1.48	0.42	0.83	0.83		
	2	1.18	0.49	5.1	0.22	0.40	1.00	1.53	0.26	0.59	4.7	0.42	0.77	0.92	1.62	0.54	0.88	4.9	0.14	0.28	0.85	1.34	0.33	0.53	0.53		
	3	1.18	0.44	5.4	0.24	0.47	1.09	1.72	0.36	0.78	4.7	0.48	0.94	0.96	1.51	0.66	1.00	5.0	0.22	0.44	0.89	1.29	0.35	0.62	0.62		
	4	5.3	1.23	15106	0.35	5.2	0.22	0.48	1.11	1.66	0.45	5.0	0.47	0.98	0.93	1.52	0.61	1.16	5.2	0.24	0.45	0.86	1.21	0.42	0.75	0.75	
	5	1.25	0.47	5.6	0.17	0.35	1.21	2.16	0.63	1.47	5.0	0.51	0.91	1.13	2.01	0.81	1.40	5.3	0.28	0.58	1.05	1.75	0.66	1.13	1.13		
	6	1.26	0.44	4.9	0.26	0.51	1.06	1.69	0.51	1.37	5.2	0.39	0.81	0.89	1.64	0.73	1.20	5.5	0.20	0.33	0.85	1.53	0.63	1.03	1.03		
	7	1.26	0.44	5.2	0.32	0.59	1.17	1.91	0.58	1.36	5.0	0.64	1.20	1.02	1.64	0.78	1.52	5.3	0.37	0.76	0.91	1.41	0.55	0.98	0.98		
15	1	2.54	0.44	10.1	0.78	1.72	2.47	4.67	1.04	2.36	10.2	1.82	2.96	3.65	5.85	2.25	4.26	10.9	0.68	1.19	3.20	6.22	1.37	3.01	3.01		
	2	2.48	0.46	10.3	0.66	1.28	2.52	4.99	0.96	1.97	10.0	1.82	2.93	3.06	5.93	1.97	3.25	10.6	0.66	1.16	2.65	5.20	0.95	2.16	2.16		
	3	2.49	0.50	10.7	0.64	1.30	2.82	5.26	1.20	2.76	10.0	1.85	3.34	3.08	5.07	2.01	3.59	11.0	0.85	1.12	2.67	5.28	1.05	2.12	2.12		
	4	5.3	2.58	15106	0.46	10.5	0.46	1.12	2.66	5.32	1.09	2.67	10.2	1.76	3.21	3.22	5.39	2.12	3.83	11.2	0.80	1.68	2.67	5.26	1.04	1.88	1.88
	5	2.65	0.52	10.2	0.81	1.72	2.56	5.05	1.14	2.82	10.6	1.76	3.43	2.59	4.52	1.97	4.14	11.7	0.79	1.44	2.04	4.84	0.97	2.04	2.04		
	6	2.62	0.52	10.4	0.68	1.34	2.74	5.86	1.25	3.02	10.5	2.13	3.62	3.22	5.48	2.32	4.23	11.4	0.93	2.00	2.57	5.32	1.08	2.14	2.14		
	7	2.62	0.50	10.3	0.76	1.42	2.69	5.43	1.24	2.86	10.5	2.06	3.95	2.93	5.10	2.21	4.77	11.6	1.01	2.32	4.91	5.00	1.09	2.67	2.67		

Table 5-3 (continued)

Run No.	Wave No.	T (sec)	H (ft)	β	α	Measured Kinematics						Linear Wave Theory						Stream Function Theory								
						LSQ			WPII			U-Tube			LSQ			WPII			U-Tube					
						K	RMS (lbs)	MAX (lbs)	RMS (lbs)	MAX (lbs)	RMS (lbs)	K	RMS (lbs)	MAX (lbs)	RMS (lbs)	MAX (lbs)	K	RMS (lbs)	MAX (lbs)	RMS (lbs)	MAX (lbs)	K	RMS (lbs)	MAX (lbs)		
16	1	3.47	0.46	13.5	0.85	1.61	3.17	6.41	0.89	1.56	14.7	2.63	4.54	5.27	9.40	3.20	6.26	14.3	0.72	1.49	4.20	8.01	1.48	3.38		
	2	3.38	0.48	13.9	0.78	1.67	3.19	7.02	1.23	2.77	13.8	3.37	5.70	5.72	10.05	3.73	6.37	14.5	1.31	2.28	4.59	8.20	1.89	3.19		
	3	3.40	0.46	14.1	0.78	1.70	4.24	8.63	1.55	3.63	14.1	3.66	5.46	5.80	10.35	3.97	7.30	14.3	1.51	2.88	4.59	8.52	1.97	3.59		
17	4	5.3	0.49	151.06	0.49	14.4	1.10	2.03	4.17	8.78	1.69	3.59	14.2	3.70	6.21	5.48	9.90	3.91	6.84	14.7	1.64	3.69	4.18	7.82	1.79	3.11
	5	3.46	0.50	14.4	0.91	1.66	3.84	8.04	1.32	2.93	14.7	3.55	5.63	5.78	10.48	3.99	7.65	14.2	1.56	3.20	4.56	9.19	2.02	3.58		
	6	3.44	0.50	14.0	0.62	1.28	3.77	7.94	1.21	2.59	14.4	3.28	5.25	5.81	9.76	3.79	7.10	14.4	1.20	2.67	4.72	9.01	1.97	4.04		
18	7	3.32	0.52	13.3	1.03	2.12	3.67	7.16	1.40	2.76	14.0	3.49	5.50	5.36	9.55	3.76	7.09	13.8	1.57	3.17	4.20	7.72	1.85	3.34		
	1	3.75	0.43	14.3	0.94	1.84	3.50	7.14	1.03	2.47	16.0	3.42	6.15	6.04	10.40	3.90	6.83	15.4	0.89	1.55	4.62	9.20	1.48	3.06		
	2	3.62	0.49	15.3	0.96	2.00	4.15	8.88	1.37	3.09	14.6	4.06	6.84	6.35	11.39	4.45	8.39	15.7	1.76	3.37	5.00	9.56	2.24	3.97		
(30) 18	3	3.56	0.40	15.8	1.20	2.40	4.50	9.41	1.65	3.13	14.9	4.04	5.96	6.36	11.64	4.36	7.12	14.9	2.03	3.75	5.37	10.64	2.66	4.81		
	4	5.3	0.49	15.9	0.93	2.17	4.19	9.02	2.07	2.78	15.4	3.92	5.73	6.18	10.94	4.34	8.21	15.7	1.64	3.27	4.72	9.08	2.00	3.69		
	5	3.84	0.48	14.6	1.13	2.28	3.92	8.36	1.37	2.78	16.4	4.38	6.55	6.62	12.52	4.91	9.67	15.8	1.91	3.82	4.82	9.38	2.20	4.72		
(31) 19	6	3.69	0.46	15.0	0.94	1.94	3.89	8.67	1.25	3.34	15.1	3.75	5.63	6.46	10.85	4.35	8.36	15.8	1.69	3.27	5.28	11.07	2.46	5.64		
	7	3.46	0.42	14.9	0.88	1.84	4.17	8.84	1.31	3.38	14.8	4.12	6.15	5.72	10.34	4.28	7.27	14.1	1.82	3.57	7.55	10.55	2.40	3.18		
	8	2.02	0.35	10.9	0.53	0.89	1.66	3.28	0.58	1.08	9.3	1.07	1.80	1.56	2.97	1.11	2.15	10.0	0.37	0.78	1.26	2.72	0.42	0.71		
(30) 18	9	2.02	0.33	10.0	0.37	0.90	0.75	3.46	0.55	1.34	8.6	1.22	1.98	1.96	3.67	1.23	2.04	9.6	0.36	0.72	1.71	2.54	0.55	1.01		
	10	1.80	0.33	11.3	0.35	0.55	1.88	3.74	0.62	1.24	8.3	1.05	2.06	1.66	2.84	1.16	2.09	9.2	0.55	0.89	1.48	2.56	0.82	1.47		
	11	1.84	0.41	10.2	0.30	0.65	0.89	3.24	0.61	1.17	8.5	0.85	1.46	2.11	3.94	1.08	2.23	9.5	0.41	0.82	2.05	3.23	0.87	1.53		
(31) 19	12	1.83	0.38	10.7	0.42	0.89	2.01	4.14	0.72	1.60	8.4	0.87	1.49	2.03	3.55	1.03	2.92	9.1	0.42	0.83	1.96	2.97	0.81	1.46		
	13	1.93	0.34	11.1	0.62	1.21	2.24	4.09	0.98	1.21	8.8	1.17	1.90	2.03	4.03	1.21	2.27	9.8	0.54	0.97	1.89	2.75	0.75	1.62		
	14	2.00	0.39	10.5	0.65	1.19	2.38	4.53	1.14	2.29	9.2	1.24	2.35	2.19	3.87	1.30	2.46	10.0	0.64	1.16	2.03	3.61	0.84	1.55		
20	1	2.37	0.33	12.8	0.49	0.82	2.22	4.00	0.63	1.40	11.1	1.58	2.92	2.73	4.65	1.63	2.73	11.8	0.39	0.92	2.35	4.35	0.66	1.44		
	2	2.35	0.38	15.2	0.41	0.77	2.07	3.73	0.52	1.11	10.8	1.57	2.51	2.33	4.57	1.57	2.57	11.8	0.53	0.85	2.35	4.40	0.59	1.21		
	3	2.21	0.35	12.5	0.53	1.24	2.32	4.52	0.69	1.29	10.2	1.72	2.85	2.48	4.59	1.75	3.01	11.5	0.78	1.42	2.18	3.43	0.98	1.95		
(31) 19	4	6.0	2.22	13344	0.38	13.2	0.33	0.67	2.73	5.41	0.83	1.61	10.3	1.84	2.91	3.14	6.08	2.05	3.97	11.6	0.69	1.43	2.84	4.86	1.31	2.15
	5	2.25	0.39	12.9	0.35	0.65	2.47	5.18	0.71	1.55	10.2	1.75	2.85	2.64	5.07	1.77	2.98	11.5	0.53	1.17	2.24	3.77	0.80	1.59		
	6	2.23	0.44	12.6	0.52	1.21	2.55	5.28	0.86	1.53	10.1	1.74	2.72	2.58	5.10	1.78	3.04	11.4	0.64	1.05	2.23	3.67	0.93	1.85		
(31) 19	7	2.31	0.43	12.0	0.73	1.60	3.04	5.57	1.40	2.43	10.7	1.71	2.79	2.81	5.40	1.80	3.48	11.6	0.68	1.23	2.48	4.10	1.04	2.22		
	8	2.00	0.39	10.5	0.65	1.19	2.38	4.53	1.14	2.29	9.2	1.24	2.35	2.19	3.87	1.30	2.46	10.0	0.64	1.16	2.03	3.61	0.84	1.55		
	9	2.78	0.40	15.6	0.48	1.11	3.12	5.52	0.66	1.59	13.1	2.51	3.89	3.67	6.56	2.55	4.56	13.9	1.01	1.63	2.85	4.52	1.09	2.12		
20	10	2.85	0.42	14.8	0.68	1.32	3.03	6.00	0.75	1.64	12.9	2.46	4.37	3.94	8.09	2.59	4.99	14.1	1.22	2.20	3.54	6.97	1.58	2.50		
	11	2.81	0.41	15.7	0.61	1.30	3.12	6.79	0.82	1.67	13.1	2.77	4.18	4.21	7.81	2.94	5.17	14.6	1.26	2.28	3.59	6.70	1.58	2.48		
	12	2.79	0.41	14.2	0.65	1.26	3.08	5.87	0.91	1.65	13.4	2.77	4.51	3.97	7.11	2.84	5.11	13.7	1.02	2.23	3.06	5.18	1.16	2.12		
20	13	2.69	0.42	13.8	0.96	2.05	3.72	7.79	1.54	3.48	13.2	2.43	4.00	3.81	6.45	2.52	4.01	13.0	1.17	2.37	3.21	5.40	1.45	2.45		

Table 5-3 (continued)

Run No.	Wave No.	T (sec)	H (ft)	β	α	Measured Kinematics						Linear Wave Theory						Stream Function Theory								
						LSQ			WPII			U-Tube			LSQ			WPII			U-Tube			LSQ		
						K	RMS (lbs)	MAX (lbs)	K	RMS (lbs)	MAX (lbs)	K	RMS (lbs)	MAX (lbs)	K	RMS (lbs)	MAX (lbs)	K	RMS (lbs)	MAX (lbs)	K	RMS (lbs)	MAX (lbs)	K	RMS (lbs)	MAX (lbs)
21	1	4.84	0.63	13.5	2.01	4.87	5.49	10.04	2.06	5.53	16.4	3.35	7.28	6.04	9.90	3.62	6.59	13.7	2.16	4.08	4.60	8.75	2.28	4.51		
	2	4.92	0.67	14.4	1.75	3.29	5.21	8.06	1.84	3.73	16.5	2.95	6.08	4.33	8.61	4.07	8.58	14.1	2.76	5.62	3.36	7.52	3.91	7.24		
	3	4.93	0.70	13.4	2.13	3.98	5.32	9.84	2.15	3.96	16.0	3.50	6.79	5.40	9.49	4.10	7.94	14.7	3.06	5.86	4.40	9.88	3.40	6.60		
	4	4.93	18913	0.65	13.9	1.45	2.95	5.82	11.07	1.69	4.22	16.4	3.06	5.64	6.03	10.82	3.59	6.53	14.3	2.25	4.24	4.64	9.73	2.41	5.04	
	5	4.91	0.66	14.2	1.64	4.72	5.73	11.17	1.77	5.30	16.2	3.06	6.08	5.38	9.66	3.54	6.72	14.4	2.92	6.52	4.55	10.78	3.18	5.95		
	6	4.92	0.62	14.7	2.13	4.43	6.41	12.51	2.40	5.73	16.6	3.11	6.99	10.48	12.50	6.94	14.0	3.02	5.94	4.81	10.17	3.19	5.37			
	7	4.88	0.65	14.8	2.06	4.35	6.05	11.07	2.18	4.53	16.4	3.38	6.88	5.58	9.21	3.68	8.50	14.0	3.08	6.11	4.75	10.15	3.30	5.28		
22	1	3.71	0.47	15.7	0.81	1.57	3.67	7.60	0.90	1.74	15.7	3.22	5.53	5.79	10.62	3.77	7.03	15.3	0.89	1.64	4.24	7.23	1.37	2.65		
	2	3.75	0.48	15.6	0.80	1.79	3.82	7.64	0.95	1.91	15.7	2.85	4.64	5.79	10.21	3.50	6.58	15.6	0.65	1.37	4.48	8.56	1.48	3.73		
	3	3.61	0.48	16.7	0.91	1.85	4.42	9.49	1.42	3.57	14.3	3.50	5.71	6.13	10.35	4.01	8.08	15.9	1.50	2.55	5.02	8.99	2.17	4.15		
	4	5.3	15166	0.43	17.1	1.41	2.92	4.68	10.48	1.76	4.13	15.0	3.50	5.82	5.76	10.16	3.72	6.29	14.7	1.66	3.23	4.78	8.90	2.05	4.06	
	5	3.74	0.45	16.8	0.98	2.22	4.65	10.40	1.75	4.14	15.2	3.75	5.50	6.54	11.32	4.41	8.02	16.1	1.54	3.02	5.25	9.91	2.33	4.09		
	6	3.82	0.42	16.2	1.07	2.36	4.06	9.87	1.34	3.82	15.7	3.94	5.94	6.58	11.75	4.54	8.61	16.2	1.57	3.31	5.12	10.84	2.20	4.67		
	7	3.78	0.46	15.6	1.12	2.48	4.24	9.24	1.57	3.46	15.2	3.84	5.86	6.89	11.65	4.67	8.97	16.5	1.76	3.32	5.69	11.52	2.78	5.50		
23	1	4.34	0.40	13.7	1.61	3.33	4.63	9.61	1.78	3.23	15.7	1.47	2.88	5.63	9.6	1.77	8.82	14.7	2.67	4.91	5.27	8.73	2.71	5.46		
	2	4.21	0.45	13.9	1.91	4.12	5.46	10.58	2.27	4.29	14.6	2.88	5.12	7.92	12.99	7.96	8.85	14.5	2.28	4.11	7.39	12.68	3.81	6.47		
	3	4.21	0.47	14.9	1.38	2.59	5.60	11.67	1.89	4.67	14.5	1.59	3.19	8.10	13.48	4.36	7.66	14.8	1.64	3.20	7.01	12.42	3.26	6.14		
	4	4.6	17405	0.42	14.9	1.69	3.78	5.57	11.89	2.05	4.88	14.5	2.30	4.70	7.20	12.90	3.50	7.70	14.4	2.29	4.35	7.70	13.44	4.16	7.32	
	5	4.01	0.44	15.0	1.69	3.32	4.53	8.59	1.36	2.43	14.4	2.28	4.73	9.13	15.65	5.39	9.71	13.6	2.14	4.44	6.69	11.22	3.26	6.63		
	6	4.11	0.48	15.6	1.32	2.69	4.91	8.67	1.48	2.47	15.1	2.19	4.20	6.97	11.94	6.28	13.7	1.88	4.07	6.35	10.89	2.81	5.94			
	7	4.09	0.55	13.3	1.32	2.43	4.53	8.59	1.36	2.51	14.4	2.28	4.73	9.13	15.65	5.39	9.71	14.2	2.14	3.94	8.60	15.22	5.15	9.89		
24	1	4.40	0.54	10.5	1.70	3.81	4.95	10.20	1.87	3.85	12.4	2.54	4.39	7.75	13.39	3.96	7.87	10.7	1.47	3.51	6.78	11.81	2.81	5.53		
	2	4.38	0.55	11.0	2.29	5.75	5.38	11.14	2.49	5.26	11.9	3.20	5.96	8.66	15.82	5.14	10.45	11.5	1.47	3.77	7.75	13.98	3.90	7.29		
	3	4.45	0.54	10.5	2.10	3.81	4.35	10.20	1.87	3.85	12.2	3.53	6.39	8.16	14.05	4.60	10.40	11.9	1.39	3.17	7.00	12.20	2.93	5.34		
	4	3.7	21638	0.54	11.3	2.41	5.47	6.14	12.38	2.83	6.37	12.4	3.38	6.25	8.11	13.94	4.57	10.11	10.9	1.49	3.40	6.98	12.19	2.94	5.79	
	5	4.44	0.41	11.5	1.92	3.68	6.08	13.06	2.65	6.71	12.0	3.10	4.98	7.97	14.01	4.55	9.38	10.9	1.43	3.55	6.83	12.34	2.98	5.89		
	6	4.37	0.40	11.0	2.10	4.47	6.00	12.70	2.48	6.33																
	7	4.41	0.41	11.0	2.10	4.47	6.00	12.70	2.48	6.33																
25	1	3.32	0.87	5.1	0.82	1.46	5.09	6.67	1.59	3.10	5.4	1.08	1.97	4.11	6.01	1.59	2.84	5.0	0.85	1.42	4.23	5.71	1.04	2.00		
	2	3.30	0.81	5.6	0.84	1.59	5.26	6.83	1.76	3.52	5.5	1.09	2.07	4.18	5.86	1.52	2.67	5.2	0.82	1.47	4.30	6.02	0.97	1.97		
	3	3.36	0.88	5.2	0.90	1.79	5.03	6.65	1.63	3.59	5.6	1.22	2.23	1.09	6.13	1.88	3.30	5.2	0.87	1.65	4.16	5.76	1.18	2.30		
	4	2.5	3.35	0.85	5.0	0.91	1.93	4.98	6.73	1.53	3.16	5.8	1.19	2.35	3.70	5.48	1.94	3.80	5.3	0.87	1.51	3.82	5.68	1.18	2.47	
	5	3.39	0.92	4.9	0.83	1.68	5.11	7.25	1.73	3.79	5.5	1.16	2.29	3.47	5.32	1.84	4.05	5.1	0.87	1.40	3.64	5.52	1.21	2.44		
	6	3.32	0.85	5.1	0.99	1.85	5.26	7.86	2.05	4.36	5.5	1.37	2.63	3.79	5.91	2.08	4.05	5.1	0.94	1.85	3.87	5.82	1.26	2.34		
	7	3.39	0.88	5.0	0.98	1.93	5.40	8.39	2.30	5.04	5.3	1.19	2.40	3.74	6.26	1.80	3.25	4.9	1.05	1.94	3.92	5.69	1.25	2.58		

Table 5-3 (continued)

Run No.	Wave No.	T (sec)	H (ft)	B	u	Measured Kinematics						Linear Wave Theory						Stream Function Theory												
						LSQ			WPII			U-Tube			LSQ			WPII			U-Tube			LSQ			WPII			
						K	RMS	MAX	(lbs)	(lbs)	(lbs)	K	RMS	MAX	(lbs)	(lbs)	K	RMS	MAX	(lbs)	(lbs)	K	RMS	MAX	(lbs)	(lbs)	K	RMS	MAX	(lbs)
26	1	3.01	0.42	14.7	1.03	2.48	3.00	6.48	1.08	2.33	14.4	1.91	3.47	3.07	5.95	2.02	3.53	14.9	0.52	1.19	2.21	5.09	0.71	1.59	5.74	5.74	5.74	5.74		
	2	2.86	0.38	14.3	0.78	2.25	2.78	6.80	0.83	1.99	13.3	2.10	3.36	3.26	5.64	2.15	3.96	14.5	0.85	1.82	2.67	5.31	3.02	1.27						
	3	2.78	0.40	16.2	0.80	1.80	3.17	6.72	0.96	1.94	12.7	2.44	4.03	3.36	5.85	2.47	4.43	11.4	1.26	2.40	2.84	6.60	1.27	2.29						
	4	6.0	13344	0.40	15.7	0.66	3.42	7.58	1.08	2.50	12.7	2.56	4.10	1.08	8.06	2.71	4.78	14.5	1.18	2.64	3.66	7.43	1.60	2.65						
	5	2.68	0.45	15.4	0.72	1.30	3.59	7.53	1.18	2.45	12.6	2.69	4.50	4.07	7.66	2.83	5.07	13.4	1.37	2.76	3.59	6.50	1.79	2.99						
	6	2.67	0.45	15.4	0.66	1.41	3.68	7.52	1.39	2.86	12.5	2.48	3.96	3.91	6.91	2.64	4.60	13.4	1.12	2.35	3.36	5.86	1.51	2.68						
	7	2.70	0.42	15.3	0.71	1.49	3.97	7.92	1.57	3.39	13.1	2.52	4.51	3.99	7.15	2.65	4.52	13.1	1.07	2.25	3.37	5.59	1.49	2.87						
Random Waves						Random Waves						Random Waves						Random Waves						Random Waves						
32	1	4.7	1.95	17108	0.62	8.4	0.79	1.79	2.08	3.40	0.84	1.51	8.2	1.46	4.20	3.30	8.11	2.66	5.80	8.6	2.20	3.90	3.31	8.55	2.46	6.00	8.39	8.39	8.39	8.39
	2	3.8	3.50	21181	0.92	11.8	3.67	7.19	5.37	10.29	4.55	7.75	10.4	3.63	7.58	4.03	8.90	4.72	9.39	9.2	3.85	8.69	4.37	8.52	4.83					
	3	2.5	2.97	31172	0.62	5.0	2.60	4.49	3.61	6.35	2.83	5.14	5.2	4.15	9.47	8.49	16.95	8.68	15.95	4.9	3.91	9.18	8.28	16.86	8.28					
	4	4.7	2.99	16391	0.83	9.9	1.56	3.37	3.37	6.50	1.77	3.74	10.6	6.54	12.53	7.75	18.14	9.28	20.70	11.1	7.22	12.42	8.68	19.60	10.00					
	5	2.5	2.89	76234	0.86	3.5	1.74	4.51	6.73	10.24	14.23	21.40	3.4	2.96	7.81	9.75	16.42	16.29	24.02	3.3	3.3	2.69	7.73	9.10	14.54	15.36				
	1	4.3	1.96	18794	0.53	7.1	1.92	3.60	2.94	5.34	2.11	3.67	6.6	1.98	3.71	3.06	6.28	2.50	4.66	6.9	1.95	3.78	3.14	6.57	2.51	5.13	5.13	5.13	5.13	
	2	4.1	2.34	19624	0.53	6.5	0.80	1.88	3.00	4.79	1.23	2.53	7.6	1.66	2.85	3.44	6.11	2.11	3.01	7.0	1.00	1.71	3.19	5.41	1.65					
	3	3.8	2.65	20850	0.57	8.7	3.37	3.34	2.01	3.37	4.19	2.29	4.51	8.0	2.95	5.54	4.71	8.36	3.63	7.07	8.2	2.21	4.11	4.35	8.28	2.87				
	4	3.7	2.88	21875	0.81	6.9	2.66	5.11	4.24	7.48	2.78	5.81	8.1	2.74	4.61	4.29	7.91	2.89	4.56	4.7	1.84	2.98	3.87	7.39	2.03					
	5	5.0	1.61	16077	0.61	8.6	1.57	3.00	2.09	5.48	1.61	3.02	6.7	2.58	5.67	3.75	9.26	3.65	7.57	7.1	2.26	4.80	3.58	9.02	3.31					

Table 5-4 Summary of RMS error (χ) and energy attenuation in acceleration spectra

Run No.	Wave No.	t_{meas} (sec)	m_e/m_o (%)	$F_{\text{max}}^{\text{meas}}$ (lbs)	Measured Kinematics				Linear Wave Theory				Stream Function Wave Theory						
					K ($\times 10^{-5}$)	C_d	C_m	RMS/ F_{max} (%)	\bar{u} (ft/sec)	K ($\times 10^{-5}$)	C_d	C_m	RMS/ F_{max} (%)	K ($\times 10^{-5}$)	C_d	C_m	RMS/ F_{max} (%)		
1	1	1.18	1.04	6.36	0.52	1.29	-0.02	2.56	5.0	-0.07	0.51	1.27	-2.55	1.27	-2.54	1.96	5.9		
	2	1.04	1.04	5.71	0.46	1.15	-0.65	2.29	8.9	-0.07	0.45	1.13	2.14	2.02	2.14	2.02	2.7		
	3	1.04	1.06	5.84	0.48	1.21	0.18	2.31	7.3	-0.07	0.45	1.12	0.78	2.06	1.12	0.78	2.05		
	4	2.0	1.06	96.45	5.93	0.46	1.14	0.04	2.33	7.4	-0.07	0.46	1.15	1.31	1.15	1.31	1.9		
	5	1.06	1.06	5.83	0.47	1.18	-0.46	2.32	7.7	-0.06	0.45	1.13	0.76	2.03	1.13	0.76	2.03		
	6	1.06	1.06	5.91	0.47	1.19	-0.48	2.33	7.1	-0.06	0.45	1.13	0.74	2.02	1.13	0.74	2.02		
	7	1.06	1.06	5.90	0.46	1.15	-0.69	2.32	7.5	-0.05	0.44	1.09	1.14	2.05	1.14	2.05	1.9		
2	1	0.36	0.36	2.04	0.15	0.38	4.05	2.73	8.1	-0.02	0.15	0.38	1.9	2.06	1.8	0.38	1.80	2.06	
	2	0.36	0.35	1.99	0.17	0.43	3.82	2.65	8.2	-0.02	0.15	0.38	3.09	2.03	1.1	0.38	1.10	2.03	
	3	0.35	0.35	1.98	0.13	0.33	5.55	2.61	9.1	-0.01	0.15	0.36	0.70	2.04	0.5	0.36	0.70	2.04	
	4	2.0	0.16	90.13	2.04	0.15	0.37	3.25	2.68	7.8	-0.01	0.15	0.37	-4.52	2.03	2.2	-4.53	2.03	2.2
	5	0.35	0.35	1.99	0.18	0.45	0.82	2.65	8.9	-0.02	0.15	0.39	0.15	2.05	0.4	0.15	0.38	2.06	
	6	0.35	0.35	1.98	0.14	0.36	0.75	2.63	8.3	-0.01	0.15	0.36	-0.12	2.05	0.8	0.15	0.36	2.06	
	7	/	0.35	2.01	0.16	0.40	1.08	2.64	8.4	-0.02	0.15	0.37	-0.28	2.06	0.5	0.15	0.37	-0.28	
3	1	1.04	0.99	5.69	0.54	1.70	-0.58	2.38	4.3	-0.04	0.52	1.64	0.10	2.06	2.5	0.52	1.63	0.10	
	2	1.04	0.99	5.54	0.49	1.55	-0.48	2.29	4.5	-0.04	0.51	1.58	-0.84	2.06	1.3	0.50	1.57	-0.84	
	3	1.01	0.99	5.77	0.53	1.64	-0.16	2.32	4.8	-0.05	0.52	1.61	0.11	2.06	1.1	0.51	1.57	0.11	
	4	2.5	1.01	97.62	5.60	0.55	1.72	-0.80	2.30	5.2	-0.06	0.52	1.63	0.57	2.05	1.8	0.52	1.62	0.58
	5	1.00	0.99	5.69	0.51	1.58	-1.07	2.32	4.8	-0.05	0.52	1.61	-0.02	2.07	1.3	0.51	1.60	-0.03	
	6	0.99	0.99	5.68	0.50	1.55	-1.37	2.31	5.4	-0.03	0.50	1.55	-0.24	2.09	1.1	0.50	1.55	-0.25	
	7	1.01	0.99	5.67	0.51	1.60	-1.56	2.31	5.6	-0.04	0.51	1.59	-0.02	2.07	1.1	0.51	1.58	-0.02	
4	1	1.88	0.88	10.07	0.90	2.82	-0.18	2.26	1.6	-0.04	0.92	2.88	0.06	1.99	2.5	0.91	2.83	0.06	
	2	1.88	0.88	10.15	0.86	2.69	0.04	2.26	1.2	-0.01	0.90	2.82	0.26	1.98	2.0	0.90	2.81	0.26	
	3	1.87	1.05	10.25	0.86	2.69	-0.28	2.31	2.0	-0.04	0.92	2.88	0.39	2.05	2.1	0.90	2.82	0.40	
	4	2.5	1.84	98.45	10.35	0.96	2.99	-0.22	2.29	1.7	-0.05	0.92	2.86	0.62	2.06	2.1	0.90	2.81	0.64
	5	1.88	1.00	10.20	0.93	2.90	-0.44	2.28	1.0	-0.02	0.91	2.84	0.01	2.01	1.8	0.89	2.78	0.01	
	6	1.89	1.08	10.18	0.85	2.65	-0.71	2.28	1.1	-0.02	0.92	2.86	0.03	2.00	1.9	0.90	2.80	0.03	
	7	1.89	1.09	10.19	0.86	2.88	-0.95	2.29	1.5	0.00	0.90	2.82	0.25	2.00	2.1	0.90	2.81	0.27	
5	1	3.24	1.26	16.86	1.55	4.83	0.06	2.29	5.6	-0.23	1.71	5.34	0.15	1.89	4.9	1.60	5.00	0.16	
	2	3.26	1.27	17.21	1.59	4.97	0.10	2.34	6.3	-0.24	1.73	5.41	0.08	1.92	5.5	1.62	5.06	0.08	
	3	3.37	1.37	17.53	1.57	4.90	0.23	2.32	7.2	-0.24	1.79	5.58	0.17	1.83	6.4	1.64	5.19	0.18	
	4	3.12*	97.84	17.35	1.68	5.25	0.13	2.28	7.7	0.17	1.61	5.03	1.14	1.89	7.6	1.52	4.73	1.24	
	5	4	2.5	3.34	17.40	1.48	4.61	0.22	2.26	8.3	-0.21	1.75	5.47	0.22	1.81	7.4	1.63	5.08	0.24
	6	3.37	3.37	17.45	1.49	4.67	0.11	2.10	7.5	-0.17	0.73	5.40	0.66	1.80	6.9	1.60	5.00	0.73	1.90
	7	3.32	17.41	1.54	4.80	0.01	2.29	7.3	-0.14	4.80	0.70	5.25	0.70	1.82	6.9	1.66	5.06	0.77	1.91

Table 5-4 (continued)

Run No.	Wave No.	T _{meas} (sec)	H _{meas} (ft)	m _o '/m _o (%)	Measured Kinematics						Linear Wave Theory						Stream Function Wave Theory					
					F _{max} meas (lbs)	R (x10 ⁻⁵)	K	C _d	C _m	RMS/F _{max} (%)	ū (ft/sec)	R (x10 ⁻⁵)	K	C _d	C _m	RMS/F _{max} (%)	R (x10 ⁻⁵)	K	C _d	C _m	RMS/F _{max} (%)	
1	1	0.93	4.20	0.53	2.46	-0.34	2.20	4.9	-0.01	1.53	2.43	0.60	2.09	0.52	2.42	0.61	2.10	1.7				
2	2	0.91	4.43	0.61	2.80	-0.10	2.24	6.8	-0.11	0.61	2.81	-0.02	2.11	0.60	2.75	-0.02	2.12	2.3				
3	3	0.92	4.21	0.51	2.37	-0.01	2.22	4.5	-0.03	0.55	2.55	0.13	2.07	3.5	0.54	2.50	0.13	2.07	1.3			
6	4	0.94	94.60	4.14	0.55	2.53	-0.12	2.21	1.6	-0.03	0.55	2.53	-0.64	2.06	6.1	0.54	2.47	-0.64	2.13	4.9		
5	5	0.94	4.16	0.54	2.47	-0.10	2.26	1.9	-0.02	0.54	2.51	-0.18	2.12	7.1	0.53	2.45	-0.17	2.13	4.9			
6	6	0.95	4.12	0.54	2.47	-0.10	2.26	1.9	-0.02	0.55	2.53	-0.32	2.06	7.0	0.54	2.47	-0.31	2.08	4.5			
7	7	0.95	4.13	0.51	2.36	0.26	2.20	1.5	-0.01	0.55	2.52	0.39	2.02	6.2	0.54	2.47	0.40	2.04	3.8			
1	2.39	10.47	1.36	6.27	0.17	2.13	3.5	-0.11	1.42	6.58	0.70	1.93	9.5	1.32	6.11	0.74	1.98	4.5				
2	2.44	10.66	1.37	6.32	0.10	2.15	3.5	-0.08	1.43	6.61	0.29	1.93	10.8	1.35	6.24	0.30	1.98	4.4				
3	2.45	11.07	1.36	6.27	0.22	2.11	5.3	-0.12	1.46	6.76	0.47	1.86	12.8	1.35	6.26	0.49	1.92	6.9				
4	3.7	99.02	10.47	1.34	6.20	0.21	2.11	6.1	-0.11	1.46	6.72	0.78	1.83	13.8	1.35	6.22	0.82	1.90	8.1			
5	2.76	11.40	1.36	6.30	0.24	2.10	6.1	-0.04	1.58	7.31	0.46	1.64	12.3	1.57	7.24	0.47	1.70	7.4				
6	2.48	11.06	1.39	6.42	0.30	2.06	7.9	-0.05	1.43	6.63	0.46	1.80	13.8	1.40	6.45	0.45	1.86	9.6				
7	2.67	11.08	1.33	6.17	0.15	2.04	7.2	-0.05	1.53	7.09	0.21	1.67	13.9	1.51	6.96	0.19	1.73	9.0				
1	4.33	16.95	2.15	9.95	0.74	1.95	11.0	-0.30	2.66	12.28	0.31	1.67	17.3	2.26	10.46	0.37	0.83	7.0				
2	4.42	16.14	2.23	10.32	0.67	1.87	11.3	-0.28	2.69	12.44	0.25	1.59	19.0	2.32	10.74	0.30	1.75	8.7				
3	4.50	18.16	2.21	10.19	0.54	1.90	10.6	-0.22	2.70	12.46	0.13	1.57	20.0	1.16	11.16	0.15	1.76	7.9				
28(8)	4	98.63	17.27	2.15	9.95	0.74	1.95	11.0	-0.30	2.56	11.82	0.02	1.59	21.7	2.46	11.38	0.02	1.78	8.1			
5	4.33	17.46	2.51	11.59	0.26	1.97	10.2	-0.23	2.61	12.05	0.02	1.67	21.6	2.32	10.71	0.01	1.86	9.0				
6	4.42	17.73	2.33	10.79	0.31	1.87	12.9	-0.22	2.65	12.25	0.13	1.57	21.6	2.37	10.95	0.13	1.87	9.3				
7	4.40	18.63	2.44	11.29	0.25	1.93	13.9	-0.18	2.60	12.02	0.08	1.63	21.6	2.39	11.05	0.06	1.83	10.3				
1	0.60	2.31	0.43	2.44	0.69	2.38	12.1	-0.02	0.37	2.10	-0.65	1.98	6.1	0.36	2.04	-0.67	1.99	4.2				
2	0.62	2.37	0.46	2.63	0.80	2.41	9.8	-0.02	0.38	2.18	0.18	1.95	6.1	0.37	2.12	0.15	1.95	6.1				
3	0.60	2.25	0.47	2.70	0.68	2.40	6.6	-0.01	0.36	2.08	2.98	1.91	4.8	0.35	2.03	3.00	1.91	5.8				
9	4	90.34	2.14	0.42	2.43	0.71	2.34	7.3	-0.01	0.36	2.06	-2.93	1.87	5.0	0.35	2.01	-2.96	0.87	6.3			
5	0.66	1.98	0.42	2.44	-0.01	2.21	6.8	-0.01	0.39	2.24	-2.49	1.60	3.6	0.39	2.22	-2.51	1.60	6.7				
6	0.67	1.94	0.39	2.26	0.28	2.19	9.7	-0.03	0.41	2.36	-0.10	1.63	4.9	0.40	2.29	-0.11	0.64	5.9				
7	0.69	1.91	0.35	2.00	0.84	2.08	8.8	0.00	0.41	2.33	0.03	1.44	6.1	0.42	2.37	0.04	1.44	7.4				
1	1.01	5.14	0.81	4.64	-0.04	2.24	2.8	-0.02	0.84	4.84	0.46	1.92	3.0	0.85	4.87	0.46	1.92	8.0				
2	1.38	5.14	0.83	4.75	0.07	2.22	3.1	-0.04	0.84	4.82	0.24	1.95	3.8	0.82	4.69	0.22	1.95	7.3				
3	1.36	5.17	0.84	4.82	0.13	2.19	4.1	-0.06	0.84	4.85	-0.04	1.95	4.8	0.79	4.56	-0.06	1.95	6.7				
10	4	4.6	4.97	0.79	4.52	0.08	2.09	4.7	-0.03	0.85	4.94	0.61	1.95	6.2	0.86	4.94	0.60	1.75	9.3			
5	1.43	4.75	0.77	4.45	0.03	2.04	4.9	-0.05	0.88	5.05	0.46	1.71	6.4	0.85	4.86	0.47	1.71	7.5				
6	1.43	5.01	0.77	4.42	0.37	2.06	7.2	0.00	0.84	4.82	0.73	1.72	7.9	0.88	5.04	0.72	1.71	11.4				
7	1.40	4.67	0.79	4.53	0.38	2.05	6.6	-0.03	0.85	4.86	0.50	1.76	6.3	0.84	4.81	0.50	1.76	10.3				

Table 5-4 (continued)

Run No.	Wave No.	H_{meas} (ft)	m_e/f_m (%)	Measured Kinematics				Linear Wave Theory				Stream Function Wave Theory							
				R ($\times 10^{-5}$)	K ($\times 10^{-5}$)	C_d	C_m	RMS/ F_{max} (%)	\bar{U} (ft/sec)	R ($\times 10^{-5}$)	K	C_d	C_m	RMS/ F_{max} (%)	R ($\times 10^{-5}$)	K	C_d	C_m	RMS/ F_{max} (%)
1	2	3.56	11.43	2.04	11.73	0.58	1.95	15.1	-0.19	2.23	12.82	0.53	1.74	8.9	2.10	12.11	0.57	1.74	20.5
2	3.57	11.71	2.04	11.76	0.45	2.00	10.1	-0.18	2.23	12.79	0.31	1.80	6.5	2.12	12.20	0.35	1.81	17.5	
3	3.65	11.40	2.04	11.75	0.35	1.94	11.5	-0.03	2.16	12.42	0.33	1.70	7.6	2.28	13.11	0.36	1.67	21.9	
29(11)	4	4.6	11.09	2.04	11.73	0.35	1.98	11.5	-0.10	2.13	12.24	0.48	1.76	11.1	2.14	12.30	0.54	1.74	23.6
5	3.58	10.85	2.08	11.94	0.48	1.94	11.1	-0.10	2.11	12.14	0.73	1.66	12.4	2.13	12.21	0.82	1.63	24.4	
6	3.45	10.47	2.15	12.36	0.50	1.90	11.6	-0.20	2.18	12.52	0.77	1.56	16.0	2.02	11.59	0.90	1.53	24.4	
7	3.49	10.72	1.99	11.43	0.66	8.9	-0.14	2.14	12.30	0.70	1.66	9.8	2.11	12.11	0.78	1.62	23.6		
1	4.30	13.31	2.60	14.94	0.44	1.98	14.7	-0.43	2.84	16.32	0.36	1.83	10.6	2.39	13.91	0.46	1.77	24.9	
2	4.22	13.53	2.65	15.22	0.50	1.94	9.3	-0.40	2.77	15.92	0.13	1.83	15.8	2.36	13.58	0.17	1.91	15.9	
3	4.29	13.81	2.40	13.76	0.34	1.93	10.5	-0.21	2.67	15.34	0.10	1.74	17.2	2.55	14.63	0.15	1.82	16.2	
12	4	4.6	12.32	2.30	13.24	0.40	1.82	14.3	-0.31	2.73	15.67	-0.12	1.64	21.0	2.45	14.07	-0.18	1.73	17.6
5	4.06	12.68	2.35	13.48	0.49	1.88	14.5	-0.30	2.63	14.95	0.24	1.93	14.2	2.34	13.63	0.27	1.89	17.1	
6	3.96	10.88	2.36	13.55	0.60	1.84	13.4	-0.40	2.63	15.10	0.14	1.77	22.8	2.20	14.24	0.16	1.87	16.8	
7	4.14	13.64	2.37	13.62	0.62	1.84	14.3	-0.18	2.56	14.70	0.60	1.78	14.6	2.48	12.90	0.04	1.84	16.1	
1	0.70	2.30	0.44	2.90	1.04	2.42	6.4	0.01	0.42	2.81	-0.32	1.92	9.9	0.44	2.90	-0.33	1.94	5.4	
2	0.72	2.28	0.41	2.74	0.89	2.40	6.7	-0.01	0.43	2.86	0.23	1.87	8.3	0.44	2.90	0.23	1.89	4.9	
3	0.74	2.14	0.40	2.65	-0.12	2.39	4.1	0.00	0.45	2.95	-0.52	1.79	6.9	0.46	3.06	-0.51	1.80	3.0	
13	4	5.3	95.49	2.13	0.38	2.50	-0.43	2.29	7.1	0.01	0.47	3.08	-0.73	1.69	11.0	0.48	3.20	-0.74	0.66
5	0.77	1.99	0.38	2.50	-0.87	2.28	5.1	0.02	0.47	3.12	0.03	1.64	8.9	0.49	3.24	0.04	1.65	4.4	
6	0.80	2.13	0.40	2.63	-0.70	2.34	7.6	0.01	0.48	3.20	0.02	1.61	13.6	0.50	3.34	0.06	1.62	10.4	
7	0.32	2.21	0.36	2.38	-0.23	2.38	9.3	-0.01	0.49	3.26	-0.10	1.63	10.1	0.50	3.33	-0.10	1.64	7.9	
1	1.17	3.94	0.77	5.08	0.68	2.10	6.1	0.00	0.70	4.62	0.18	1.86	12.2	0.74	4.89	0.17	1.89	4.8	
2	1.18	3.83	0.77	5.11	0.61	5.6	0.00	0.71	4.69	0.38	1.83	11.2	0.75	4.94	0.38	1.86	3.4		
3	1.18	3.97	0.81	5.35	0.43	2.12	6.2	0.01	0.72	4.73	0.43	1.86	12.2	0.76	5.00	0.45	1.89	5.8	
14	4	5.3	1.33	3.94	0.78	5.15	0.13	2.12	5.5	0.02	0.75	4.95	0.40	1.78	12.0	0.79	5.24	0.42	
5	1.25	3.63	0.85	5.60	-0.27	2.13	4.6	0.02	0.76	5.04	-0.08	1.76	14.0	0.80	5.34	-0.05	1.79	7.6	
6	1.26	3.70	0.74	4.92	-0.10	2.02	6.9	0.04	0.79	5.21	0.21	1.66	10.5	0.83	5.52	0.22	1.68	5.3	
7	1.26	4.20	0.79	5.23	-0.15	2.16	7.4	0.00	0.76	5.00	-0.39	0.74	15.2	0.80	5.30	0.41	0.78	8.8	
1	2.54	8.35	1.53	10.13	0.54	2.03	9.4	-0.03	1.54	10.19	0.06	1.67	21.9	1.65	10.93	0.09	1.79	8.1	
2	2.48	8.73	1.56	10.34	0.37	1.98	7.6	-0.03	1.50	9.95	0.28	1.64	20.9	1.60	10.62	0.27	1.77	7.5	
3	2.49	8.88	1.65	10.70	0.16	1.98	7.2	0.03	1.52	10.03	0.28	1.62	20.8	1.67	11.03	0.31	1.74	9.6	
15	4	5.3	2.58	8.36	1.58	10.45	1.99	5.4	0.00	1.54	10.20	0.28	1.56	22.8	1.69	11.21	0.32	1.68	9.6
5	2.65	9.11	1.53	10.15	0.24	1.95	9.9	0.02	1.60	10.59	0.55	1.45	19.3	1.77	11.68	0.59	1.55	8.6	
6	2.52	8.91	1.56	10.35	0.12	2.00	7.7	-0.02	1.58	10.45	0.35	1.50	23.9	1.71	11.35	0.40	1.65	10.4	
7	2.62	9.06	1.56	10.31	0.17	2.00	8.4	0.03	1.59	10.51	0.48	1.49	22.7	1.75	11.59	0.52	1.62	11.2	

Table 5-4 (continued)

Run No.	Wave No.	T _{meas} (sec)	H _{meas} (ft)	m _o /m _o (%)	Measured Kinematics						Linear Wave Theory						Stream Function Wave Theory					
					F _{max} meas (lbs)	R (x10 ⁻⁵)	K	C _d	C _m	RMS/F _{max} (%)	u (ft/sec)	R (x10 ⁻⁵)	K	C _d	C _m	RMS/F _{max} (%)	R (x10 ⁻⁵)	K	C _d	C _m	RMS/F _{max} (%)	
1	1	3.47	11.82	2.04	13.48	0.50	1.77	7.2	.20	2.23	14.73	.25	1.47	22.2	2.16	14.29	0.28	1.64	6.1	6.1		
2	2	3.38	13.50	2.12	13.93	0.41	1.95	5.8	-0.09	2.08	13.78	0.22	1.62	24.9	2.18	14.46	0.25	1.84	9.7	9.7		
3	3	3.40	99.08	12.95	2.12	14.07	0.31	2.00	6.0	-0.14	2.14	14.14	0.25	1.59	28.3	2.16	14.29	0.27	1.84	11.7	11.7	
16	4	5.3	3.45	13.17	2.18	14.42	0.31	1.98	8.4	-0.11	2.14	14.20	0.26	1.53	28.1	2.22	14.69	0.40	1.78	12.4	12.4	
5	5	3.46	12.49	2.18	14.42	0.35	1.90	7.3	-0.21	2.23	14.74	0.25	1.48	28.4	2.14	14.18	0.27	1.72	12.5	12.5		
6	6	3.44	11.66	2.12	14.03	0.31	1.90	5.3	-0.16	2.17	14.36	0.20	1.53	28.1	2.17	14.38	0.20	1.75	10.3	10.3		
7	7	3.32	12.77	2.01	13.30	0.31	1.88	8.1	-0.18	2.12	14.01	0.30	1.53	27.4	2.08	13.78	0.32	1.77	12.3	12.3		
-86-																						
1	1	3.75	13.59	2.17	14.34	0.54	1.86	6.9	-0.23	2.42	16.00	0.29	1.49	25.2	2.33	15.42	0.32	1.72	6.6	6.6		
2	2	3.62	14.68	2.31	15.32	0.38	1.90	6.6	-0.06	2.08	13.78	0.22	1.62	24.9	2.18	14.46	0.25	1.84	9.7	9.7		
3	3	3.40	98.64	12.95	2.38	15.77	0.39	1.95	8.6	-0.17	2.65	14.38	0.26	1.62	28.7	2.25	14.87	0.22	1.88	14.4	14.4	
4	4	5.3	3.71	12.75	2.21	15.93	0.34	1.86	7.3	-0.14	2.32	15.36	0.31	1.44	30.8	2.37	15.70	0.33	1.70	12.8	12.8	
5	5	3.84	13.48	2.21	14.62	0.45	1.91	8.4	-0.24	2.47	16.35	0.31	1.36	32.5	2.38	15.77	0.36	1.67	14.2	14.2		
6	6	3.69	13.38	2.27	15.00	0.37	1.93	7.0	-0.10	2.28	15.10	0.21	1.46	28.0	2.13	15.81	0.20	1.71	12.7	12.7		
7	7	3.46	13.83	2.25	14.88	0.37	1.87	6.4	-0.23	2.23	14.79	0.37	1.54	29.8	2.13	14.13	0.44	1.84	13.2	13.2		
30(18)	4	6.0	97.99	6.04	1.46	10.93	0.56	1.89	8.6	-0.04	1.25	9.34	0.66	1.68	17.5	1.33	10.00	0.69	1.75	6.0	6.0	
5	5	1.83	6.47	1.42	10.65	0.56	1.89	8.6	-0.02	1.10	10.10	0.21	1.46	28.0	2.13	9.50	0.47	1.79	5.6	5.6		
6	6	1.93	6.53	1.48	11.96	0.24	9.3	0.01	1.17	8.77	0.47	1.95	17.7	1.31	9.78	0.43	2.02	6.5	6.5			
7	7	2.00	6.74	1.40	10.52	0.10	9.7	-0.02	1.22	9.16	0.34	1.88	18.3	1.33	9.99	0.32	1.95	9.5	9.5			
1	1	2.37	8.06	1.71	12.78	0.58	1.92	6.1	-0.06	1.47	11.05	0.37	1.80	19.6	1.58	11.84	0.39	1.95	4.8	4.8		
2	2	2.35	7.86	1.63	12.19	0.59	1.88	5.2	-0.03	1.44	10.80	0.58	1.75	19.9	1.53	11.84	0.61	1.85	6.8	6.8		
3	3	2.21	8.28	1.67	12.51	0.53	1.93	6.4	0.03	1.36	10.20	0.58	1.90	20.8	1.53	11.47	0.57	2.02	9.5	9.5		
4	4	6.0	98.27	7.83	1.76	13.21	0.30	1.92	4.3	0.04	1.38	10.31	0.14	1.91	23.4	1.55	11.58	0.12	2.05	8.9	8.9	
5	5	2.25	1.75	1.24	12.89	0.34	1.91	4.4	0.01	1.37	10.23	0.45	1.86	22.6	1.54	11.53	0.46	2.00	6.9	6.9		
6	6	2.23	7.96	1.69	12.63	0.35	1.95	6.5	0.00	1.35	10.13	0.55	1.92	21.9	1.52	11.40	0.35	2.05	8.0	8.0		
7	7	2.31	8.30	1.61	12.03	0.11	2.03	8.8	-0.04	1.42	10.67	0.44	1.96	20.6	1.55	11.58	0.44	2.07	8.2	8.2		
1	1	3.00	9.73	2.07	15.48	0.44	1.72	8.0	-0.16	1.93	14.50	0.39	1.53	22.7	1.97	14.73	0.39	1.68	8.4	8.4		
2	2	2.78	9.97	2.09	15.63	0.43	1.79	4.8	-0.09	1.75	13.11	0.41	1.69	25.2	1.85	13.85	0.47	1.86	10.2	10.2		
3	3	2.85	98.76	9.77	2.09	1.98	14.83	0.46	1.78	7.2	-0.05	1.72	12.89	0.30	1.72	26.1	1.88	14.09	0.56	1.88	13.0	13.0
4	4	6.0	2.81	8.96	2.12	15.88	0.36	1.79	4.6	-0.04	1.75	13.12	0.28	1.60	28.4	1.95	14.50	0.26	1.81	13.0	13.0	
5	5	2.79	9.78	1.89	14.20	0.35	1.80	6.6	-0.13	1.78	13.35	0.36	1.66	28.3	1.83	13.68	0.39	1.85	11.4	11.4		
6	6	2.69	10.23	1.84	13.77	0.19	9.4	-0.17	1.76	13.15	0.33	1.92	23.7	1.73	12.95	0.40	1.87	12.8	12.8			
31(19)	4	6.0	98.27	1.75	1.24	12.89	0.34	1.91	4.4	0.01	1.37	10.23	0.45	1.86	22.6	1.54	11.53	0.46	2.00	6.9	6.9	
20	4	6.0	98.76	9.77	2.09	15.63	0.43	1.79	4.8	-0.09	1.75	13.11	0.41	1.69	25.2	1.85	13.85	0.47	1.86	10.2	10.2	
7	7	2.79	9.78	1.89	14.20	0.35	1.80	6.6	-0.13	1.78	13.35	0.36	1.66	28.3	1.83	13.68	0.39	1.85	11.4	11.4		

Table 5-4 (continued)

Run No.	Wave No.	T _{meas} (sec)	H _{meas} (ft)	m ₀ '/m ₀ (%)	F _{max} _{meas} (lbs)	Measured Kinematics				Linear Wave Theory				Stream Function Wave Theory				
						R (x10 ⁻⁵)	K	C _d	C _m	RMS/F _{max} (%)	u (ft/sec)	R (x10 ⁻⁵)	K	C _d	C _m	RMS/F _{max} (%)		
1	1	4.84	20.76	2.57	13.47	0.57	1.83	9.7	-0.43	3.10	16.41	0.55	1.54	2.59	13.70	0.68	10.4	
2	2	4.92	19.48	2.75	14.40	0.61	1.83	9.0	-0.39	3.12	16.51	0.72	1.40	2.66	14.06	0.92	14.2	
3	3	4.93	99.40	2.56	13.43	0.58	1.81	10.3	-0.35	3.02	15.97	0.64	1.45	16.9	2.78	0.76	14.8	
21	4	4.2	99.40	2.66	13.93	0.45	1.78	7.6	-0.35	3.10	16.39	0.53	1.48	16.0	2.70	0.65	11.8	
5	5	4.91	20.03	2.70	14.18	0.50	1.82	8.2	-0.31	3.06	16.16	0.62	1.50	2.72	14.36	0.74	14.6	
6	6	4.92	19.83	2.80	14.70	0.45	1.85	10.8	-0.41	3.13	16.57	0.59	1.51	15.7	2.65	1.39	15.2	
7	7	4.88	20.96	2.82	14.82	0.53	1.86	9.8	-0.39	3.10	16.37	0.62	1.55	16.1	2.64	1.71	14.7	
1	3.71	12.89	2.37	15.66	0.48	1.70	6.3	-0.22	2.39	15.73	0.29	1.43	25.0	2.32	15.29	0.36	6.8	
2	3.75	12.55	2.36	15.64	0.46	1.69	6.4	-0.18	2.38	15.67	0.27	1.45	22.7	2.37	15.64	0.31	5.2	
3	3.61	13.22	2.53	16.73	0.33	1.74	6.9	-0.02	2.17	14.32	0.22	1.52	26.5	2.41	15.86	0.23	11.3	
22	4	5.3	98.92	12.72	2.59	17.13	0.37	1.81	11.1	-0.20	2.28	15.02	0.33	1.63	27.5	2.23	14.68	0.31
5	5	3.56	3.74	12.32	2.54	16.80	0.26	1.76	8.0	-0.09	2.31	15.20	0.21	1.44	30.4	16.07	0.22	12.5
6	6	3.82	12.45	2.44	16.17	0.39	1.79	8.6	-0.13	2.38	15.72	0.26	1.41	31.6	2.46	16.09	0.27	12.6
7	7	3.78	12.36	2.36	15.60	0.30	1.75	9.0	-0.05	2.30	15.16	0.17	1.41	31.1	2.50	16.45	0.16	14.2
1	4.34	13.32	2.38	13.69	0.58	1.91	12.1	-0.24	2.72	15.65	0.43	1.68	11.1	2.56	14.69	0.49	21.0	
2	4.21	13.22	2.39	13.74	0.47	1.87	11.6	-0.18	2.60	14.94	0.07	1.76	14.2	2.52	14.47	0.06	17.3	
3	4.21	13.73	2.72	13.93	0.36	1.85	13.9	-0.11	2.55	14.62	0.08	1.65	21.0	2.57	14.79	0.08	11.2	
23	4	4.12	98.86	12.93	2.60	14.41	0.40	1.89	10.7	-0.13	2.51	14.45	-0.05	1.80	21.3	2.50	14.38	-0.03
5	5	4.6	12.74	2.61	15.02	0.42	1.82	13.3	-0.21	2.52	14.45	0.14	1.82	18.0	2.37	13.63	0.13	16.8
6	6	4.11	13.50	2.72	15.64	0.56	1.89	9.8	-0.29	2.62	15.08	0.21	1.77	16.1	2.38	13.67	0.20	13.9
7	7	4.09	12.54	2.31	13.26	0.51	1.78	10.5	-0.15	2.51	14.43	-0.18	1.66	18.2	2.47	14.18	-0.27	17.1
1	4.40	15.51	2.28	10.54	0.60	1.89	11.0	-0.29	2.59	12.43	0.13	1.66	16.4	2.31	10.69	0.15	8.8	
2	4.38	16.96	2.34	10.79	0.57	1.94	11.0	-0.26	2.66	12.27	0.01	1.69	20.3	2.32	10.74	0.00	8.8	
3	4.45	16.24	2.38	10.98	0.41	1.80	14.1	-0.10	2.57	11.89	0.02	1.57	19.7	2.48	11.74	-0.00	9.1	
24	4	4.42	98.61	17.19	2.34	10.82	0.33	1.97	12.5	-0.21	2.64	12.22	0.14	1.69	20.5	2.38	10.99	0.16
5	5	4.44	17.74	2.45	11.34	0.37	1.89	13.6	-0.26	2.59	12.42	0.14	1.65	19.1	2.35	10.85	0.15	8.4
6	6	4.37	16.10	2.50	11.54	0.27	1.84	12.0	-0.19	2.60	12.02	0.09	1.61	19.3	2.37	10.94	0.11	7.9
7	7																	

Table 5-4 (continued)

Run No.	Wave No.	T _{meas} (sec)	H _{meas} (ft)	m ₀ '/m ₀ (%)	Measured Kinematics						Linear Wave Theory						Stream Function Wave Theory					
					F _{max} meas (lbs)	R (x10 ⁻⁵)	K	C _d	C _m	RMS/F _{max} (%)	u (ft/sec)	R (x10 ⁻⁵)	K	C _d	C _m	RMS/F _{max} (%)	R (x10 ⁻⁵)	K	C _d	C _m	RMS/F _{max} (%)	
26	1	3.01	9.49	1.96	14.66	0.46	1.76	10.9	-0.13	1.92	14.36	0.57	1.54	20.1	1.99	14.91	0.66	1.64	5.5			
	2	2.83	9.36	1.90	14.26	0.47	1.73	8.4	-0.07	1.78	13.31	0.49	1.60	22.5	1.93	14.49	0.51	1.73	9.1			
	3	2.78	9.20	2.16	16.19	0.41	1.76	8.3	-0.01	1.69	12.68	0.53	1.62	25.5	1.92	14.36	0.52	1.79	13.1			
	4	6.0	9.20	2.09	15.67	0.31	1.80	7.2	0.00	1.69	12.69	0.28	1.69	27.9	1.94	14.51	0.23	1.87	12.8			
	5	5	9.34	2.06	15.43	0.29	1.80	7.7	-0.09	1.68	12.62	0.26	1.76	28.8	1.78	13.36	0.20	1.96	14.7			
	6	2.67	9.22	2.12	16.88	0.19	1.74	7.1	-0.08	1.67	12.50	0.24	1.72	26.7	1.78	13.35	0.22	1.90	12.2			
	7	2.70	9.86	2.04	15.28	0.16	1.87	7.2	-0.16	1.75	13.12	0.29	1.85	25.6	1.75	13.08	0.30	2.03	10.8			
Random Waves																						
32	1	4.68	1.95	9.41	8.36	0.36	1.84	8.4	0.34	1.40	8.18	0.10	1.64	26.2	1.47	8.59	0.01	1.71	23.5			
	2	3.78	3.50	18.70	2.49	11.75	0.83	2.04	19.6	-0.31	2.1	10.44	1.24	1.65	19.4	1.94	9.06	1.34	1.74	20.6		
	3	2.52	2.97	13.25	5.04	0.51	1.76	19.6	-0.31	1.65	5.20	-1.72	1.16	31.3	1.57	4.94	-1.98	1.22	29.5			
	4	4.74	2.99	13.83	1.66	9.85	0.71	1.95	11.3	-0.05	1.79	10.62	0.26	47.3	1.87	11.05	1.59	0.01	52.5			
	5	2.52	2.89	14.71	2.64	3.46	0.24	0.89	11.8	-0.41	2.62	3.43	-0.55	0.83	20.1	2.50	3.28	-0.60	0.86	18.3		
	34	1	4.26	1.96	8.82	1.34	7.14	0.03	2.16	21.8	0.14	0.24	6.62	-0.22	1.62	22.5	1.30	6.90	-0.31	1.64	22.1	
	2	4.08	2.34	8.57	1.27	6.45	0.39	2.23	9.3	-0.20	1.49	7.61	-0.02	1.79	19.4	1.37	5.99	-0.04	1.87	11.7		
	3	3.84	2.65	11.90	1.81	8.69	0.73	2.18	16.9	0.22	1.66	7.98	-0.10	1.57	24.8	1.72	8.25	-0.08	1.69	18.6		
	4	3.66	2.89	13.57	1.50	6.88	0.60	2.13	19.6	-0.20	1.77	8.07	0.31	1.74	20.2	1.61	7.36	0.33	1.86	13.6		
	5	4.98	1.61	4.17	1.39	8.62	0.02	1.73	37.5	0.17	1.08	6.72	-1.17	1.08	61.9	1.14	7.10	-1.22	1.25	54.1		

Table 5-5 RMS errors for the 4-term MOJS equation
 (MK = measured kinematics, LW = linear wave theory, SF = stream function wave thec

Run No.	Wave No.	T (sec)	RMS			Run No.	Wave No.	T (sec)	RMS			
			MK	LW	SF				F _{max}	MK	LW	SF
1	1		5.0	5.7	5.9		1			4.9	3.7	1.7
	2		8.9	2.8	6.4		2			6.8	1.7	2.3
	3		7.3	1.8	1.9		3			4.5	3.5	1.3
	4	2.0	7.4	2.3	2.4	6	4	3.7		1.6	6.1	3.5
	5		7.7	1.6	1.7		5			1.9	7.1	4.9
	6		7.1	1.9	2.1		6			1.1	7.0	4.5
	7		7.5	1.9	1.9		7			1.5	6.2	3.8
2	1		8.1	1.7	1.8		1			3.5	10.4	4.5
	2		8.2	1.1	1.1		2			3.5	11.2	4.4
	3		9.1	0.5	0.5		3			5.3	13.4	7.8
	4	2.0	7.8	2.2	2.2	7	4	3.7		6.1	14.3	8.8
	5		8.9	0.4	0.4		5			6.1	12.9	8.4
	6		8.3	0.8	0.8		6			7.9	14.0	9.9
	7		8.3	0.5	0.5		7			7.2	14.0	9.3
3	1		4.3	2.5	2.5		1			11.0	28.3	18.4
	2		4.5	1.3	1.2		2			23.4	26.3	16.7
	3		4.8	1.1	1.3		3			20.0	23.2	14.4
	4	2.5	5.2	1.8	1.6	28(8)	4	3.7		30.1	21.9	9.4
	5		4.8	1.3	1.3		5			10.2	22.1	10.0
	6		5.4	1.1	1.0		6			24.1	23.9	14.0
	7		5.6	1.1	0.9		7			31.9	22.6	12.7
4	1		1.6	2.5	1.8		1			12.1	6.1	4.2
	2		1.2	2.0	1.5		2			9.8	6.0	6.1
	3		2.0	2.1	2.6		3			6.6	5.3	6.2
	4	2.5	1.7	2.1	2.3	9	4	4.6		7.3	5.0	6.3
	5		1.0	1.8	1.3		5			6.8	3.6	6.7
	6		1.1	1.9	1.5		6			9.7	4.9	5.9
	7		1.5	2.1	1.8		7			8.8	6.4	7.6
5	1		5.6	5.3	4.0		1			2.8	3.5	8.3
	2		6.3	5.9	5.5		2			3.1	3.7	7.3
	3		7.2	6.9	6.5		3			4.1	4.8	6.7
	4	2.5	7.7	8.2	5.8	10	4	4.6		4.7	6.8	9.7
	5		8.3	7.7	6.3		5			4.9	6.9	7.8
	6		7.5	7.5	6.1		6			7.2	8.4	11.8
	7		7.3	7.4	6.1		7			6.6	6.8	10.6

Table 5-5 (continued)

Run No.	Wave No.	T (sec)	RMS			Run No.	Wave No.	T (sec)	RMS			
			MK	LW	SF				F _{max}	MK	LW	SF
29(11)	1		15.1	37.1	40.1			1		26.8	26.0	20.4
	2		10.0	31.0	35.1			2		5.8	29.1	26.2
	3		41.6	24.7	35.5			3		6.0	31.7	29.1
	4	4.6	11.5	30.3	38.3	16	4	5.3		8.3	33.3	28.7
	5		57.7	34.8	42.1			5		33.7	31.7	25.4
	6		49.8	37.5	37.9			6		33.8	31.3	23.4
	7		53.5	37.9	43.4			7		30.0	32.1	28.3
12	1		14.7	23.4	41.9			1		29.7	26.0	15.9
	2		55.5	20.4	35.4			2		26.1	30.7	22.5
	3		49.5	21.3	28.3			3		35.0	30.6	26.8
	4	4.6	38.3	21.0	17.6	17	4	5.3		22.0	32.9	22.6
	5		52.6	27.9	44.7			5		38.3	33.3	21.3
	6		58.0	24.0	31.4			6		25.9	29.8	18.7
	7		50.3	14.8	17.9			7		25.9	33.4	31.3
13	1		6.4	9.9	5.4			1		28.9	19.0	14.9
	2		6.7	8.4	5.1			2		5.8	21.1	8.5
	3		4.1	6.9	3.0			3		5.4	16.3	8.5
	4	5.3	7.1	11.0	5.7	30(18)	4	6.0		21.0	14.1	6.7
	5		5.1	8.9	4.4			5		6.5	13.4	6.5
	6		7.6	13.6	10.5			6		9.3	17.7	8.1
	7		9.3	10.1	7.9			7		9.7	21.7	9.5
14	1		6.1	12.2	5.0			1		50.5	25.0	31.4
	2		5.6	11.3	3.8			2		38.2	27.1	32.9
	3		6.2	12.4	6.4			3		48.6	29.1	9.5
	4	5.3	5.5	12.2	6.5	31(19)	4	6.0		43.7	26.7	8.9
	5		4.6	14.0	7.6			5		41.0	27.3	6.9
	6		6.9	10.7	5.8			6		6.5	30.9	8.0
	7		7.4	15.4	9.3			7		8.8	20.6	8.2
15	1		9.4	22.6	14.4			1		18.2	27.1	22.7
	2		7.6	22.0	15.4			2		23.9	34.6	37.1
	3		7.2	23.5	21.3			3		25.6	31.1	33.4
	4	5.3	5.4	24.7	20.5	20	4	6.0		19.4	31.9	27.5
	5		17.0	22.6	21.7			5		19.8	36.9	37.5
	6		7.6	26.2	21.2			6		28.5	36.1	38.6
	7		8.4	25.9	23.7			7		22.6	35.3	11.4

Table 5-5 (continued)

Run No.	Wave No.	T (sec)	MK	RMS	
				F _{max}	SF
21	1	4.2	27.3	21.2	25.9
	2		28.7	22.5	29.0
	3		26.8	24.0	28.6
	4		26.0	22.4	28.9
	5		28.3	23.1	30.6
	6		27.4	21.6	30.2
	7		27.0	23.0	29.4
22	1	5.3	16.9	26.5	18.2
	2		17.7	24.8	16.4
	3		15.7	29.7	20.1
	4		16.1	30.7	31.5
	5		12.6	31.8	17.9
	6		18.2	33.1	18.9
	7		18.4	31.6	16.0
23	1	4.6	56.9	23.8	37.4
	2		47.4	15.1	19.4
	3		39.3	22.2	16.8
	4		41.5	12.3	17.7
	5		47.2	22.3	32.3
	6		40.2	20.3	30.4
	7		38.4	18.2	17.1
24	1	3.7	27.2	23.0	16.6
	2		41.7	20.7	8.8
	3		28.0	19.8	9.1
	4		12.5	25.5	21.5
	5		31.6	24.0	16.3
	6		28.4	23.4	16.3
	7		4.8	6.8	5.7
25	1	2.5	4.9	7.0	4.8
	2		5.2	7.6	5.8
	3		5.2	7.4	5.8
	4		5.2	7.4	5.8
	5		4.8	7.4	5.9
	6		5.6	8.3	6.0
	7		5.7	7.4	6.6
26	1	6.0	21.1	25.9	23.1
	2		27.9	32.1	32.3
	3		21.5	35.3	36.5
	4		21.4	33.4	32.9
	5		21.9	34.4	14.7
	6		15.2	32.2	36.3
	7		21.3	37.1	10.8

10.0 FIGURES

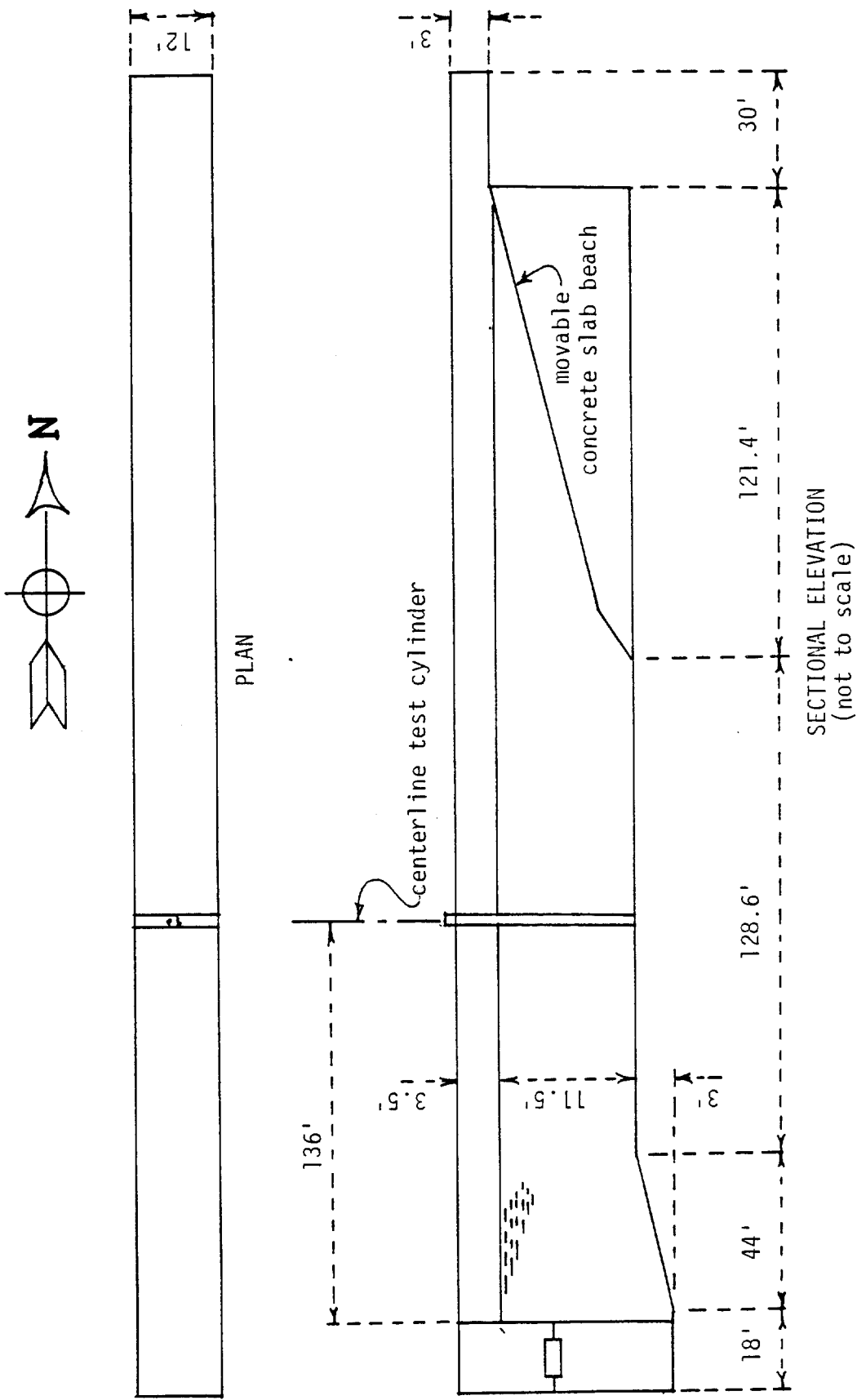


Fig. 3-1 OSU Wave Flume

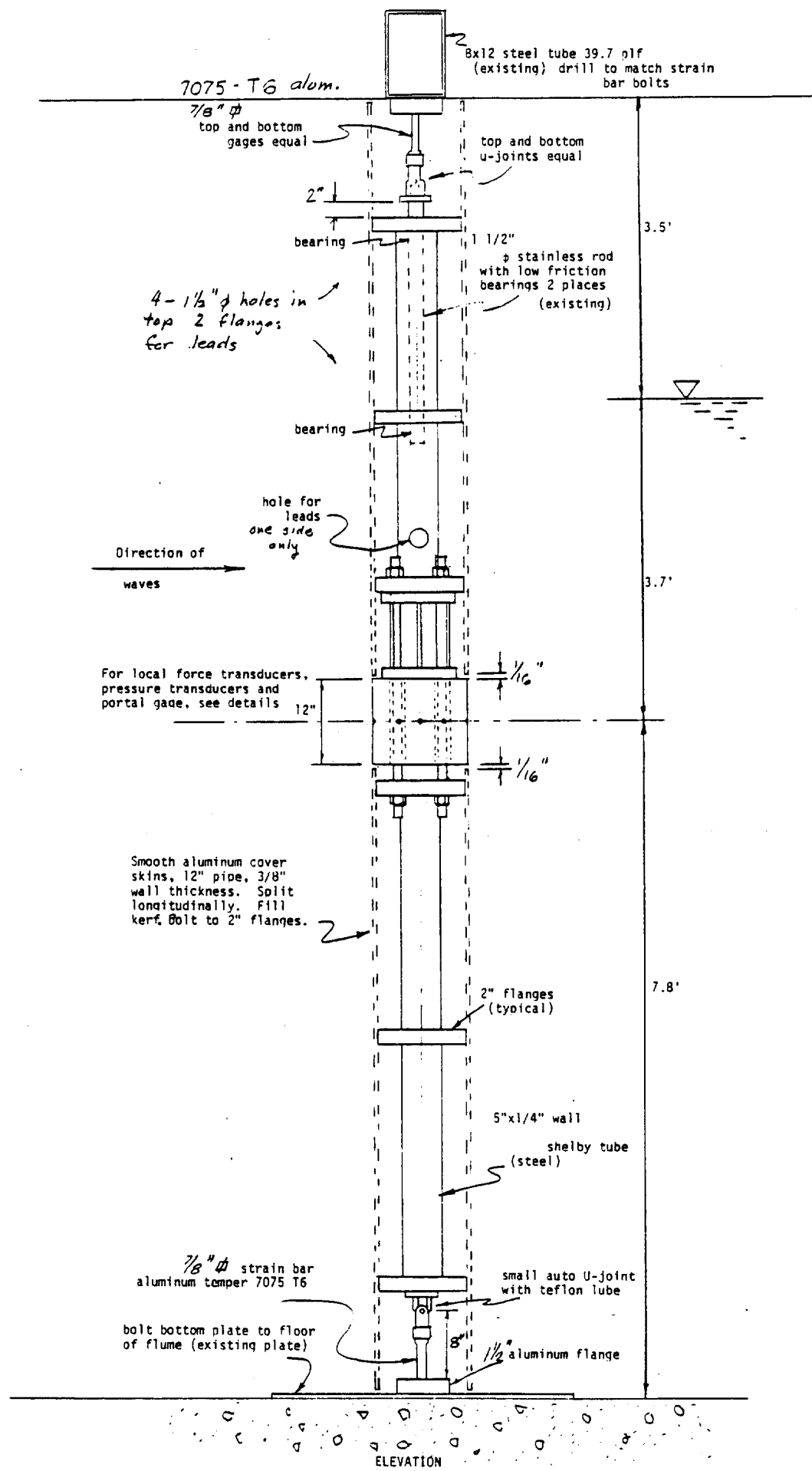


Fig. 3-2 Sectional elevation of test cylinder

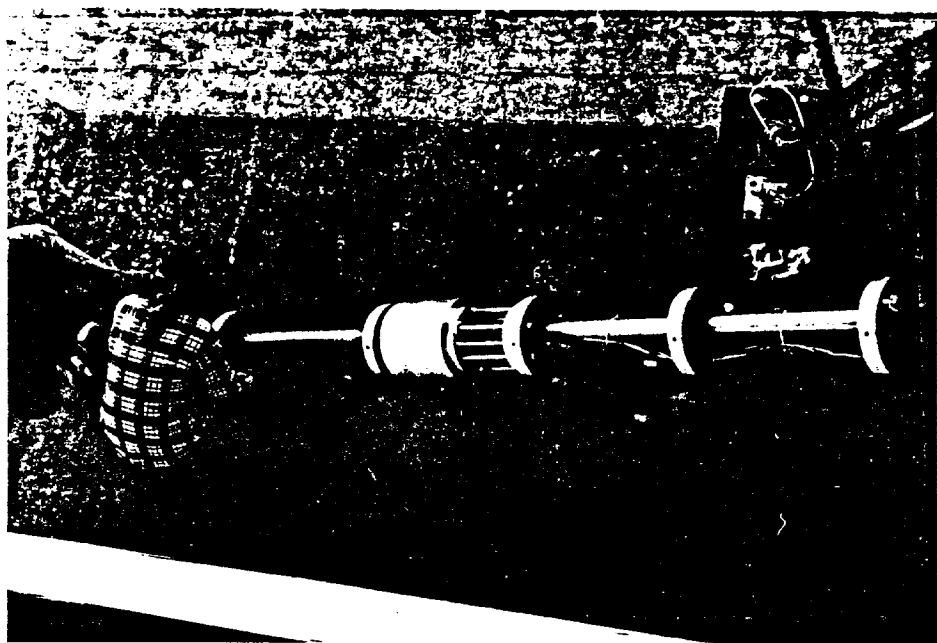


Fig. 3-3 Cylinder core during installation

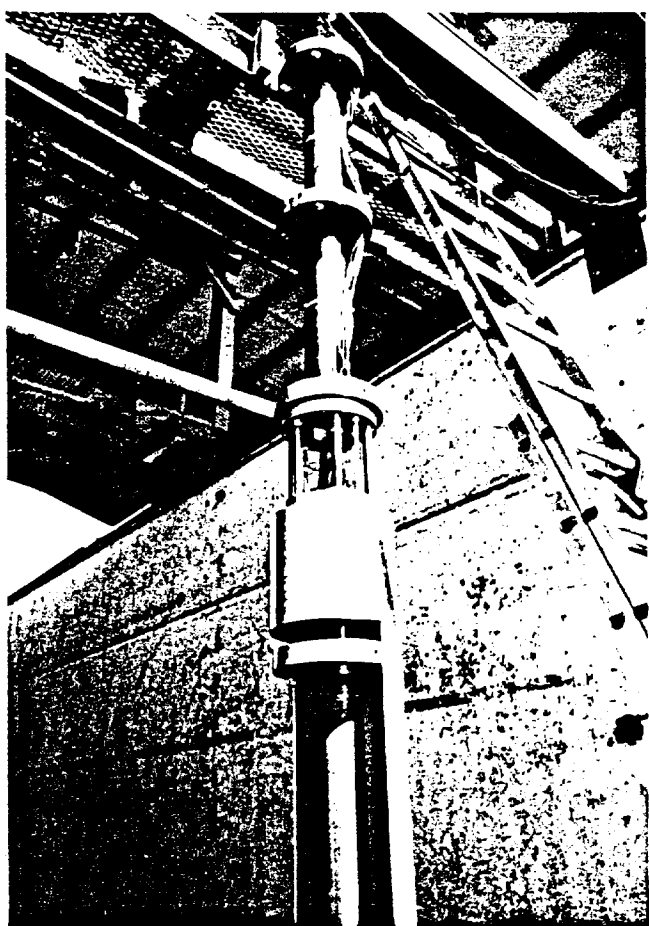


Fig. 3-4 Cylinder core in vertical position with 1/2 of lower skin in place

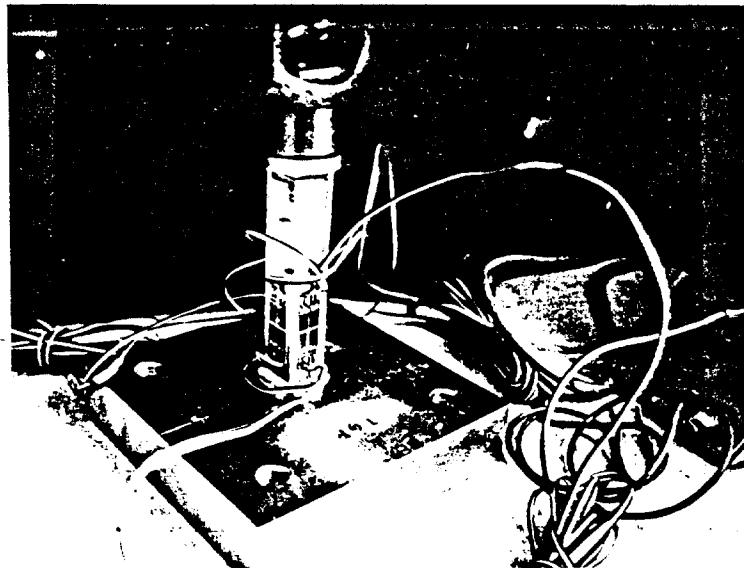


Fig. 3-5 Bottom (and top) support strain gaging

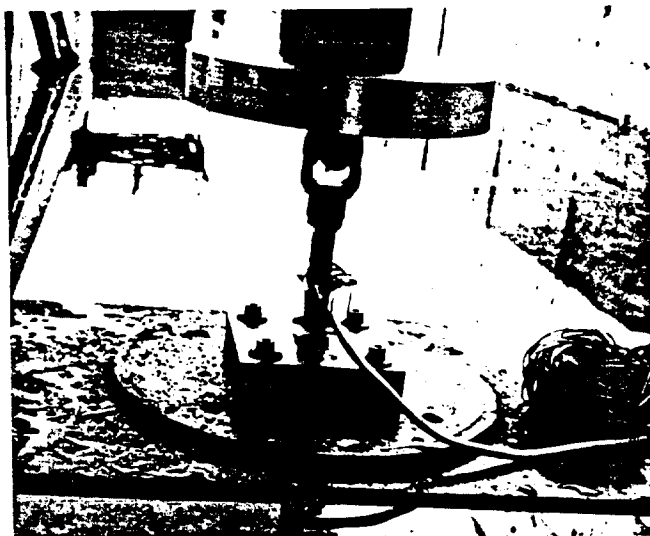


Fig. 3-6 Bottom support bolting to WRL floor



Fig. 3-7 Skin installation at bottom support

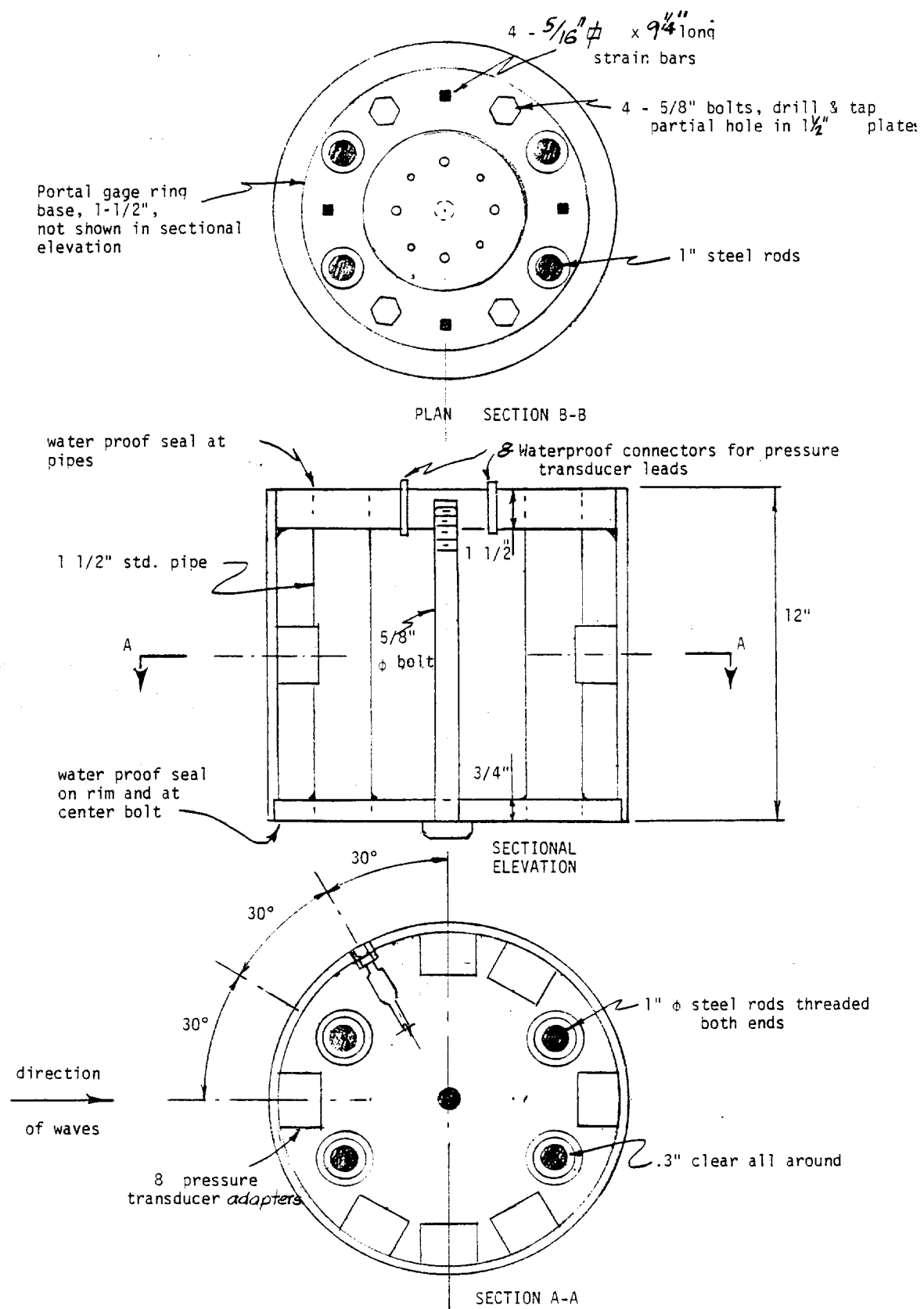


Fig. 3-8 LOCAL FORCE TRANSDUCER AND PRESSURE TRANSDUCERS (aluminum)

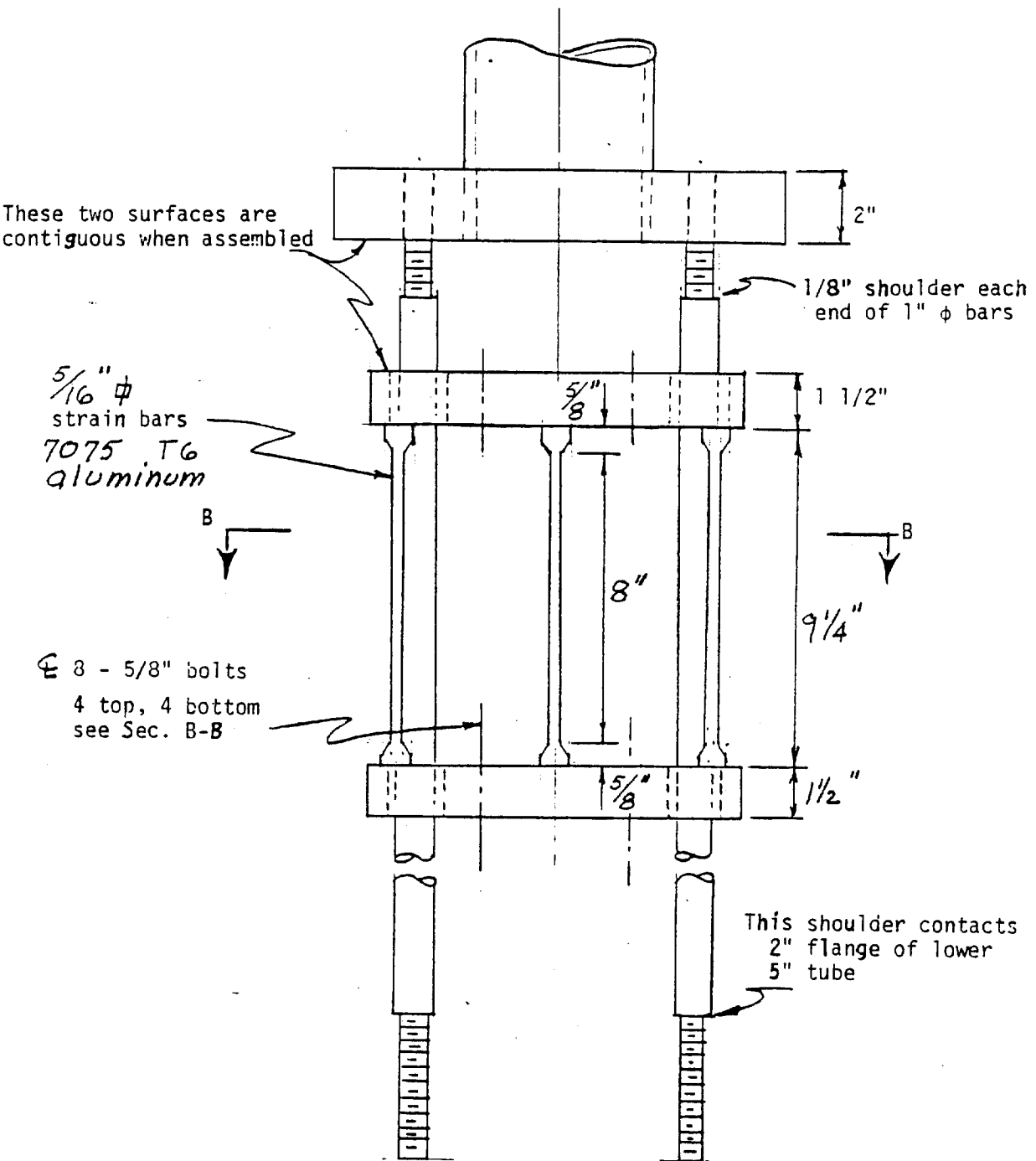
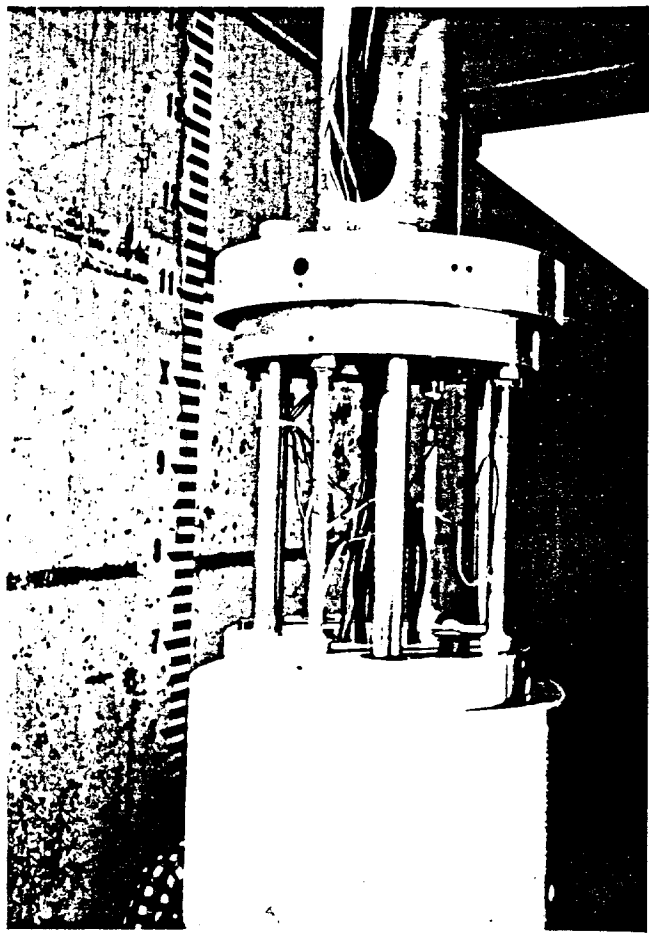
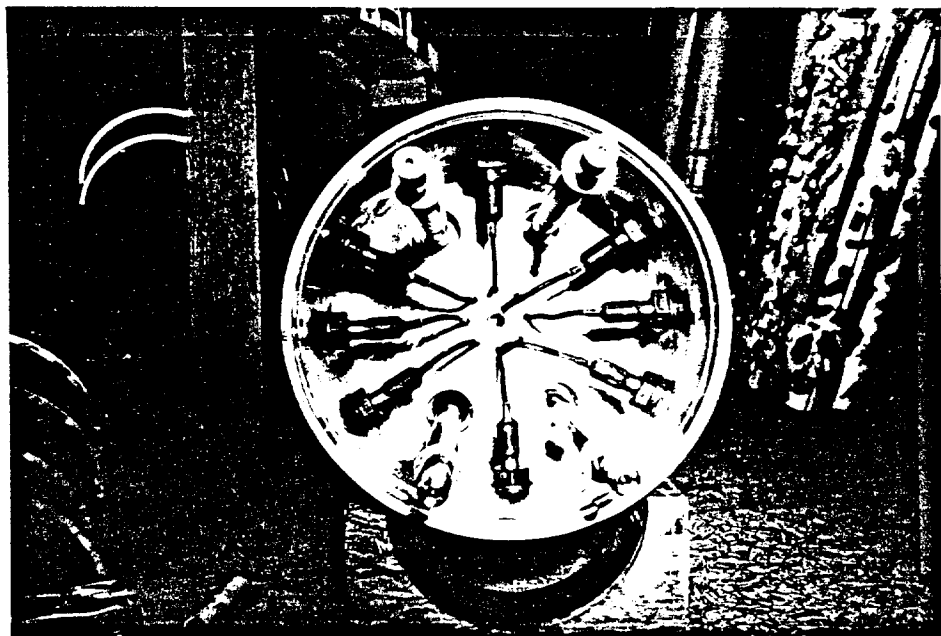


Fig. 3-9 PORTAL GAGE FOR LOCAL FORCE TRANSDUCER (exploded view)

OSU Wave Research Facility



' Fig. 3-10 Local force transducer strain bar support. Pressure ports shown prior to filling and sanding the immediate area around them.



' Fig. 3-11 Interior of the LFT with 8 pressure transducers and 4-1" round bars which provide structural continuity for the core structure.

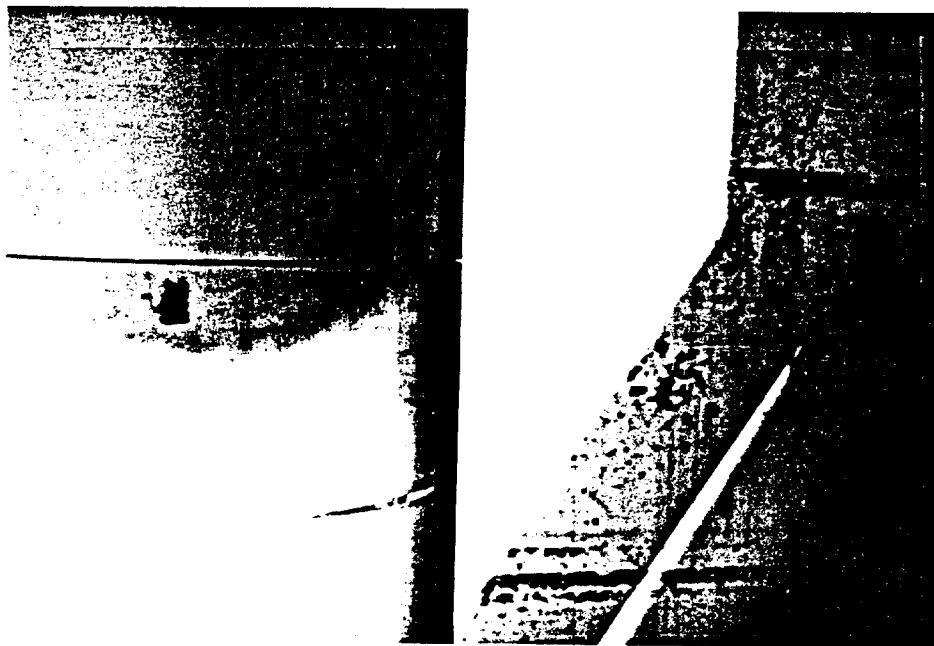


Fig. 3-12 Perfect alignment demonstrated at one azimuth position of the LFT, bottom joint

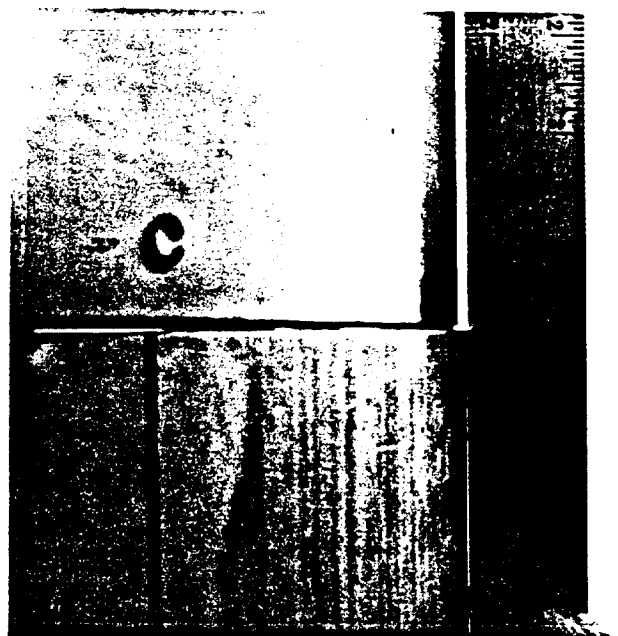
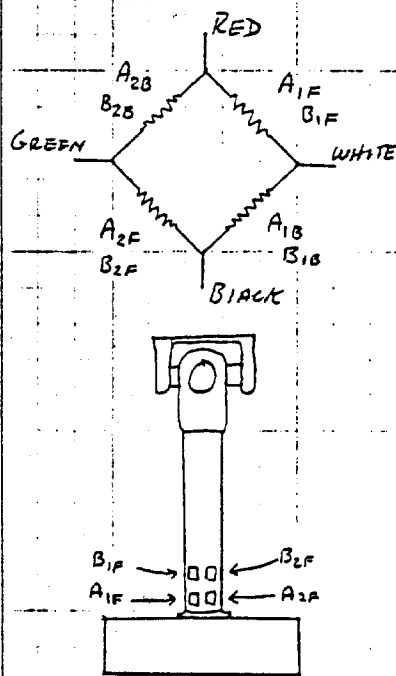


Fig. 3-13 The worst alignment for the LFT at the top joint. Offset ≈ 1.1 mm, although it looks larger because of the sun reflection.

APRIL 1983

NCEL - VERTICAL CYLINDER STRAIN GAUGE WIRING

TOP & BOTTOM FORCE BEAMS



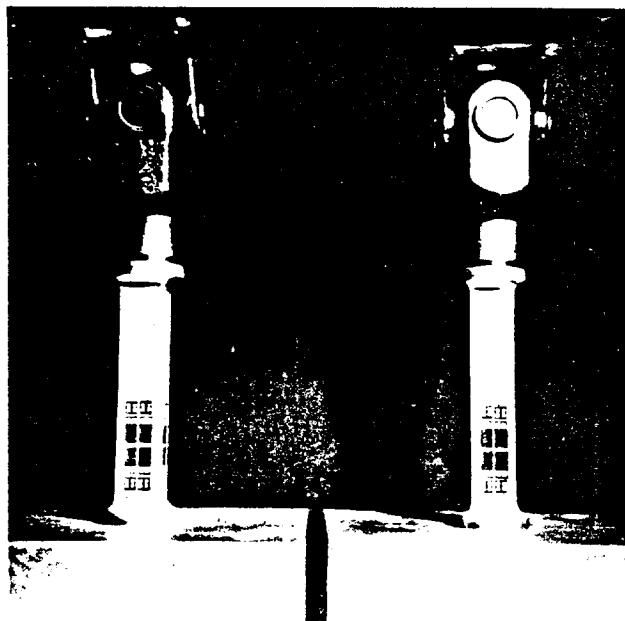
F - FRONT, B - BACK

A - MOST SENSITIVE

B - LEAST SENSITIVE

- Primary

- Backup

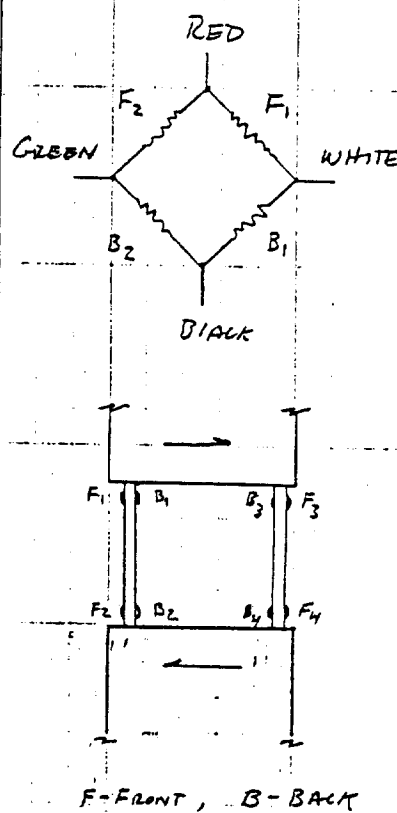


TYPE	SENSITIVE DIRECTION	GAUGE #	SENSITIVITY	EXCIT. VOLTAGE	GAIN	USE
					CALIB.	RUNS
TOP	NORTH 1	1	MOST	10V.	200	X X
	NORTH 2	2	LEAST	"	" X	
	EAST 1	3	MOST	"	" X	
	EAST 2	4	LEAST	"	" X X	X
BOTTOM	NORTH 1	5	MOST	"	" X	X
	NORTH 2	6	LEAST	"	" X	
	EAST 1	7	MOST	"	" X	X
	EAST 2	8	LEAST	"	" X	

Fig. 3-14 Bottom and top support strain gage wiring

APRIL 1983

NCEL - VERTICAL CYLINDER STRAIN GAUGE WIRING
LOCAL FORCE BEAMS



F-FRONT, B-BACK



TYPE	SENSITIVE DIRECTION	GAUGE #	SENSITIVITY	EXCIT. VOLTAGE	GAIN	CALIB.	USE RUNS
CENTER (Local)	NORTH 1	9	SAME	10V.	300	x	x
	NORTH 2	10	"	"	"	x	x
	EAST 1	11	"	"	4	x	x
	EAST 2	12	"	"	"	x	x

Gauge #9 was electronically summed with Gauge #10
" #11 " " " " " " = 12

Fig. 3-15 Local force transducer strain gage wiring

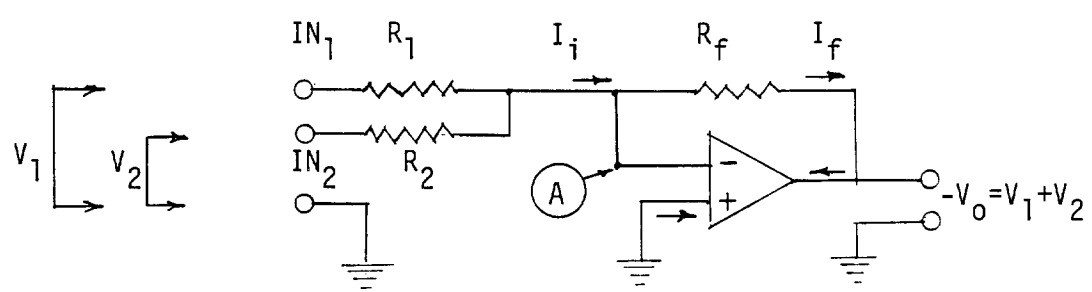


Fig. 3-16 Typical summing operational amplifier

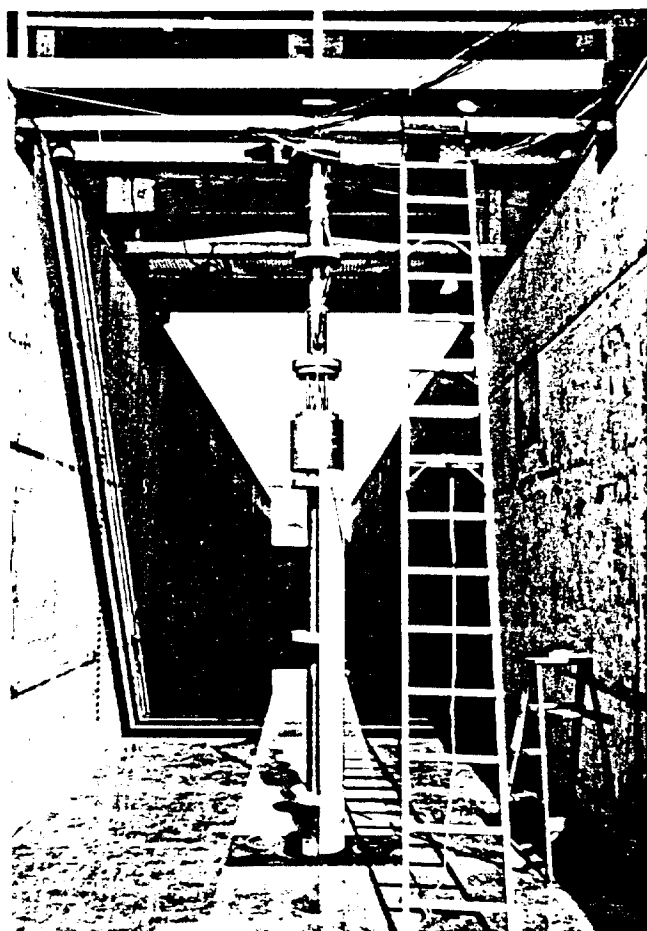


Fig. 3-17 Nearly completed installation with one of the four skins attached



Fig. 3-18 Three of the four skins bolted on. Final painting and smoothening around the pressure parts in progress.

west current meter

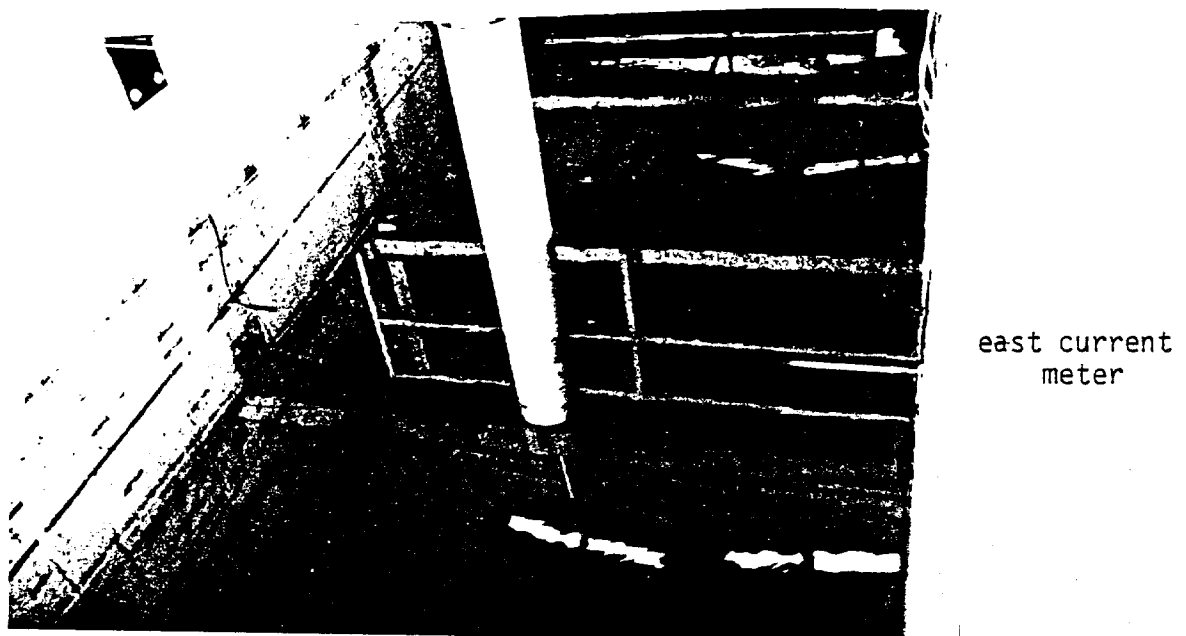


Fig. 3-19 Final arrangement just prior to testing.
Water level is at the test level.

APRIL 1983

NCEL - VERTICAL CYLINDER - RUN TIME WIRING

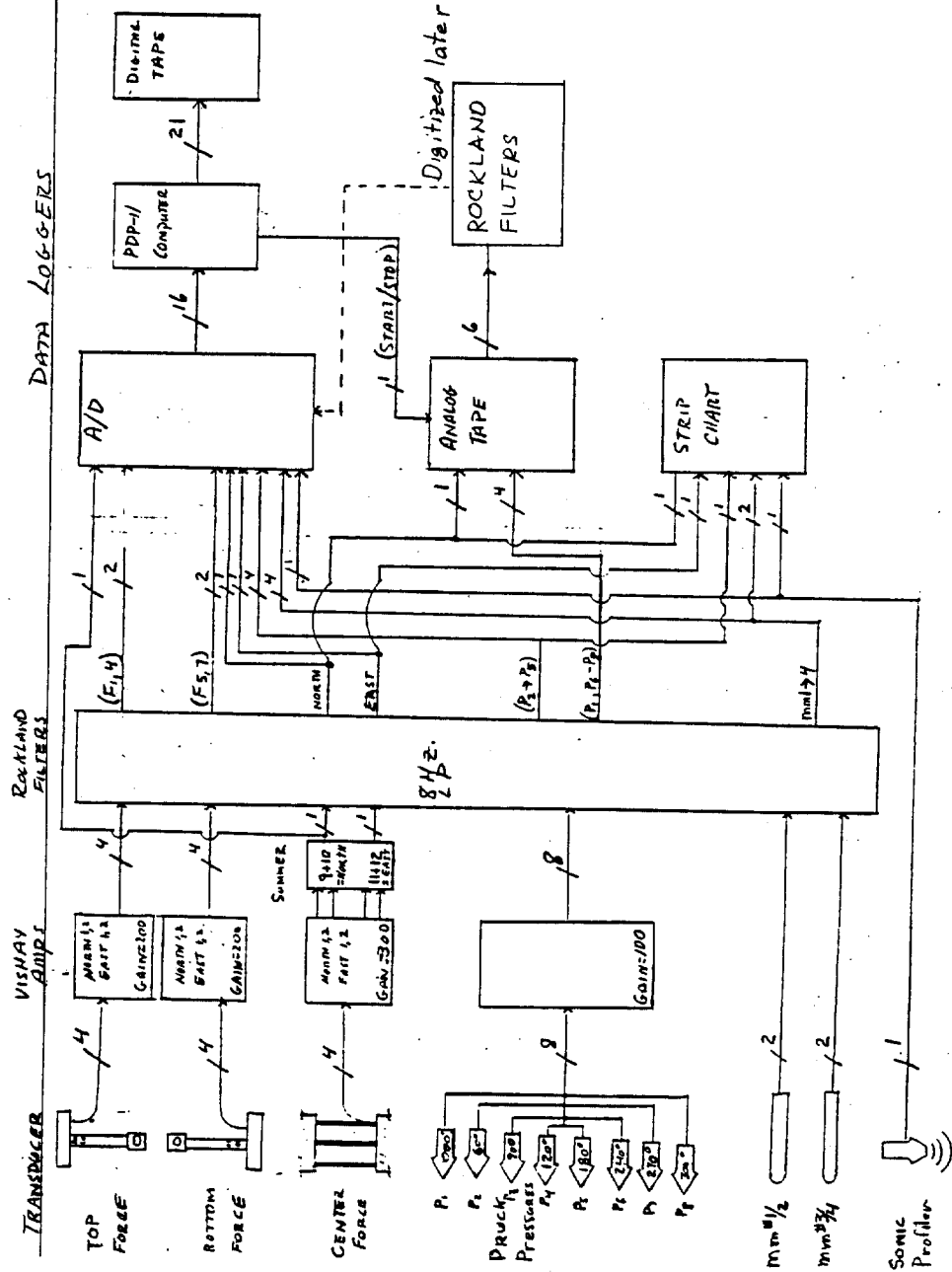


Fig. 3-20 Signal routing

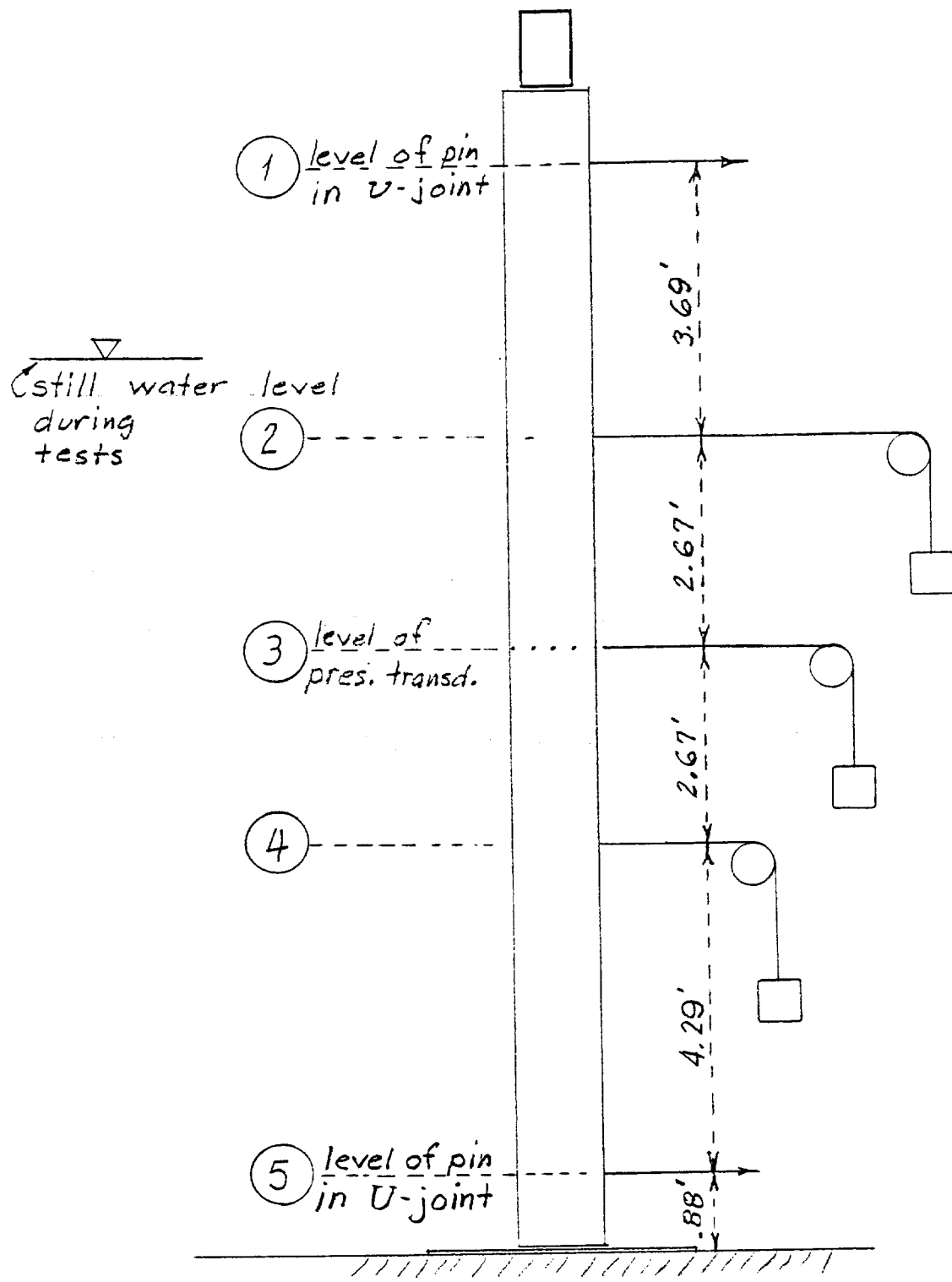


Fig. 3-21 Example of XXX Calibration



Fig. 3-22 XXX Calibration to the east in air

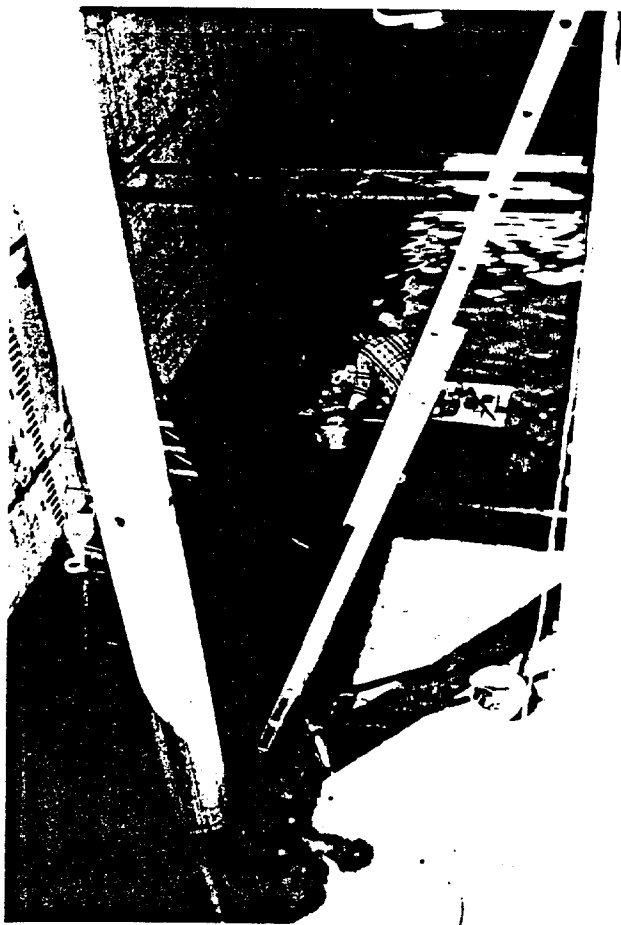


Fig. 3-23 Calibrating at position 5 with the bottom support submerged. Also shown is the horizontal truss used for calibrating at position 3. The completely assembled vertical cylinder is on the left.



Fig. 3-24 Method of applying torsional calibration loads

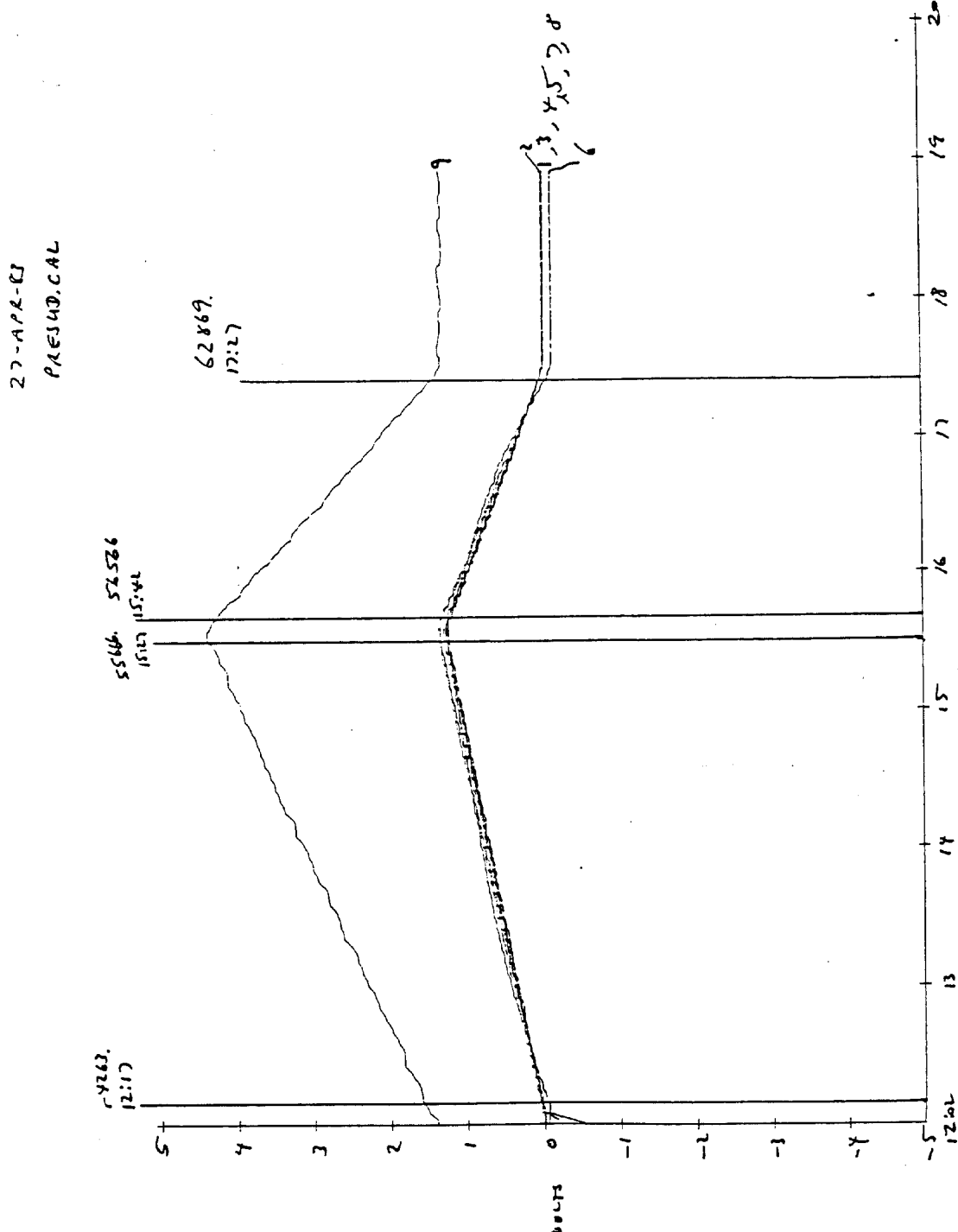


Fig. 3-25 Pressure Transducer Calibrations

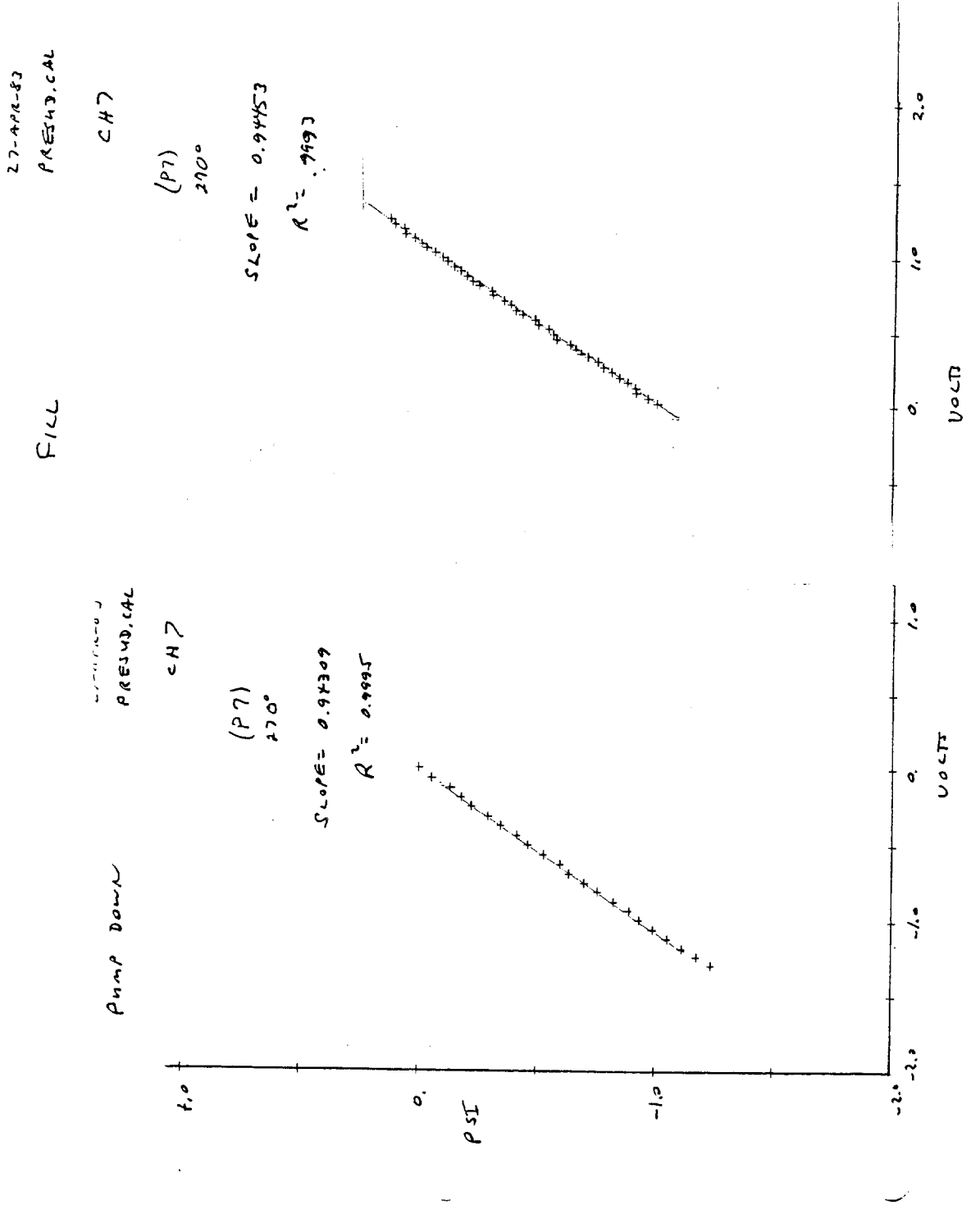


Fig. 3-26 Typical pressure transducer calibration curve

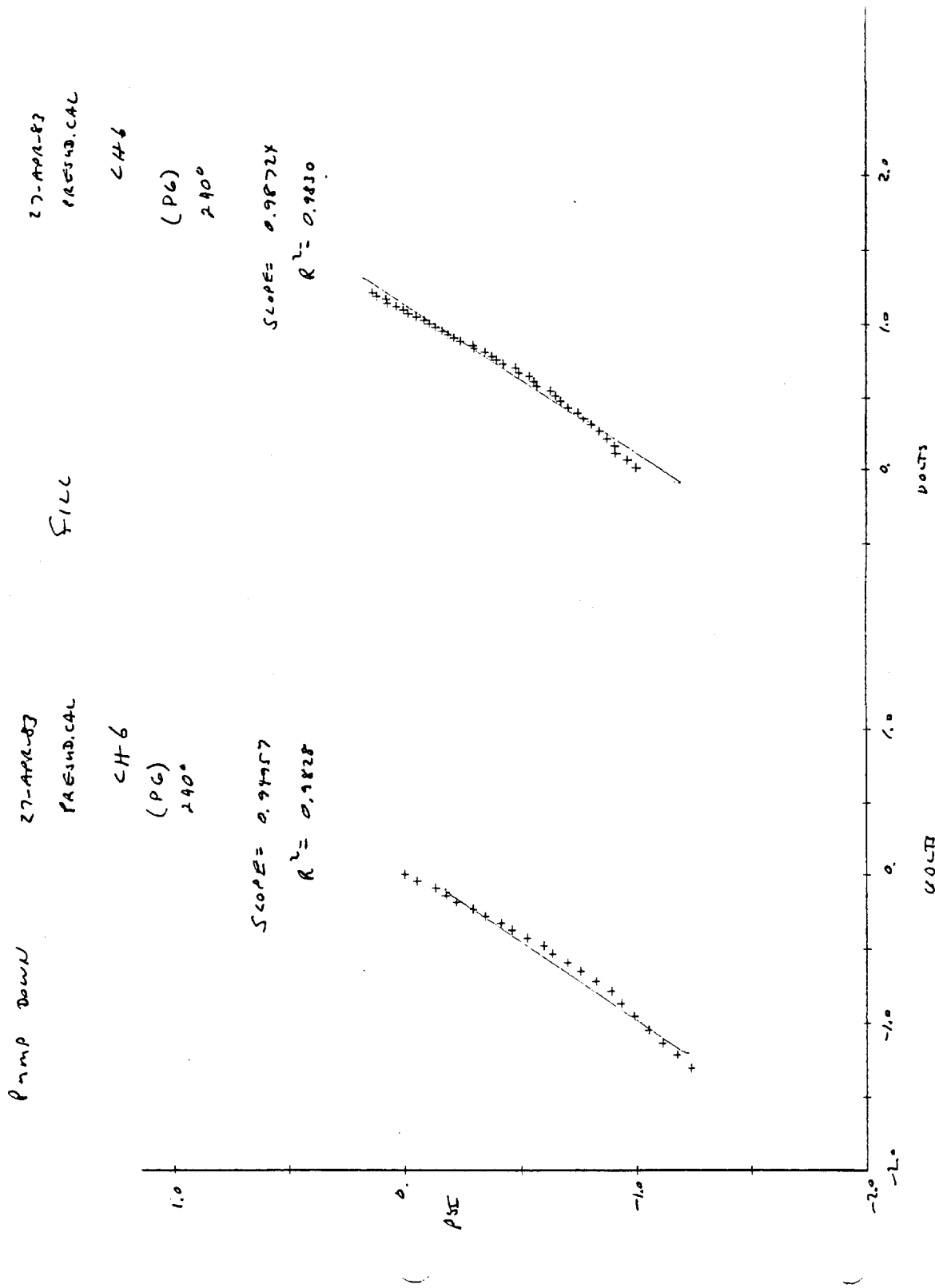


Fig. 3-27 P6 (240°) pressure transducer calibration curve. (Of the 8 meters, this is the only nonlinear one.)

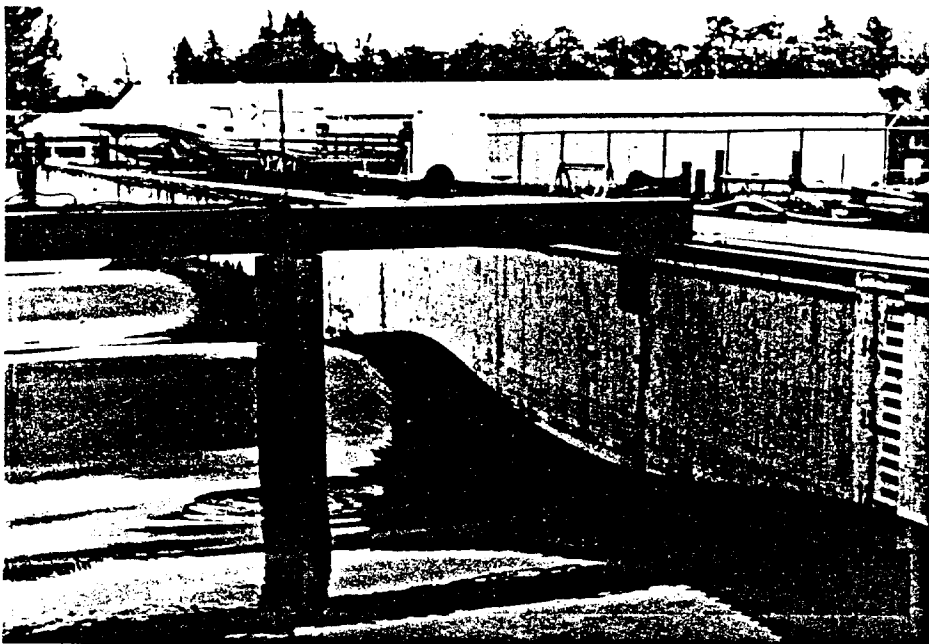


Fig. 3-28



Fig. 3-29

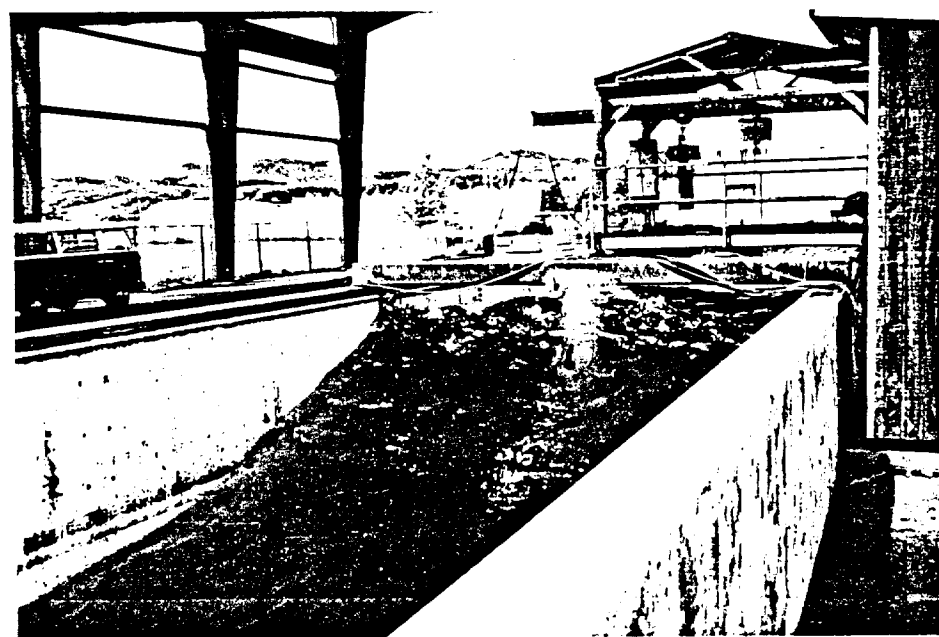


Fig. 3-30

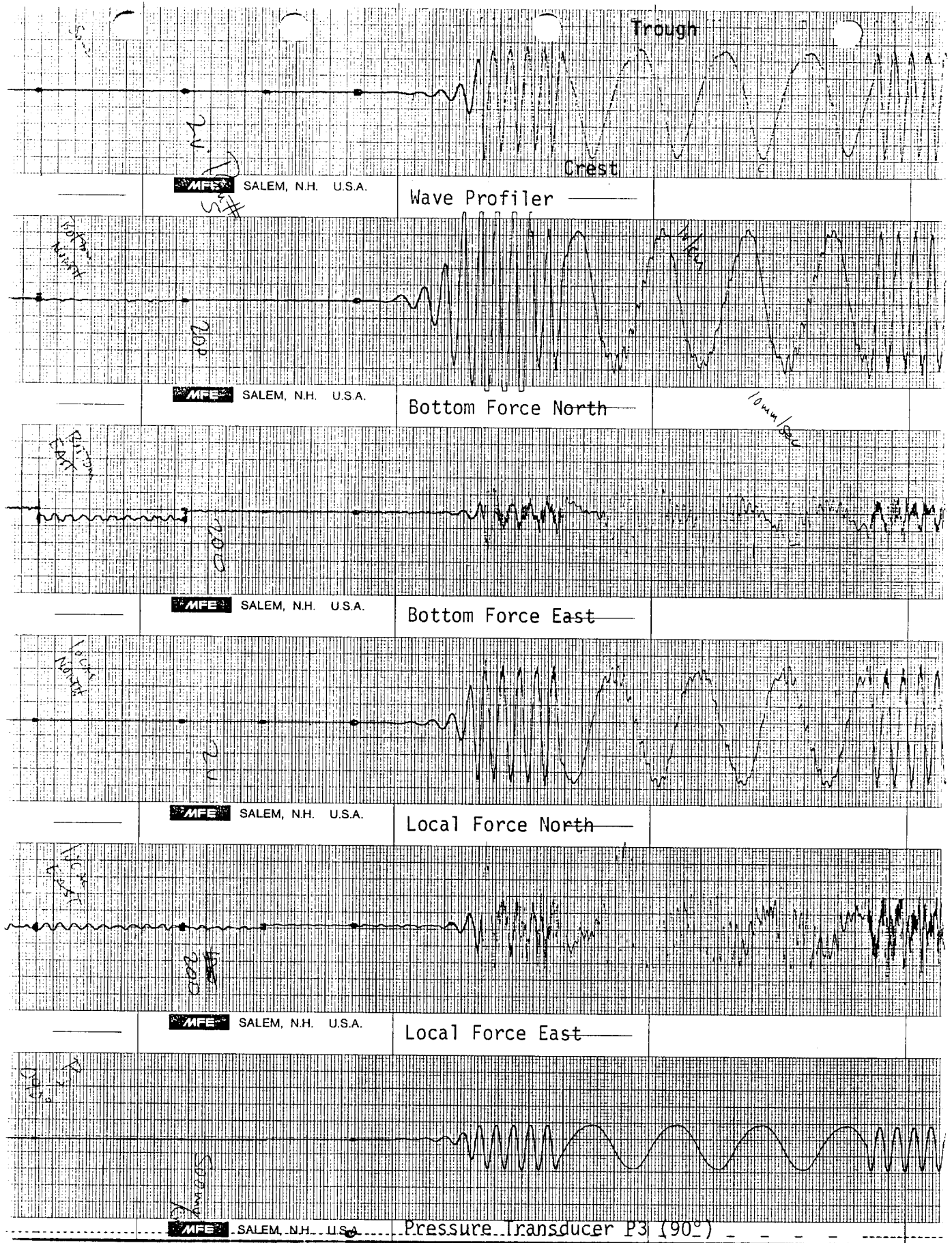


Fig. 4-1 Sample strip chart recording for Run #5

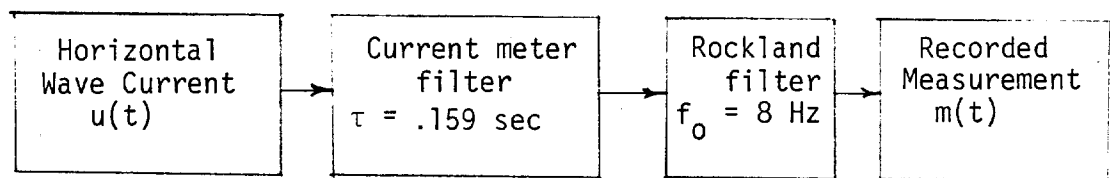
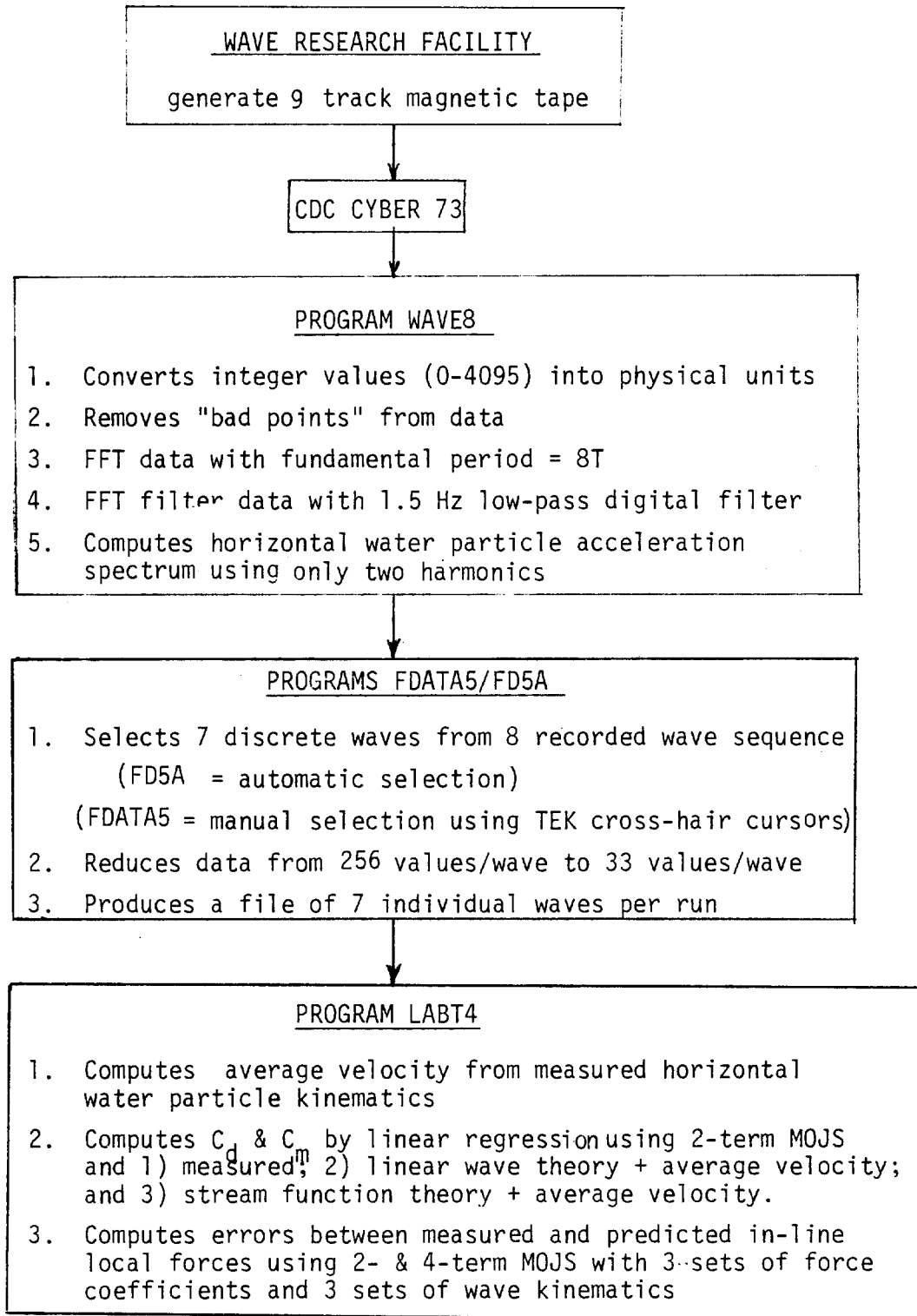


Fig. 4-2 Current measurement and recording diagram

Fig. 4-3 Flow Chart of NCEL Data Processing



R25H37.005
 2,5,3,7,0.
 21,2048,256,256,21
 WAVE PROFILE
 FT
 16,-53333,0.,1.5,0.
 E VERTICAL CURRENT
 FT/SEC
 0,-20.6,-0.159,1.5,8.
 E HORIZONTAL CURRENT
 FT/SEC
 9,20.6,-0.159,1.5,8.
 1,0,1,0,1,1
 TRANSVERSE FORCE
 LB
 6,-4.856,0.,1.5,8.
 1,0,1,1,1,1
 INLINE FORCE
 LB
 5,-4.86,0.,1.5,8.
 TOP INLINE FORCE
 LB
 1,41.345,0.,1.5,8.
 TOP TRANSVERSE FORCE
 LB
 2,4.4095,0.,1.5,8.
 BTM INLINE FORCE
 LB
 3,41.1675,0.,1.5,8.

ANALOG INLINE FORCE
 LB 17,-4.86,0.,1.5,8.
 1,0,1,1,1
 PRESSURE P1 (0 DEG)
 PSI 18,1,03554,0.,1.5,8.
 1,0,1,0,1,1
 PRESSURE P6(240 DEG)
 PSI 19,0,96752,0.,1.5,8.
 1,0,1,0,1,1
 PRESSURE P7(270 DEG)
 PSI 20,0,93050,0.,1.5,8.
 1,0,1,0,1,1
 PRESSURE P8(300 DEG)
 PSI 21,1,00447,0.,1.5,8.
 1,0,1,0,1,1
 THIS HEADER IS FOR WAVE8 PROGRAM
 27-SEP-83 0.6.
 END OF FILE

Fig. 4-4 Sample calibration constant format for Run #5

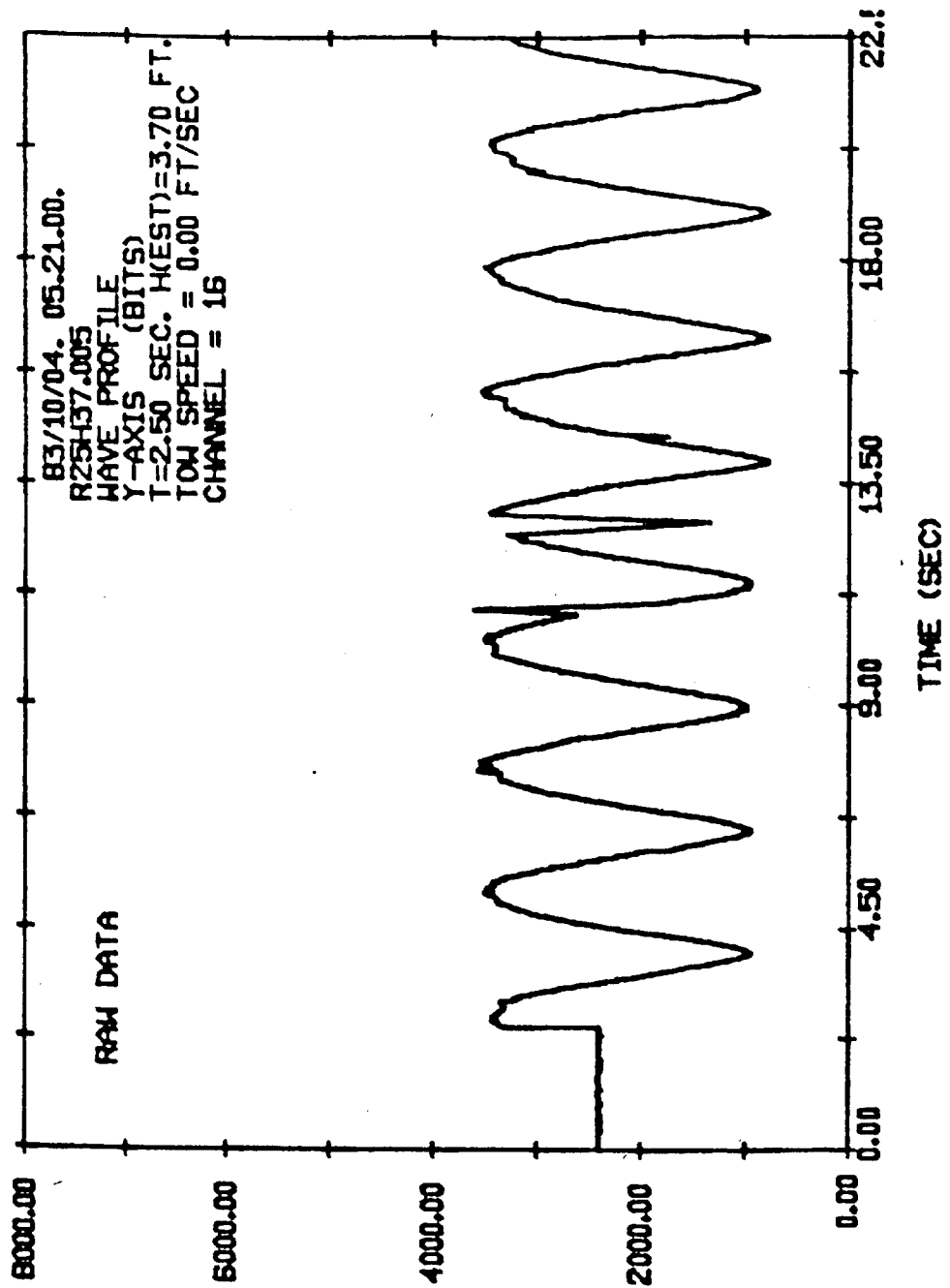


Fig. 4-5 Sample wave profile in integer values for Run #5 (note the "bad point" values in waves #3 and #4)

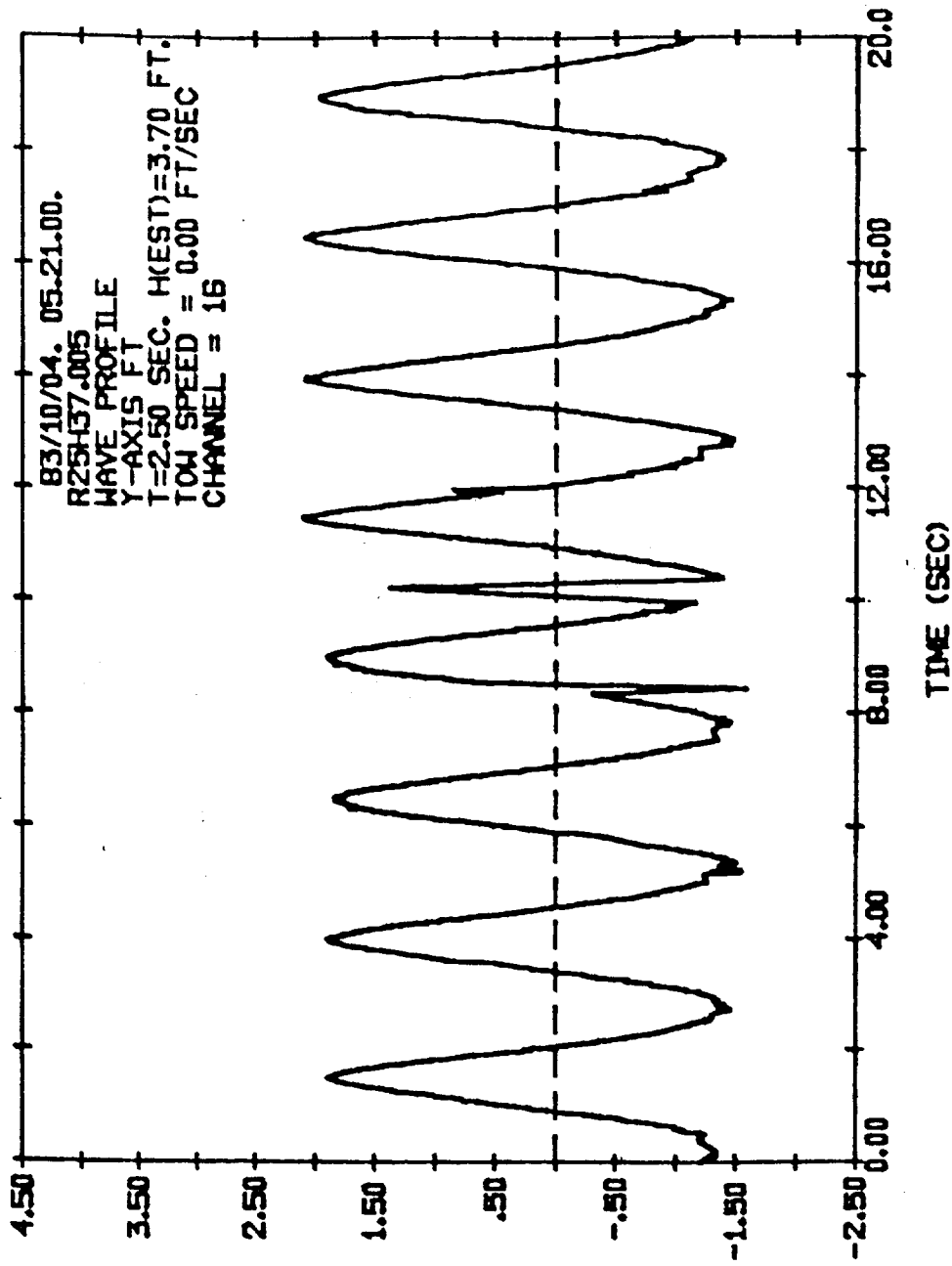


Fig. 4-6 Sample wave profile in physical units following calibration for Run #5 (note that profile is inverted from Fig. 4-5)

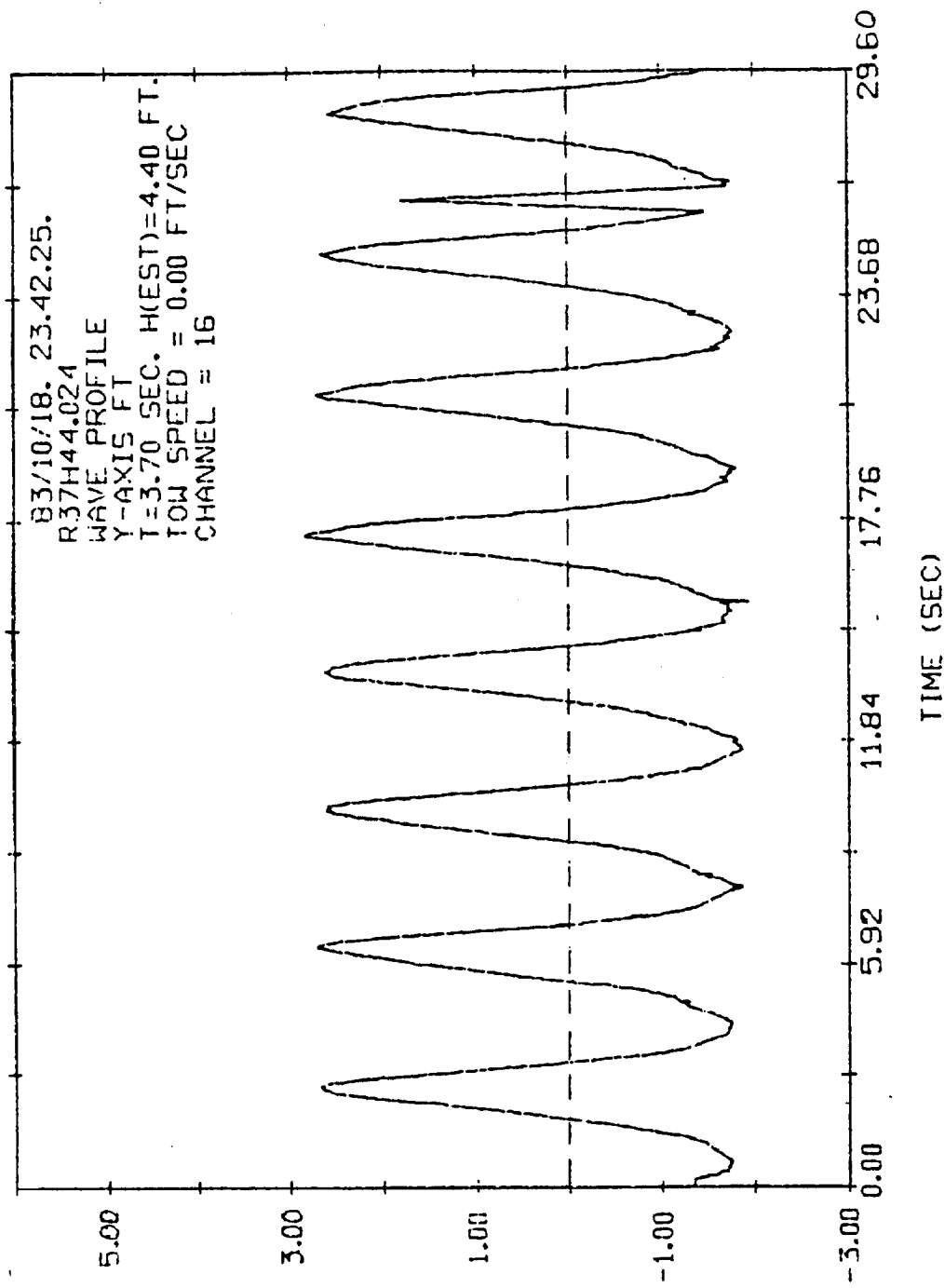


Fig. 4-7 Sample wave profile with "bad point wave" for Run #24

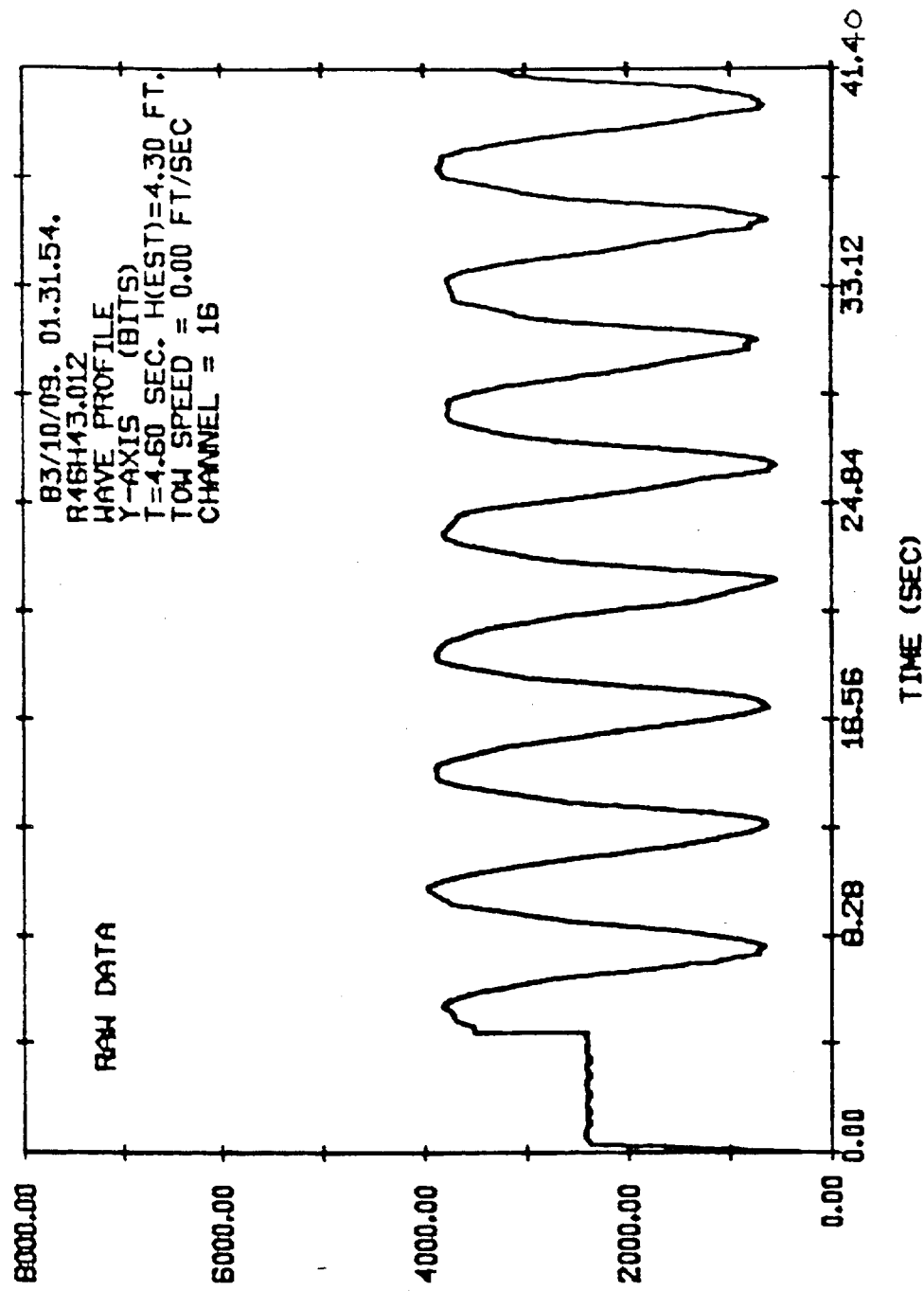


Fig. 4-8 Sample wave profile in integer values for Run #12 (note the absence of any "bad point" values)

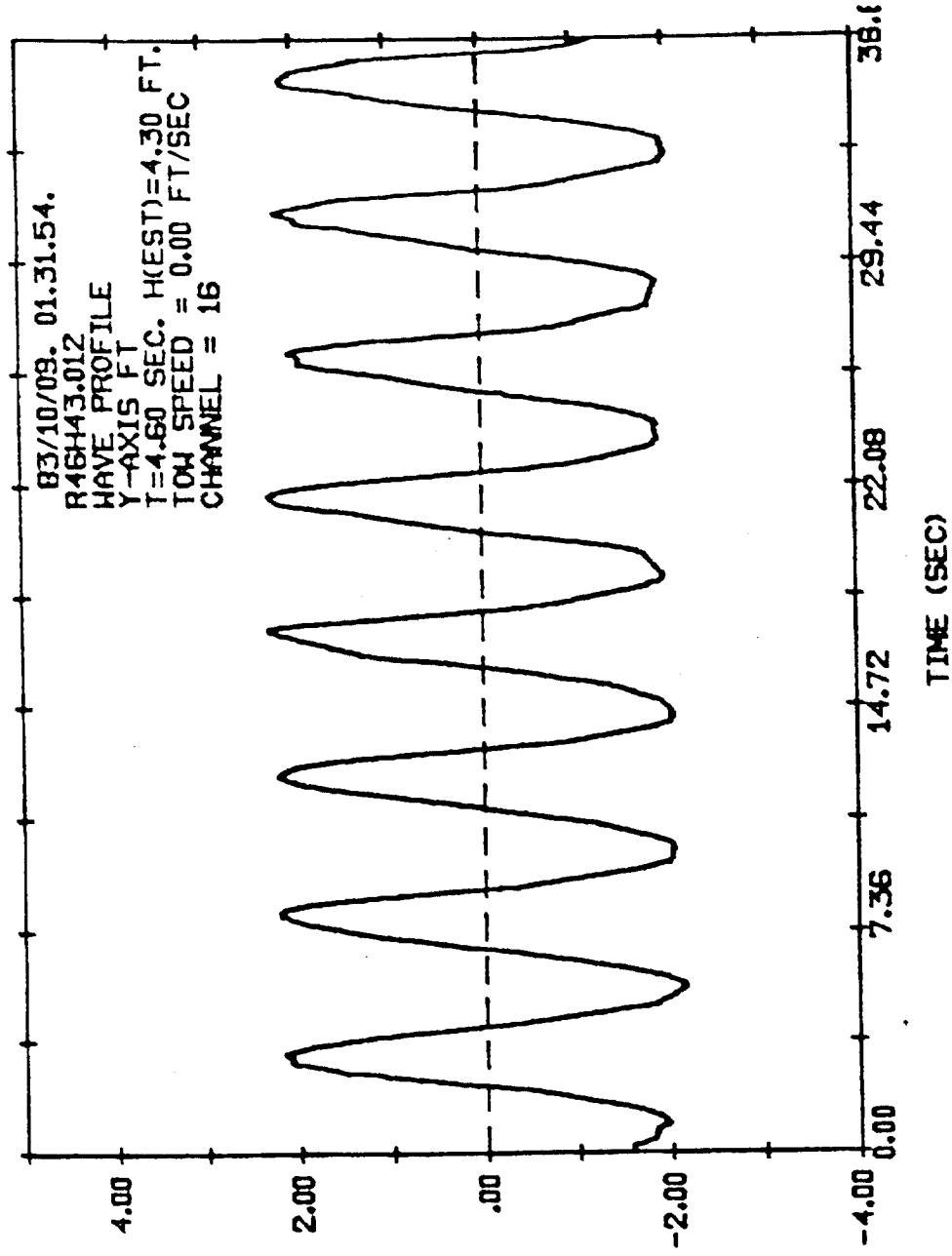


Fig. 4-9 Sample wave profile in physical units following calibration for Run #12 (note that the profile is inverted from Fig. 4-8)

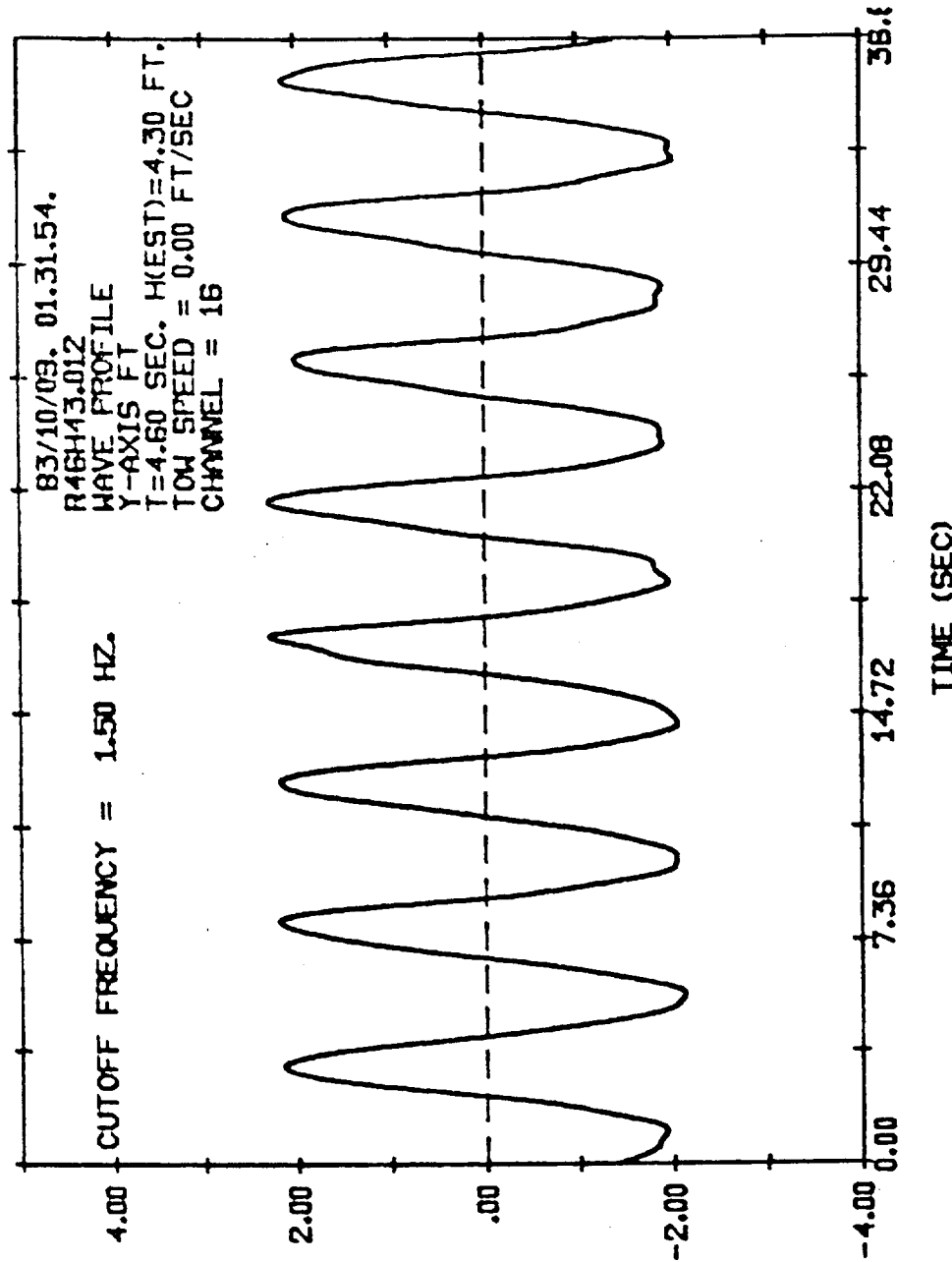


Fig. 4-10 Typical sample wave profile without any "bad points" for Run #12

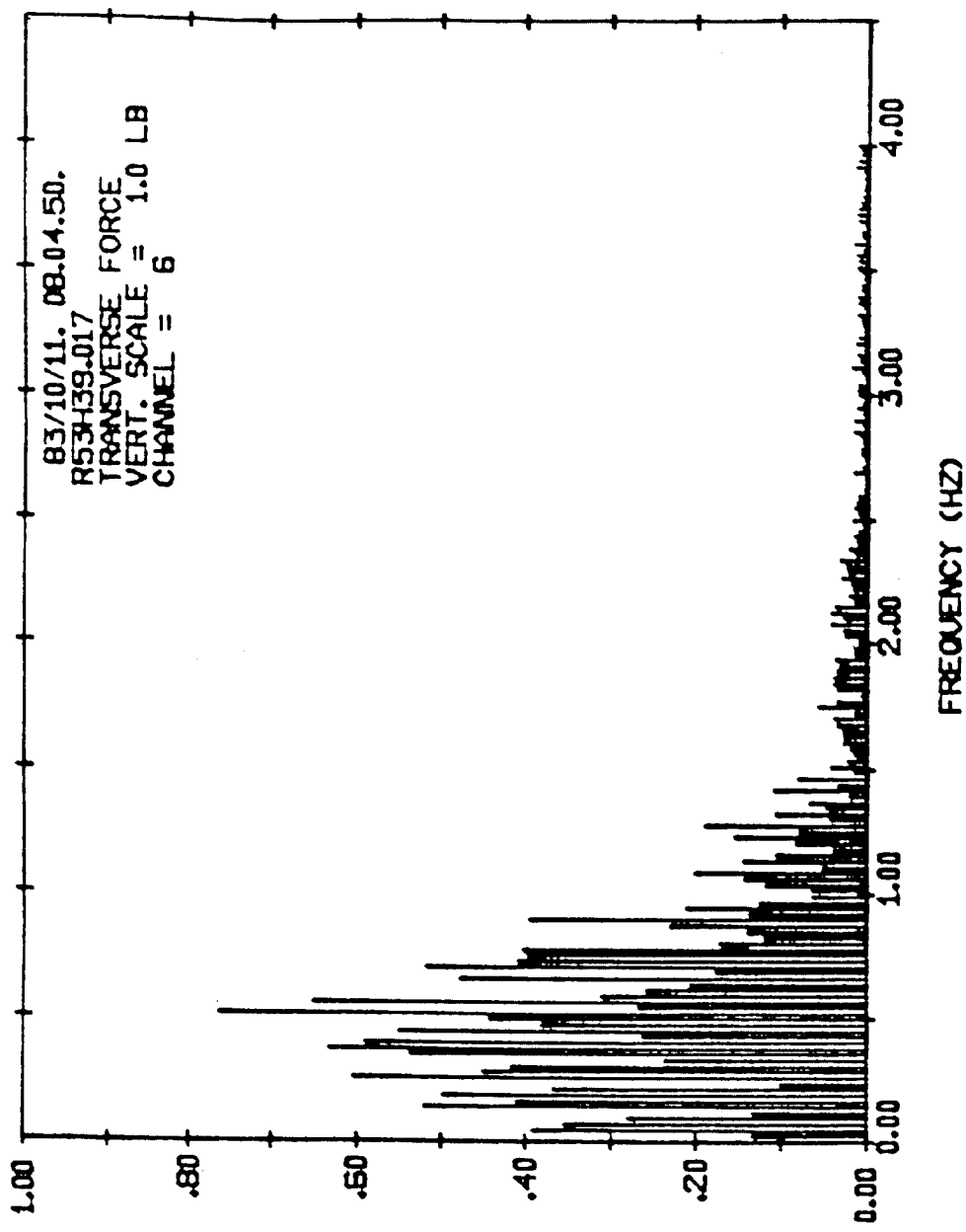


Fig. 4-11 Sample transverse force amplitude spectrum from the local force transducer for Run #30

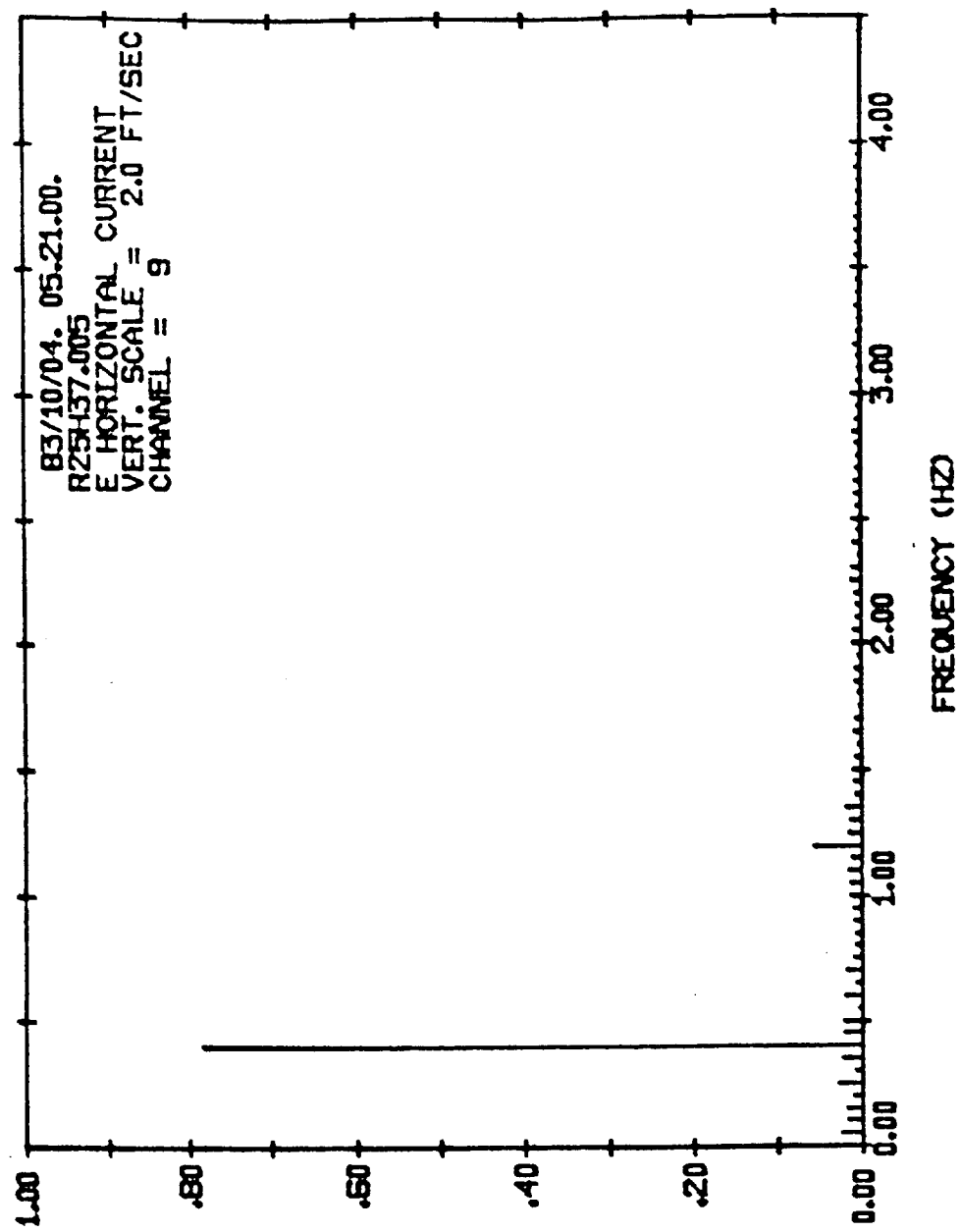


Fig. 4-12 Sample amplitude spectrum for the horizontal current for Run #5

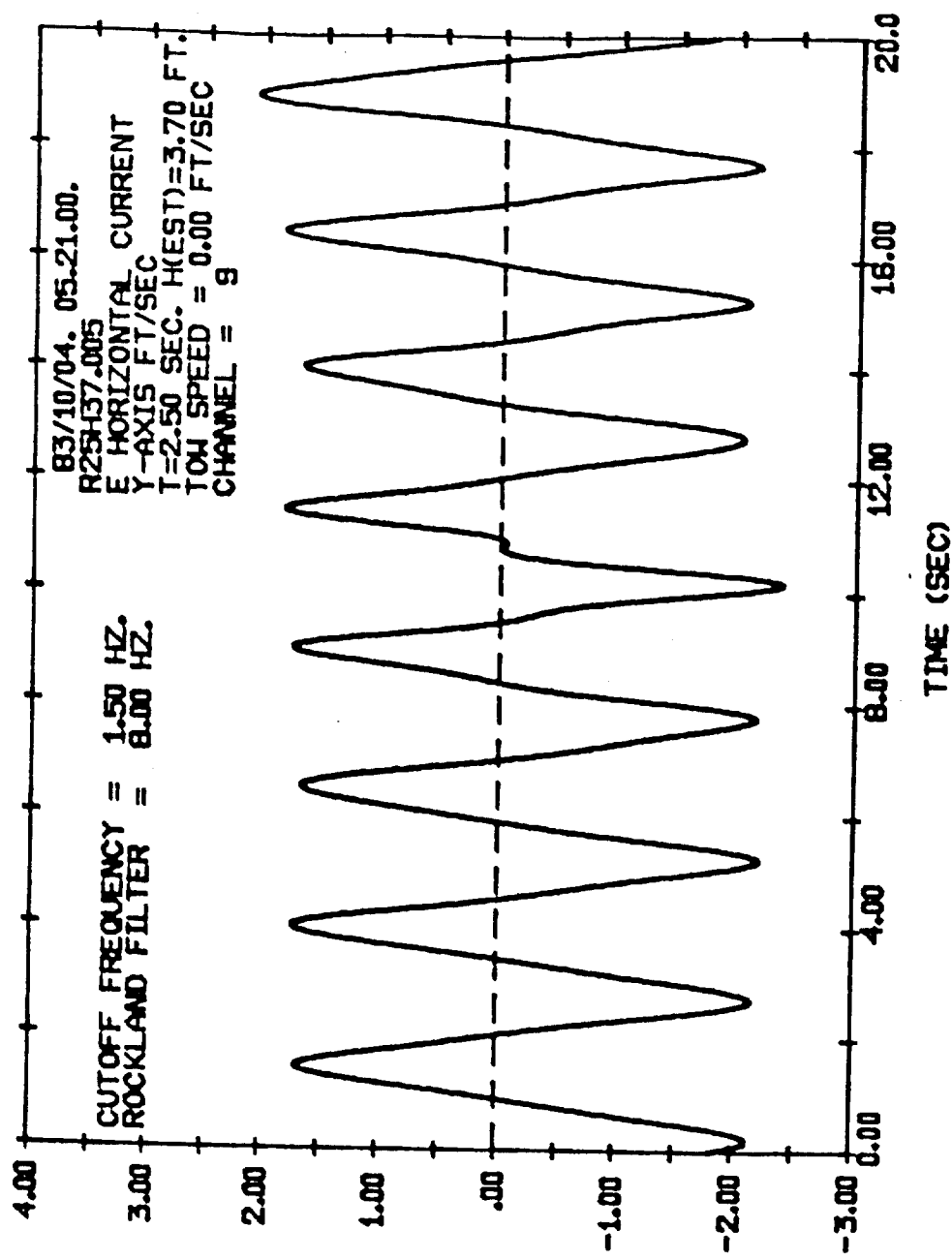


Fig. 4-13 Sample FFT filtered time series for the horizontal current for Run #5 ($f_c = 1.5 \text{ Hz}$)

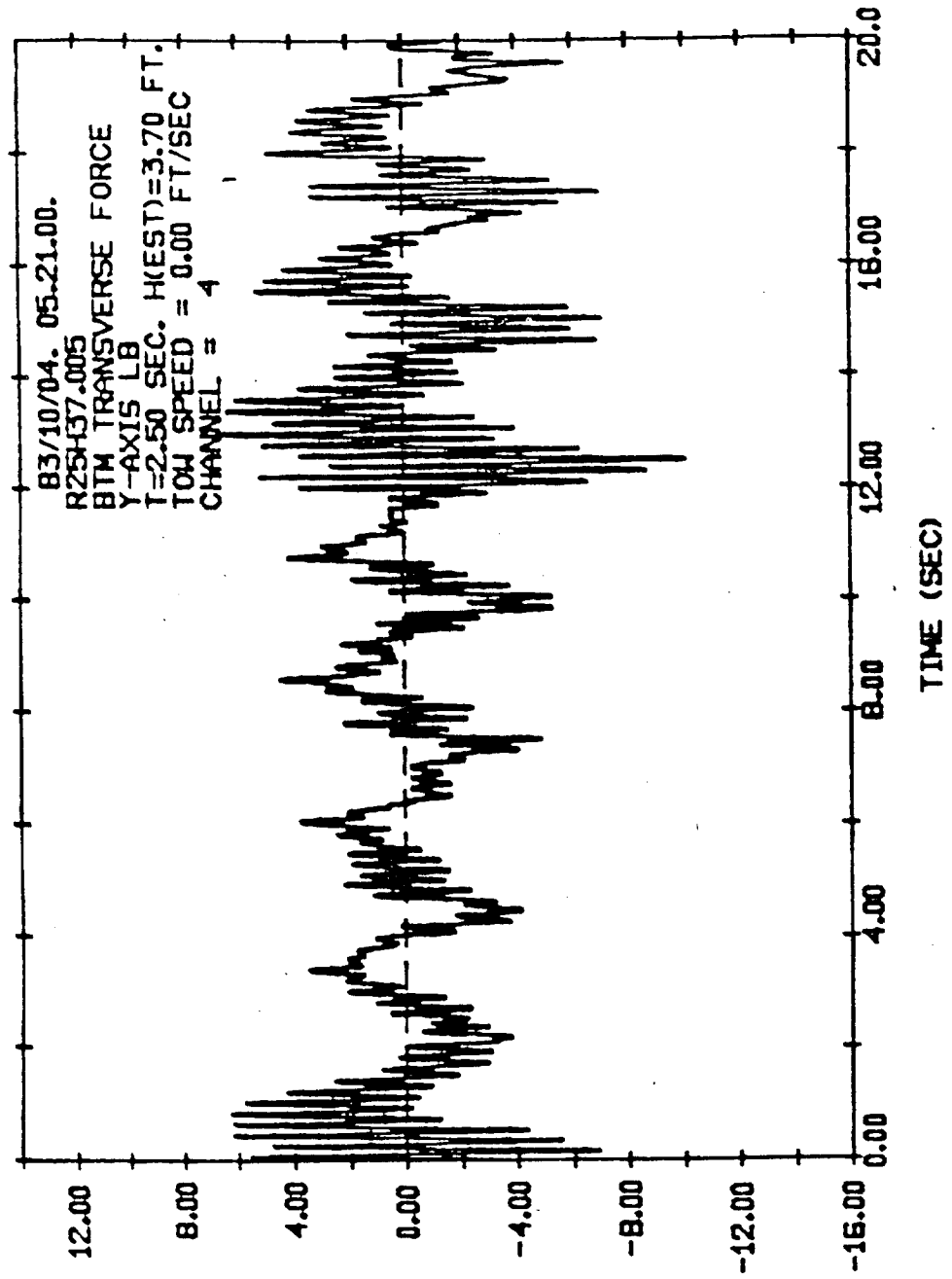


Fig. 4.14 Sample time series of the bottom transverse force before FFT filtering for Run #5

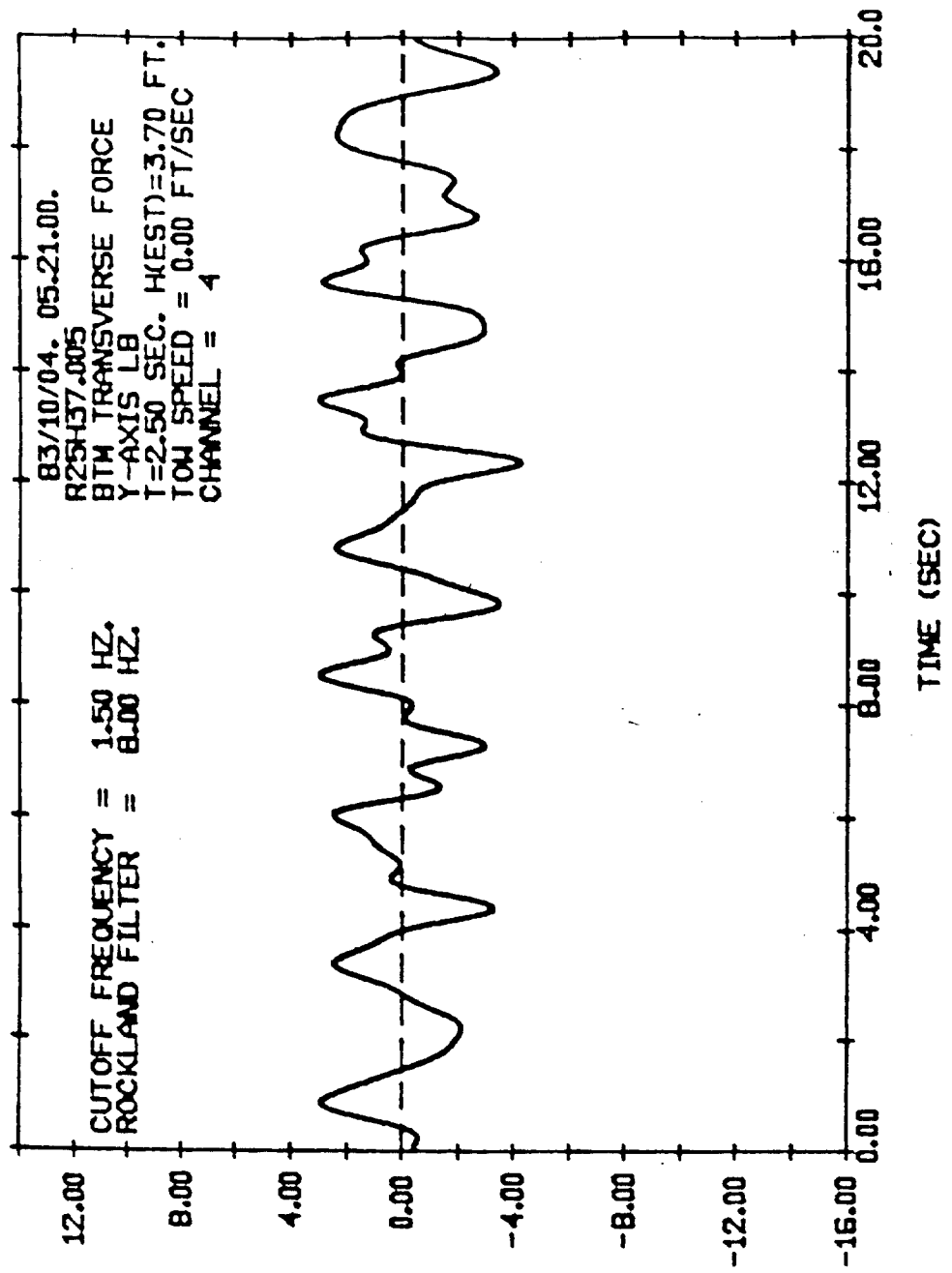


Fig. 4-15 Sample time series of the bottom transverse force after FFT filtering at $f_c = 1.5 \text{ Hz}$ for Run #5

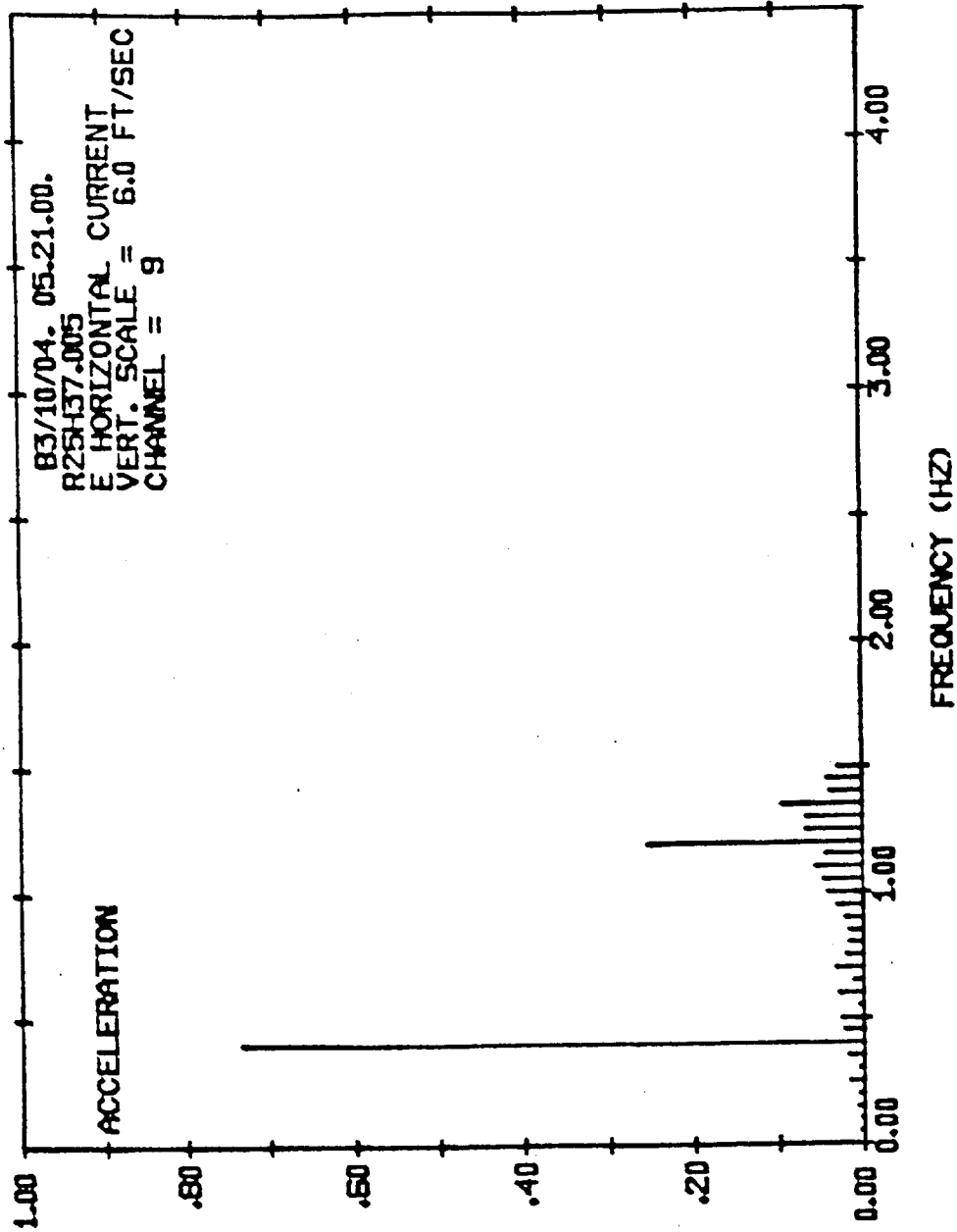


Fig. 4-16 Sample horizontal acceleration amplitude spectrum for Run #5
 computed by numerical differentiation in the frequency domain
 (Note that the units for the vertical scale should read ft/sec²)

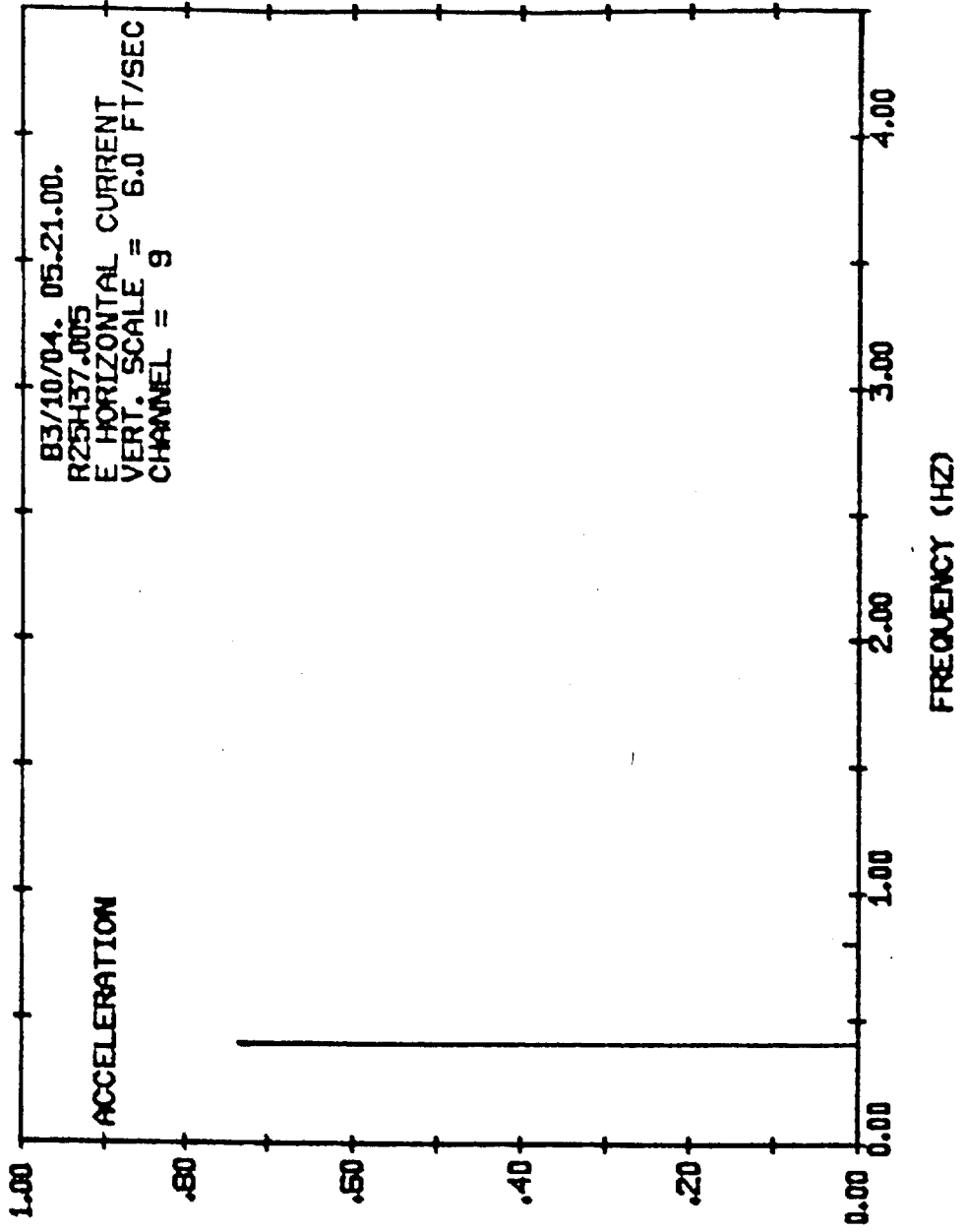


Fig. 4-17 Sample horizontal acceleration amplitude spectrum for Run #5 (note that units for the vert. scale should read ft/sec^2)

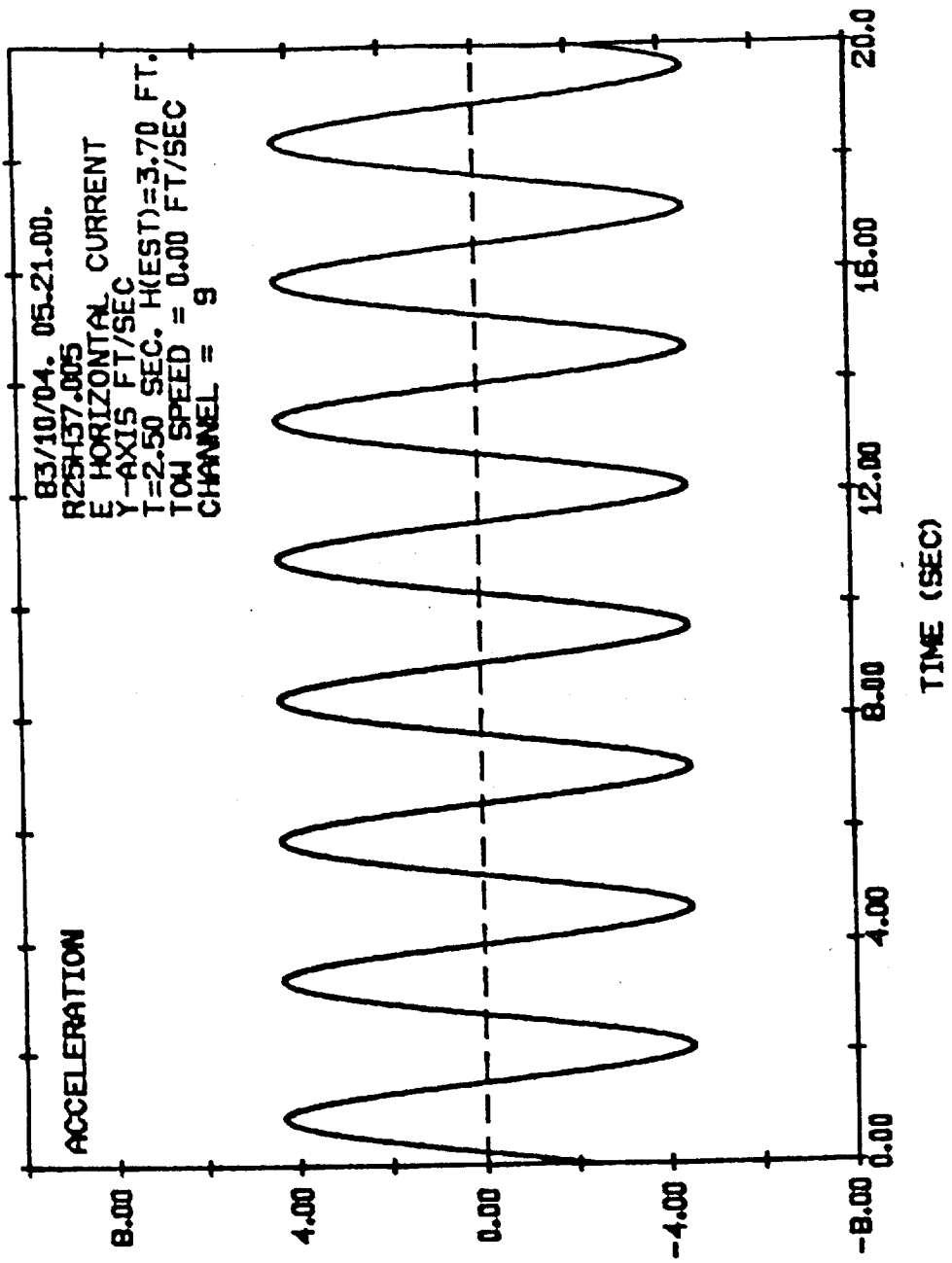


Fig. 4-18 Sample horizontal acceleration time series synthesized from amplitude spectrum in Fig. 4-13 for Run #5 (note that Y-AXIS scale should read "ft/sec²")

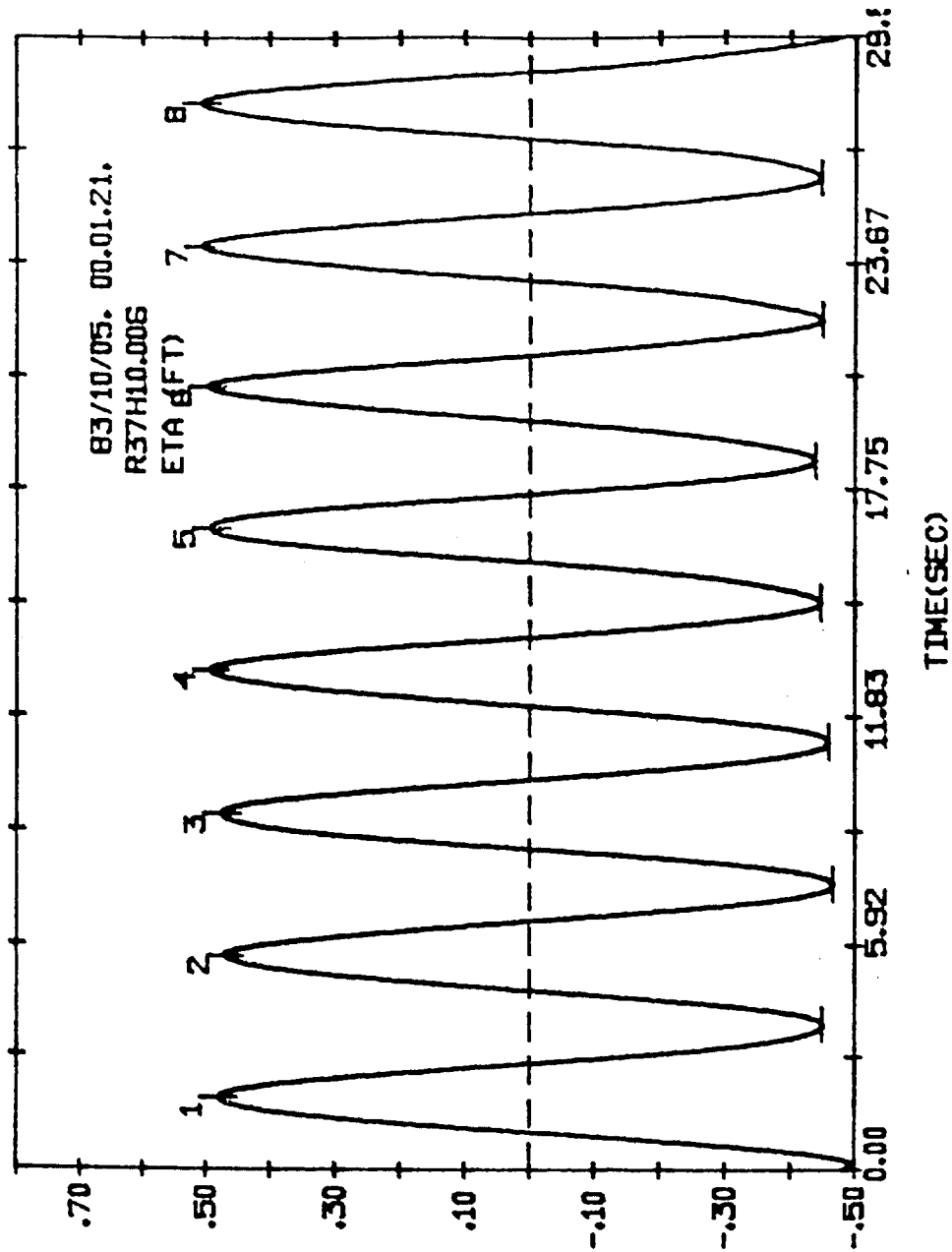


Fig. 4-15 Sample automatic selection of seven individual waves by PROGRAM FD5A for Run #6

Fig. 4-19 Sample automatic selection of seven individual waves by PROGRAM FD5A for Run #6

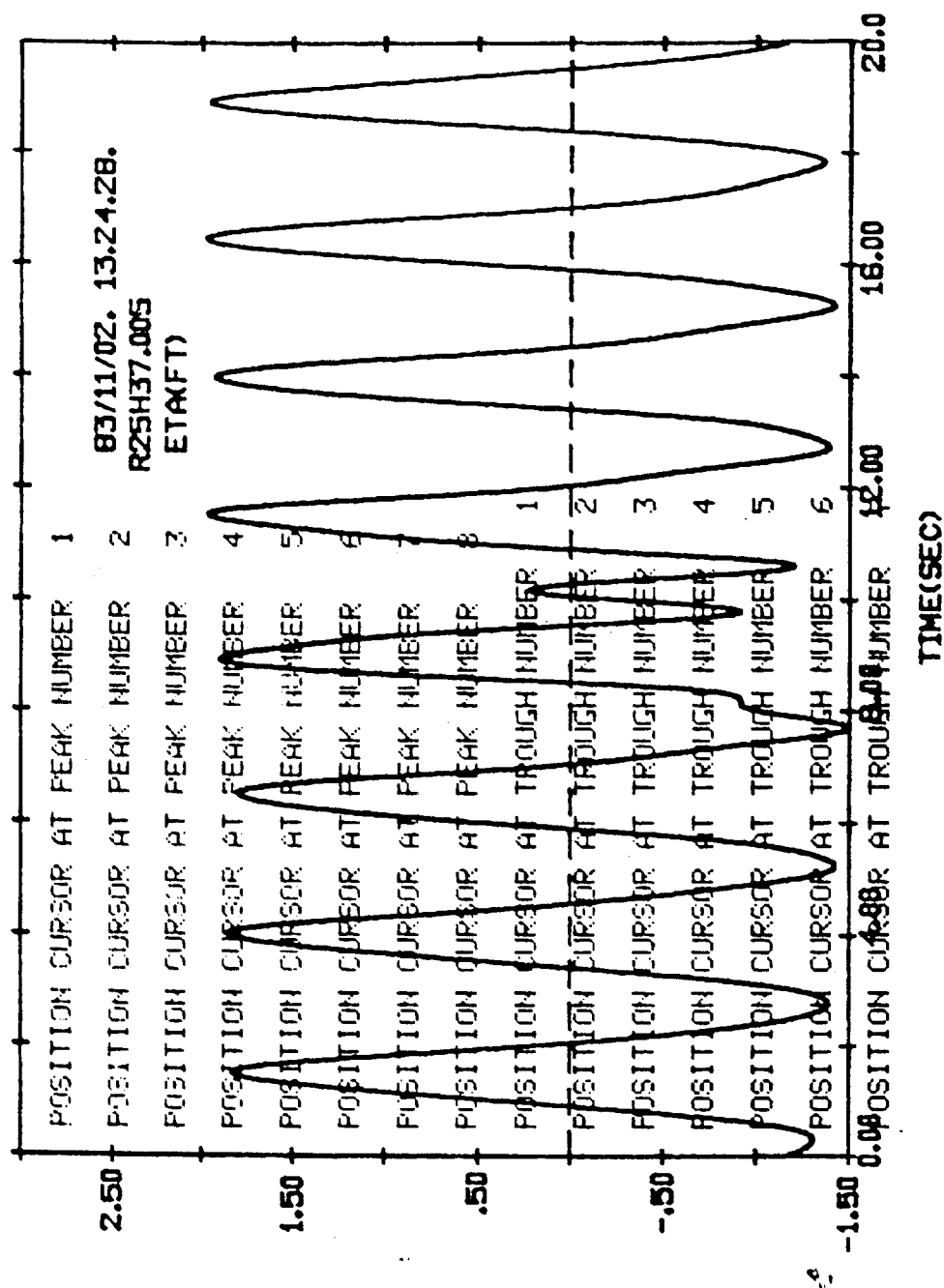


Fig. 4-20 Sample manual selection of seven individual waves by PROGRAM FDATA5 for Run #5

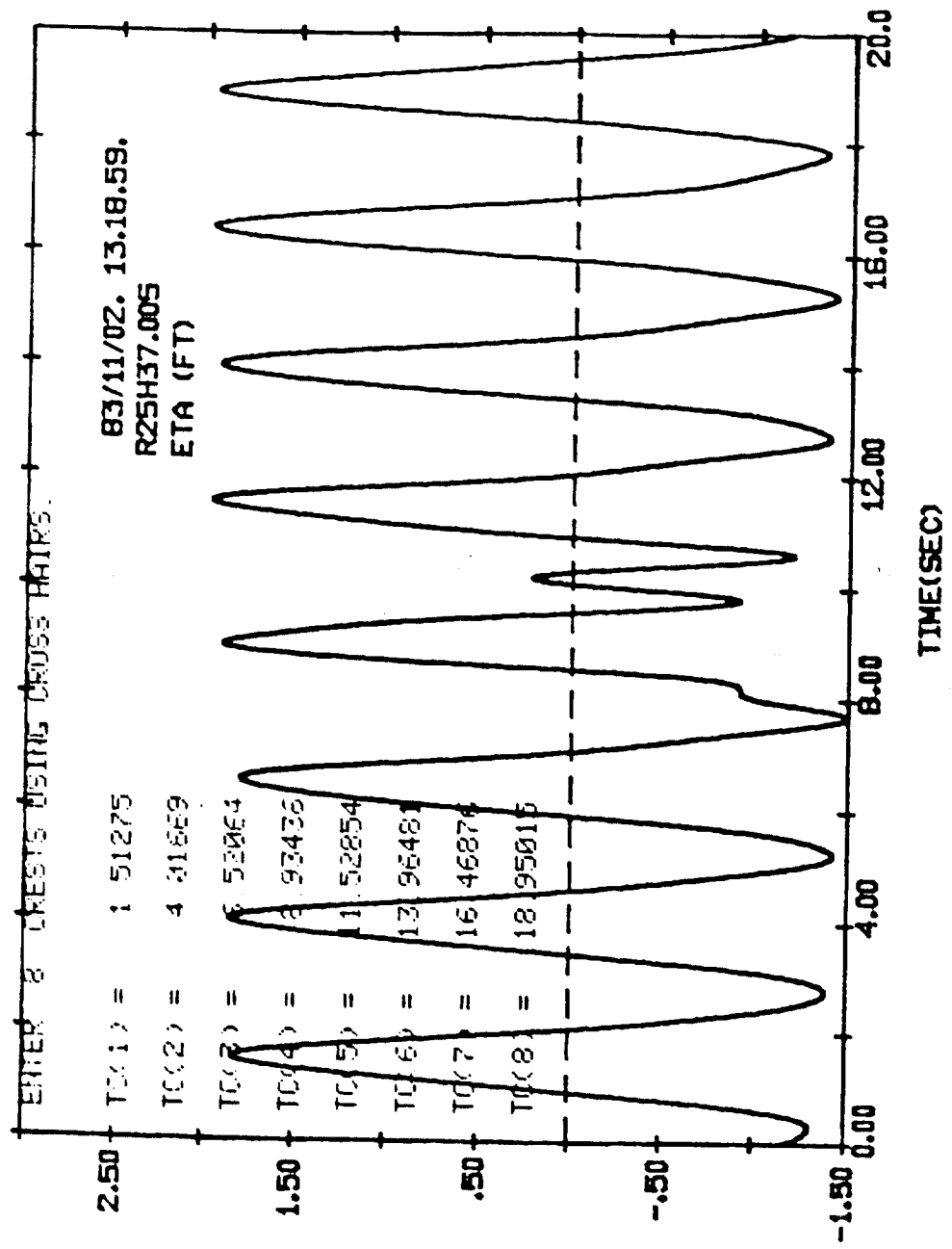


Fig. 4-21 Sample manual determination of individual wave periods by PROGRAM FDATA5 for Run #5

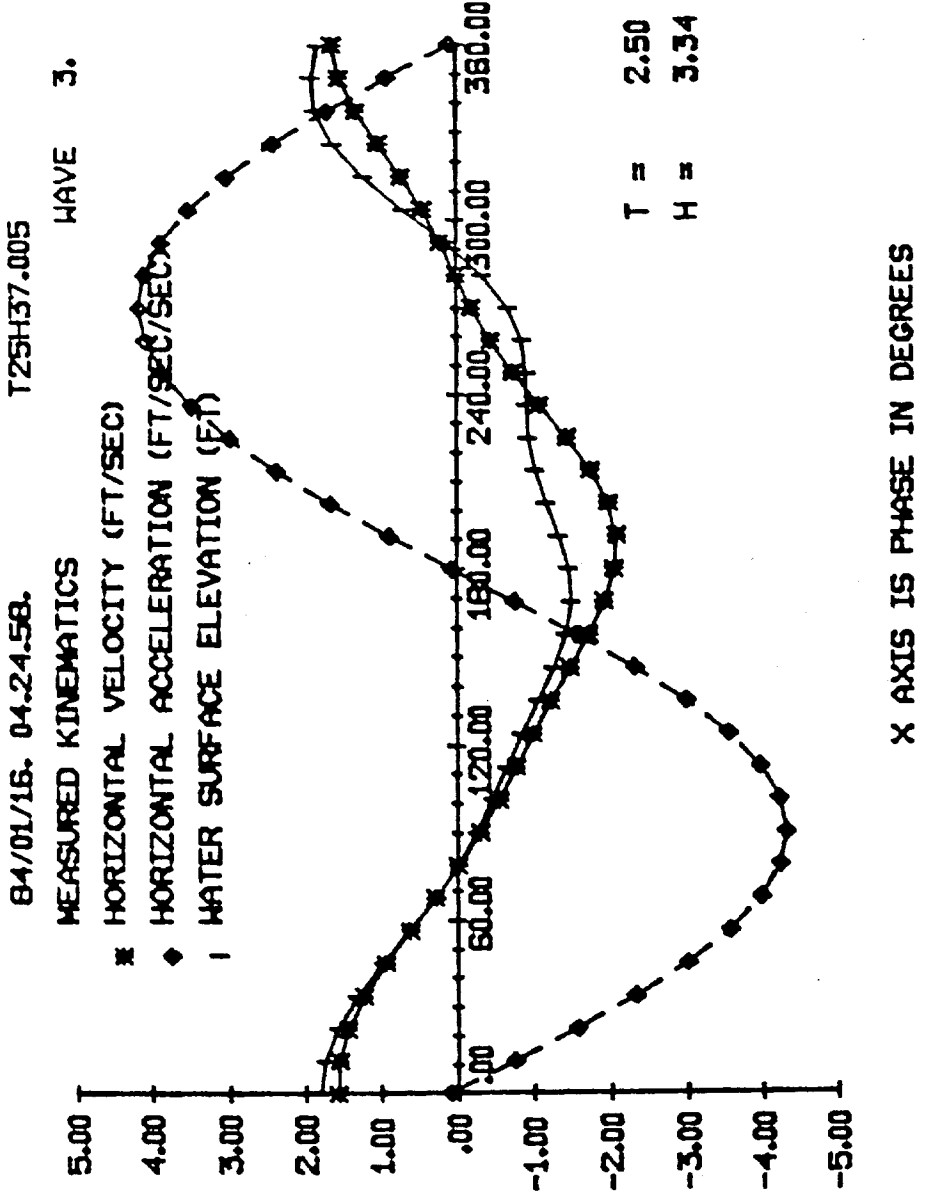


Fig. 4-22 Sample time series of measured horizontal water particle velocity and numerically computed acceleration for Wave #3 in Run #5 Spike as seen in Fig. 4-6 influences water surface profile.

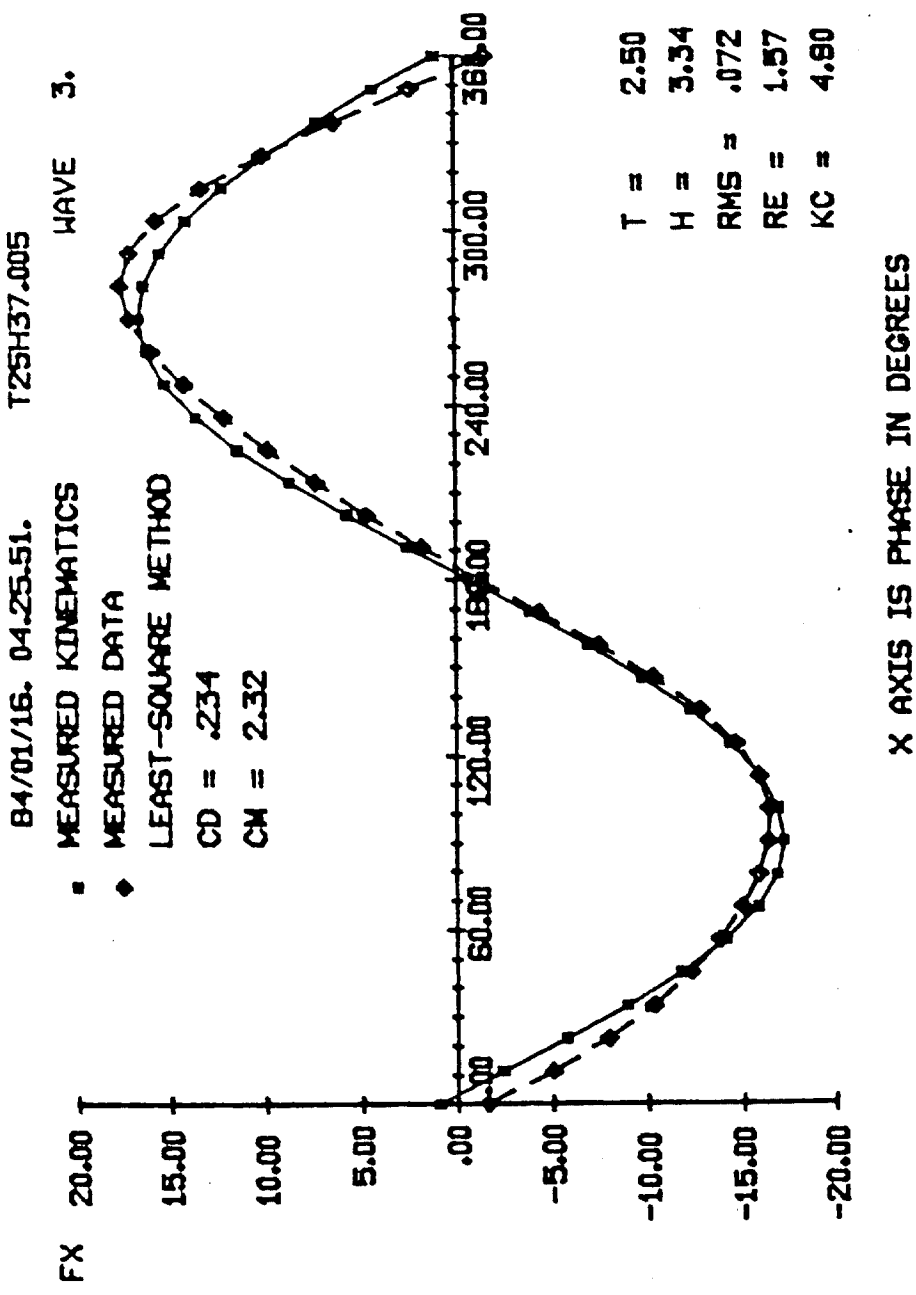


Fig. 4-23 Comparison between measured (♦) and predicted (■) local in-line force using measured kinematics and coefficients for Wave #3 in Run #5

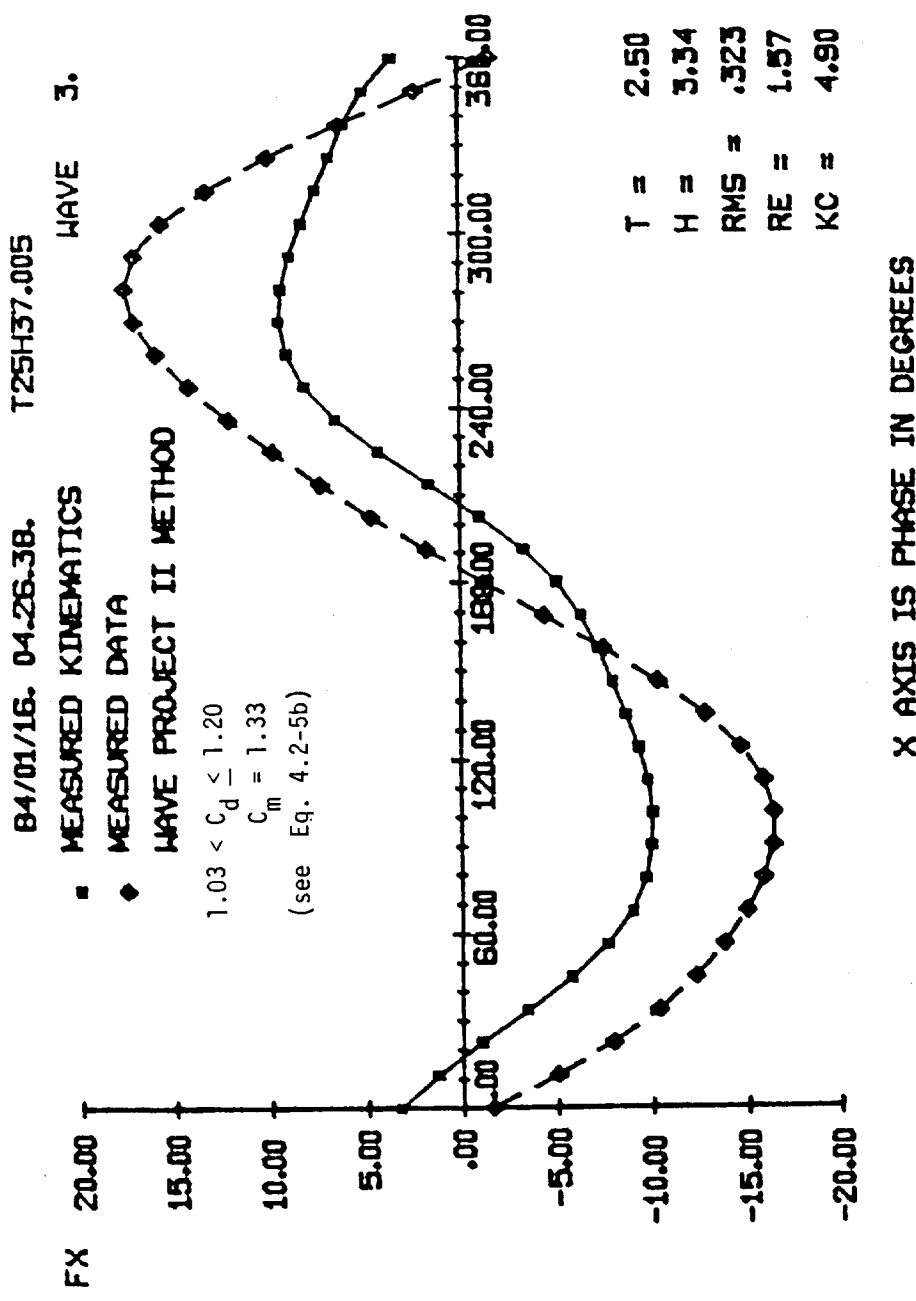
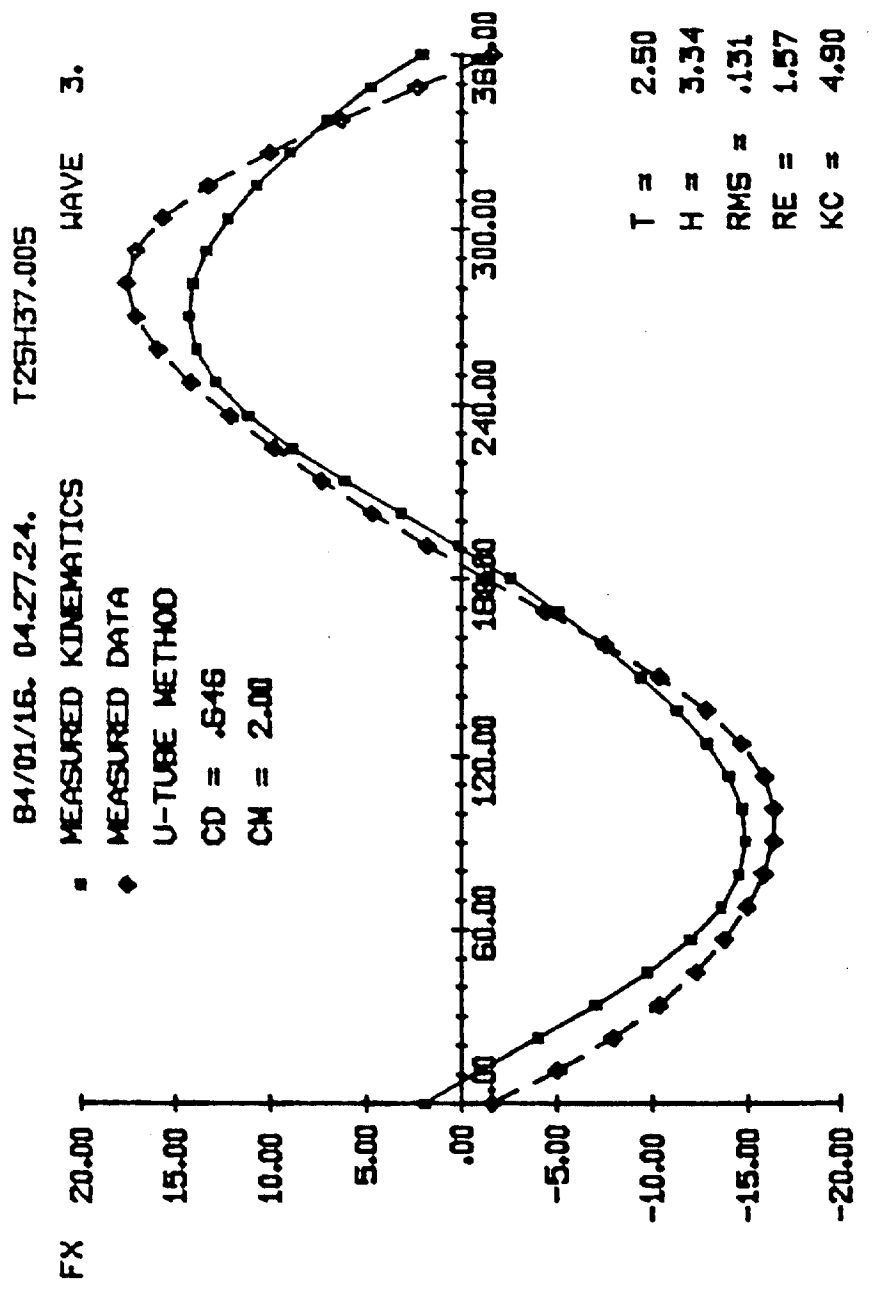


Fig. 4-24 Comparison between measured (◆) and predicted (□) local in-line force using measured kinematics and Wave Project II coefficients for Wave #3 in Run #5



X AXIS IS PHASE IN DEGREES

Fig. 4-25 Comparison between measured (♦) and predicted (■) local in-line force using measured kinematics and U-tube coefficients for Wave #3 in Run #5

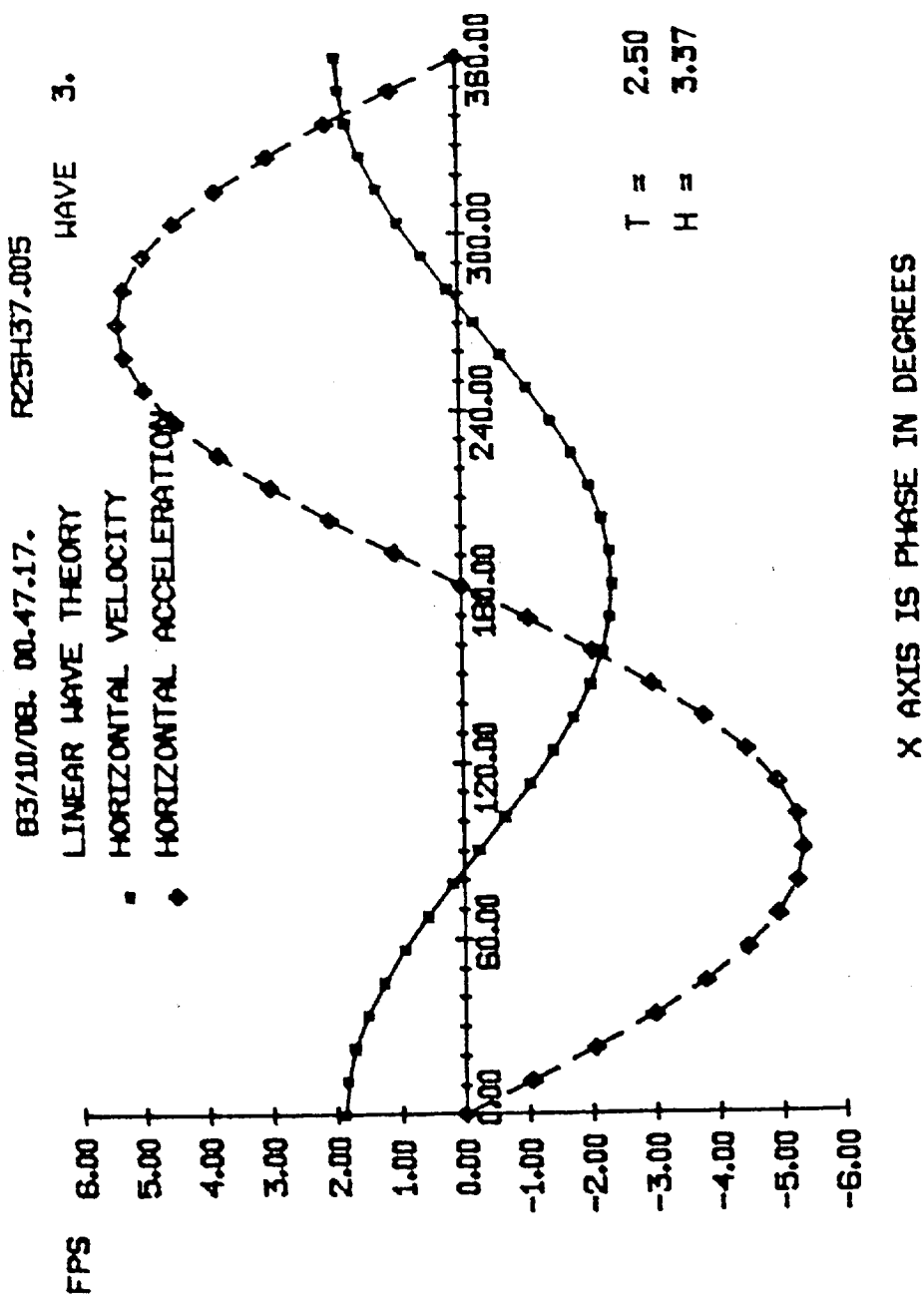


Fig. 4-26 Sample time series of LWT horizontal water particle velocity and acceleration for Wave #3 in Run #5

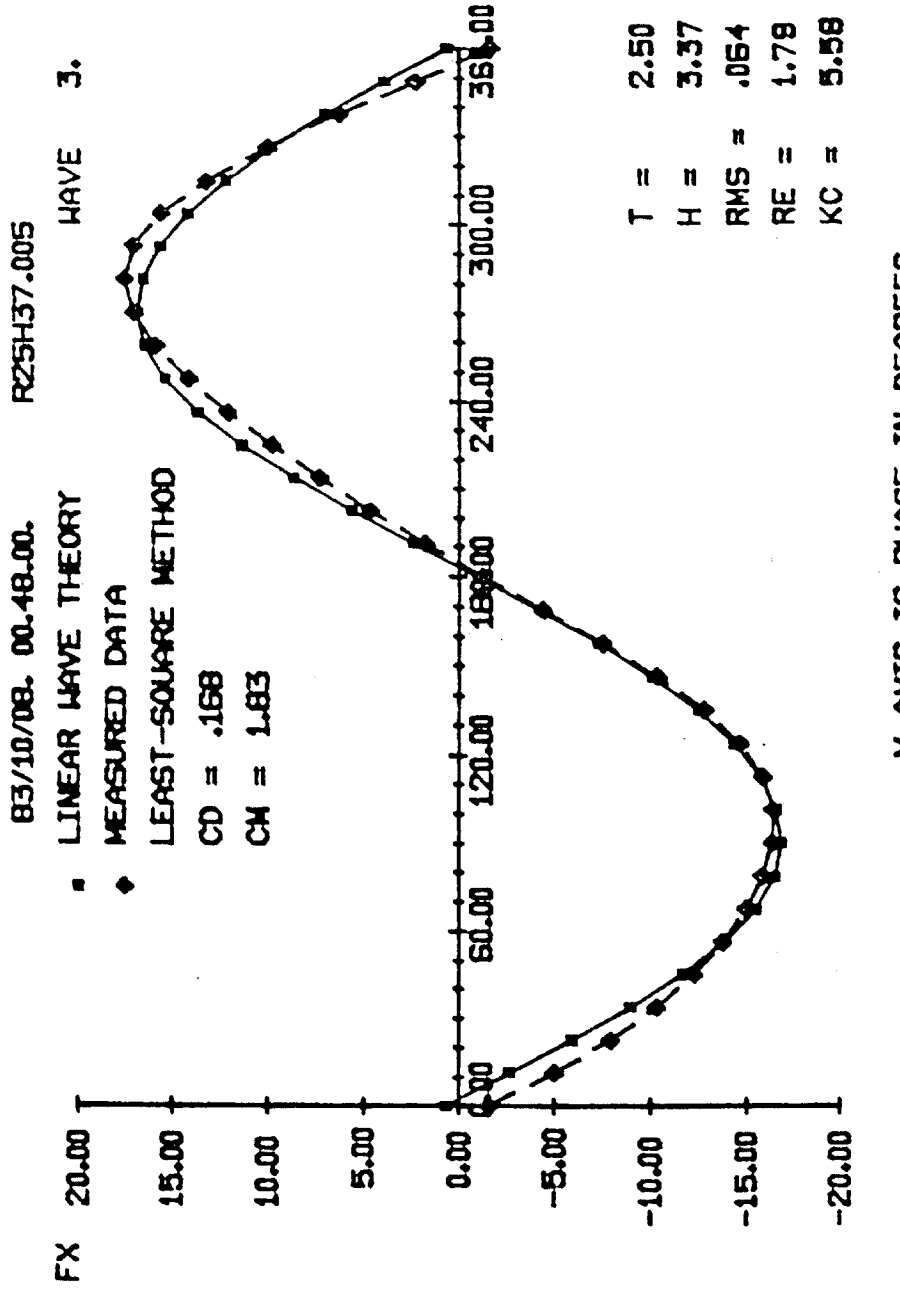


Fig. 4-27 Comparison between measured and predicted local inline force using LWT kinematics and measured coefficients for Wave #3 in Run #5

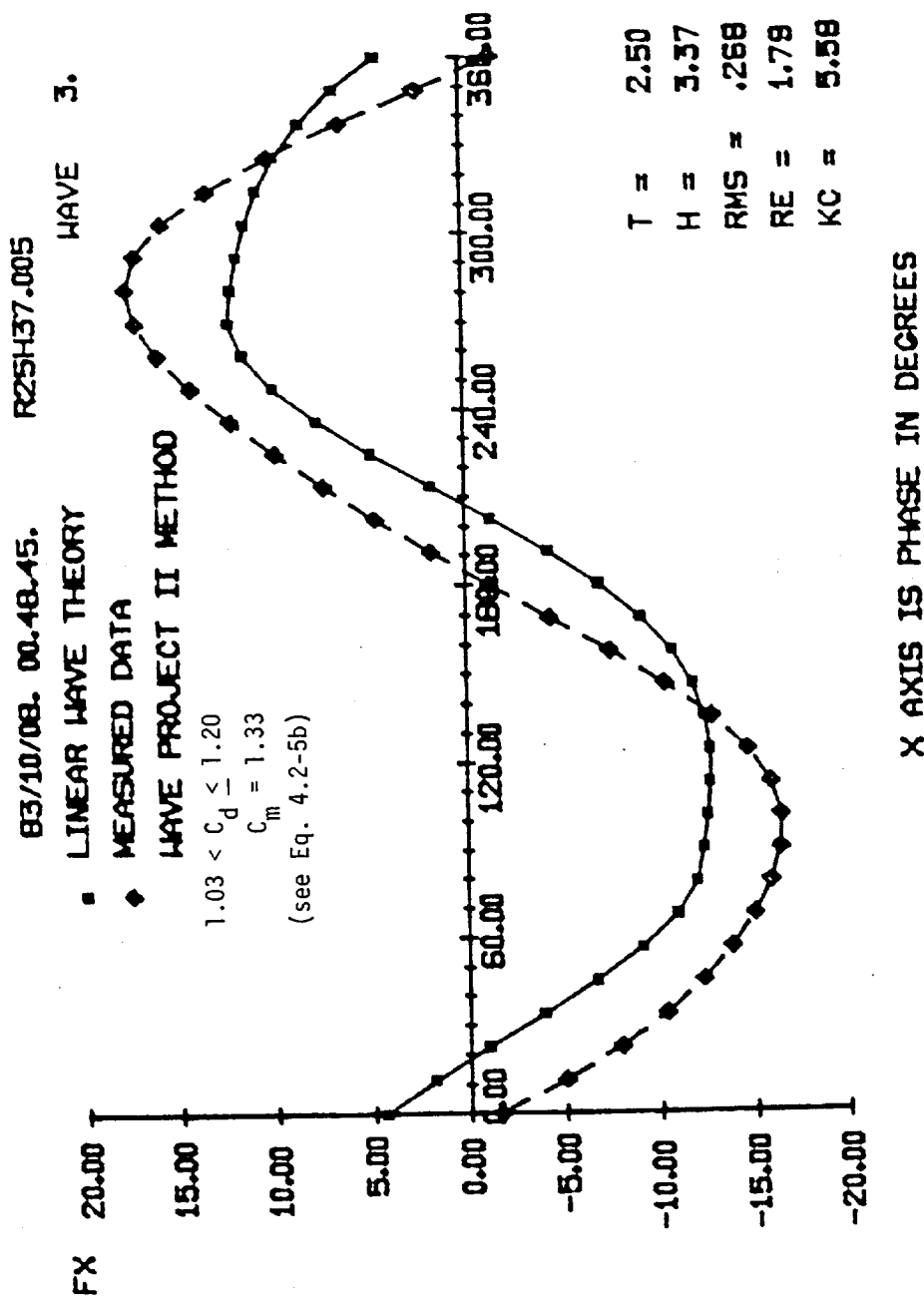


Fig. 4-28 Comparison between measured and predicted local inline force using LWT kinematics and Wave Project II coefficients for Wave #3 in Run #5

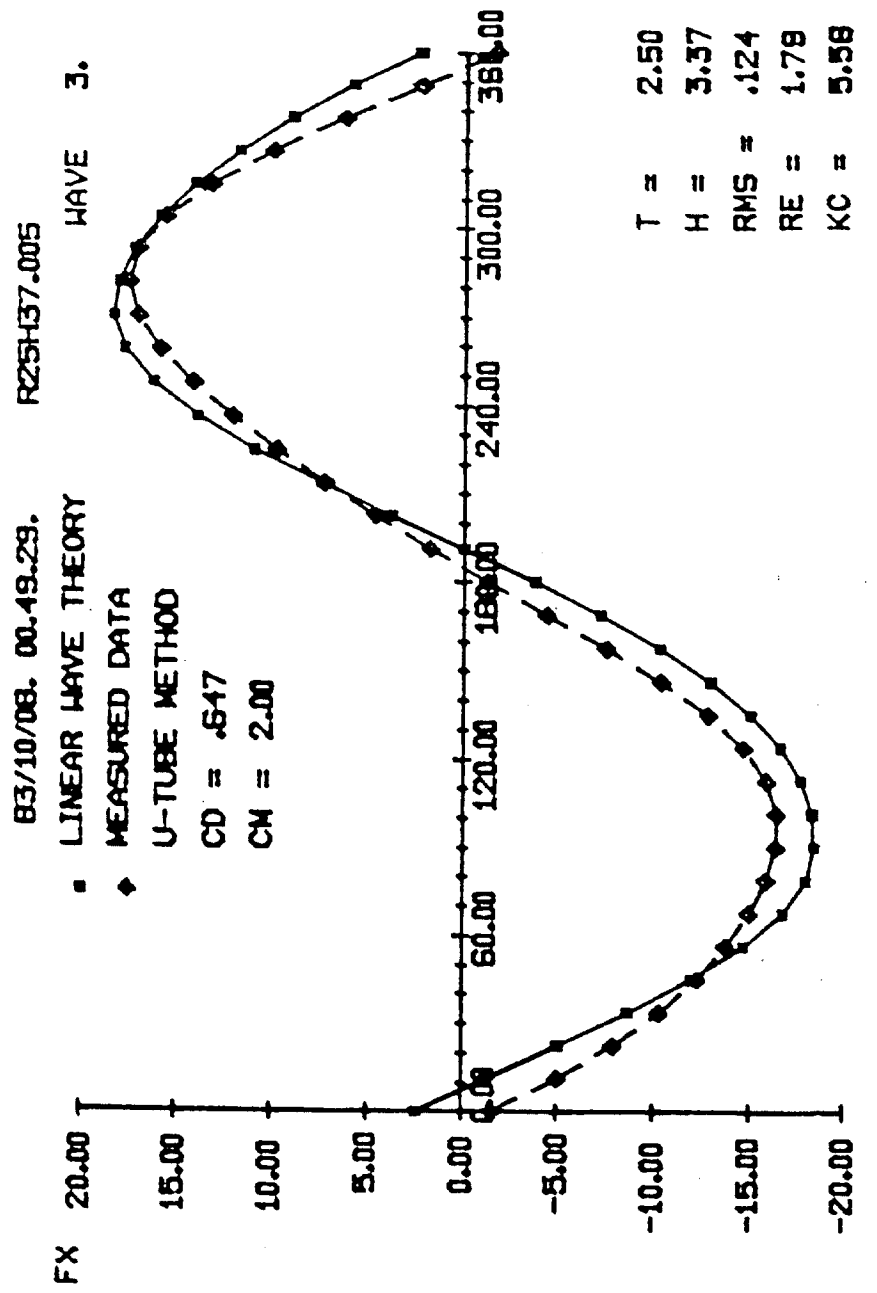


Fig. 4-29 Comparison between measured and predicted local inline force using LWT kinematics and U-tube coefficients for Wave #3 in Run #5

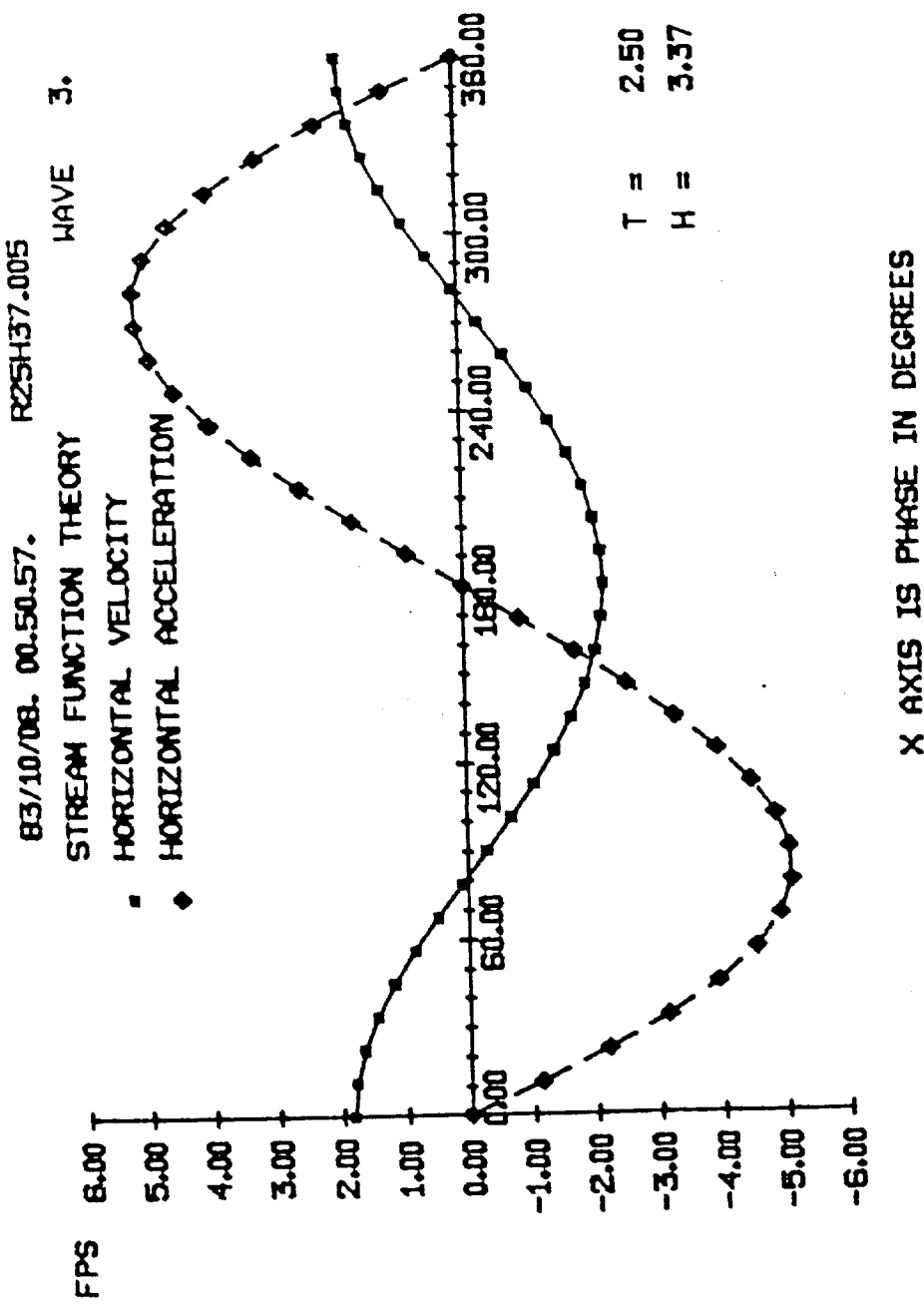
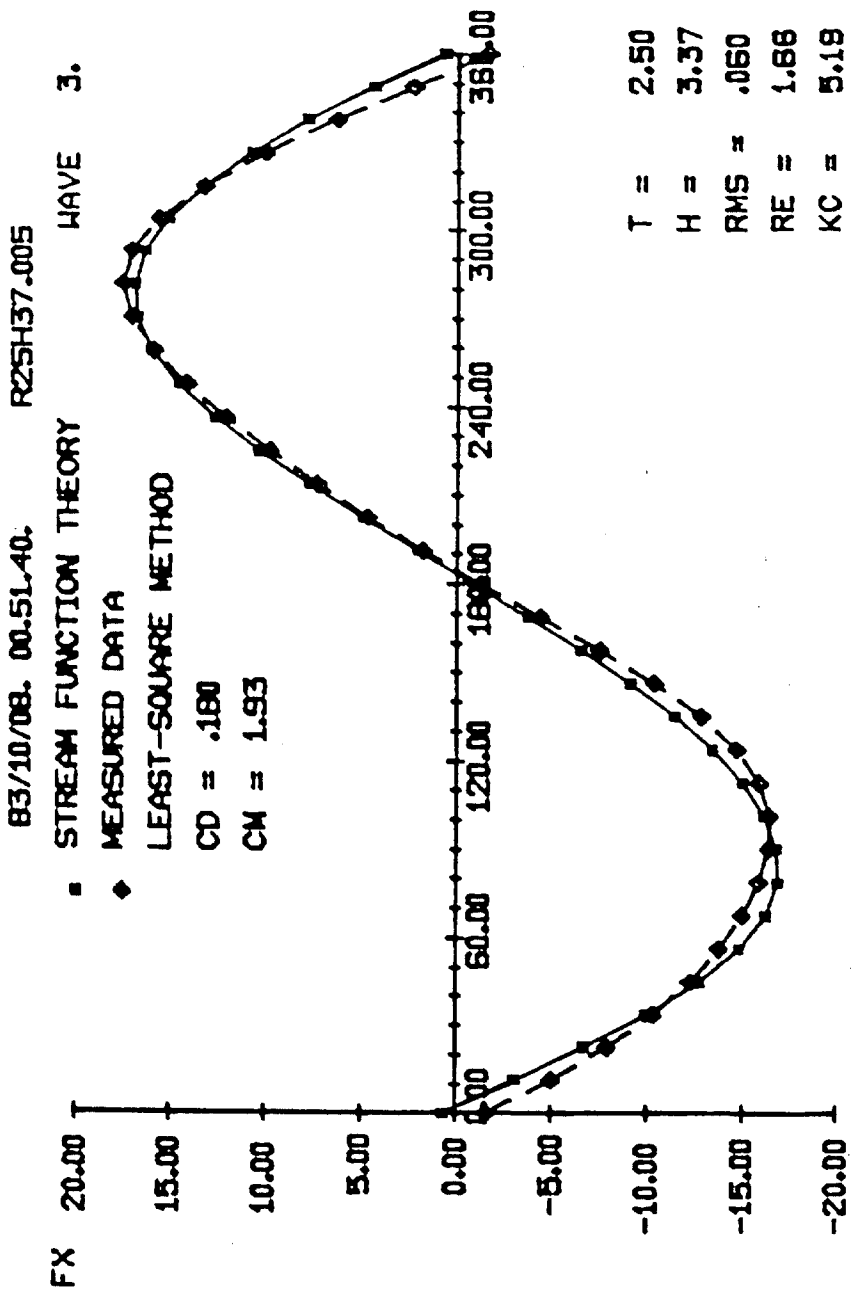


Fig. 4-30 Sample time series of stream function theory horizontal water particle velocity and acceleration for Wave #3 in Run #5



X AXIS IS PHASE IN DEGREES

Fig. 4-31 Comparison between measured and predicted local inline force using stream function wave theory kinematics and measured coefficients for Wave #3 in Run #5

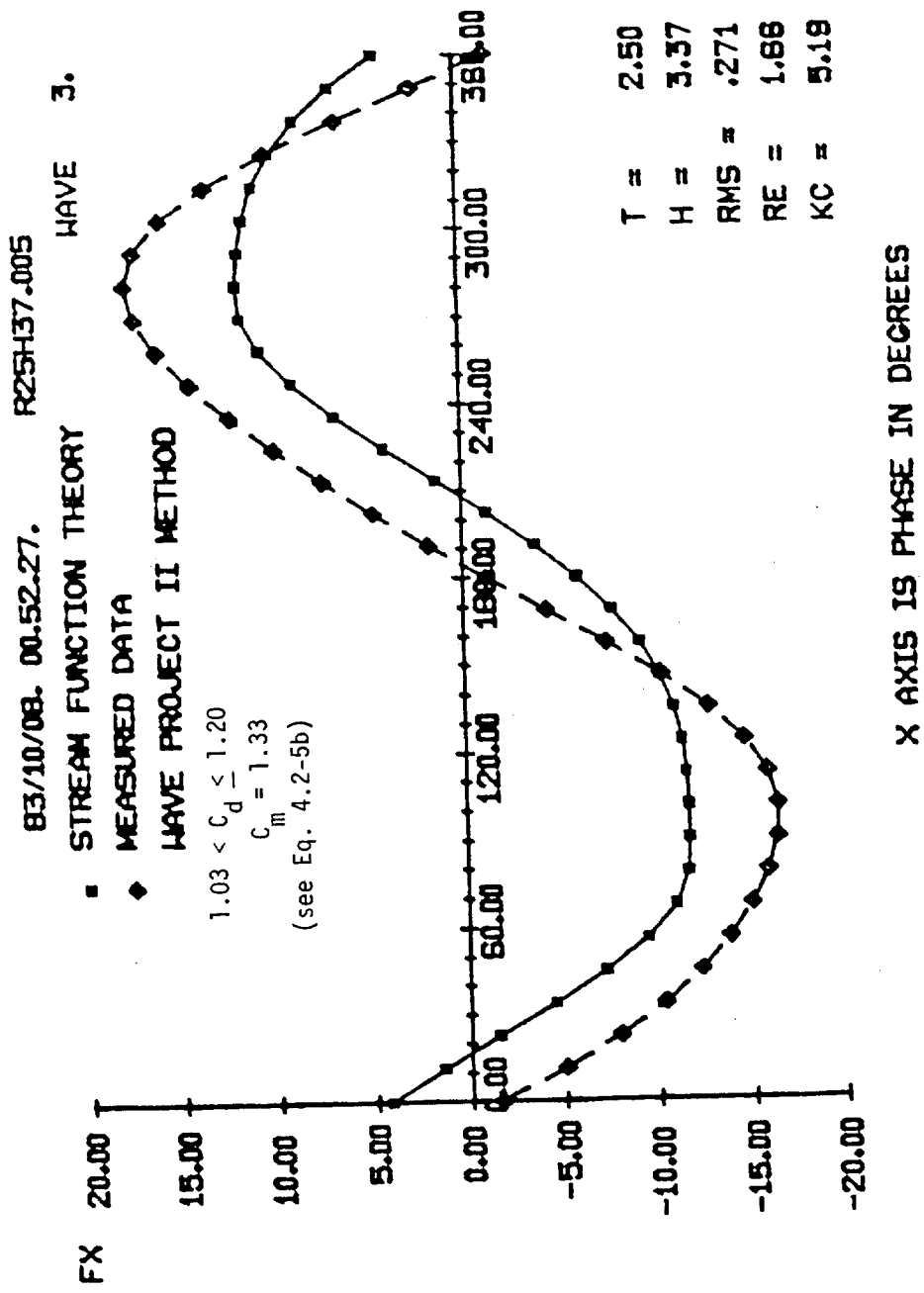


Fig. 4-32 Comparison between measured and predicted local inline force using stream function wave theory kinematics and Wave Project II coefficients for Wave #3 in Run #5

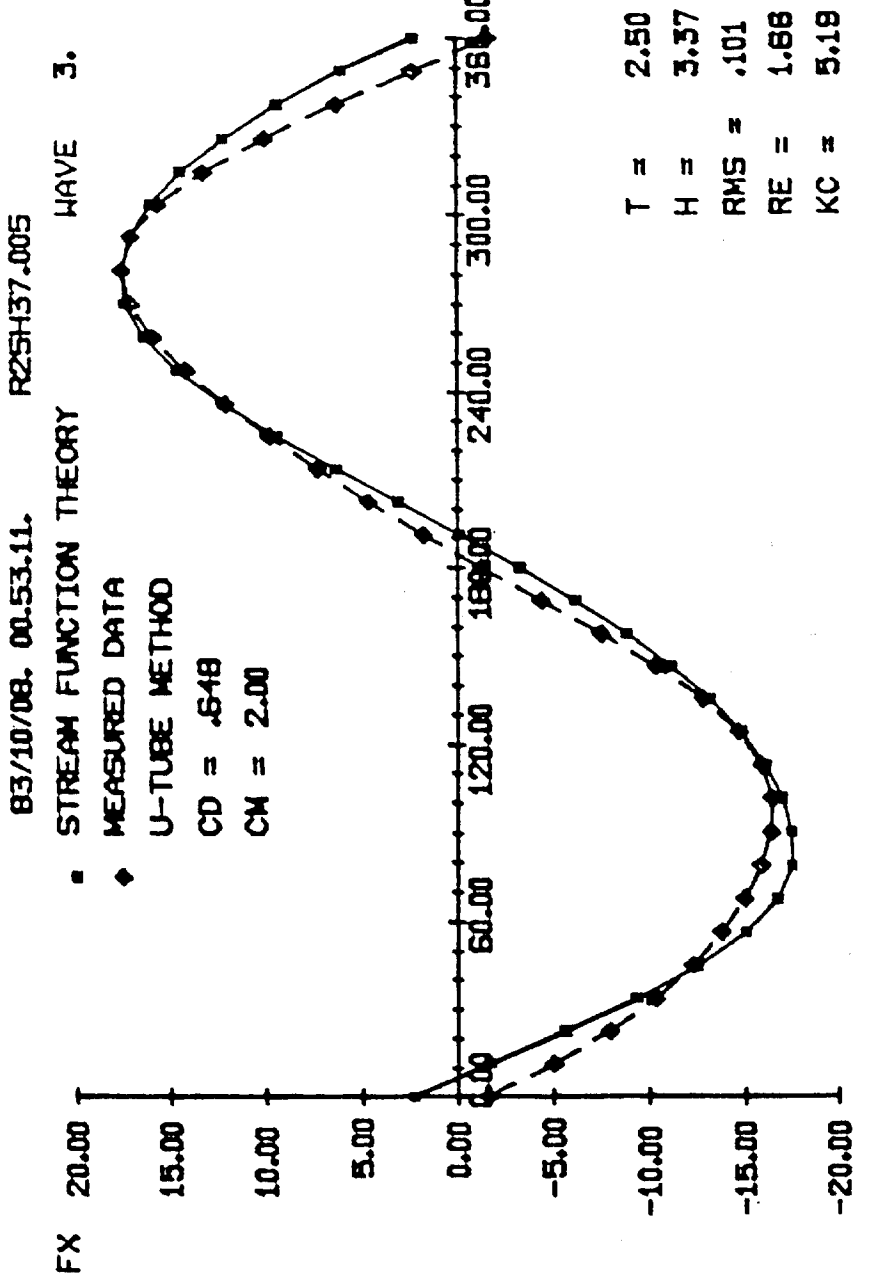


Fig. 4-33 Comparison between measured and predicted local inline force using stream function wave theory kinematics and U-tube coefficients for Wave #3 in Run #5

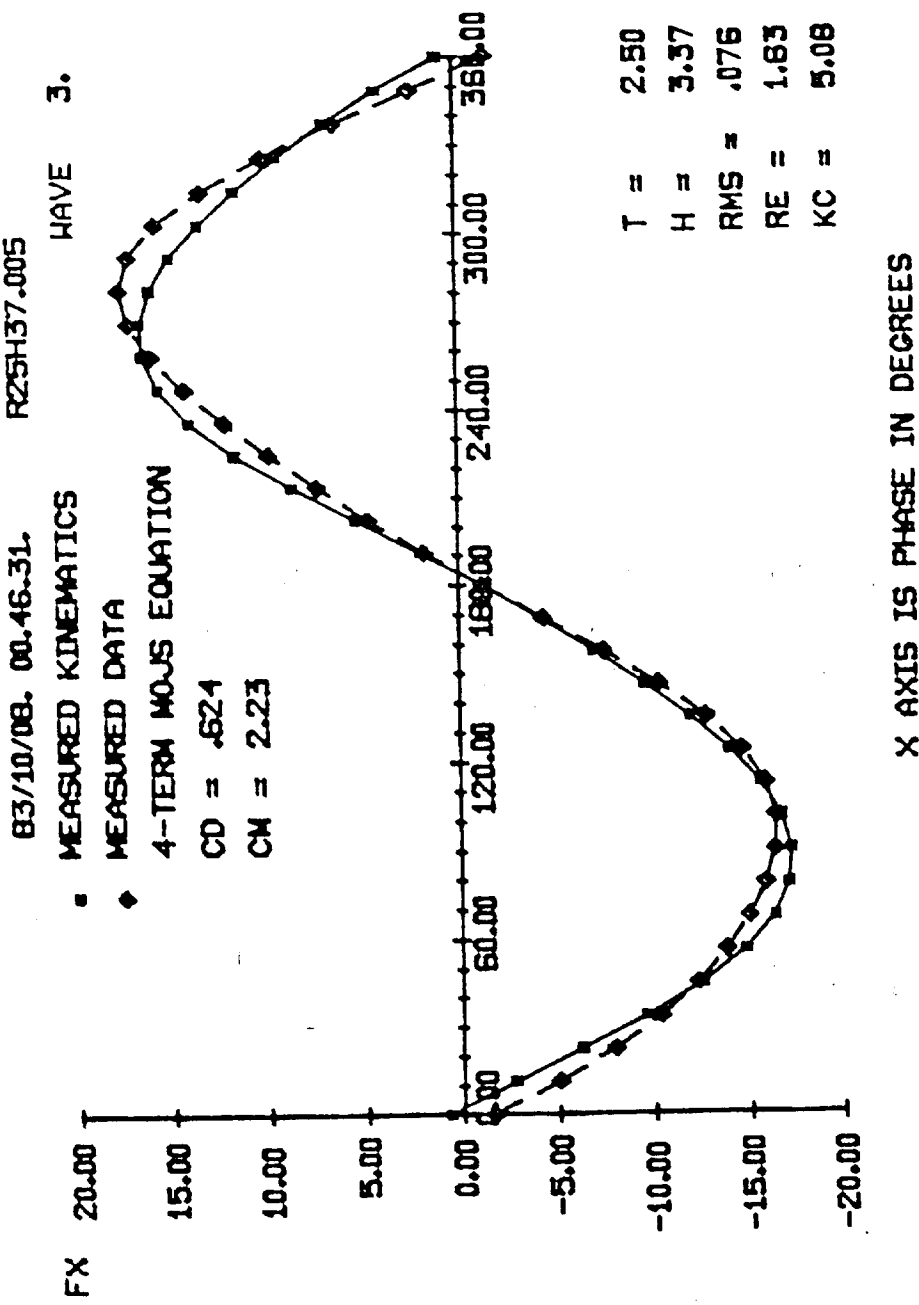


Fig. 4-34 Comparison between measured and predicted forces by the 4-term MOJS equation using measured kinematics for Wave #3 in Run #5

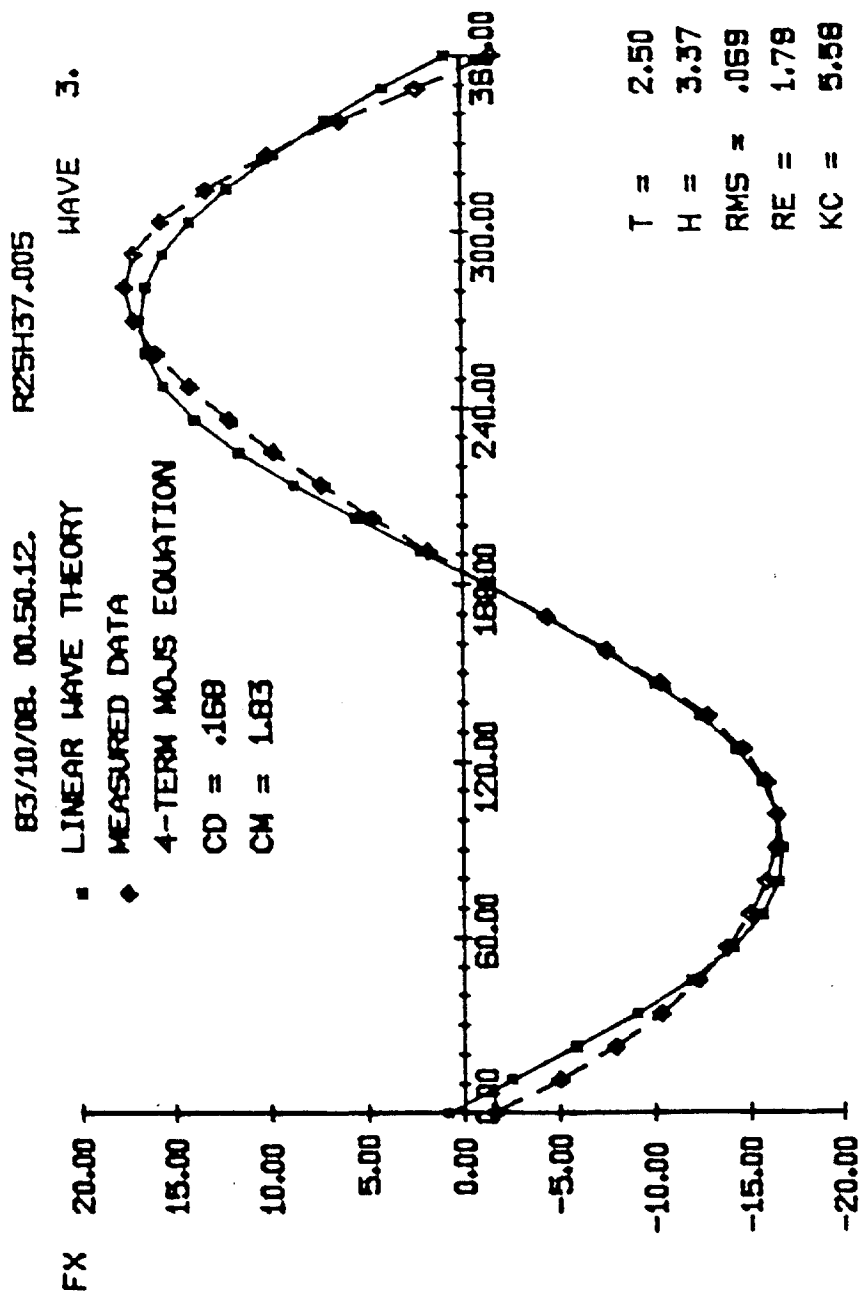


Fig. 4-35 Comparison between measured and predicted forces by the 4-term MOJS equation using LWT kinematics for Wave #3 in Run #5 (only 2 terms used since $C_m > 2.0$ and $C_d > 0.0$)

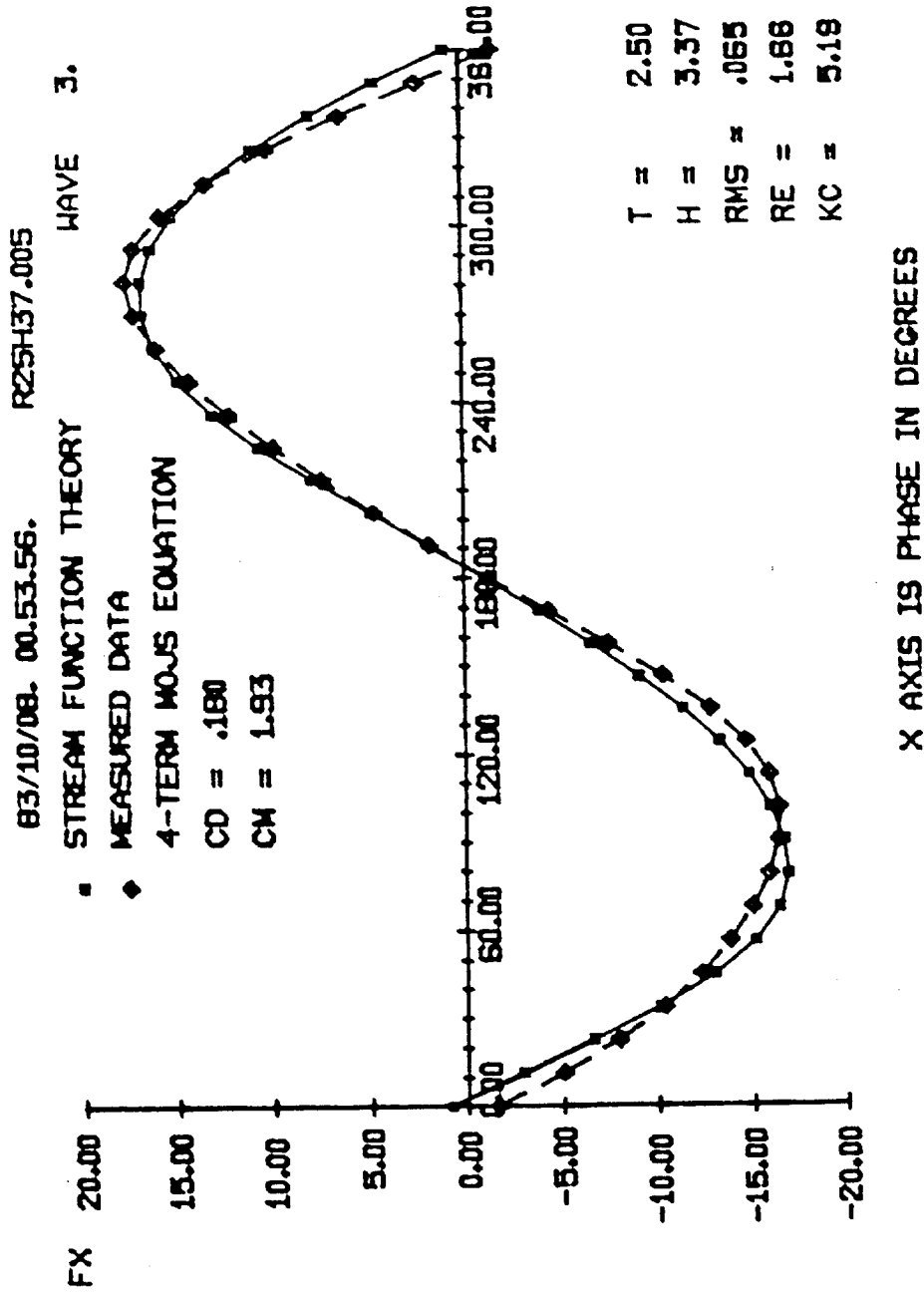


Fig. 4-36 Comparison between measured and predicted forces by the 4-term Mojs equation using stream function kinematics for Wave #3 in Run #5

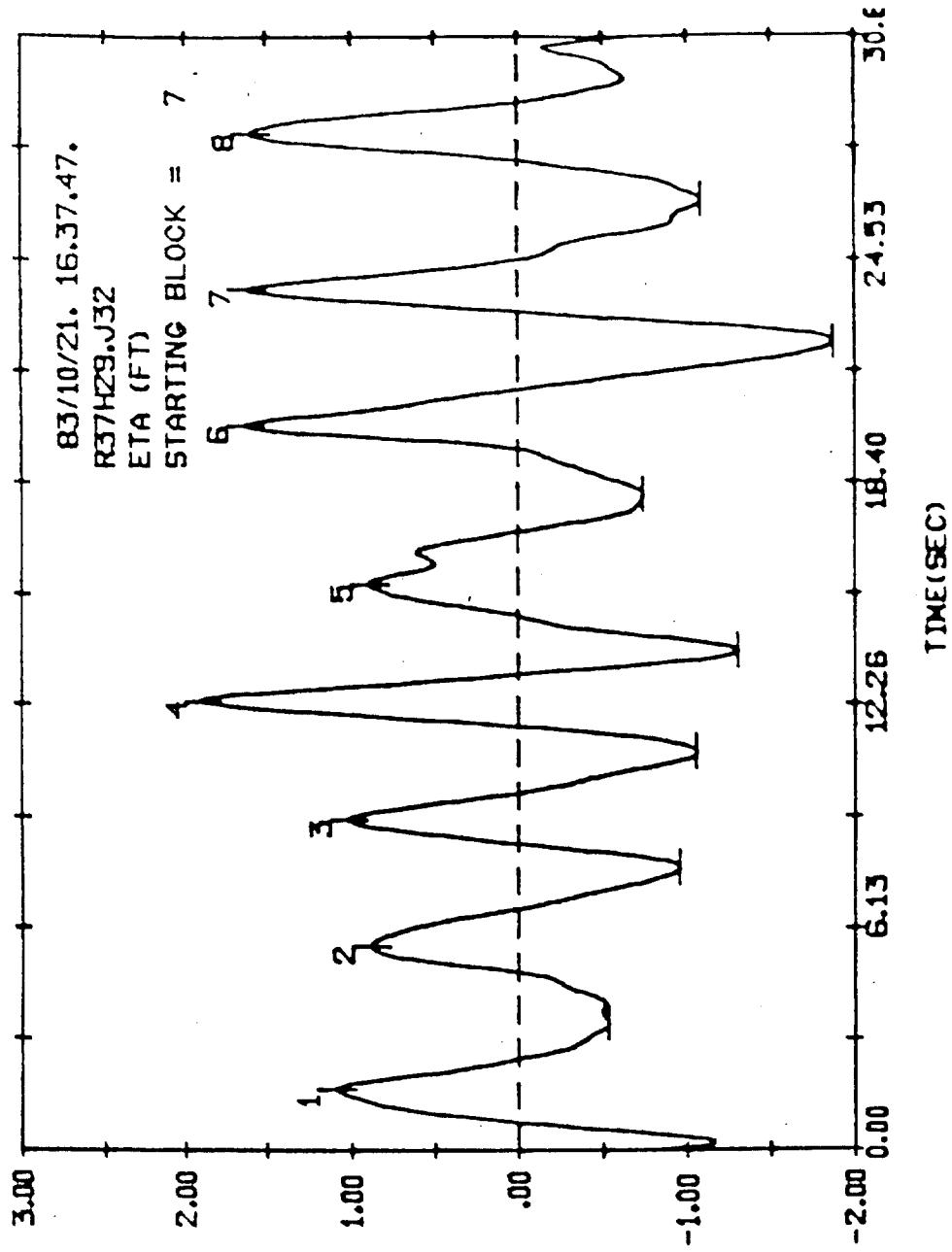


Fig. 4-37 A block of random wave profile (512 values) from random wave
 Run #32 (individual wave = #6)

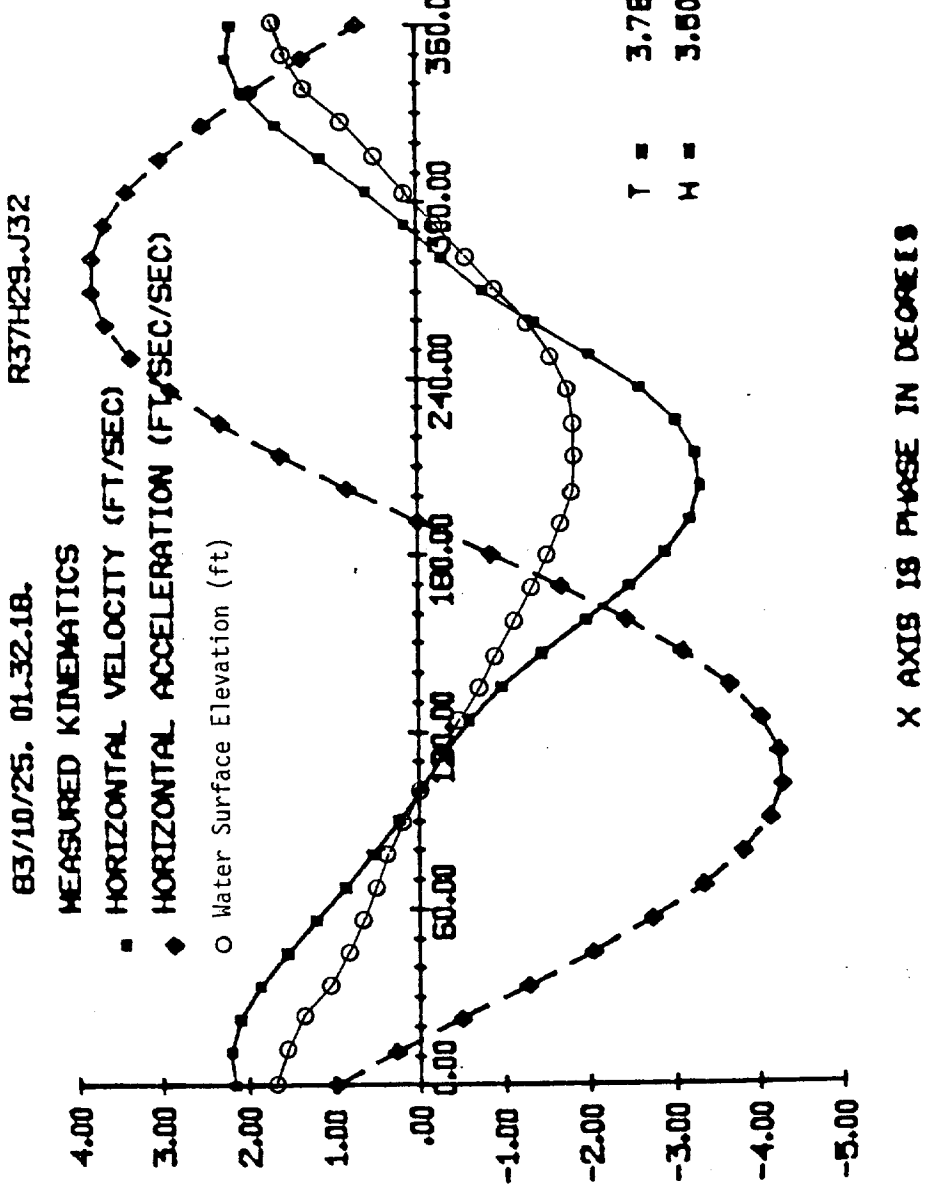


Fig. 4-38 Sample time series of measured horizontal water particle velocity and numerically computed acceleration for Wave #6, Block #7, Random Wave #32

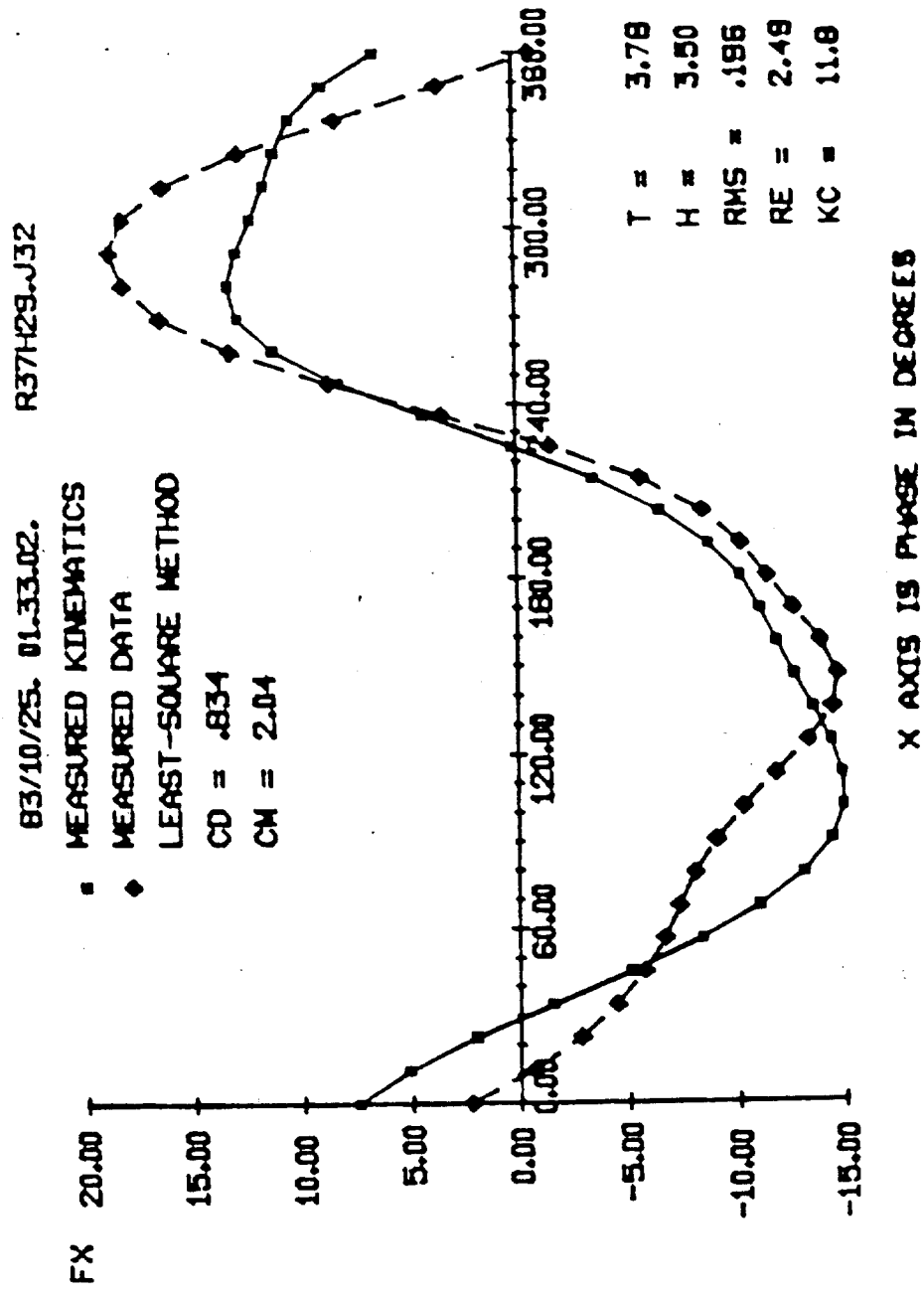


Fig. 4-39 Comparison between measured and predicted local inline force using measured kinematics and coefficients for Wave #6, Block #7, Random Wave #32

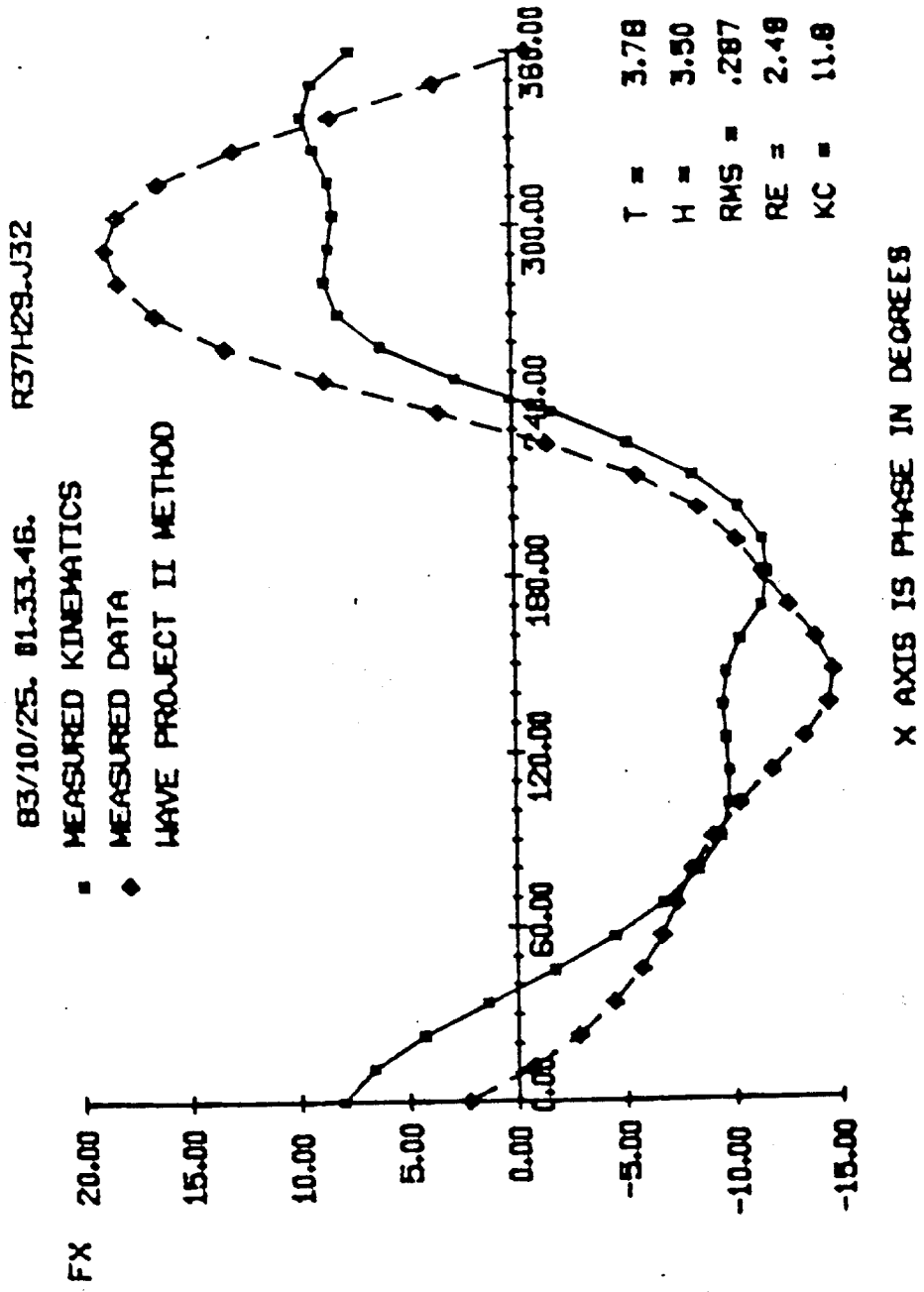


Fig. 4-40 Comparison between measured and predicted local inline force using measured kinematics and Wave Project II coefficients for Wave #6, Block #7, Random Wave #32

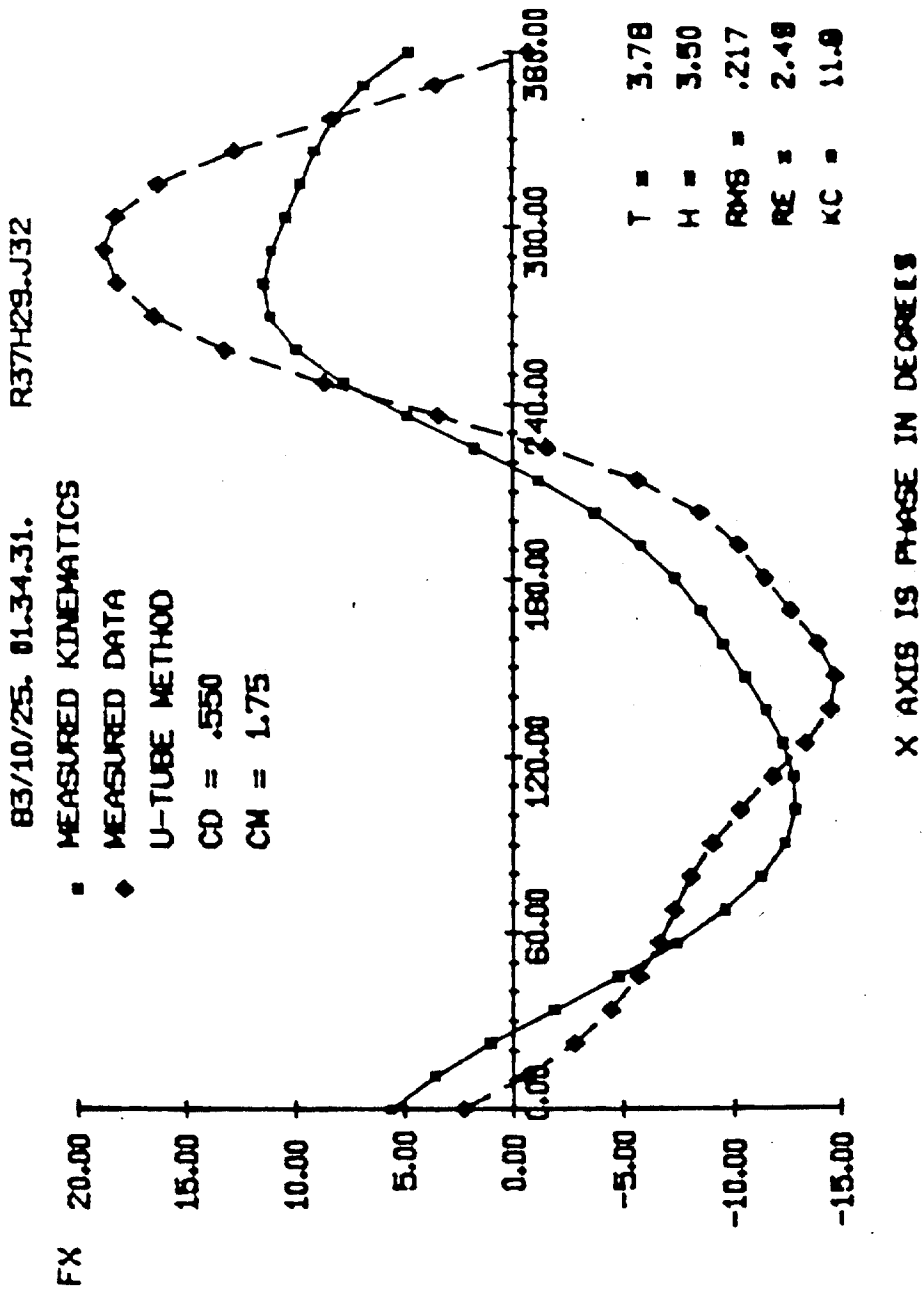


Fig. 4-41 Comparison between measured and predicted local inline force using measured kinematics and U-tube coefficients for Wave #6, Block #7, Random Wave #32

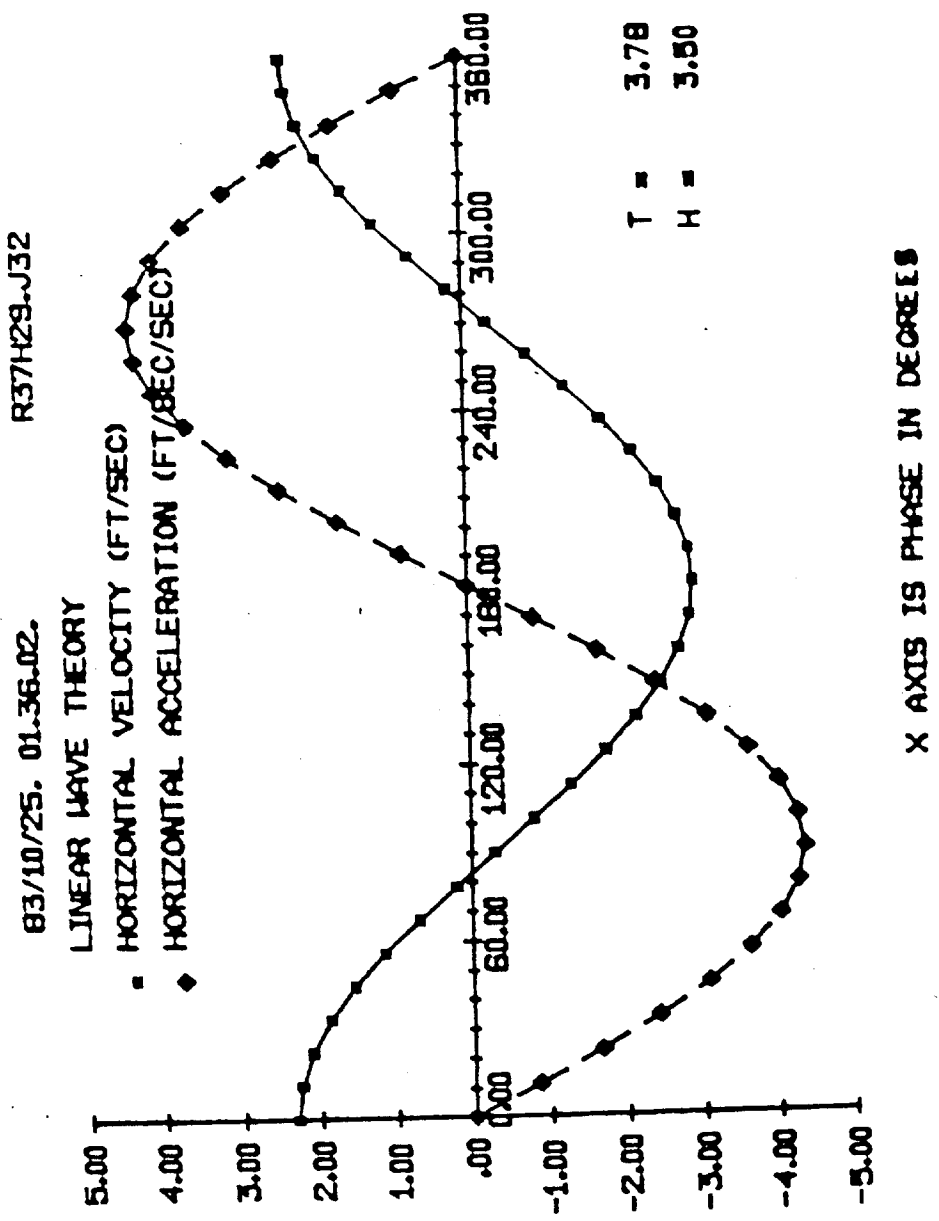


Fig. 4-42 Sample time series of LWT horizontal water particle velocity and acceleration for Wave #6, Block #7, Random Wave #32.

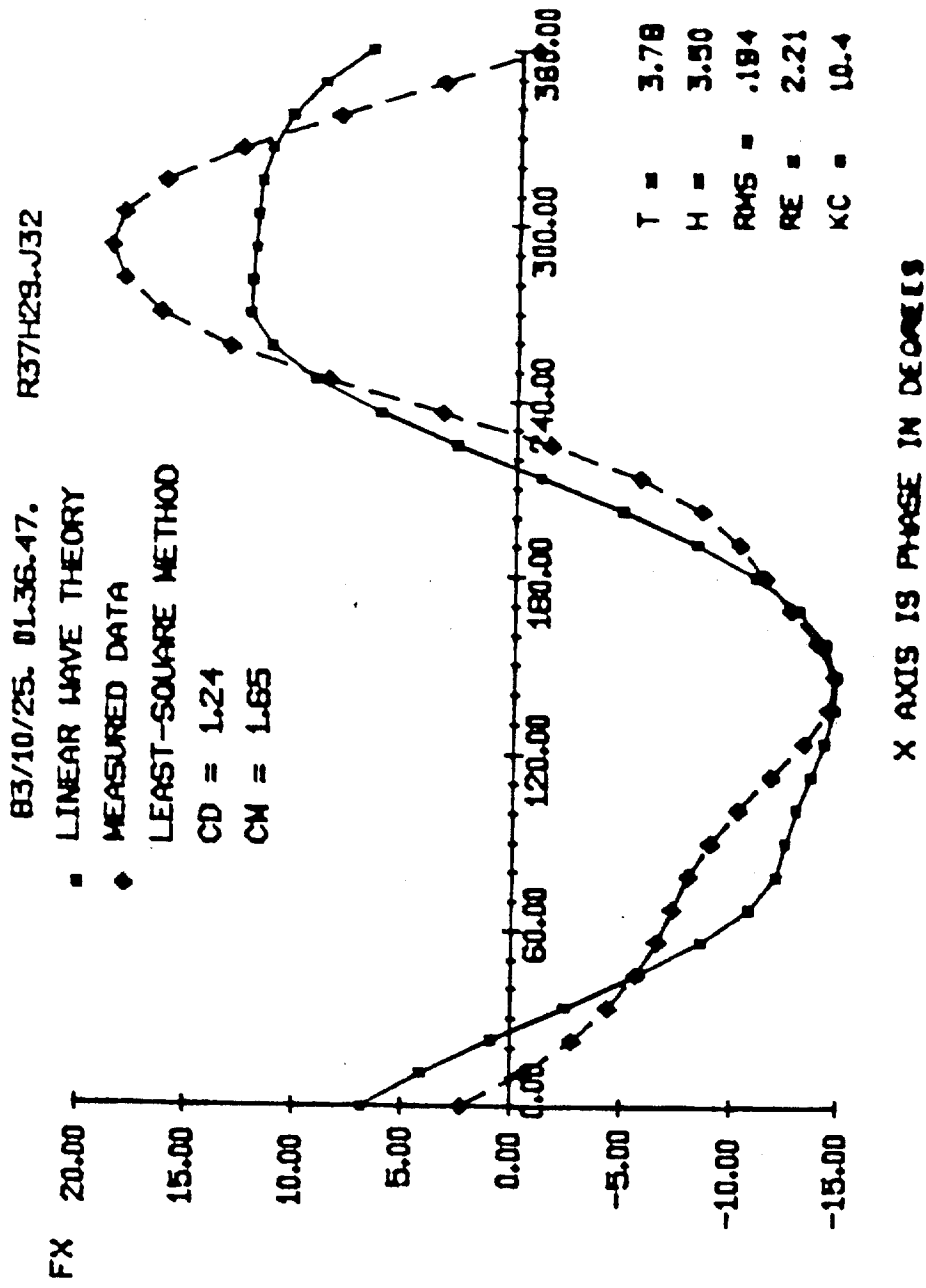


Fig. 4-43 Comparison between measured and predicted local inline force using LWT kinematics and measured coefficients for Wave #6, Block #7, Random Wave #32

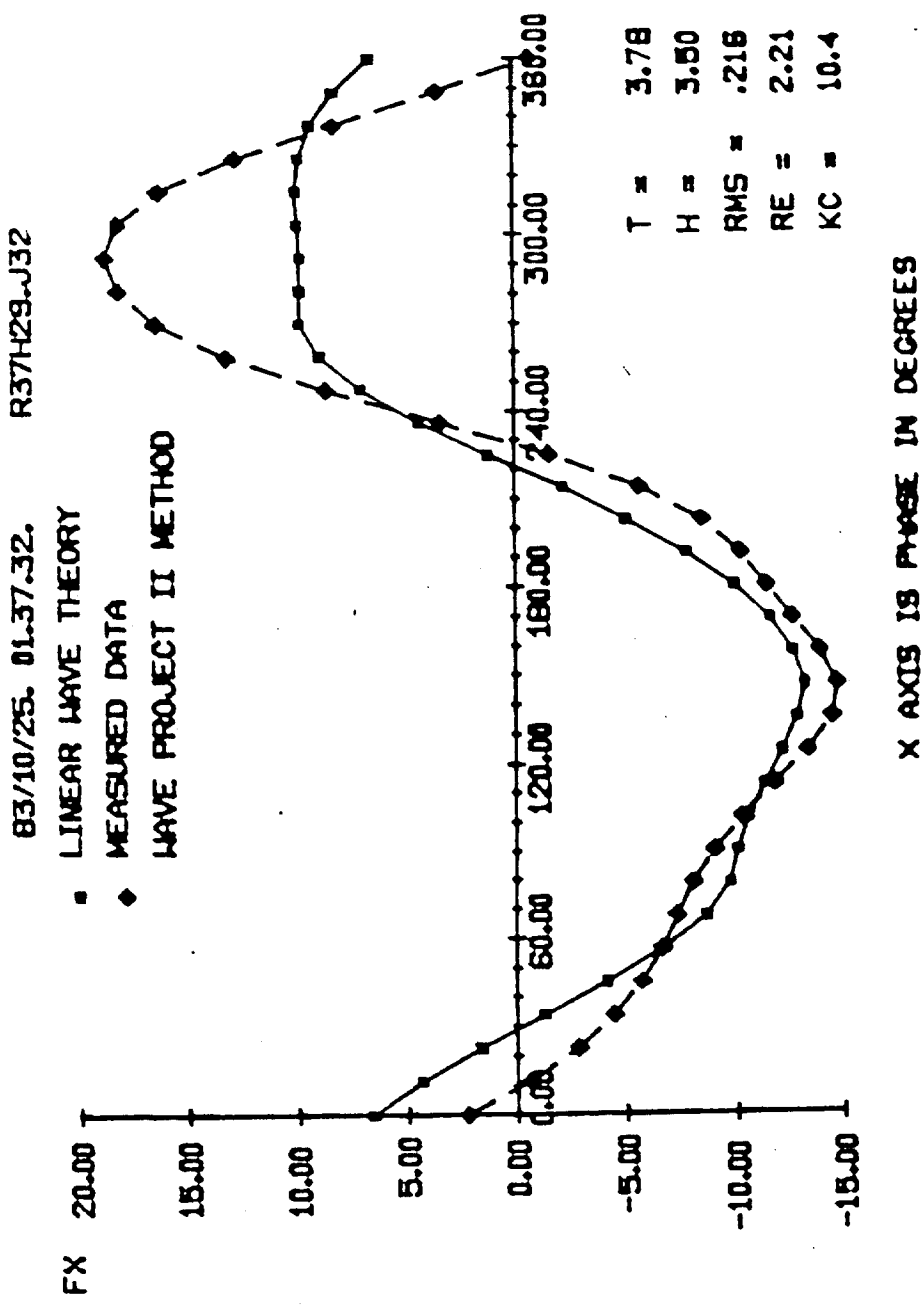


Fig. 4-44 Comparison between measured and predicted local inline force using LWT kinematics and Wave Project II coefficients for Wave #6, Block #7, Random Wave #32

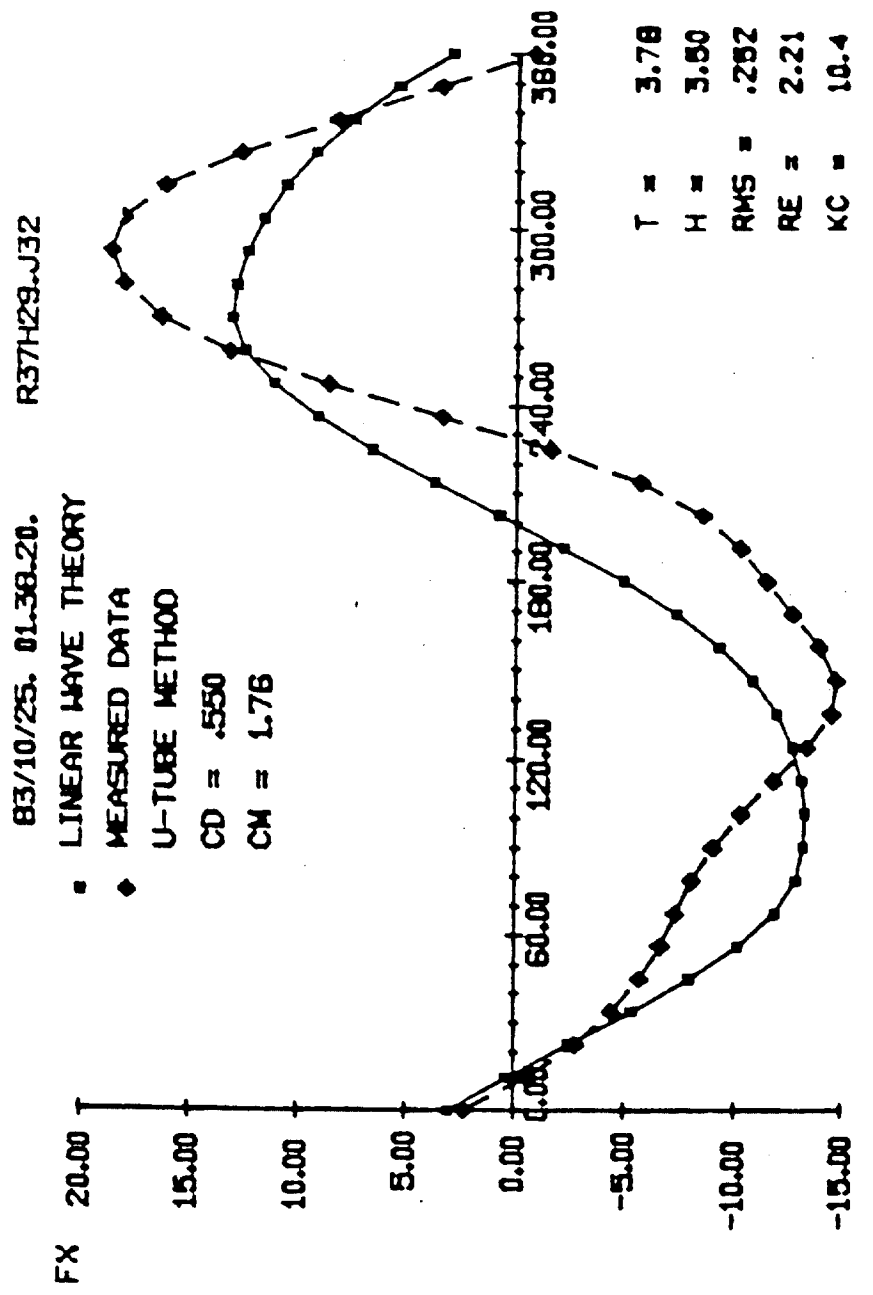


Fig. 4-45 Comparison between measured and predicted local inline force using LWT kinematics and U-tube coefficients for Wave #6, Block #7, Random Wave #32

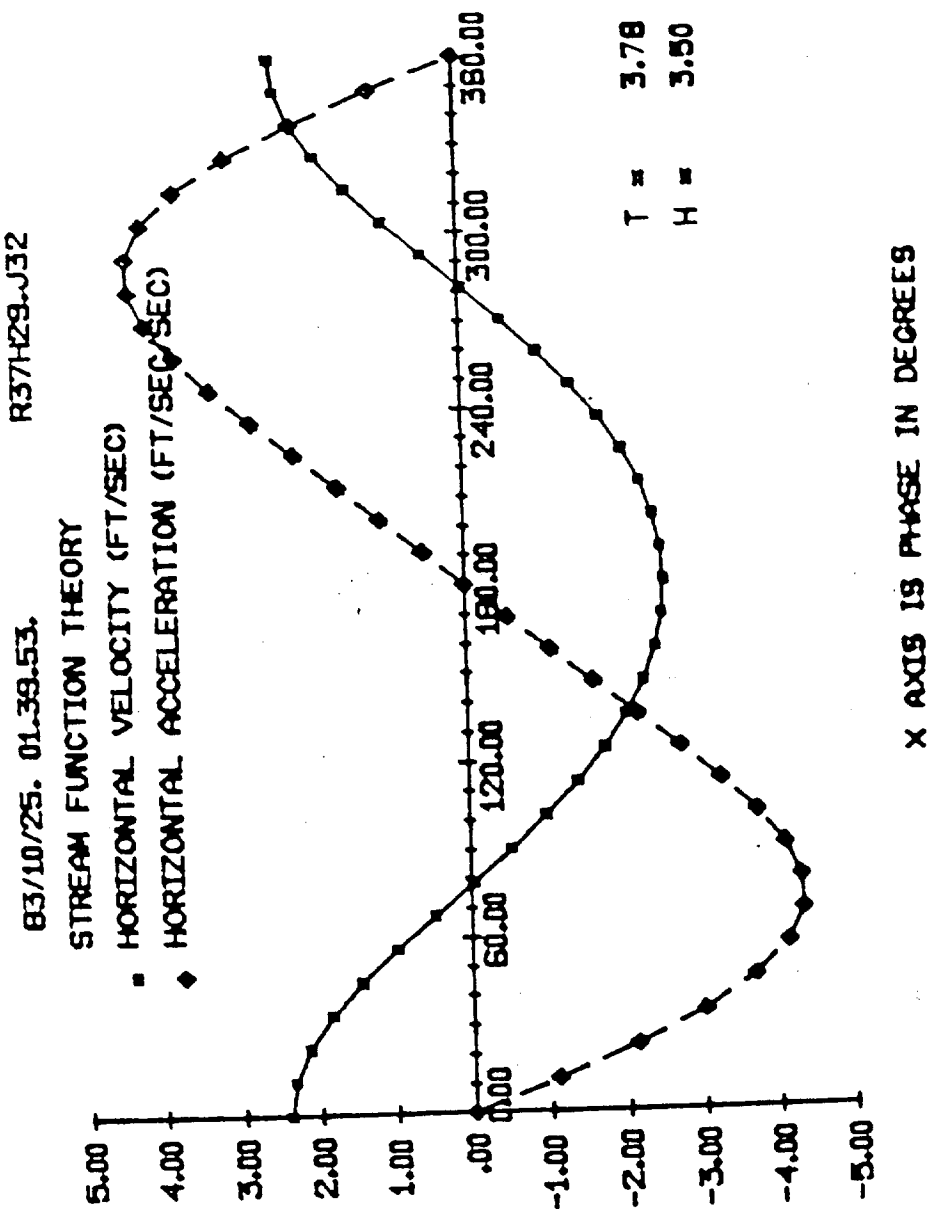


Fig. 4-46 Sample time series of stream function theory horizontal water particle velocity and acceleration for Wave #6, Block #7, Random Wave #32

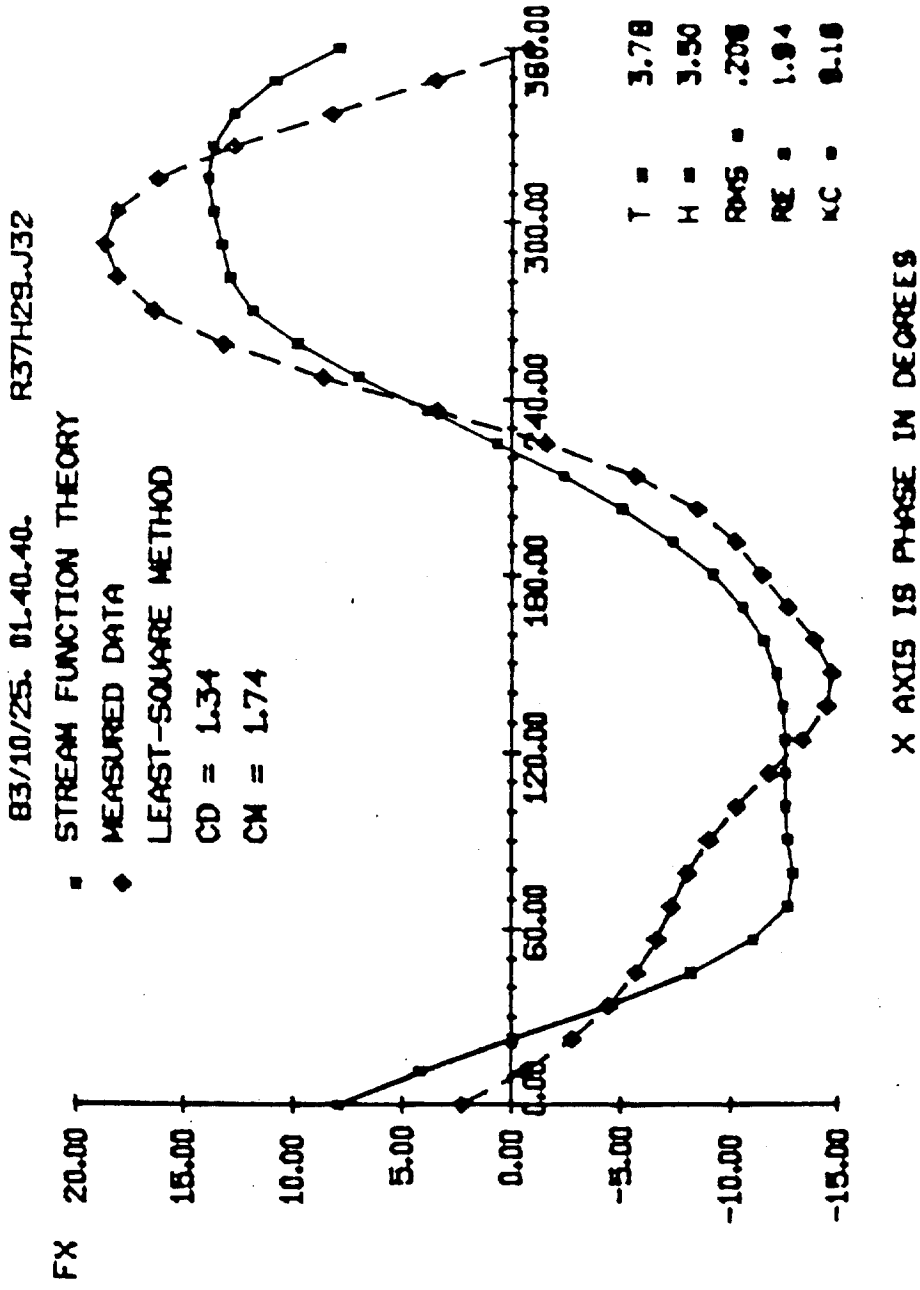


Fig. 4-47 Comparison between measured and predicted local inline force using stream function wave theory kinematics and measured coefficients for Wave #6, Block #7, Random Wave #32

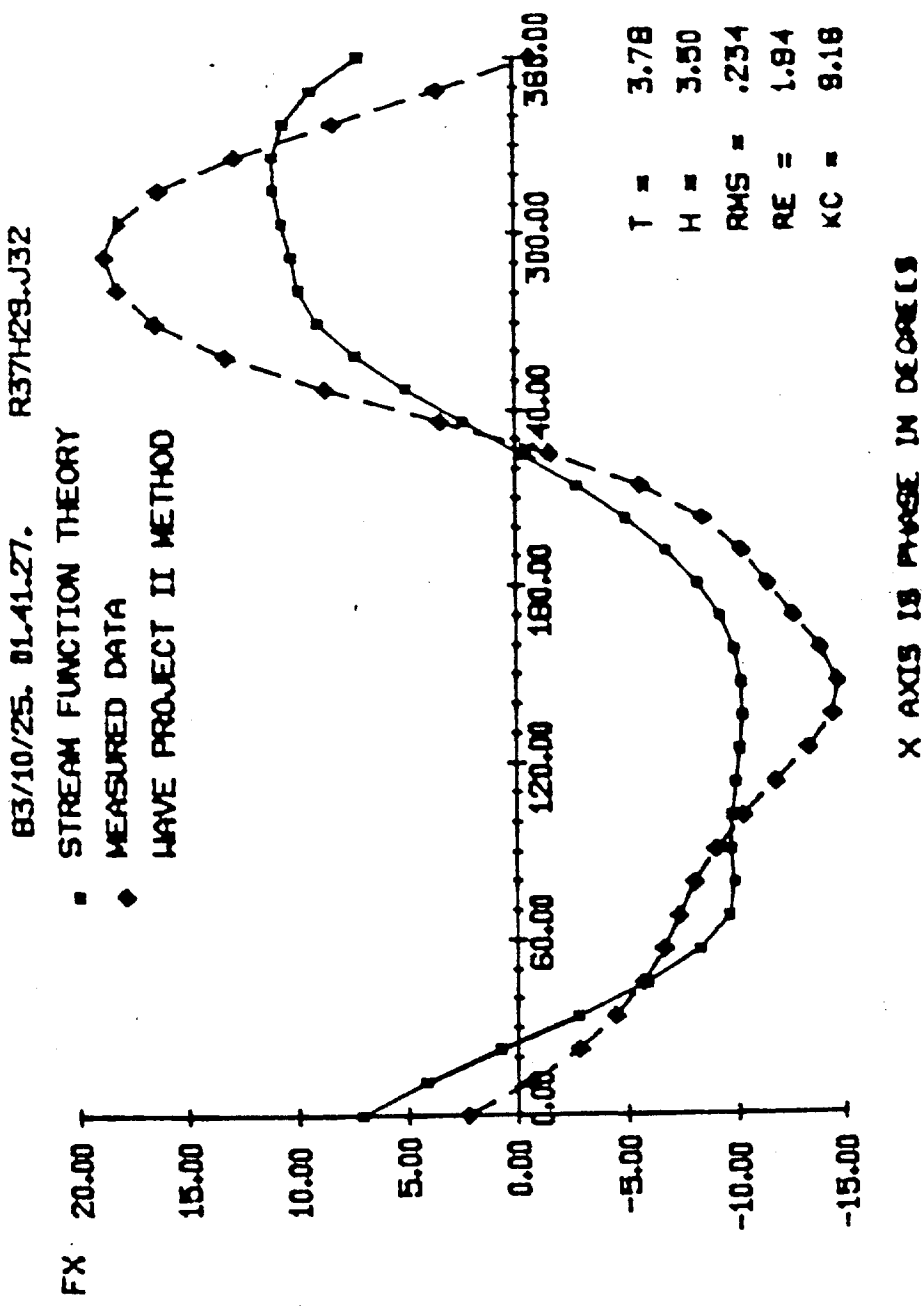


Fig. 4-48 Comparison between measured and predicted local inline force using stream function wave theory kinematics and Wave Project II coefficients for Wave #6, Block #7, Random Wave #32

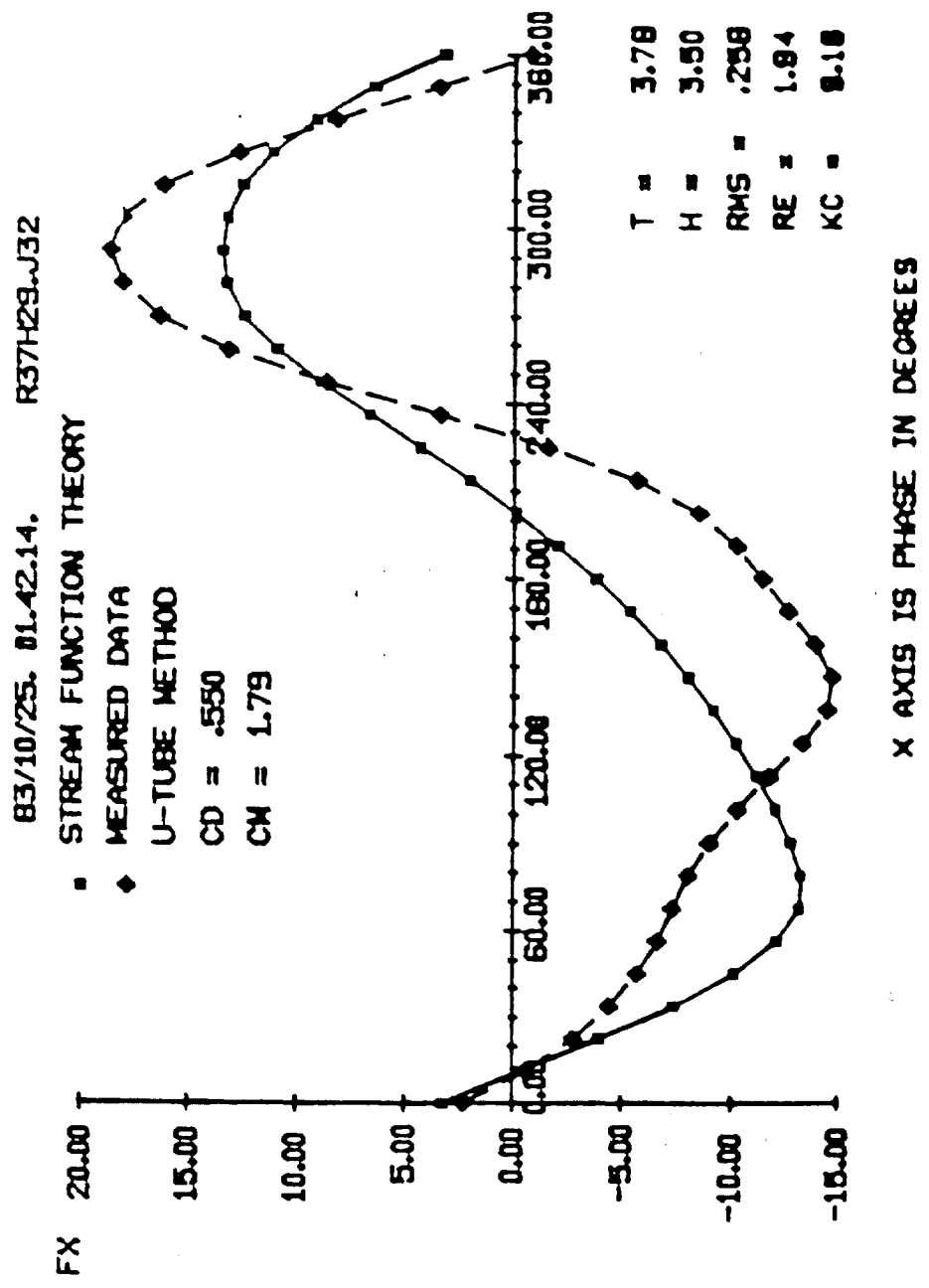


Fig. 4-49 Comparison between measured and predicted local inline force using stream function wave theory kinematics and U-tube coefficients for Wave #6, Block #7, Random Wave #32

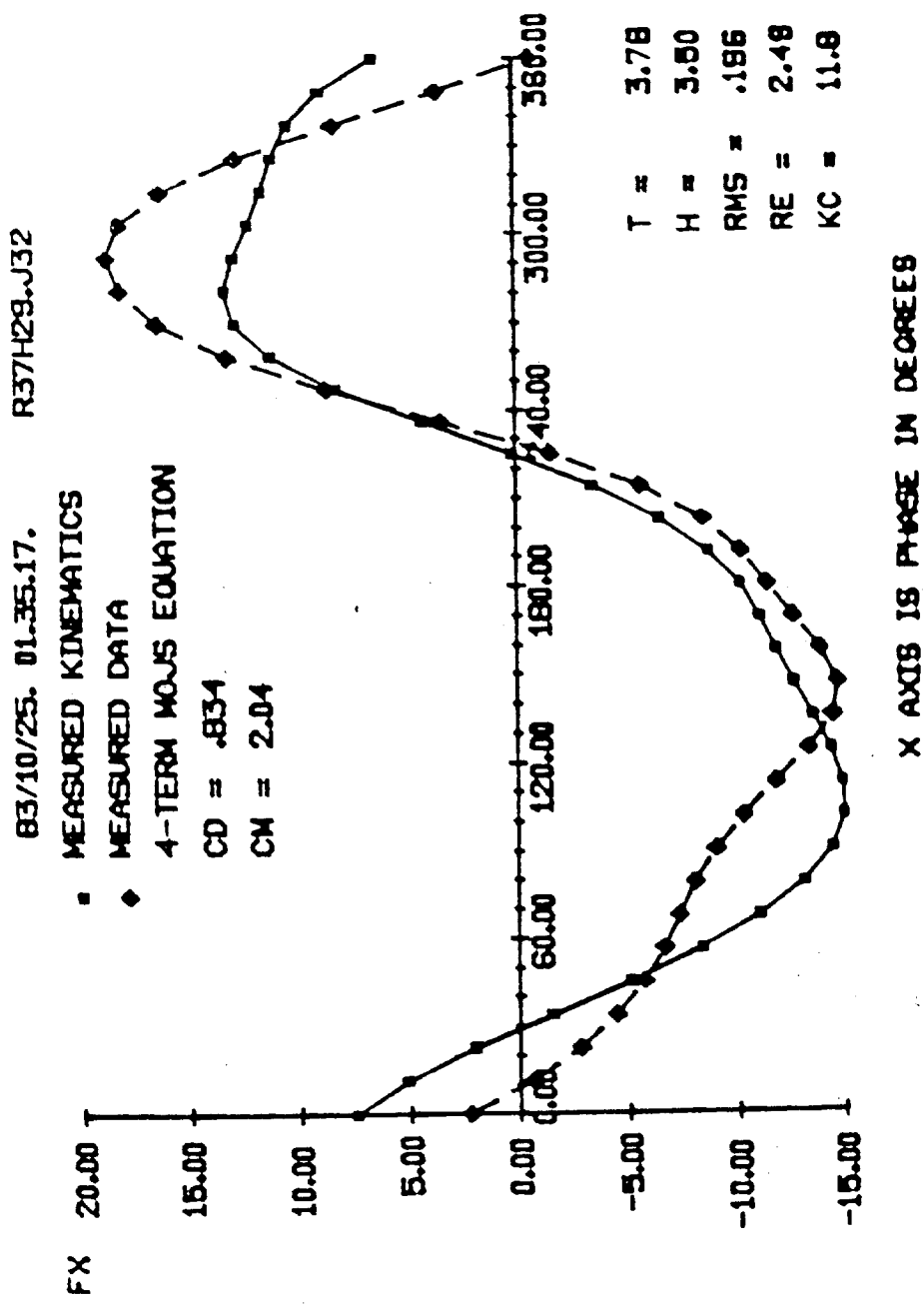


Fig. 4-50 Comparison between measured and predicted forces by the 4-term MOJS equation using measured kinematics for Wave #6, Block #7, Random Wave #32 (only 2 terms used since $C_m > 2.0$ and $C_d > 0.0$)

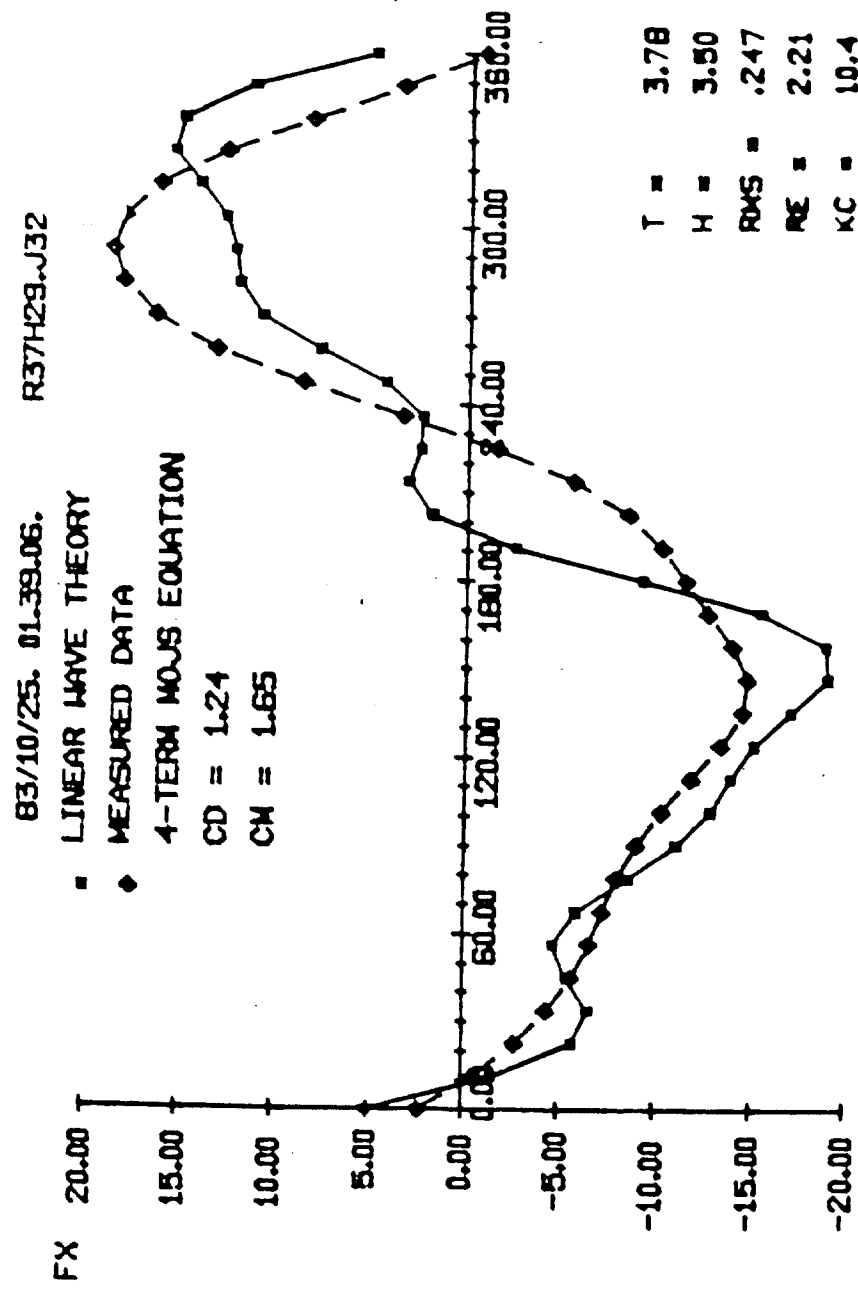


Fig. 4-51 Comparison between measured and predicted forces by the 4-term MOJS equation using linear wave theory kinematics for Wave #6 Block #7, Random Wave #32

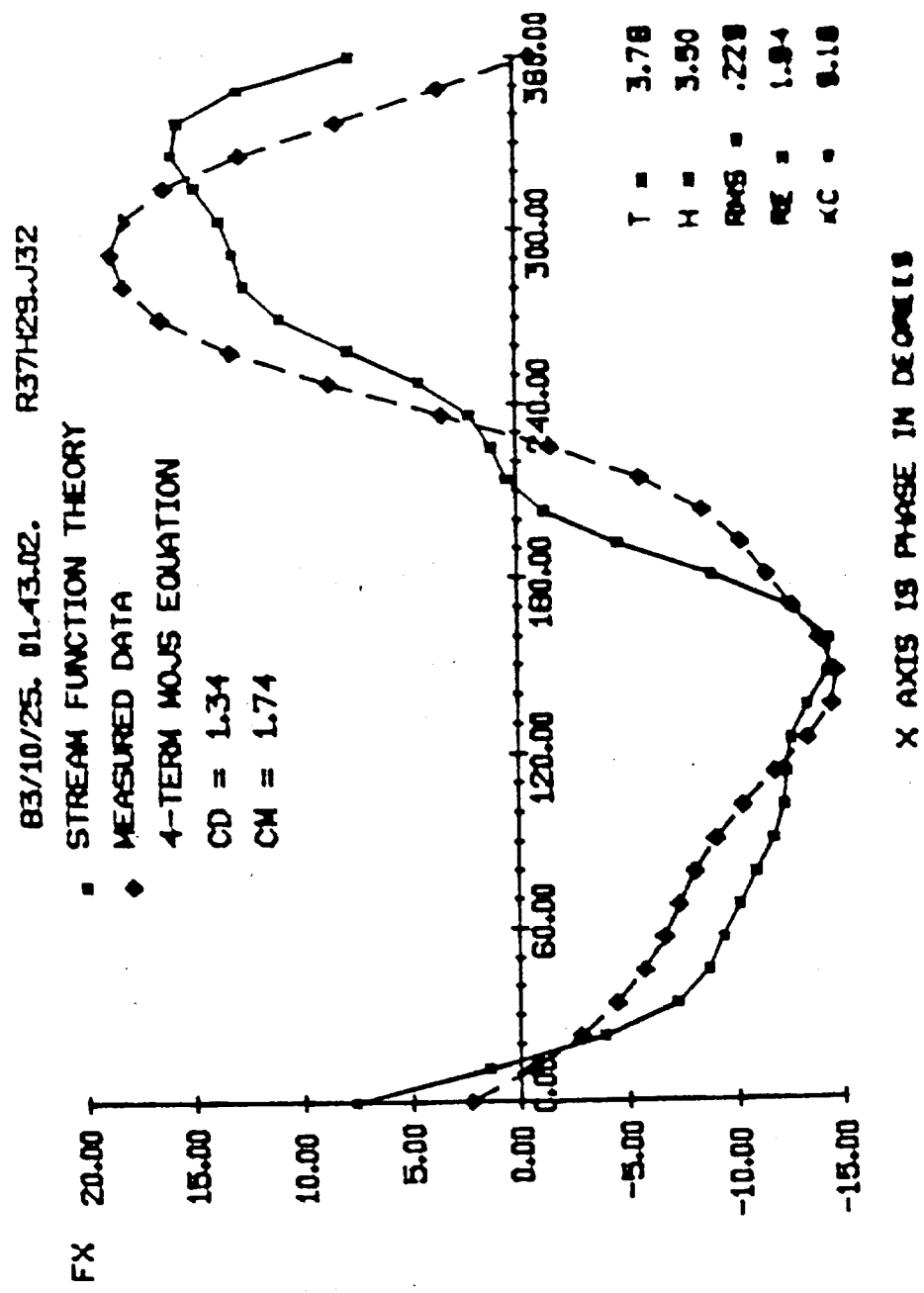


Fig. 4-52 Comparison between measured and predicted forces by the 4-term MOJS equation using stream function kinematics for Wave #6, Block #7, Random Wave #32

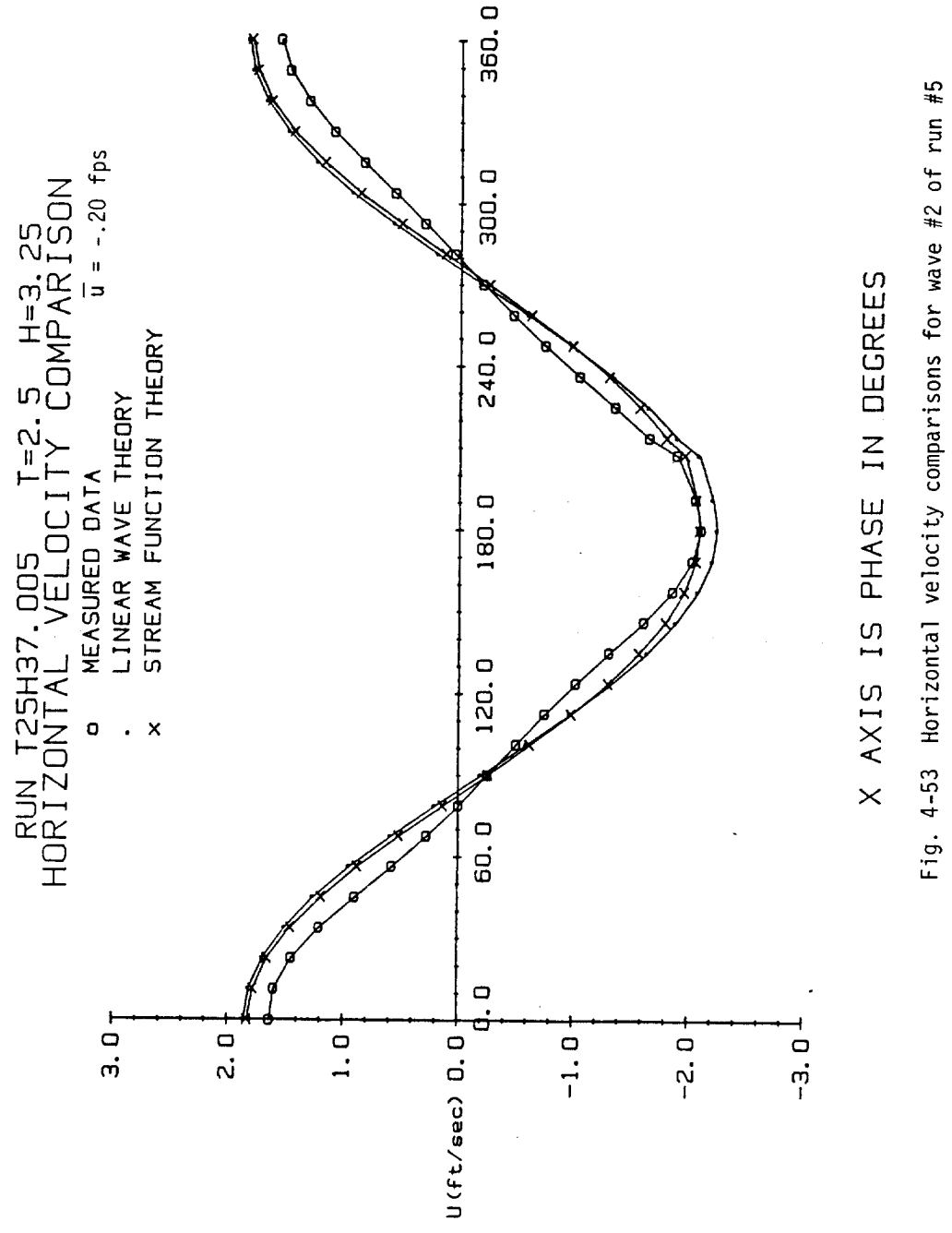


Fig. 4-53 Horizontal velocity comparisons for wave #2 of run #5

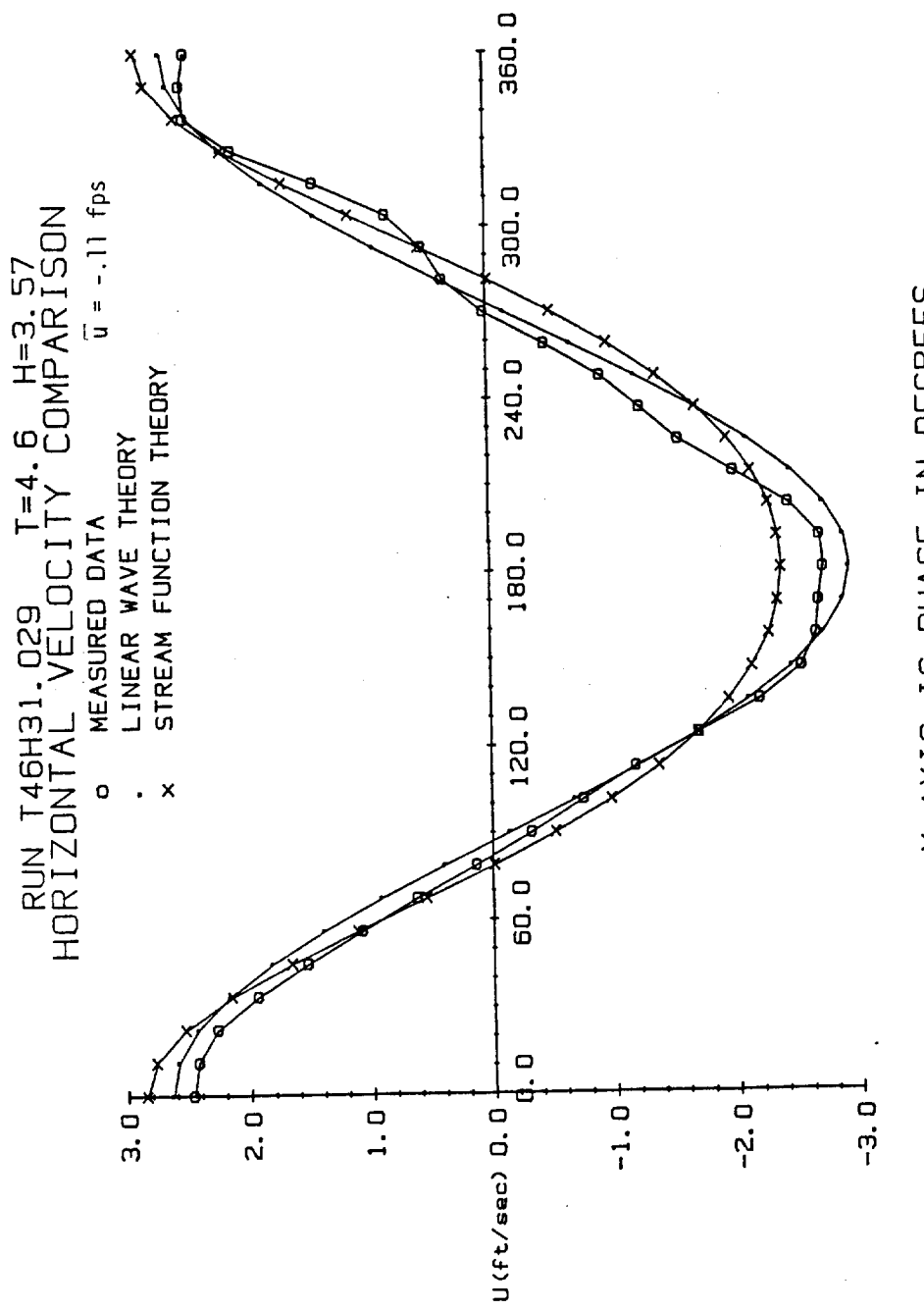
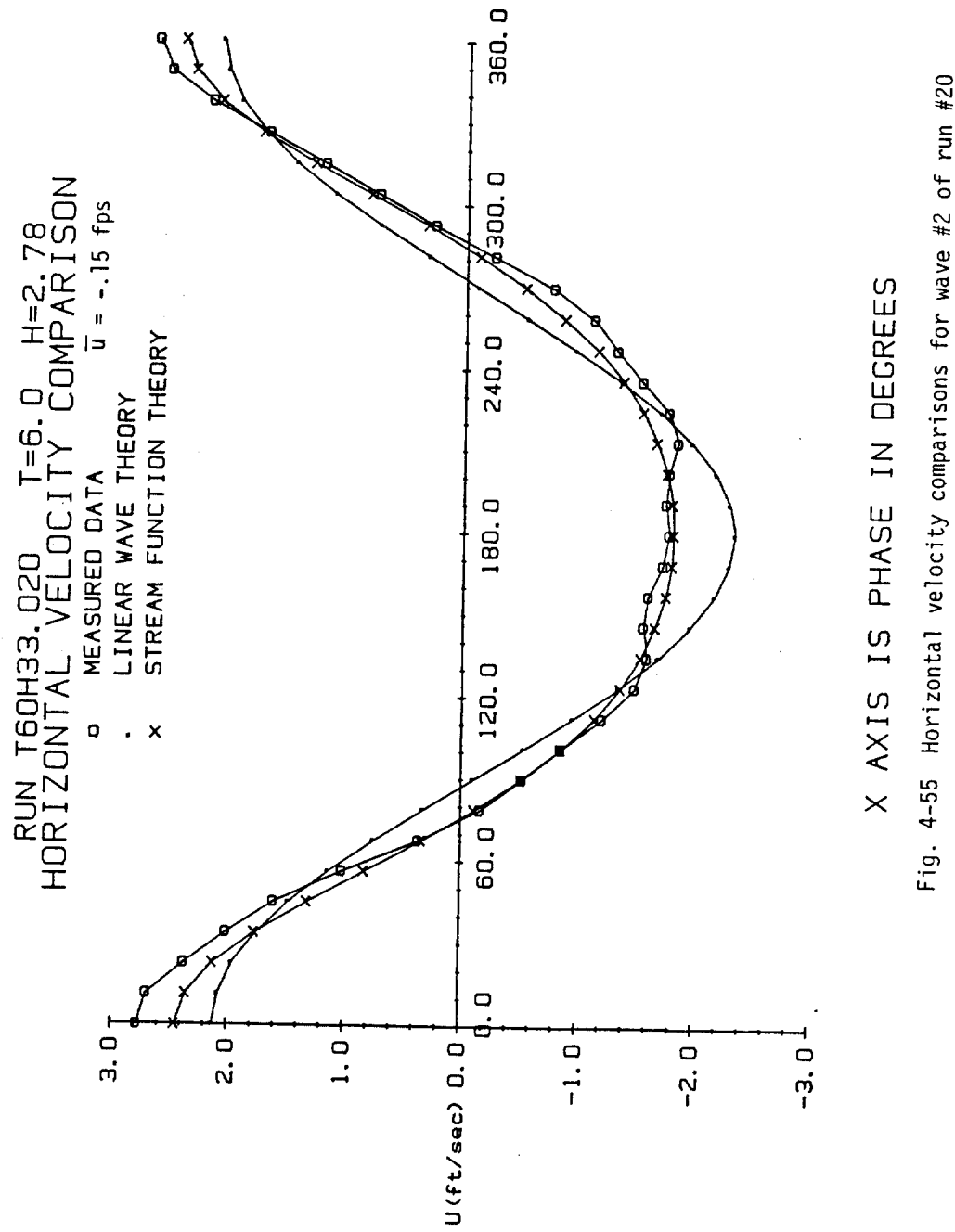


Fig. 4-54 Horizontal velocity comparisons for wave #2 of run #29



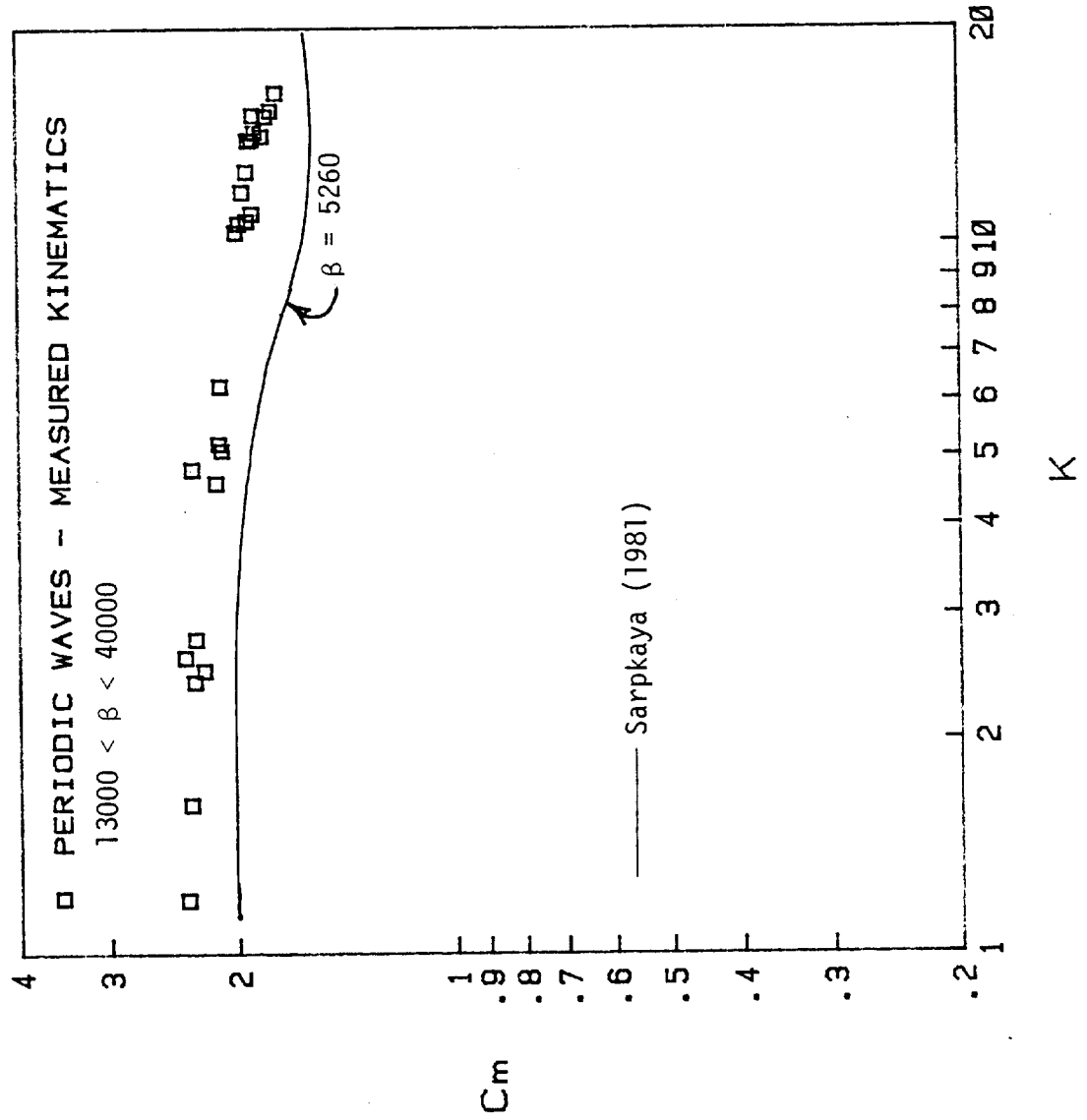
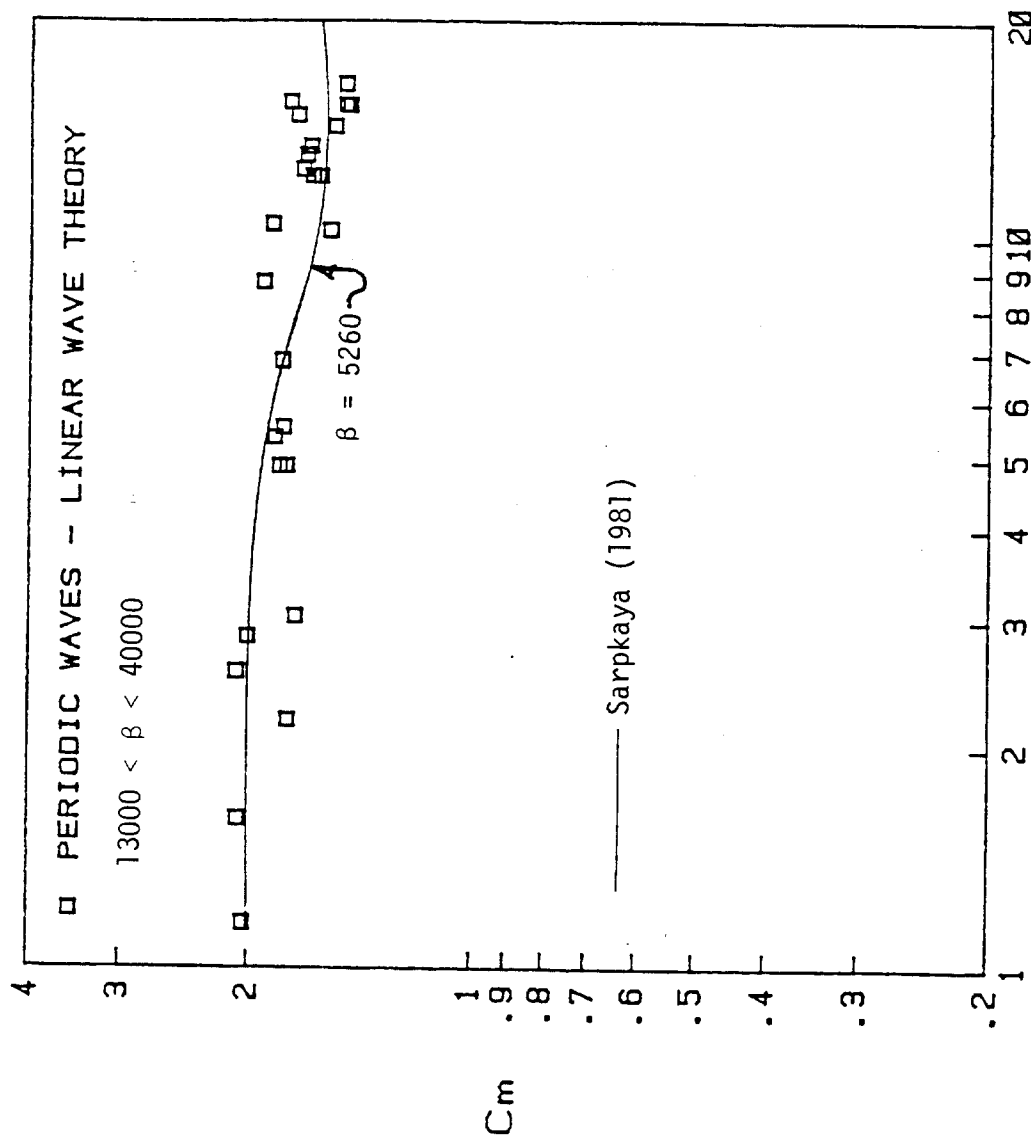


Fig. 5-1 Average inertia force coefficients for the 26 periodic wave runs for measured kinematics

Fig. 5-2 Average inertia force coefficients for the 26 periodic wave runs for linear wave theory kinematics



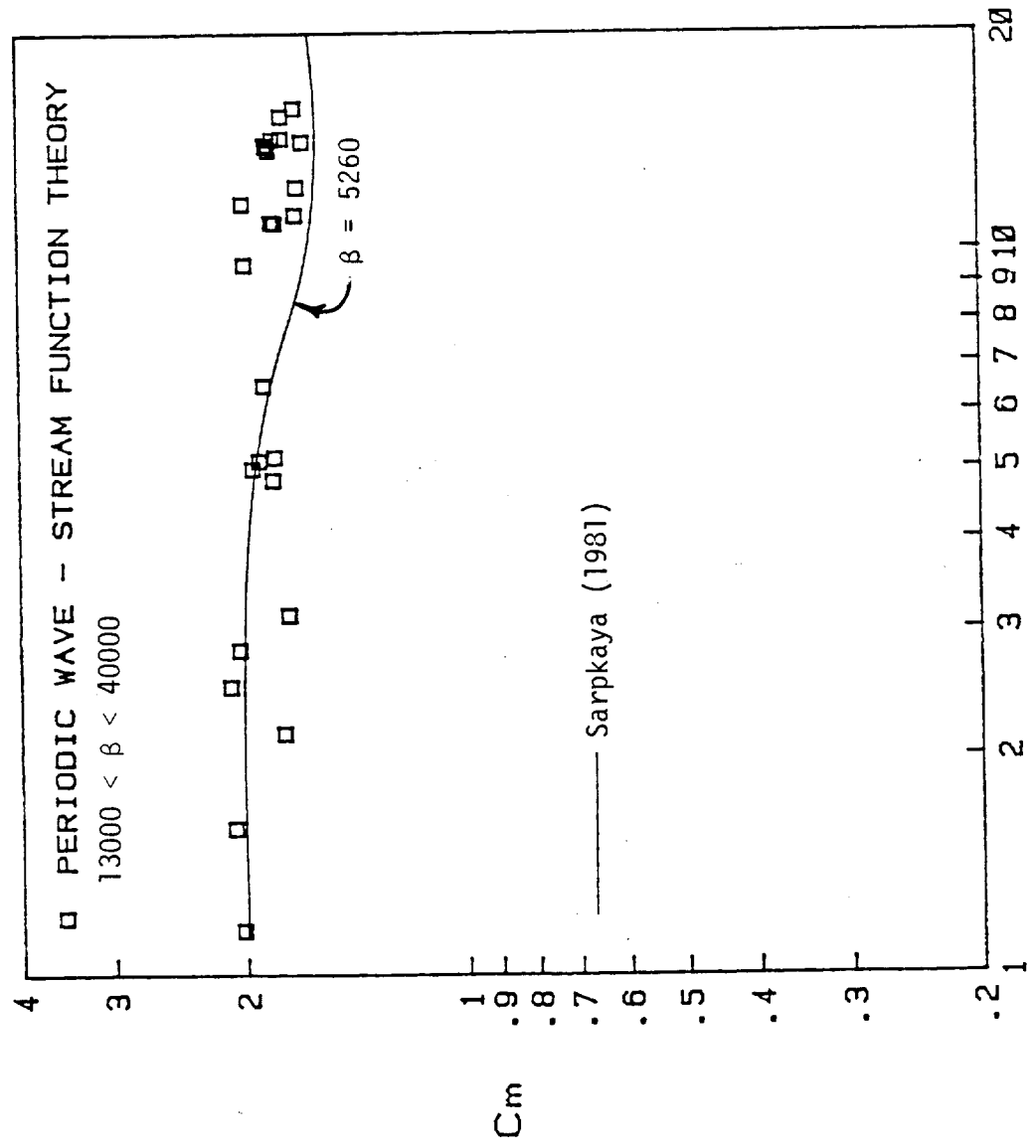


Fig. 5-3 Average inertia force coefficients for the 26 periodic wave runs for stream function wave theory kinematics

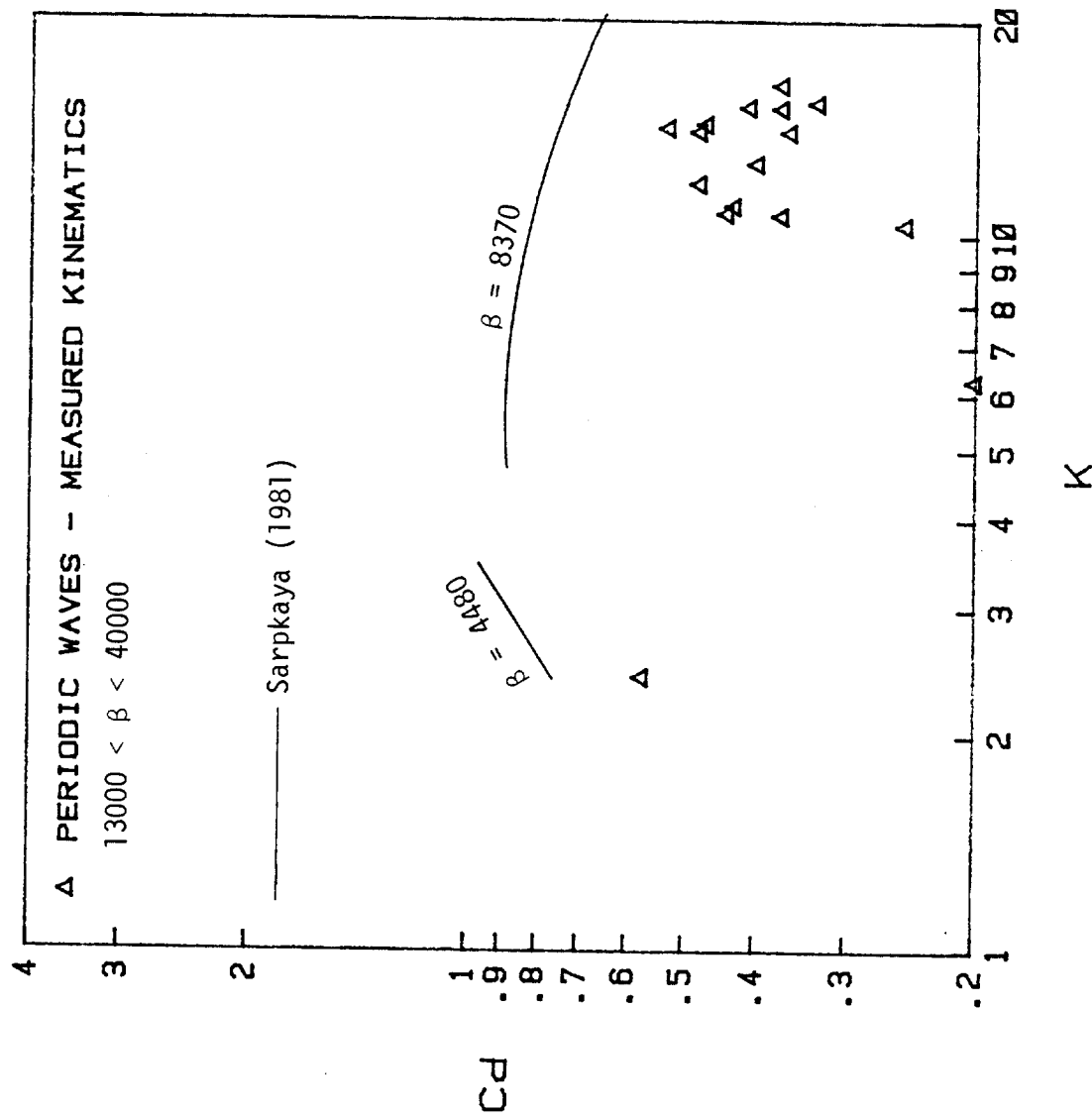


Fig. 5-4 Average drag force coefficient for the 26 periodic wave runs for measured kinematics

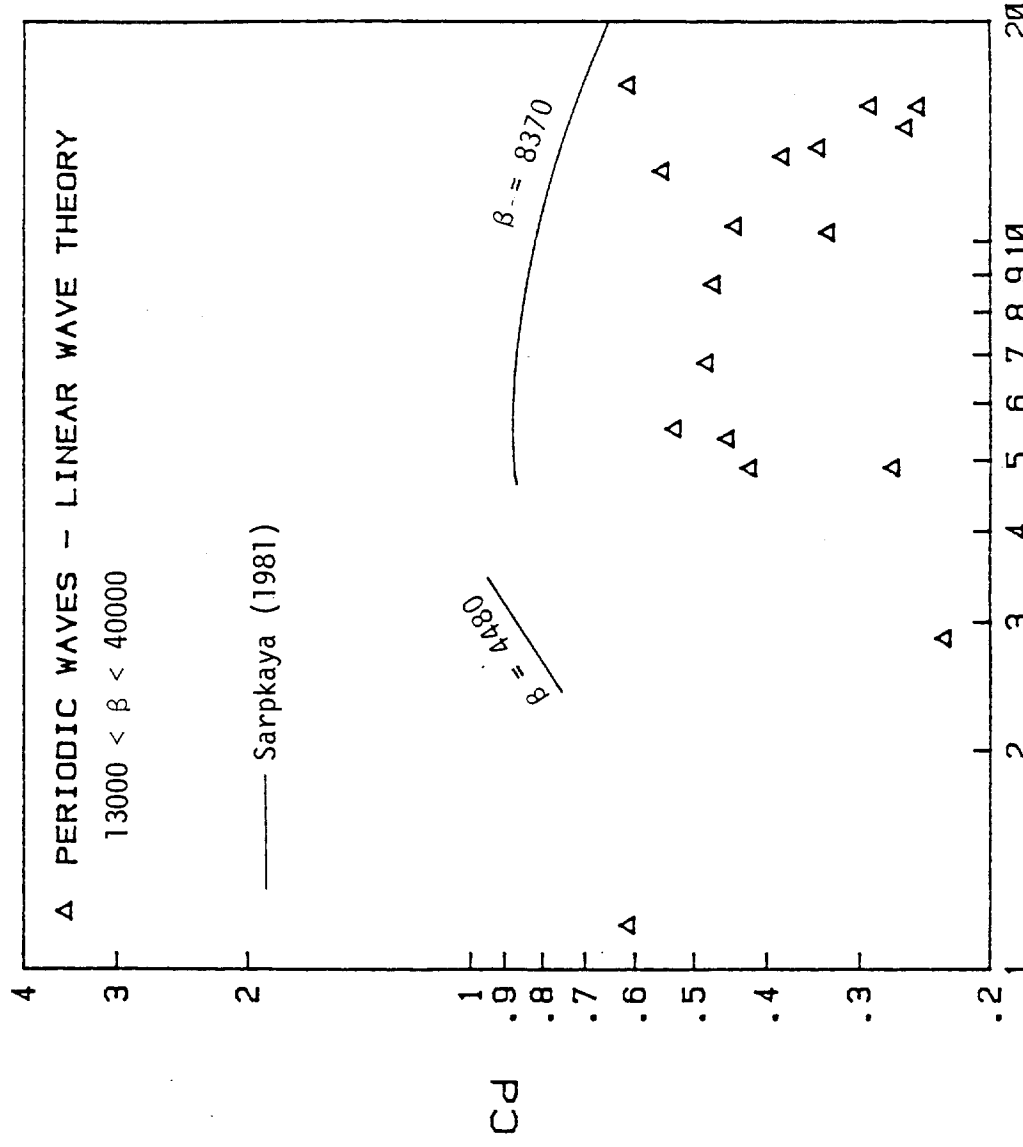


Fig. 5-5 Average drag force coefficient for the 26 periodic wave runs for linear wave theory kinematics

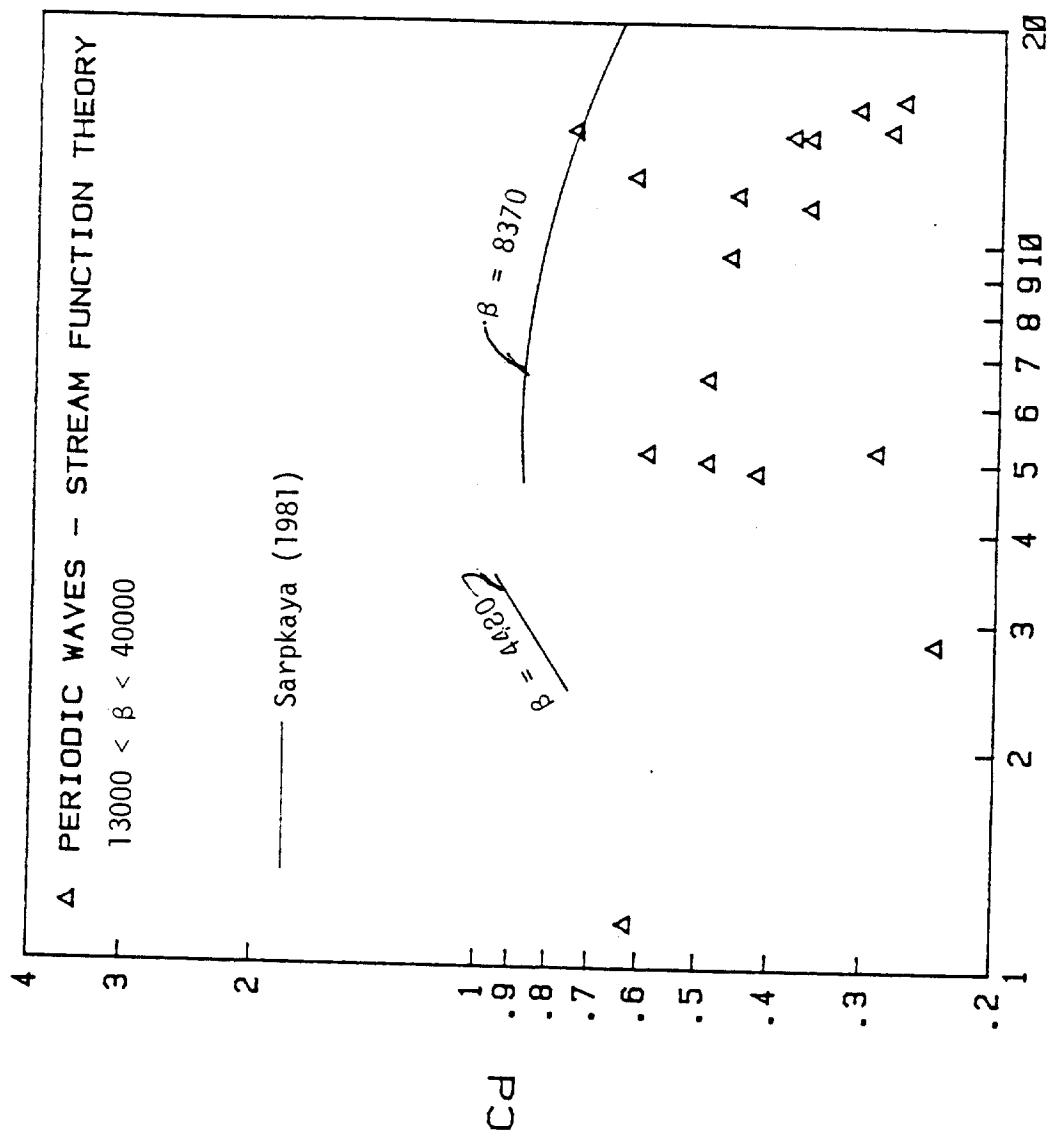


Fig. 5-6 Average drag force coefficient for the 26 periodic wave runs for stream function wave theory kinematics

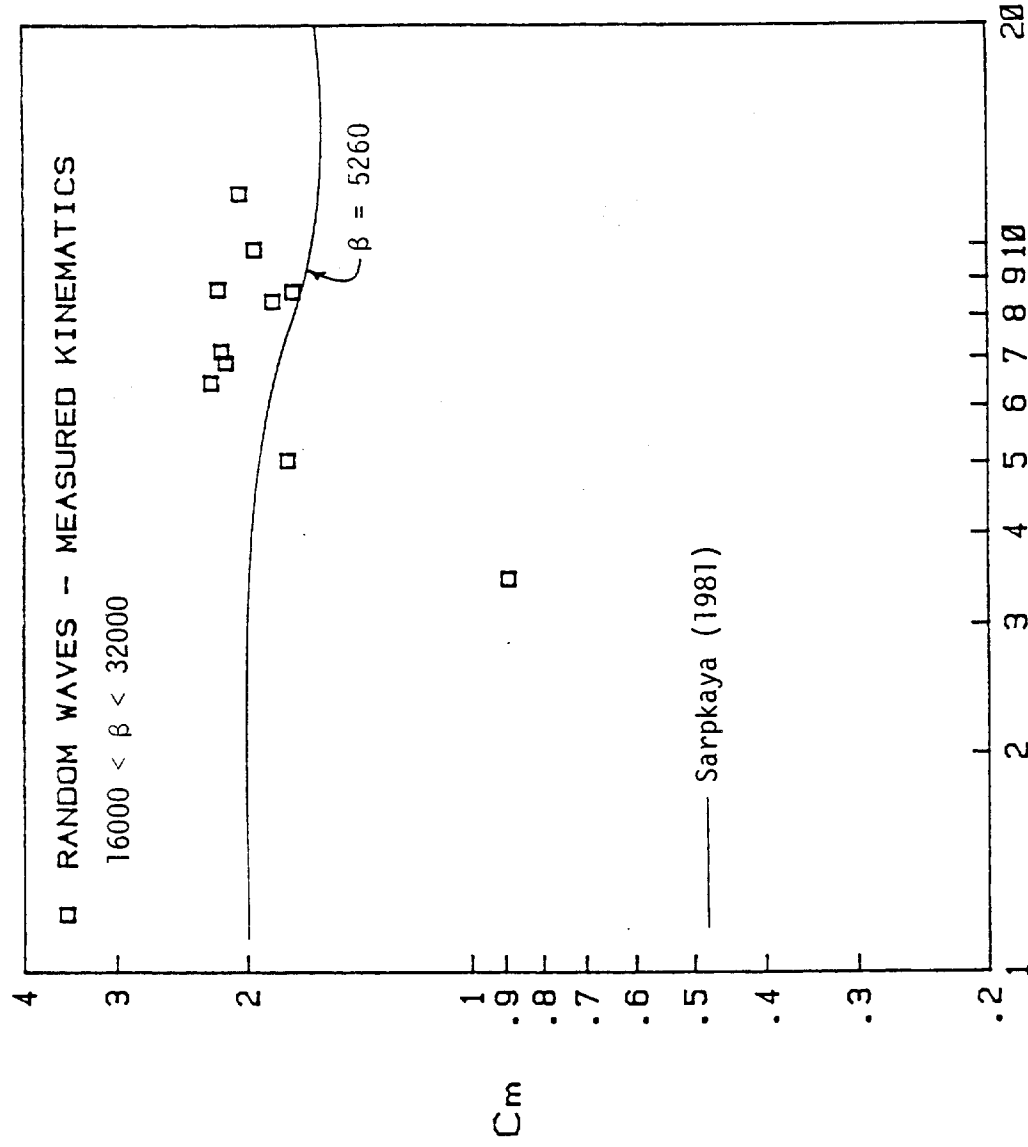


Fig. 5-7 Inertia force coefficients for the 10 individual waves from the two random wave runs using measured kinematics

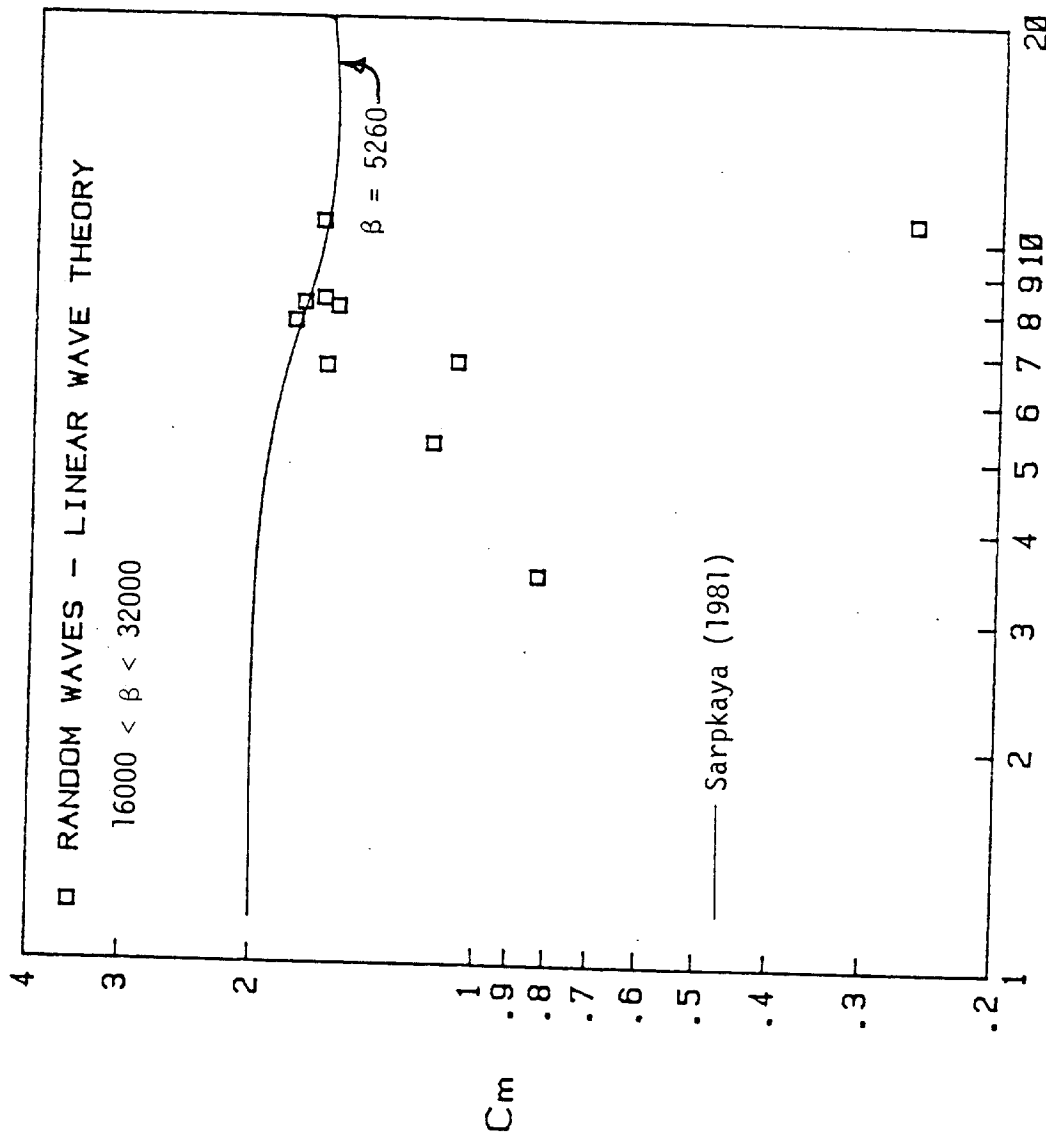


Fig. 5-8 Inertia force coefficients for the 10 individual waves selected from the two random wave runs using linear wave theory kinematics

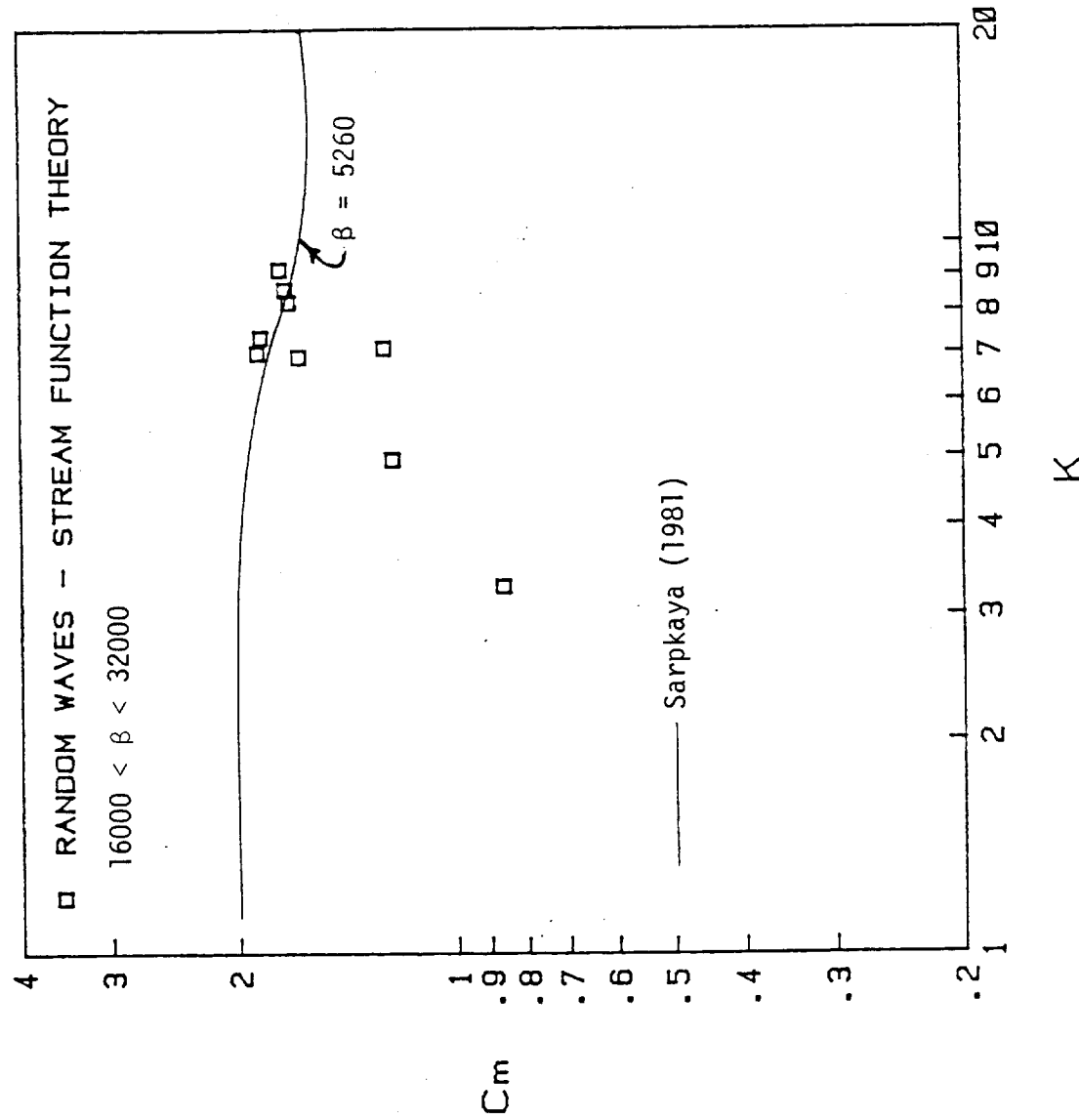


Fig. 5-9 Inertia force coefficients for the 10 individual waves selected from the two random wave runs using stream function wave theory kinematics

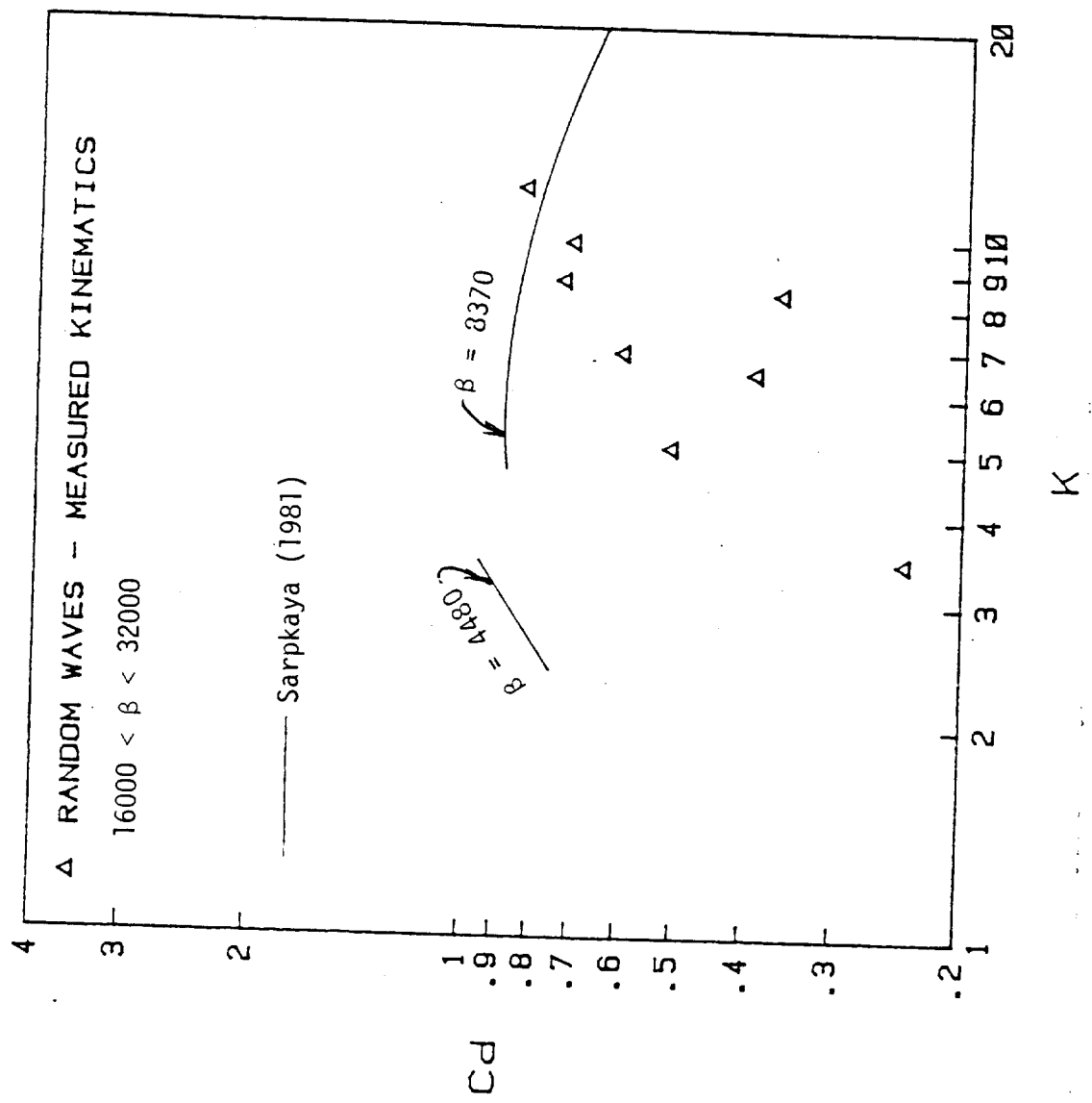


Fig. 5-10 Drag force coefficients for the 10 individual waves selected from the two random wave runs using measured kinematics (negative C_d 's not plotted)

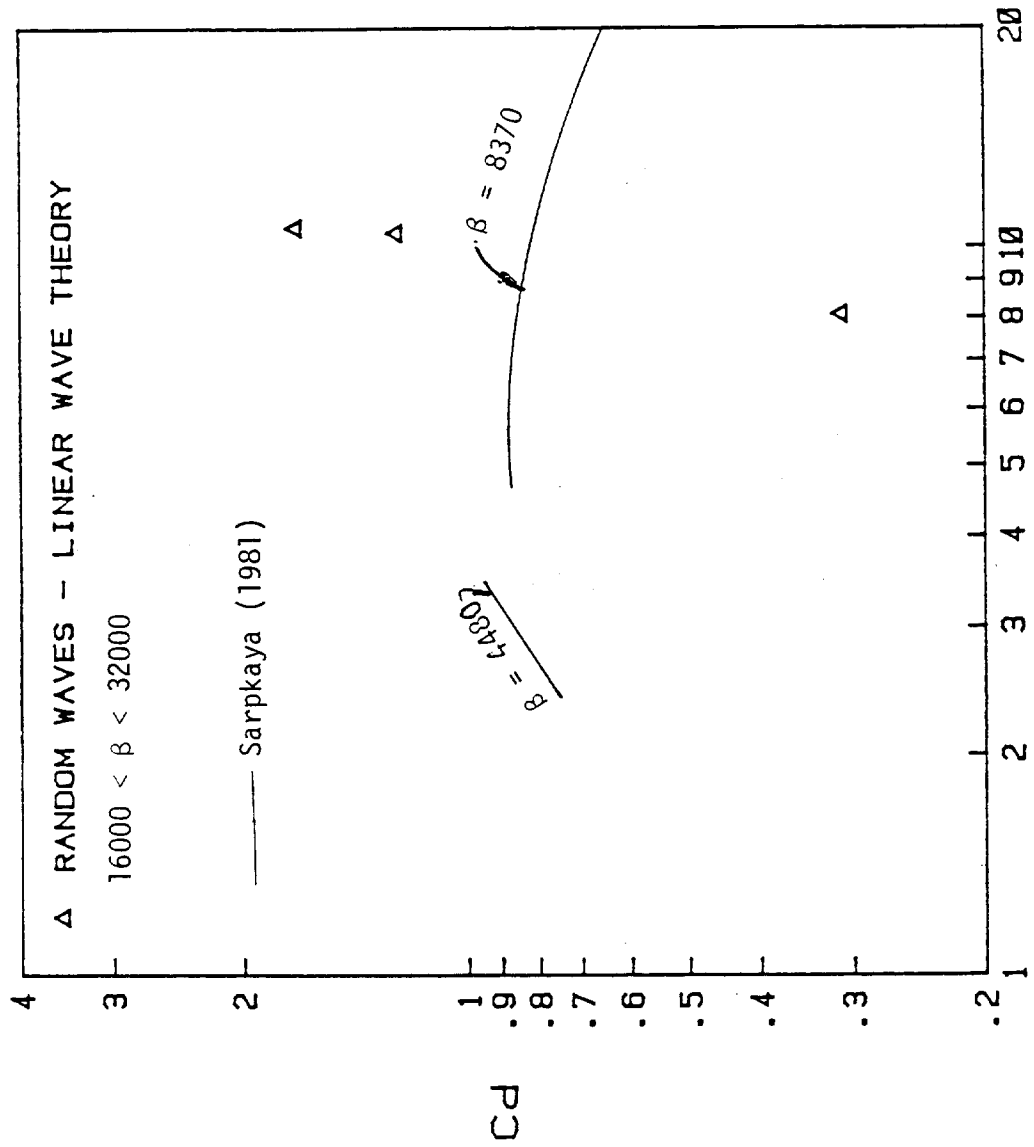


Fig. 5-11 Drag force coefficients for the 10 individual waves selected from the two random wave runs using linear wave theory kinematics (negative C_d 's not plotted)

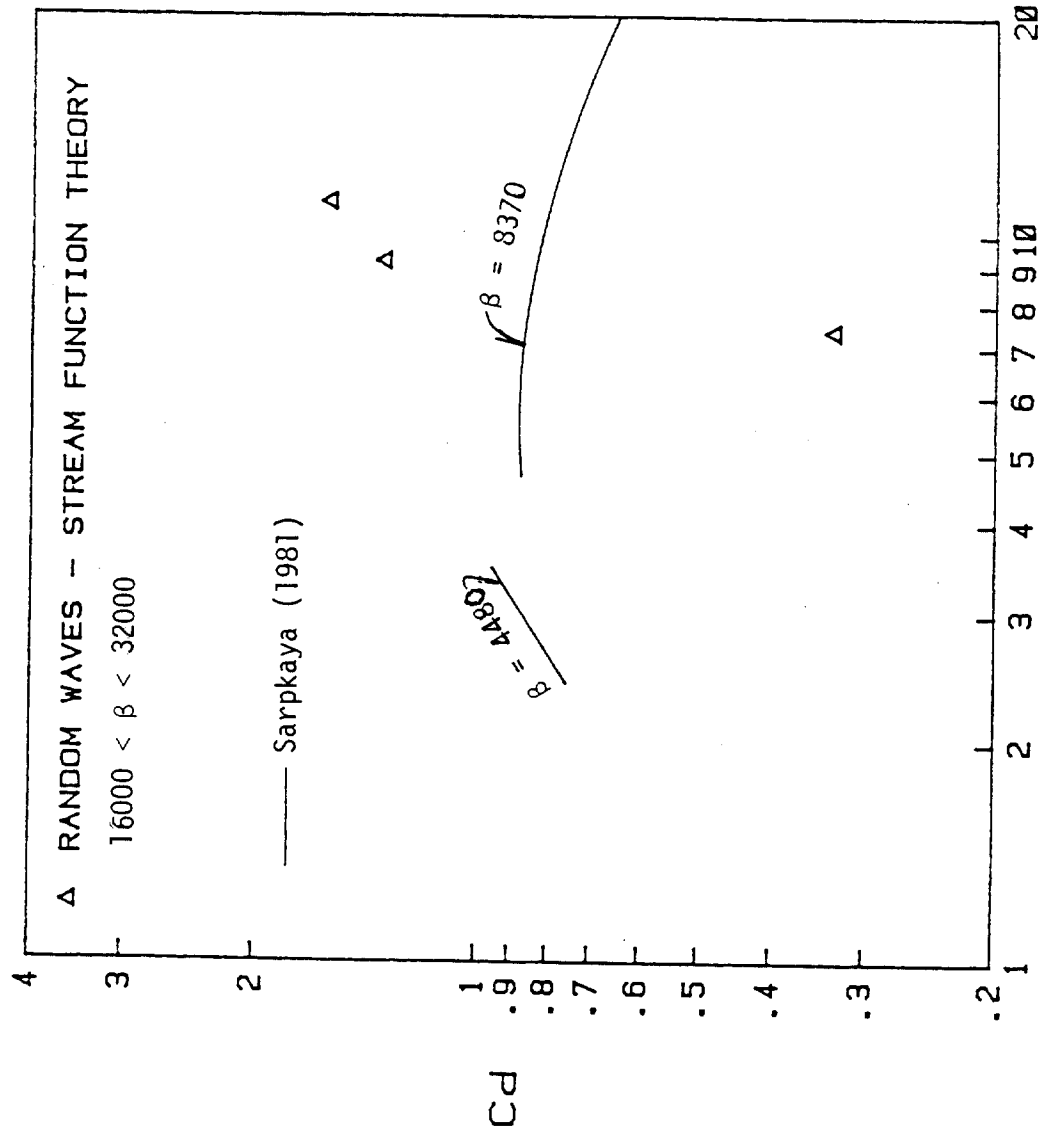


Fig. 5-12 Drag force coefficients for the 10 individual waves selected from the two random wave runs using stream function wave theory kinematics (negative C_d 's not plotted)

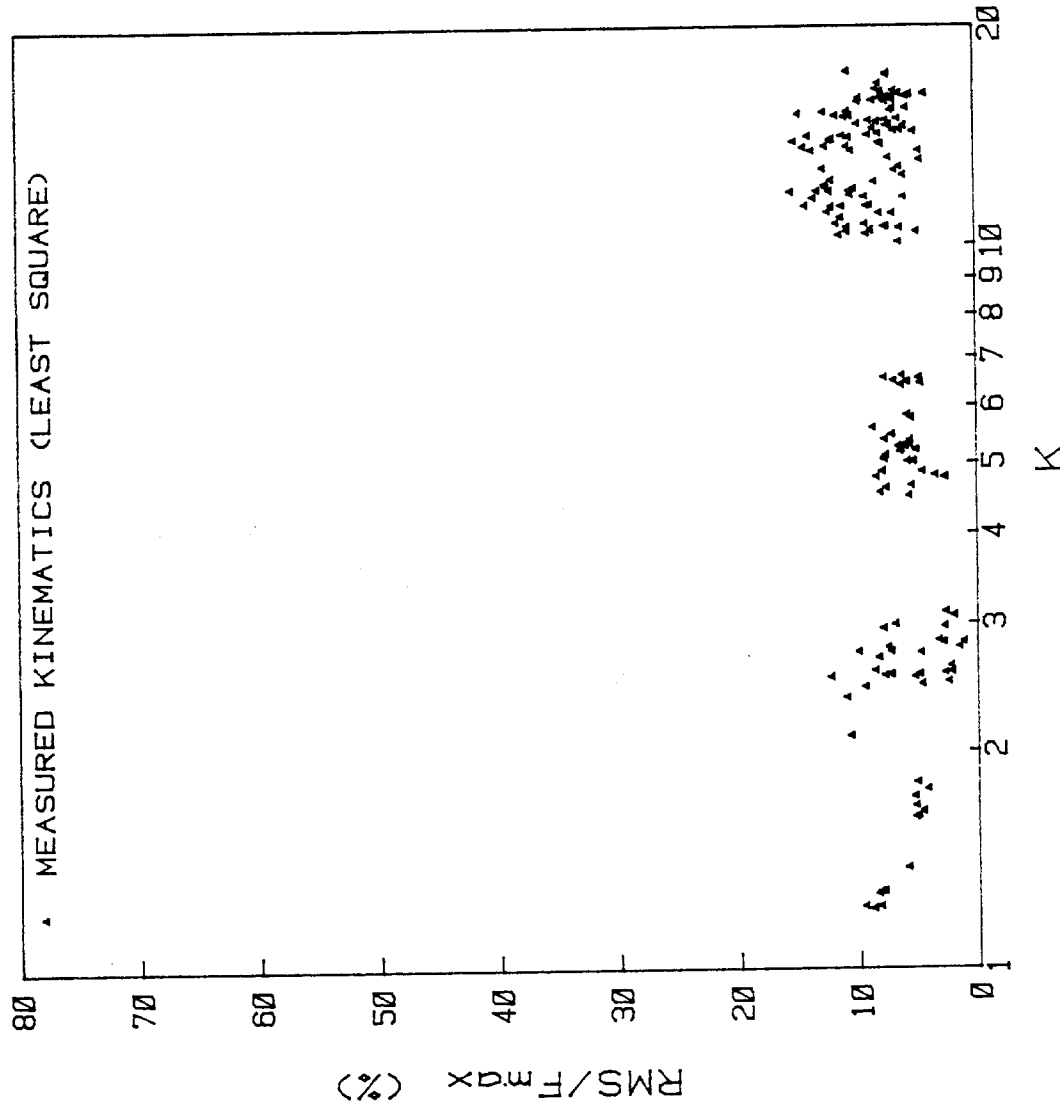


Fig. 5-13 RMS errors (%) for the 2-term MOJS equation

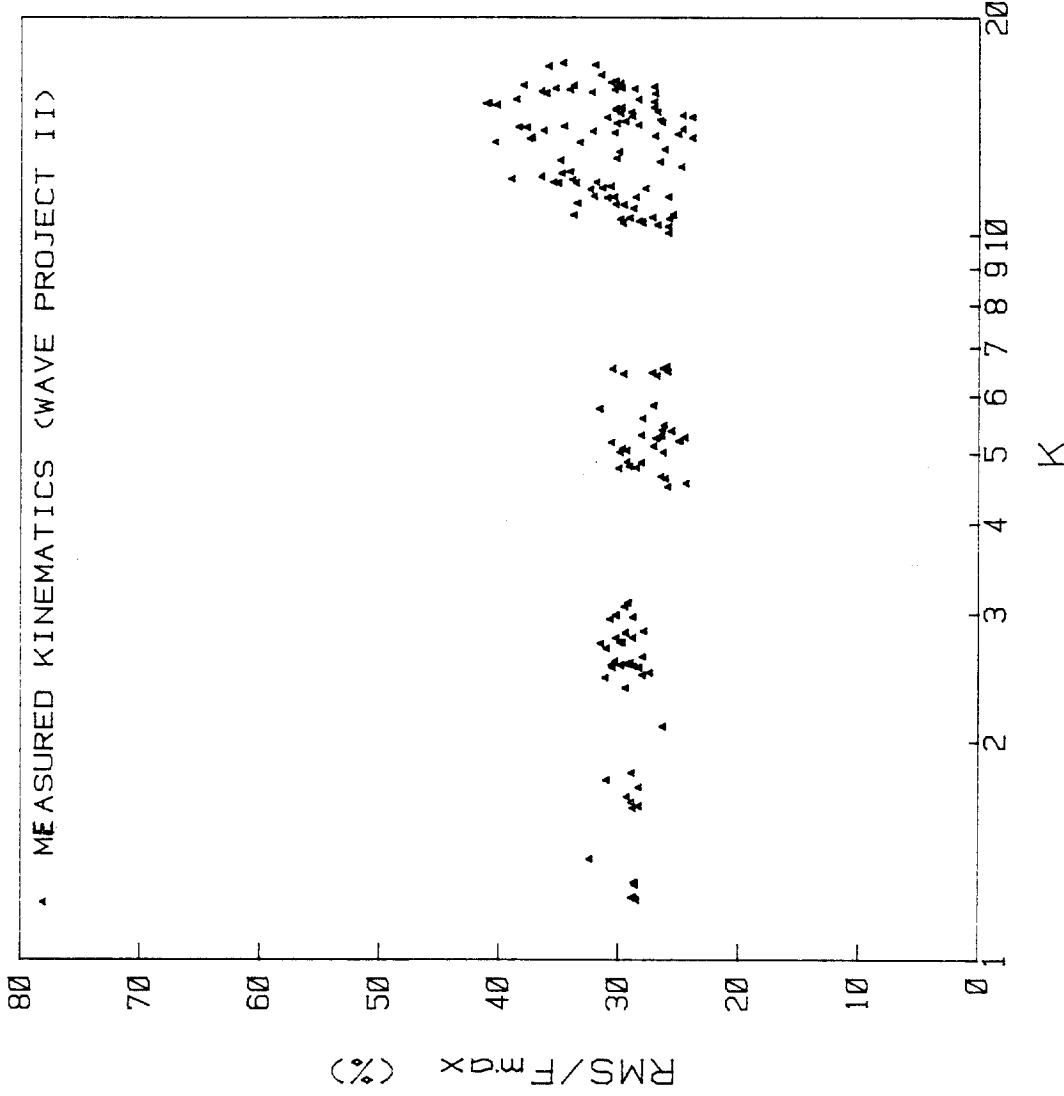


Fig. 5-14 RMS errors (%) for the 2-term MOJS equation

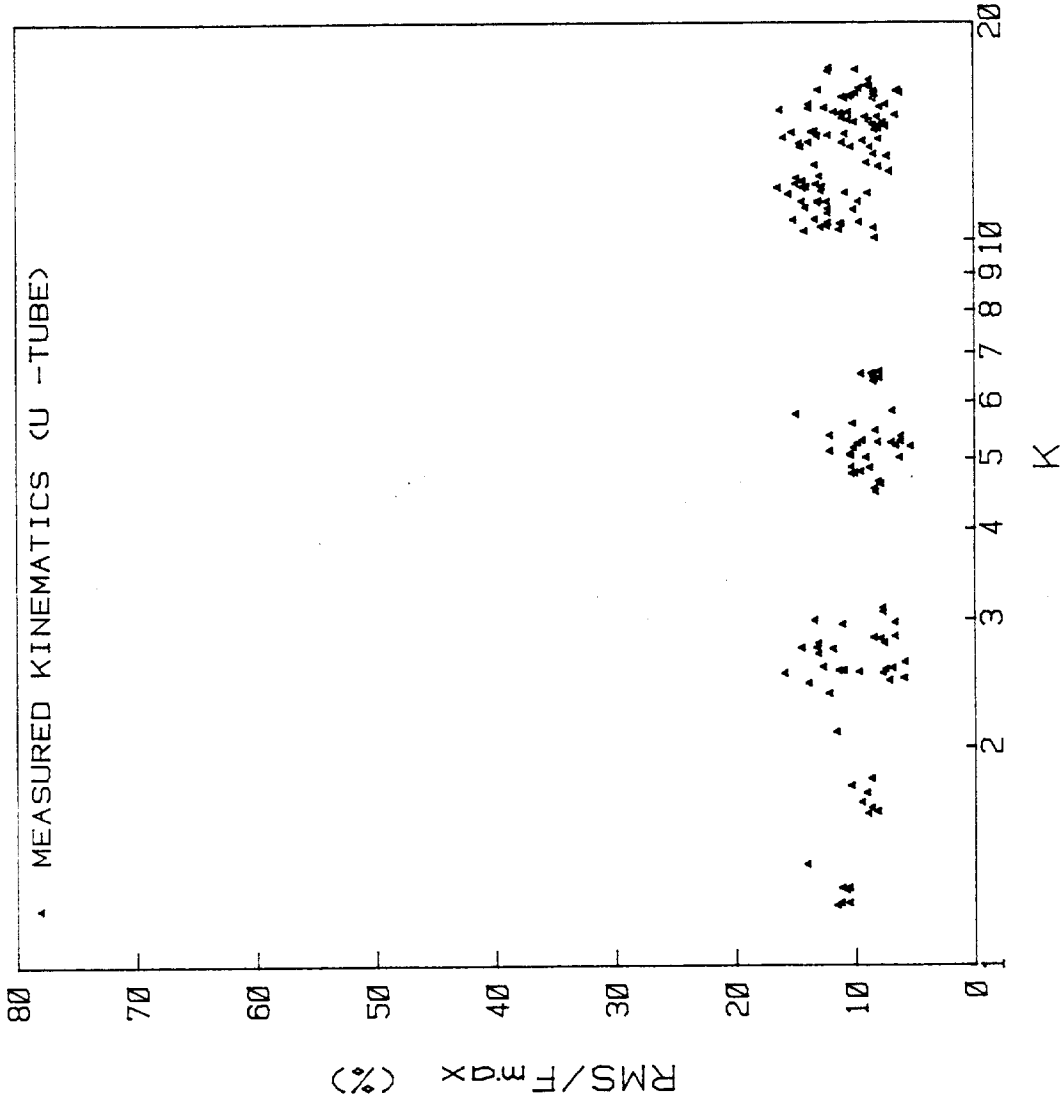


Fig. 5-15 RMS errors (%) for the 2-term MOJS equation

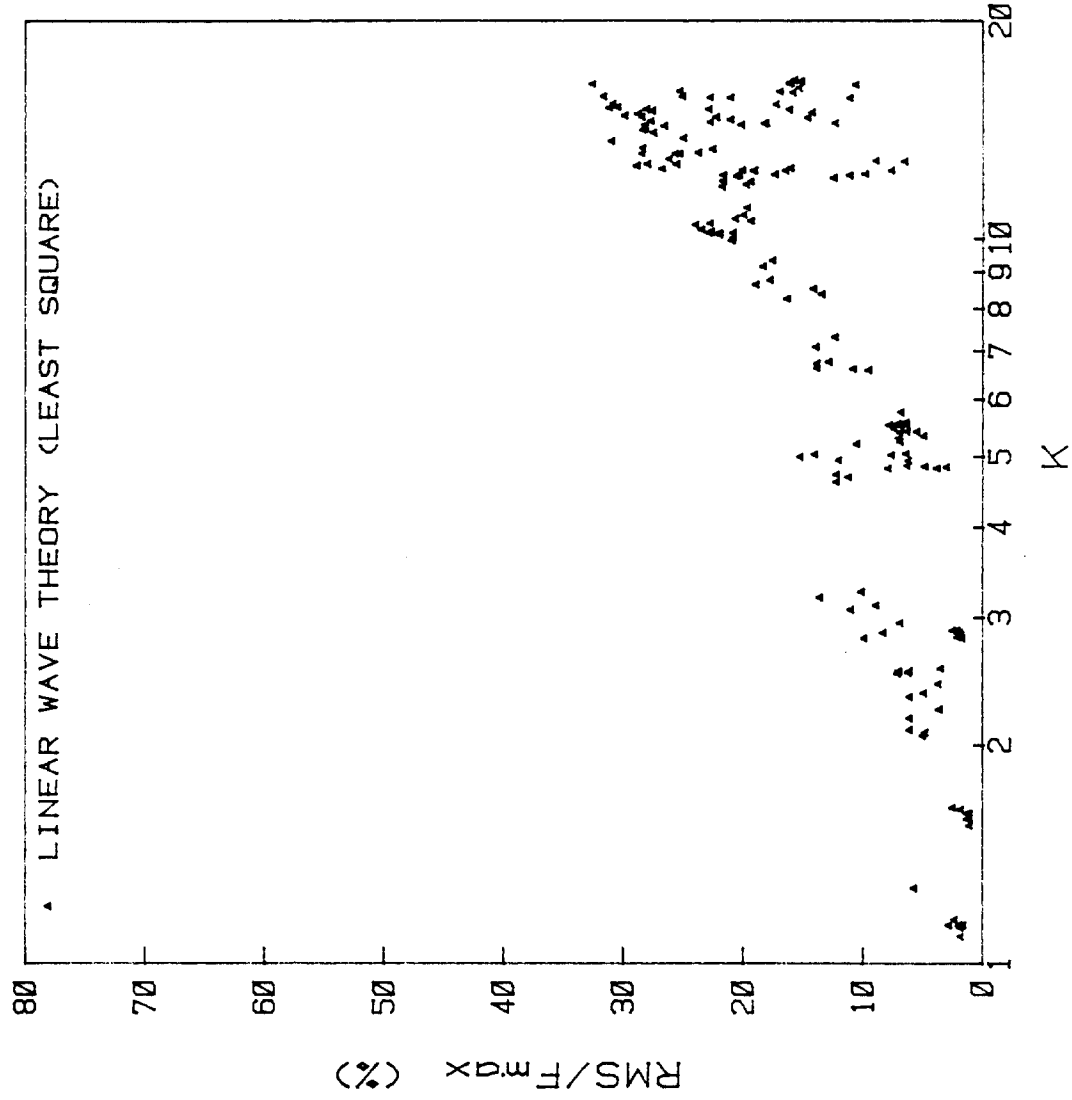


Fig. 5-16 RMS errors (%) for the 2-term MOJS equation

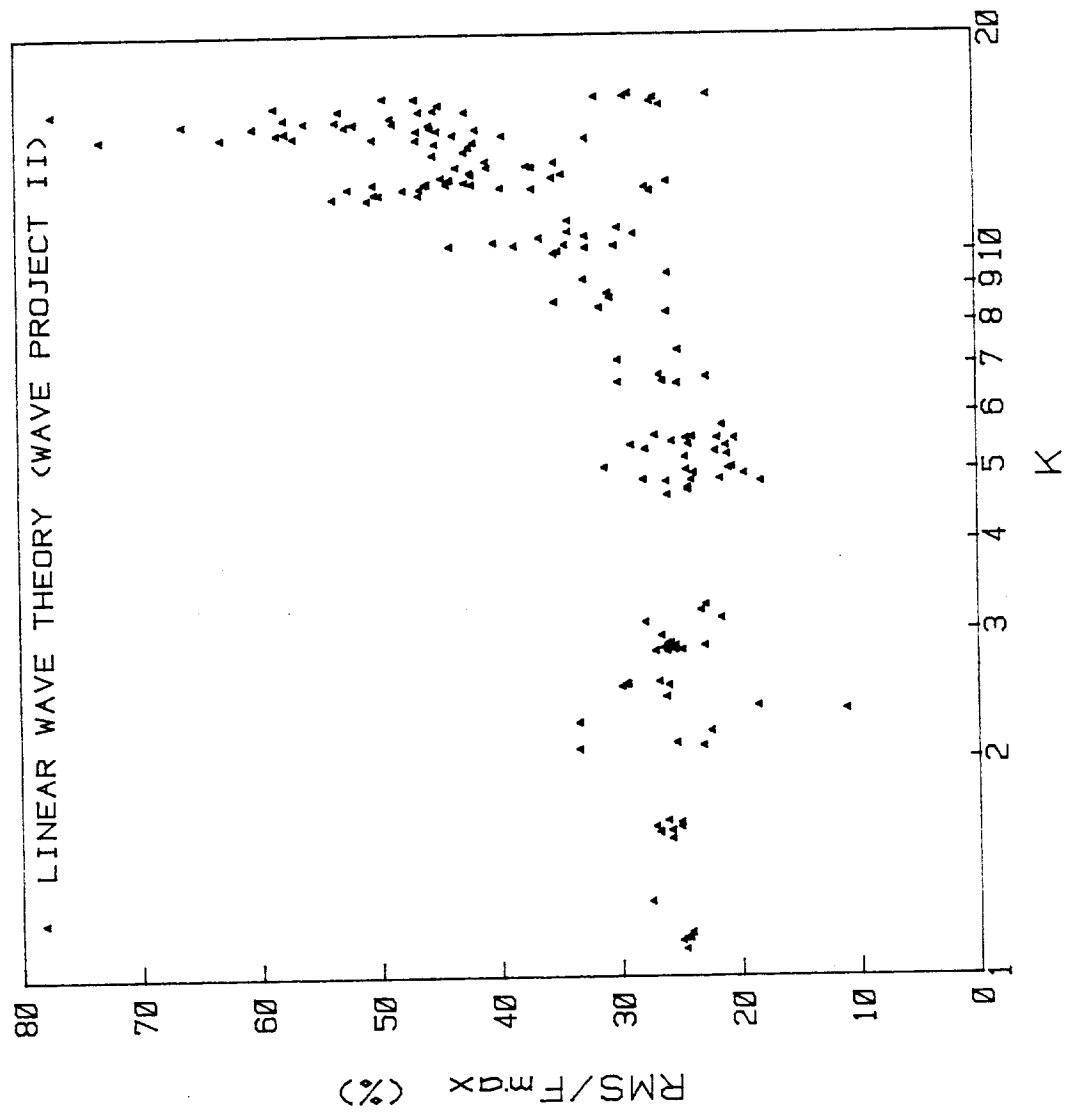


Fig. 5-17 RMS errors (%) for the 2-term MOUS equation

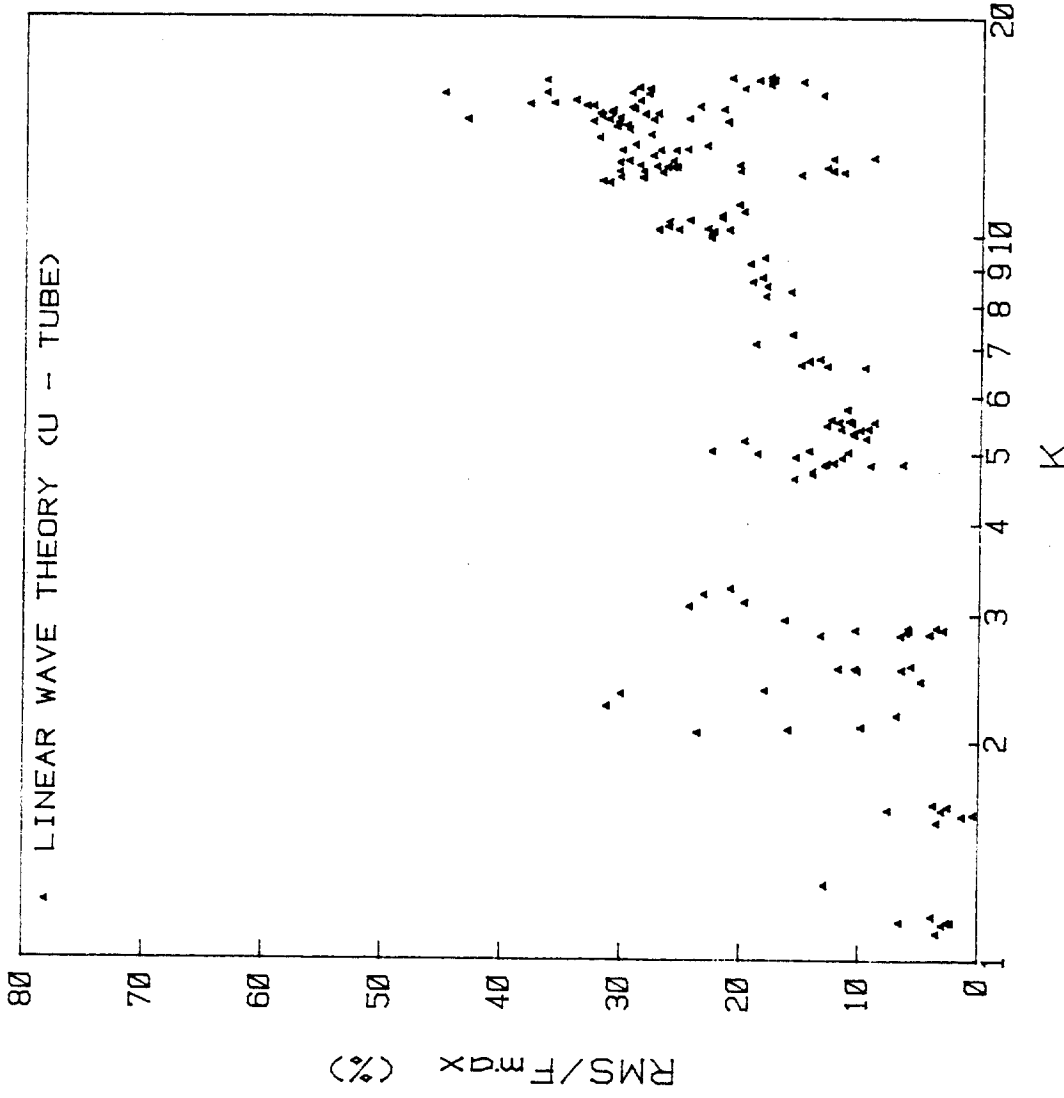


Fig. 5-18 RMS errors (%) for the 2-term MOJS equation

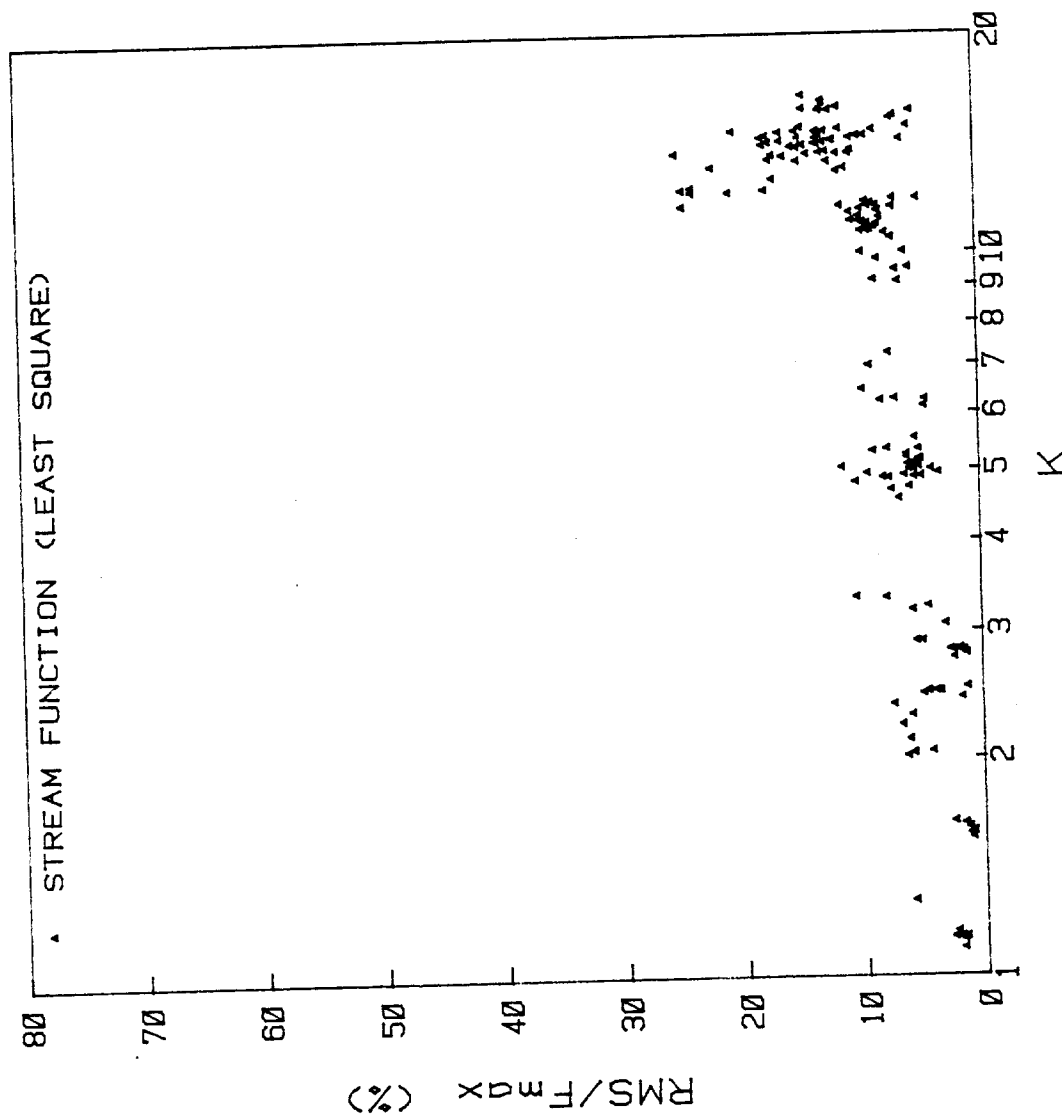


Fig. 5-19 RMS errors (%) for the 2-term MOJS equation

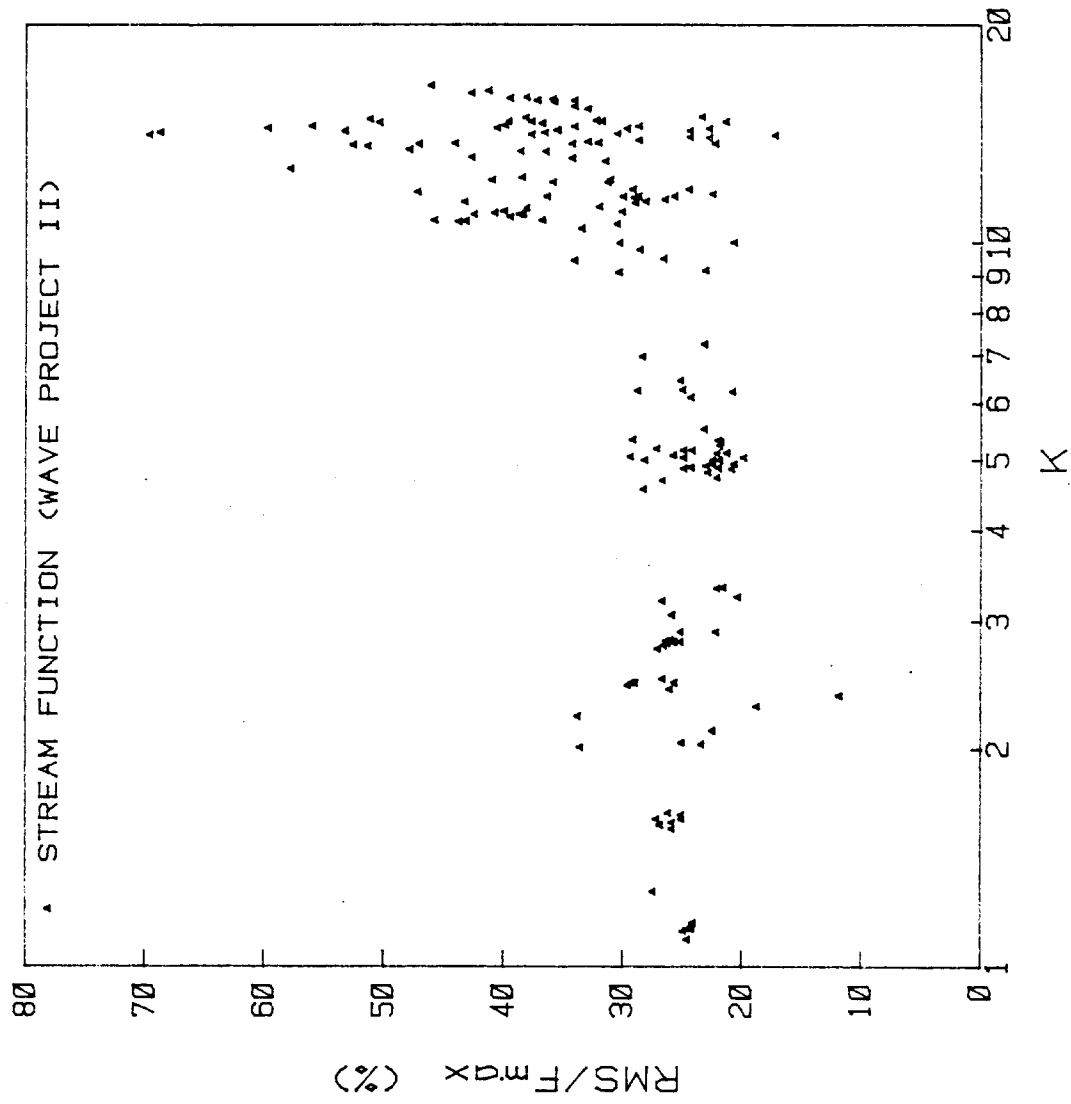


Fig. 5-20 RMS errors (%) for the 2-term MOJS equation

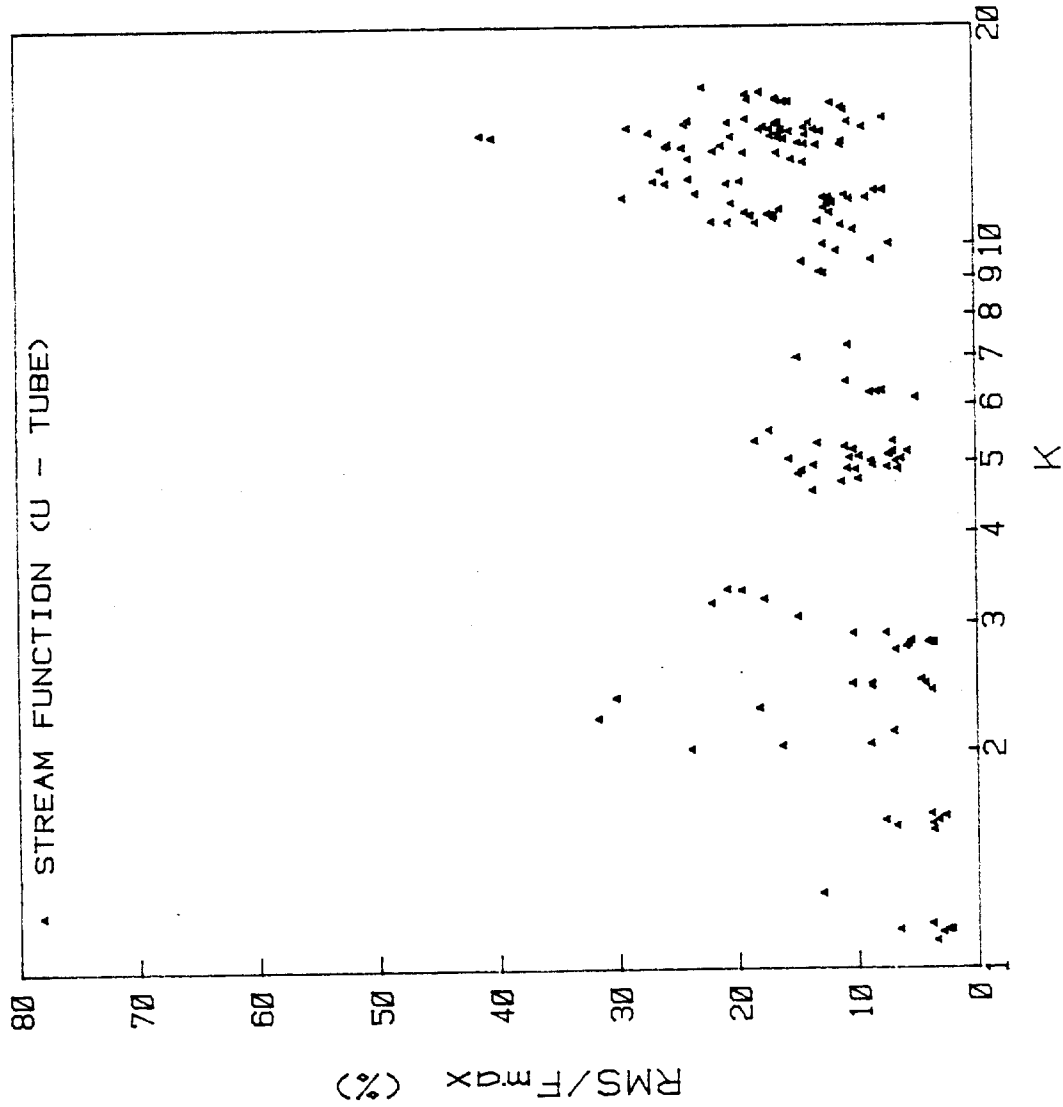


Fig. 5-21 RMS errors (%) for the 2-term MOJS equation

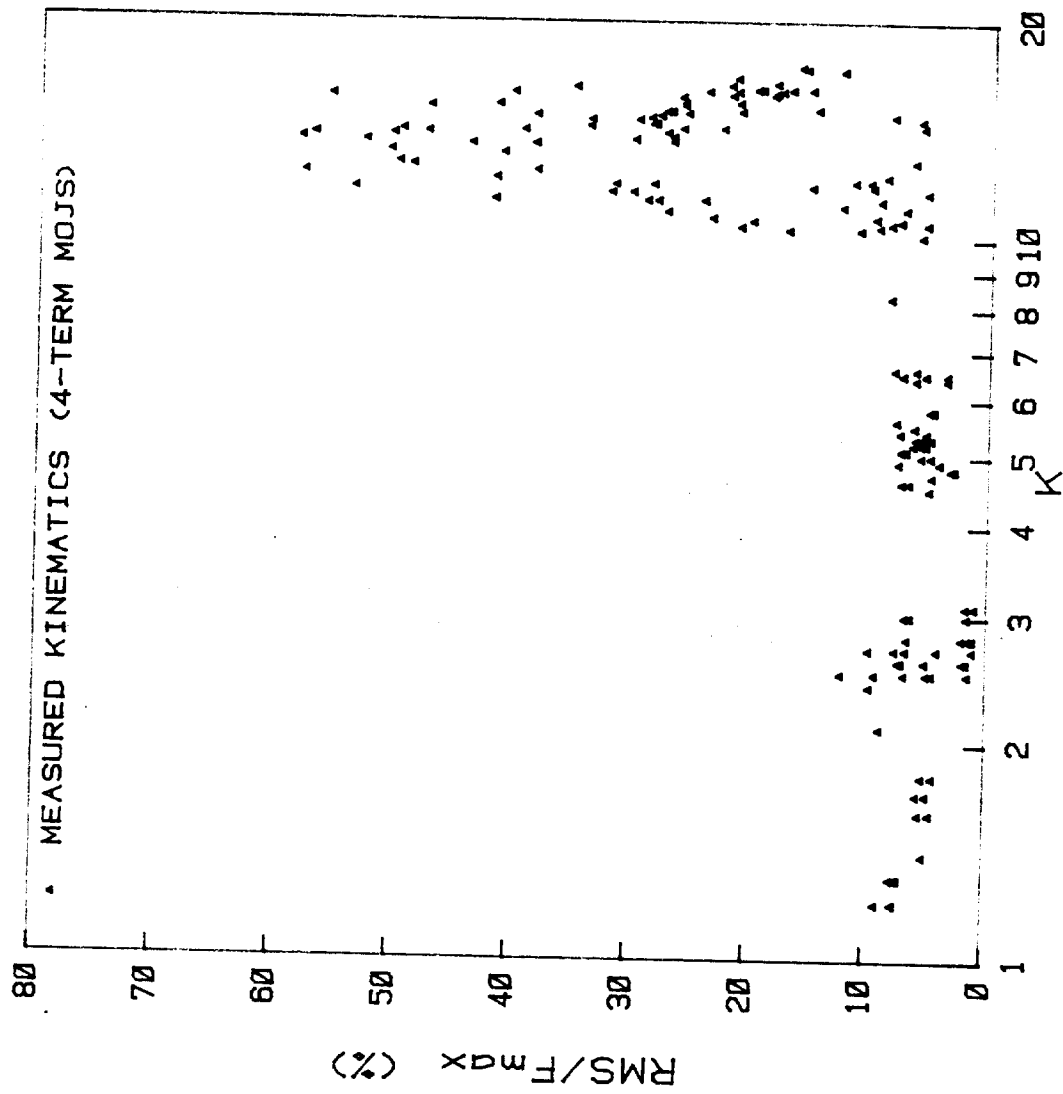


Fig. 5-22 RMS errors (%) for the 4-term MOJS equation

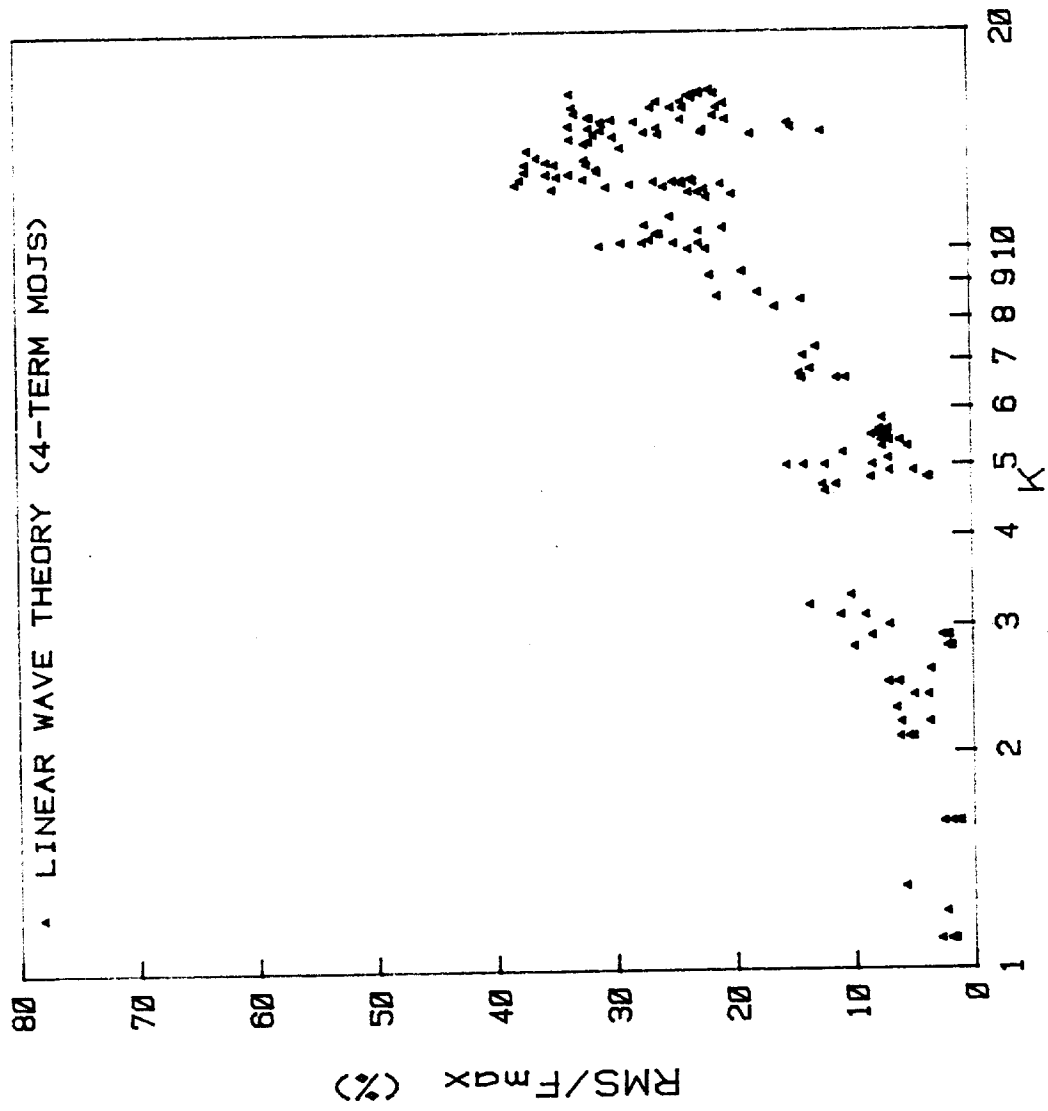


Fig. 5-23 RMS errors (%) for the 4-term MOJS equation

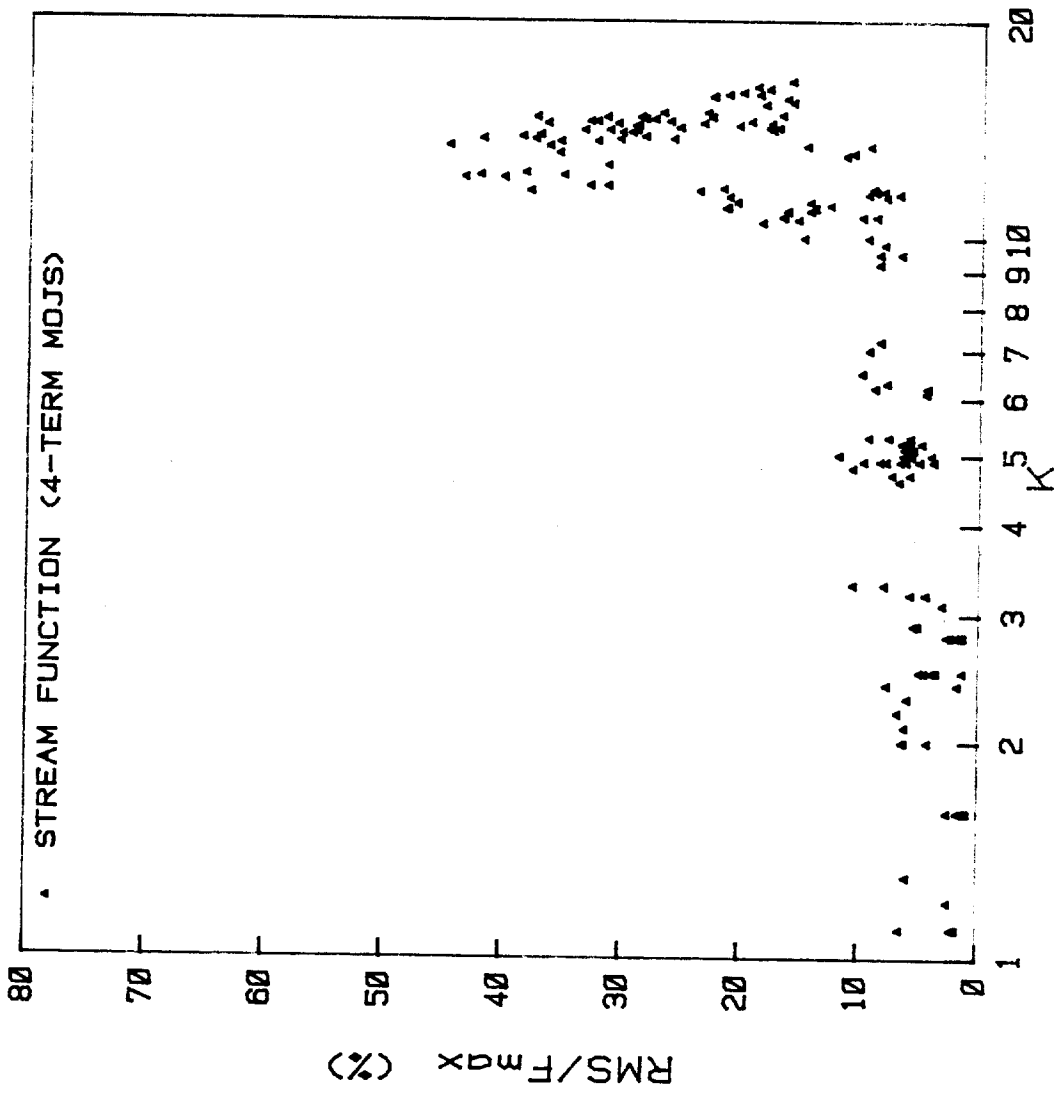
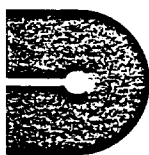


Fig. 5-24 RMS errors (%) for the 4-term MOJS equation

11.0 APPENDIX

- 11.1 Druck pressure transducer specifications
- 11.2 Parametric dependency of force coefficients on Dean number
- 11.3 Notes from Mr. Standley on how 33 points (32 time increments) were interpolated for each random wave from the assigned time increment of $\Delta t = .06$ sec.

APPENDIX 11.1
DRUCK PRESSURE TRANSDUCER SPECIFICATIONS



Druck Limited

8 Fir Tree Lane Groby
Leicestershire LE6 0FH England
Telephone Leicester (0533) 878551
Telex 341743



Thousands of Druck pressure transducers are being used throughout the world in applications where high accuracy and reliability are of importance, and the PDCR 10 series has been designed more specifically for the industrial user following years of operation of the PDCR 22 and PDCR 32 transducers in mainly aerospace environments requiring maximum performance with regard to weight, reliability and accuracy. The PDCR 10 is an extremely rugged transducer and operational ratings such as shock, vibration and overload are extremely high as is usual with microcircuit devices.

Pressure ranges extend from 1 to 5000 psi, gauge, sealed gauge or differential. The standard output of 100mV with 10 Volts excitation is available on most pressure ranges whilst still retaining high linearity and hysteresis accuracy ($\pm 0.1\%$ B.S.L.) and high overload capability.

A silicon strain gauge bridge is diffused into a single crystal silicon diaphragm using microcircuit techniques and so it is effectively atomically bonded, and this feature, combined with the fact that there is no measurable hysteresis in such diaphragm material, makes an excellent fundamental sensing element. The gauge factors of the four silicon gauges are approximately 50 times those of conventional wire strain gauges so that the output can be relatively high whilst still retaining a high overload.

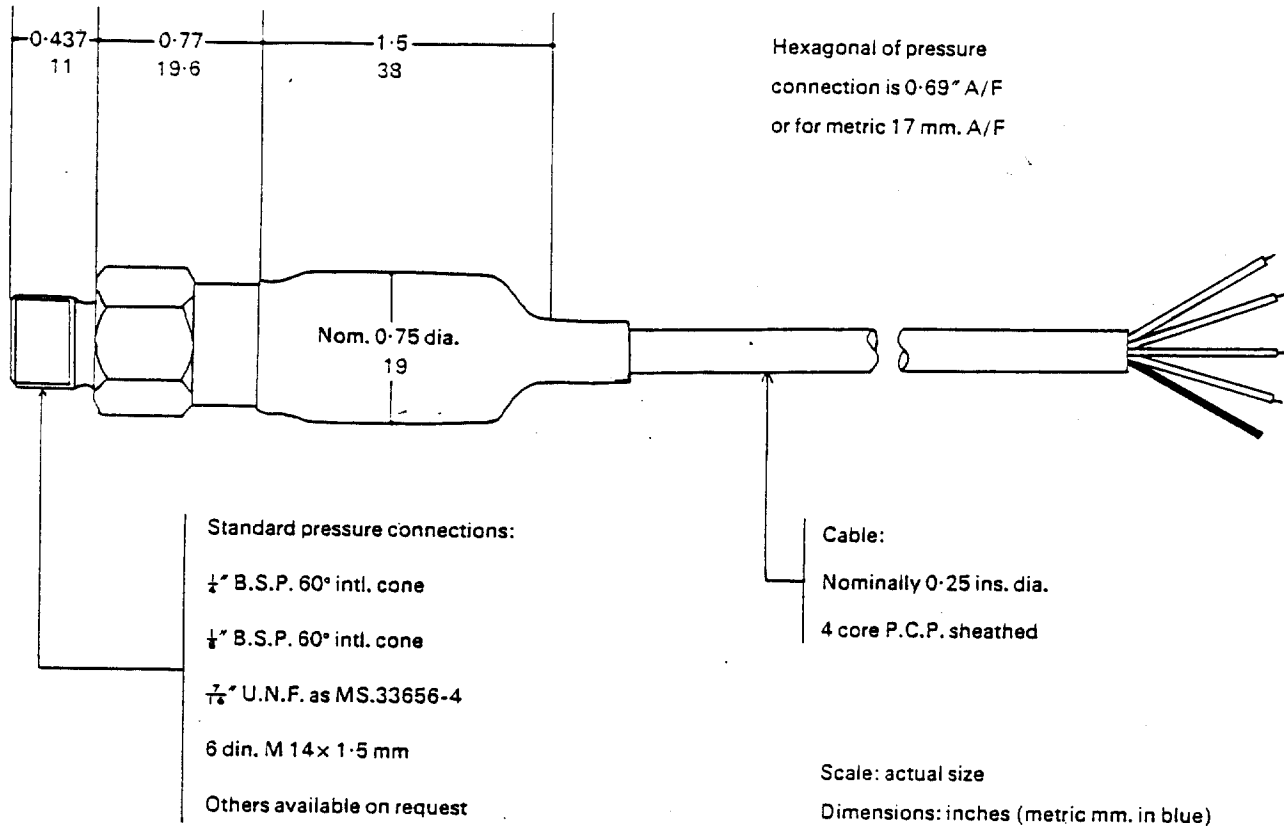
The construction of the transducer is completed using microcircuit, alloying and bonding techniques, and electron beam welding. The ancillary electronic package to give good temperature compensation, rationalisation or amplification, is encapsulated. The complete transducer, having effectively no moving parts and being both mechanically and electronically extremely rugged, is therefore ideally suited to industrial environments of extreme vibration, shock or other external effects.

Many pressure fittings are available as standard and the transducer case is of stainless steel and titanium. A polychloroprene cable is sealed into the body with a heat shrink boot. The integrity of the cable outlet seals is such that the entire transducer could be immersed to depths of at least 300 metres.

Different versions are available which include bore hole transducers suitable for continuous immersion in salt or high mineral water, and also transducers are available with a 2000 ohm resistance bridge network which makes them suitable to operate with two wire 'mA' transmitter electronics.

Also current outputs can be sufficient to drive meters and galvanometers or oscilloscope recorders directly.

Installation details for PDCR 10



The PDCR 10/D BORE HOLE TRANSDUCER has the same body dimensions as the PDCR 10 above, except that the hexagon and pressure fitting is replaced by a conical front end as illustrated in the photograph on the previous page.

Electrical Connection

Red +ve supply, White -ve supply, Yellow +ve output, Blue -ve output.

Ordering information

Please specify type number and pressure range and whether this is gauge, sealed gauge or differential. Also state temperature range of operation and survival, and degree of temperature compensation required.

For pressure fittings refer to above installation drawing but where non-standard connections are required, refer to supplier. The cable length supplied as standard is 1 metre, and longer lengths must be specified for which an extra charge will be made. Transducers can be supplied with different supply voltages and different outputs from those specified and in all cases, reference must be made to the supplier.

The manufacturer reserves the right to alter specifications without notice.
Prices also subject to change without notice.

201 487-301

Prack Inc

III Kinderkrankheit

Druck Limited
8 Fir Tree Lane, Groby, Leicester LE6 0FH,
England
Telephone: Leicester (0533) 878551
Telex: 341743

Represented by:

SCANIVALVE, INC.

P. O. BOX 20005

SAN DIEGO, CALIF. 92120 U.S.A.

TEL: 714 283-0010

Bore Hole and Depth Measurement Transducer PDCR 10/D

A version of the PDCR 10 has been specifically designed for depth measurement in bore holes, reservoirs, the sea and many other applications. It has the electrical specifications outlined on the opposite page, but a special front end has been designed which makes it ideal for dropping down small bore pipes, and discourages the ingress of particles. Extra integrity has been built into the cable seal, and combines encapsulation, O ring seals and a heat shrink boot. The pressure ranges are vented gauge for the lower depths but sealed gauge versions are normally recommended for depths above about 150 feet. High accuracy versions are available with a linearity and hysteresis combined of less than $\pm 0.06\%$ B.S.L. and temperature compensation from -2°C to $+30^{\circ}\text{C}$ of better than $0.01\%/\text{ }^{\circ}\text{C}$ for both zero and span shifts.



Options

For many years we have specialised in producing pressure transducers based on the use of an integrated silicon strain gauge diaphragm and have solved many different pressure measuring and recording problems. Three such transducers are a differential version, an amplifier transducer and a flush mounting transducer, and these are briefly mentioned below.

The PDCR 10L DIFFERENTIAL TRANSDUCER (Technical note 4) has been developed to fulfil special applications measuring low differential pressure at different line pressures where high accuracy, small size and fast response are important. These transducers have electron beam welded pressure connectors at each end and a side entry cable. The current models are suitable for liquid on the positive side and dry, non-corrosive gas on the negative side, and measurements so far have been limited to 1000 psi static pressures, although other types are being developed. The zero and sensitivity change for increasing line pressure is often negligible and the linearity and hysteresis in the negative direction, as in the positive direction, is extremely low.

Transducers containing INTEGRAL AMPLIFIERS are

also being manufactured (Technical note 5) and the more standard ones require a power supply of +12.0, -12 Volts and give output voltages of up to 5 Volts, with a low output impedance. Again, the general performance in terms of accuracy and temperature, are the same as outlined for the PDCR 10, although wider temperature ranges and higher accuracies are available.

The FLUSH MOUNTING PRESSURE TRANSDUCER, PDCR 50 (Technical note 6) has a 0.5 ins. diameter front end and a flange which enables it to be mounted into tanks and other containers such that the sensing diaphragm is flush with the wall, and hence gives fast response and accurate measurements without disturbing the flow pattern. These transducers are already proving extremely useful in marine model testing, general flow research and the process industries.

These are just a few of the transducers that we have manufactured over the years to fulfil specific requirements, so therefore, if you have pressure measuring or recording problems, it is suggested that you contact us, since we may already have solved your particular problem.

Pressure Ranges

$\pm 1, 2.5, 5, 15, 50, 100, 150, 250, 500, 1000, 1500, 2500, 3500, 5000$, lbf/in (p.s.i.).

S.I. units: 10^5 N/m^2 (bars) 0 to 6.895 kN/m^2 through to 3.447 MN/m^2 .

Intermediate ranges are available on request.

Operational Mode

Gauge, sealed gauge or differential.

Overpressure

400% with negligible calibration change and higher overload capability is available especially in lower ranges. For higher ratings please specify.

Pressure Media

Plus side, fluids compatible with quartz, titanium, and silicon dioxide.

Input and Output Impedance

Nominally 1000 ohms.

For optional 2000 ohms refer to supplier.

Excitation

10 Volts d.c. regulated. For a.c. excitation please specify.

Shock

1000g for 1 ms. in each of three mutually perpendicular axes will not affect calibration.

Output

25mV for 1 psi

30mV for 2.5 psi

60mV for 5 psi

100mV for 10 psi and above

Load impedance for quoted performance should be greater than 100 Kohms. For lower load impedances please specify.

Resolution

Infinite.

Combined Non-linearity Hysteresis

$\pm 0.1\%$ B.S.L.

Zero Offset

$\pm 3\text{mV}$.

Sensitivity Setting

$\pm 3\text{mV}$.

More accurate settings of zero and span are available for applications where interchangeability is important. Please refer to supplier.

Operational Temperature Range

—20°C to +80°C standard but this temperature range can be extended.

Temperature Effects

Any 100°C or 50°C temperature band to be specified.

Temperature error band of $\pm 0.5\%$ over 50°C or temperature error band of $\pm 1.5\%$ over 100°C.

Better temperature compensation and/or a wider temperature range is available on request. Please refer to supplier.

Natural Frequency

Typical 5000 p Hz where p is full range pressure in psi.

Acceleration Sensitivity

0.002% FSO/g for 5 psi decreasing to 0.00015% FSO/g for 1000 psi.

Weight

Approx. 140 gms.

Electrical Connection

Integral sealed cable assembly: standard length 1 metre and other lengths to order.

Mechanical outline and ordering information
See back page.

APPENDIX 11.2
PARAMETRIC DEPENDENCY OF FORCE COEFFICIENTS ON DEAN NUMBER

Ocean Wave Data. Dean and Aagaard (1969) used measured pressure forces from a prototype offshore oil platform and a least-squares regression analysis with theoretical nonlinear water particle kinematics computed by the stream function theory to compute C_d , C_m . They found that the drag coefficient varied with Reynolds number and that the inertia coefficient was essentially a constant. The Dean and Aagaard regression analysis illustrates the parametric dependence of the coefficients and explains some of the scatter observed by various investigators.

Dean and Aagaard (1969) computed C_D , C_I from a least squares fit to the measured forces by minimizing the following mean square error:

$$\epsilon^2 = \frac{1}{N} \sum_{n=1}^N \{F_m(n) - F_p(n)\}^2 \quad (1)$$

Minimizing this mean square error requires that

$$\frac{\partial \epsilon^2}{\partial C_m} = 0 \quad \text{and} \quad \frac{\partial \epsilon^2}{\partial C_d} = 0 \quad (2)$$

Equation 1 for the mean square error may be expanded into a general equation for a quadratic surface of second-degree with an origin which has been translated and rotated. The coefficients of the independent variables include products of the wave field kinematics and measured forces and determine whether or not the data are well conditioned or ill conditioned for determining true minima (Dean, 1976).

Expanding the mean square error yields the following equation for a quadratic error surface:

$$\begin{aligned}\varepsilon^2 = & \left(\frac{C_d\rho}{2}\right) \langle u^4 \rangle + \left(C_m \frac{\rho\pi D}{4}\right)^2 \langle u^2 \rangle + 2\left(\frac{C_d\rho}{2}\right) \left(C_m \frac{\rho\pi D}{4}\right) \langle u | u | \dot{u} \rangle \\ & - 2\left(\frac{C_d\rho}{2}\right) \langle F_m u | u | \rangle - 2\left(C_m \frac{\rho\pi D}{4}\right) \langle F_m \dot{u} \rangle = \langle F_m^2 \rangle \quad (3)\end{aligned}$$

in which the temporal averaging operator $\langle \cdot \rangle$ is defined by $\langle \cdot \rangle = \frac{1}{N} \sum_{n=1}^N (\cdot)_n$. This equation is the general equation for an ellipse whose origin has been translated and rotated. For data which are simple harmonic oscillations, the coordinates of the origin (x_0, y_0) are given by

$$x_0 = \left(\frac{16}{3\rho}\right) \frac{\langle F_m u | u | \rangle}{\langle u_m^4 \rangle} \quad (4a)$$

$$y_0 = \left(\frac{2}{\rho\pi}\right) \left(\frac{T}{U_m D}\right)^2 D \langle F_m \dot{u} \rangle \quad (4b)$$

To determine the suitability of the data to resolve the regression coefficients, C_d , C_m , changes in the minimum values of these coefficients for a given mean square error are minimized.

For $C_m = \text{constant}$, it may be shown that this minimization of the changes in the minimum values gives

$$\delta C_d = \frac{\sqrt{2}}{\rho} \frac{[\varepsilon_i^2 - (\varepsilon_i^2)_{\min}]^{1/2}}{[\langle u \rangle^4]^{1/2}} \quad (5a)$$

and for $C_d = \text{constant}$:

$$\delta C_m = \frac{4}{\rho\pi D} \frac{1}{\sqrt{2}} \frac{[\varepsilon_i^2 - (\varepsilon_i^2)_{\min}]^{1/2}}{[\langle \dot{u}^2 \rangle]^{1/2}} \quad (5b)$$

The ratio of the axes of the error ellipse (eccentricity) is given by

$$E = \frac{\delta C_m}{\delta C_d} = \frac{2}{\pi D} \left[\frac{\langle u^4 \rangle}{\langle \dot{u}^2 \rangle} \right]^{1/2} \quad (6)$$

For simple harmonic oscillations, this reduces to

$$E = \frac{2}{\pi D} [3/4]^{1/2} \frac{U_m}{\omega} \quad (7a)$$

$$= [3/4]^{1/2} \frac{C_m}{C_d} \frac{(F_d)_{\max}}{(F_I)_{\max}} \quad (7b)$$

The error surface for simple harmonic oscillations in dimensionless form is

$$\frac{\epsilon_i^2 - (\epsilon_i^2)_{\min}}{(F_D)^2_{\max}} = 3/8 \left(\frac{\delta C_d}{\delta C_m} \right) + 1/2 \left(\frac{F_I}{F_D} \right)_{\max} \left(\frac{\delta C_m}{\delta C_d} \right)^2 \quad (8)$$

Dean (1976) gives the following criteria for estimating the suitability of the data for determining C_d , C_m :

E	<u>Relatively Well-Conditioned to Determine</u>
0.25	C_m
0.25 - 4.0	C_d and C_m
4.0	C_d

From Eq. 7a, it is obvious that the Dean number, E , is proportional to the Keulegan-Carpenter number, K . The constant of proportionality for simple harmonic flows is

$$E/K = \frac{\sqrt{.75}}{\pi^2} \Rightarrow K = \frac{E \cdot \pi^2}{\sqrt{.75}} \approx E \times 11.4 \quad (9)$$

APPENDIX 11.3

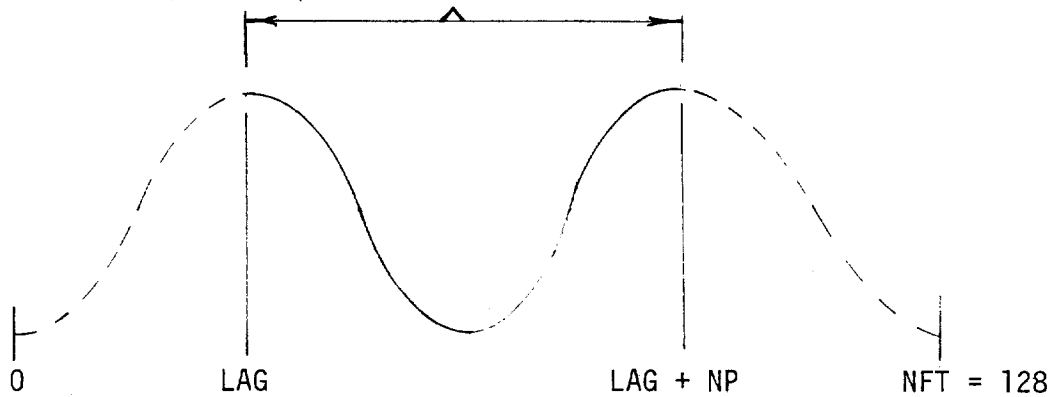
FDATAR

Choose starting peak of desired wave.

$DT = .06 \text{ sec}$

$NP = \# \text{ of points in original wave profile including both end points at spacing of } DT$

$\text{PERIOD} = (NP-1) * DT \quad \text{period of desired wave}$



$NFT = \# \text{ of points to FFT including desired wave in center}$

OUTPUT wave must have $NN = 33$ points

Spacing of output wave ($\text{delta-}t$) = $\text{TT} = \text{PERIOD}/(NN-1)$

$N = \# \text{ of spaces in total FFT window at } \text{delta-}t = TT$

FFT the data and filter at 2 Hz since original data were already filtered at 1.5 Hz

Starting at time = $LAG * DT$ compute NN points using the coefficients

$$\begin{aligned} \text{WAVE}(I) = & XR(I) + 2.* \sum_{m=2}^{NFLTR-1} XR(m) * \cos(2\pi * (m-1) * T / (N * TT)) \\ & - XI(m) * \sin(2\pi * (m-1) * T / (N * TT)) \end{aligned}$$

where $T = (LAG * DT) + TT * (I-1)$.

```

CGETHWAVE
C***** SUBROUTINE GETHWAVE(WAVE, IWAVE, NPWAVE)
C 18-OCT-83 DEBUG WRITE TO TAPE23
C 23-SEP-83
C
C WAVE IS SINGLE WAVE STARTING AT RIPEAK(IWAVE))
C WAVE WILL CONTAIN IWAVE POINTS
C
C IWAVE IS THE STARTING PEAK NUMBER IN THE SERIES
C OF WAVES CONTAINED IN R WHICH IS NPTS LONG.
C ARRAY IPEAK CONTAINS THE STARTING INDICES
C OF ALL PEAKS
C
C NPWAVE IS THE DESIRED NUMBER OF POINTS IN THE OUTPUT WAVE.
C
C 22-SEP-83 MAKE OUTPUT WAVE 129 POINTS LONG (128+DT)
C 16-SEP-83 MAKE WINDOW (128 POINTS WIDE WITH DESIRED WAVE IN MIDDLE)
C FFT THIS DATA WINDOW AND USE THE COEFFICIENTS TO
C INTERPOLATE OVER THE DESIRED WAVE IN TIME DOMAIN.
C
C
C D. STANLEY
C***** COMMON RI(1K,2),DT
C COMMON/DEBUG/DEBUG, IPLT
C COMMON/PTZ3/R(4096),NPTS, IPEAK(16)
C DIMENSION XR(128), XI(128), WAVE(129), XRTMP(128), LBL(2)
C NFT = 128
C NYQ = NFT / 2 + 1
C
C

```

```

C      * IWPWAVE IS THE DESIRED NUMBER OF POINTS IN THE OUTPUT WAVE.
C
C 22-SEP-83 MAKE OUTPUT WAVE 129 POINTS LAGS(128)*DT)
C 16-SEP-83 MAKE WINDOW(128 POINTS WIDE WITH DESIRED WAVE IN MIDDLE)
C          FFT THIS DATA WINDOW AND USE THE COEFFICIENTS TO
C          INTERPOLATE OVER THE DESIRED WAVE IN TIME DOMAIN.
C
C 15-SEP-83
C
C D. STANLEY
C***** ****
COMMON RJK(2),DT
COMMON/DEBUG/DEBUG,IPLT
COMMON/PT33/R(4096),NPTS,IPEAK(16)
DIMENSION XRC(128),XI(128),WAVE(129),XRTMP(128),LBL(2)
NFT = 128
NFTQ = NFT / 2 + 1
TWOP1 = 8 * ATAN(1.)
PI = TWOP1 / 2
IPK1 = IWAVE
IPK2 = IPK1 + 1
NP = IPEAK(IPK2) - IPEAK(IPK1) + 1
PERIOD = FLOAT(NP - 1) * DT
C
C *** FILL XRC,XI WITH WINDOW OF DATA ***
C
J = IPEAK(IPK1)
L = IPEAK(IPK2)
LAG = (NFT - NP) / 2
ISTART = J - LAG
*?

```

```

NZ = 0
IF( ISTART .LT. 0 ) THEN
  HZ = - ISTART
  ISTART = 1
  DO 8 I=1,HZ
    XRC(I) = XIC(I) = 0
  ENDIF
  IEND = HFT
  M = HFT - (LAG + NP)
  IF( (L + M) .GT. HFT ) THEN
    IEND = HFTS - L
  ENDIF
  J = ISTART - 1
  DO 9 I=HZ+1, IEND
    J = J + 1
    XRC(I) = R(J)
    XIC(I) = 0
  IF( IEND .NE. HFT ) THEN
    K = HFT - IEND
    DO 10 I=K, HFT
      XRC(I) = XIC(I) = 0
    ENDIF
    DO 11 I=1,HFT
      XRTMP(I) = XRC(I)
    IF( IPLT .NE. 0 ) THEN
      LBL(1) = 10H/WAVE VALUE
      LBL(2) = 10H
      CALL TSPLDT(XR(LAG+1),NP,LBL)
      CALL TEKPUS
      LBL(1) = 10H/WAVE WINDO
    *?

```

A16

```

LBL(2) = 10HJ
CALL TSPLTC(XR,NFT,LBL)
CALL TEKPAUS
ENDIF
C***** IF DEBUG HE. 0. THEN
C (LAG+1) IS FIRST POINT OF WAVE
C
C WRITE(23,800)LAG+1
C
FORMAT('RAW ETA WINDOW',WAVE STARTS AT ',15)
DO 79 I=1,NFT
    T = FLOAT(I-1)*DT
    WRITE(23,801)I,T,XRC(I)
790 FORMAT(I10,F10.4,F15.5)
801 ENDIF
C***** OF = 1, '(FLOAT(NFT)*DT)
C CALL FTGIA(XR,XI,NFT,0)
IFC IPLT .NE. 0 XCALL SPCLIT(XR,XI,NFT,OF)
NFLTR = NYQ
PRINT *, 'ENTER FCUT (HZ) ... 0. IF NO CUT,
READ *,FCUT
IFC FCUT .EQ. 0 GO TO 21
NFLTR = IFIX(FCUT / OF) + 2
NFT2 = NFT / 2
DO 20 I=NFLTR,NFT2
N1 = NFT + 2 - 1
XRC(I) = XRC(N1) = XI(I) = XIC(N1) = 0.
20 XRC(NYQ) = XIC(NYQ) = 0.
*?

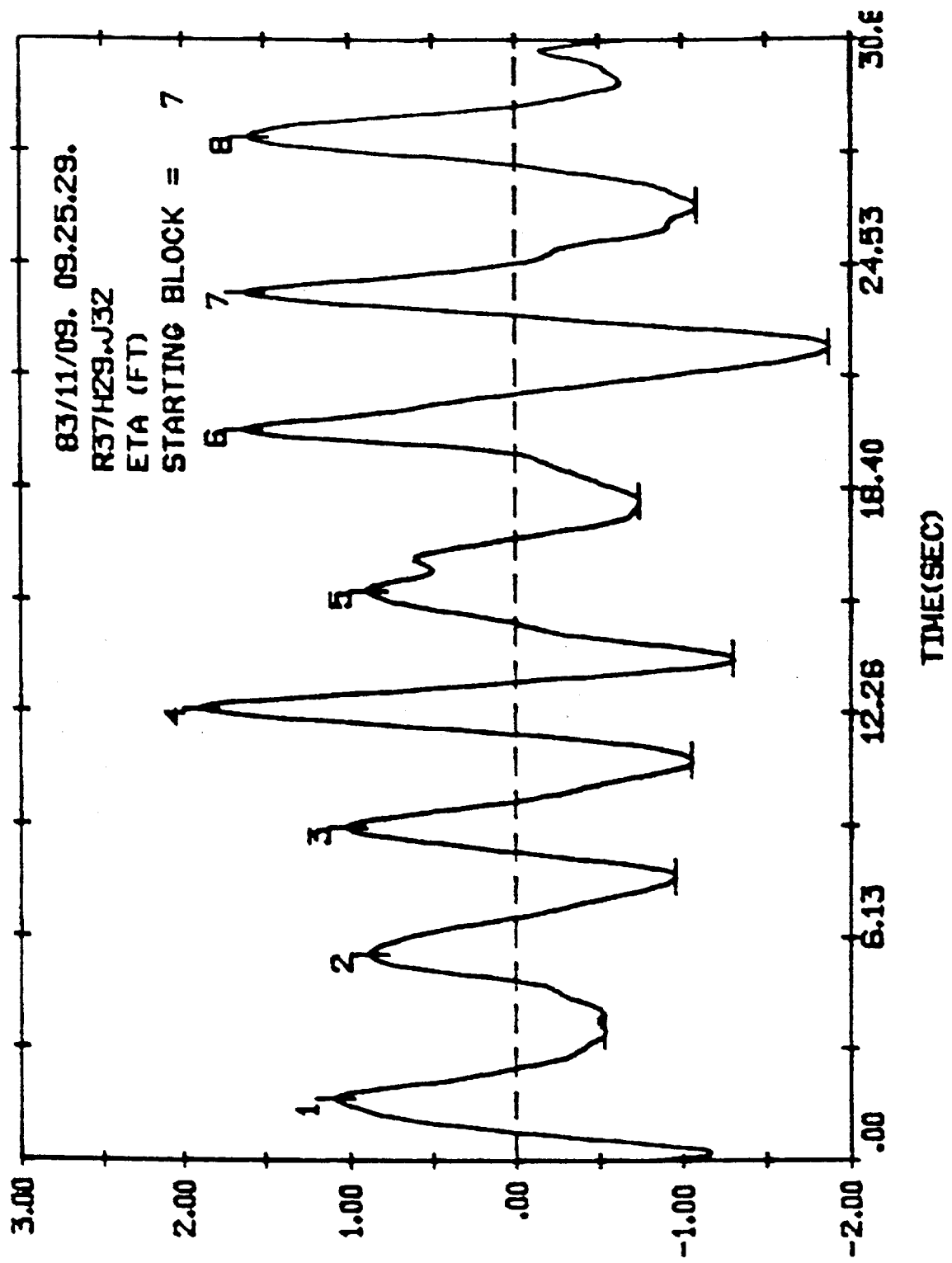
```

```

C *** RECONSTRUCT ORIGINAL WAVE WITH UNIQUE POINTS ***
C SEE EQU 5-38 IN DIGITAL SIGNAL ANALYSIS
C BY STEARNS
C COMPUTE MM POINTS (WHICH INCLUDE BOTH END POINTS)
C FOR PERIOD OF (MH-1)*TT
H/NFT = (MH-1)*(MP-1)
H IS # OF SPACES IN TOTAL WINDOW AT DELTA-T = TT
FOR THERE TO BE (MH-1) SPACES IN PERIOD
C MP IS ORIGINAL # OF POINTS IN PERIOD INCLUDING BOTH END POINTS AT DT
MH IS NEW # OF POINTS IN PERIOD INCLUDING BOTH END POINTS AT TT

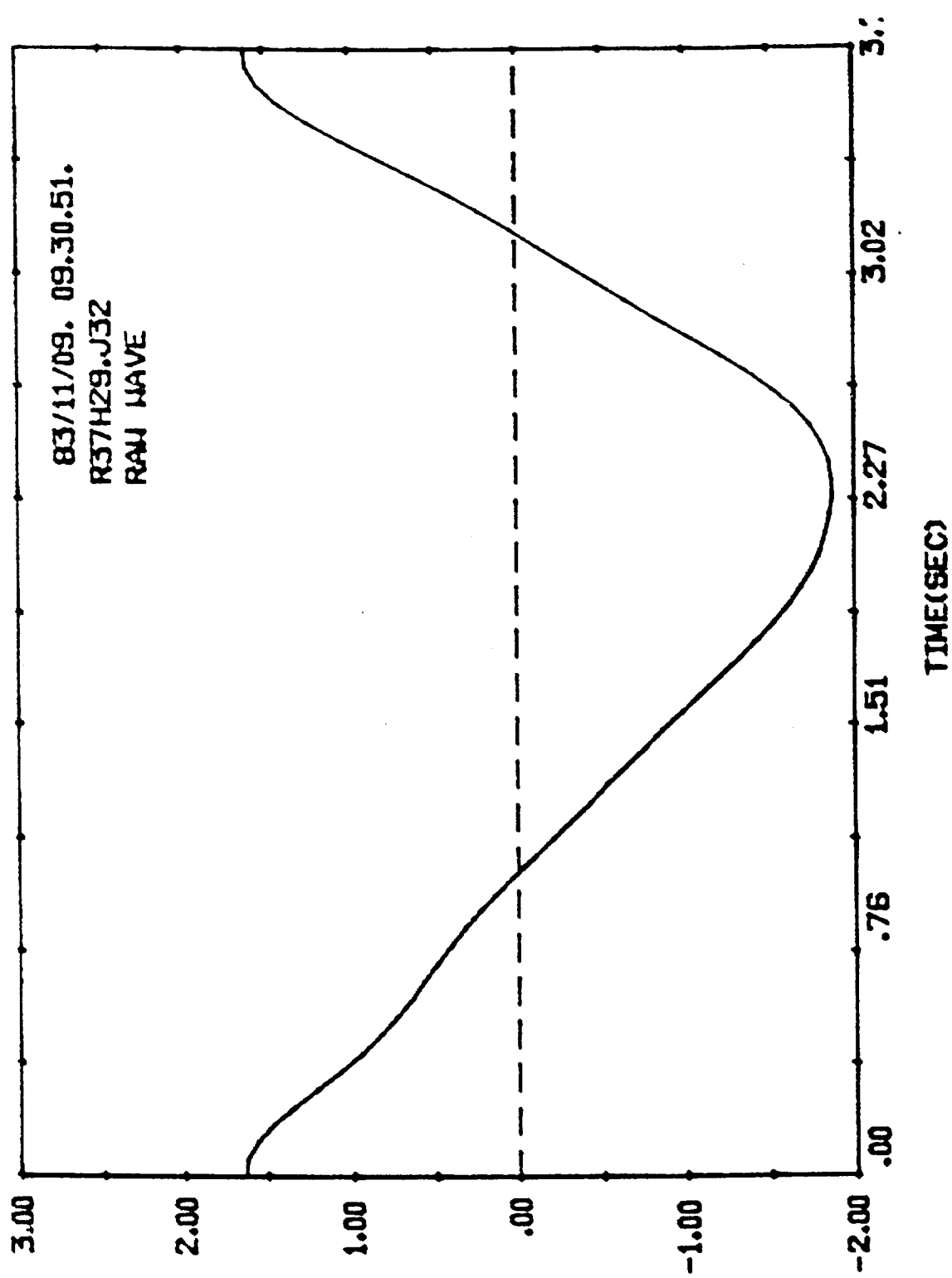
C
21 MH = NPERIOD
H = ((MH - 1) * NFT) / (MP - 1)
TT = PERIOD * FLOAT(MH - 1)
OFFSET = FLOAT(LAG) * DT
J = -1
DO 50 I=1,MH
J = J + 1
T = FLOAT(J) * TT + OFFSET
ARG = TWOPI * T / (FLOAT(MH) * TT)
SUM = 0.
DO 45 M=2,NFLTR - 1
ARGFM = FLOAT(M - 1) * ARG
SUM = SUM + XRCM * COS(ARGFM) - XICM * SIN(ARGFM)
ARGFM = FLOAT(MQ) * ARG
SUM = SUM + XRCMQ * COS(ARGFM) - XICMQ * SIN(ARGFM)
WAVE(I) = (XRC1) + 2. * SUM
50 ENCODE(20,100,LBL,WAVE)
51
*?

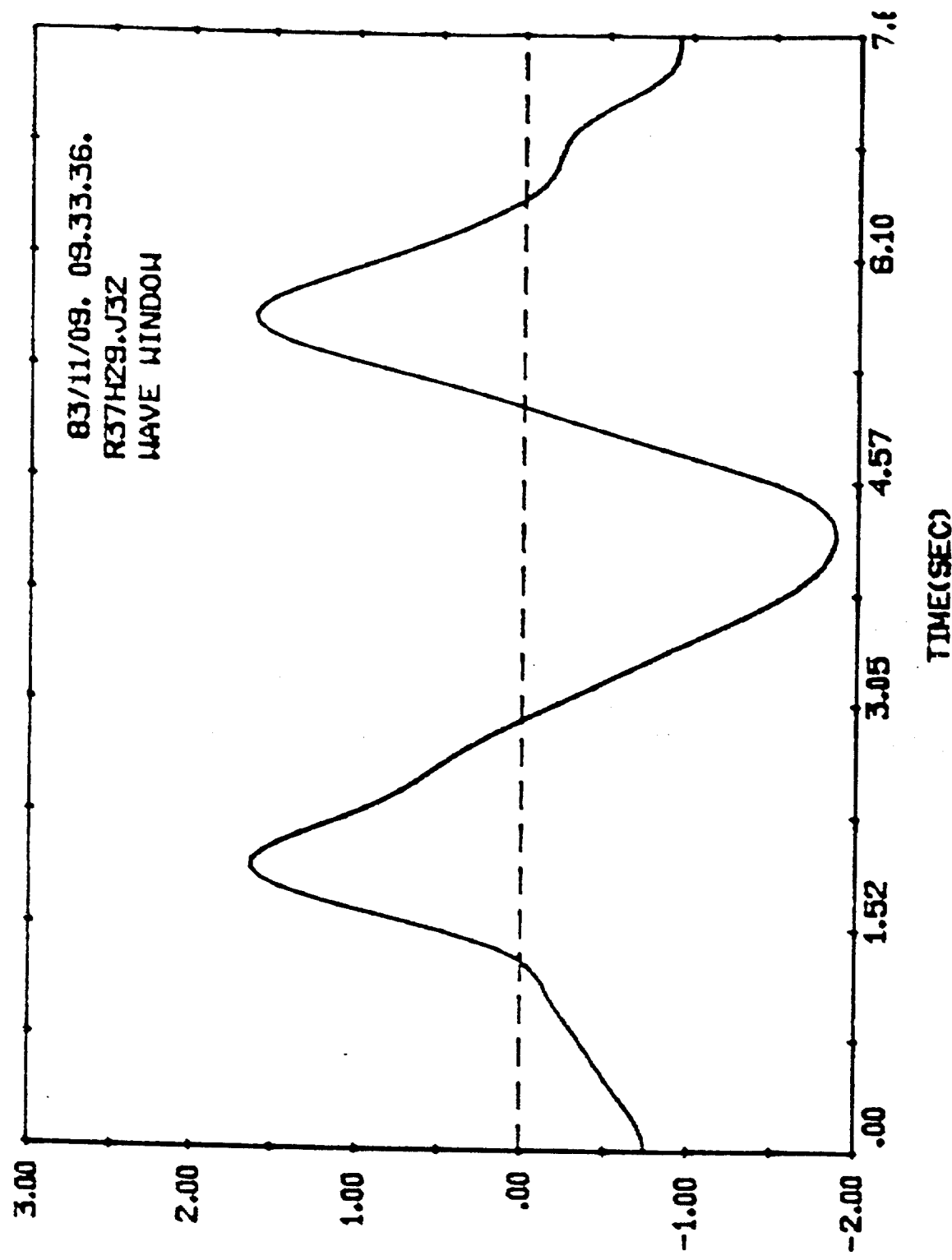
```

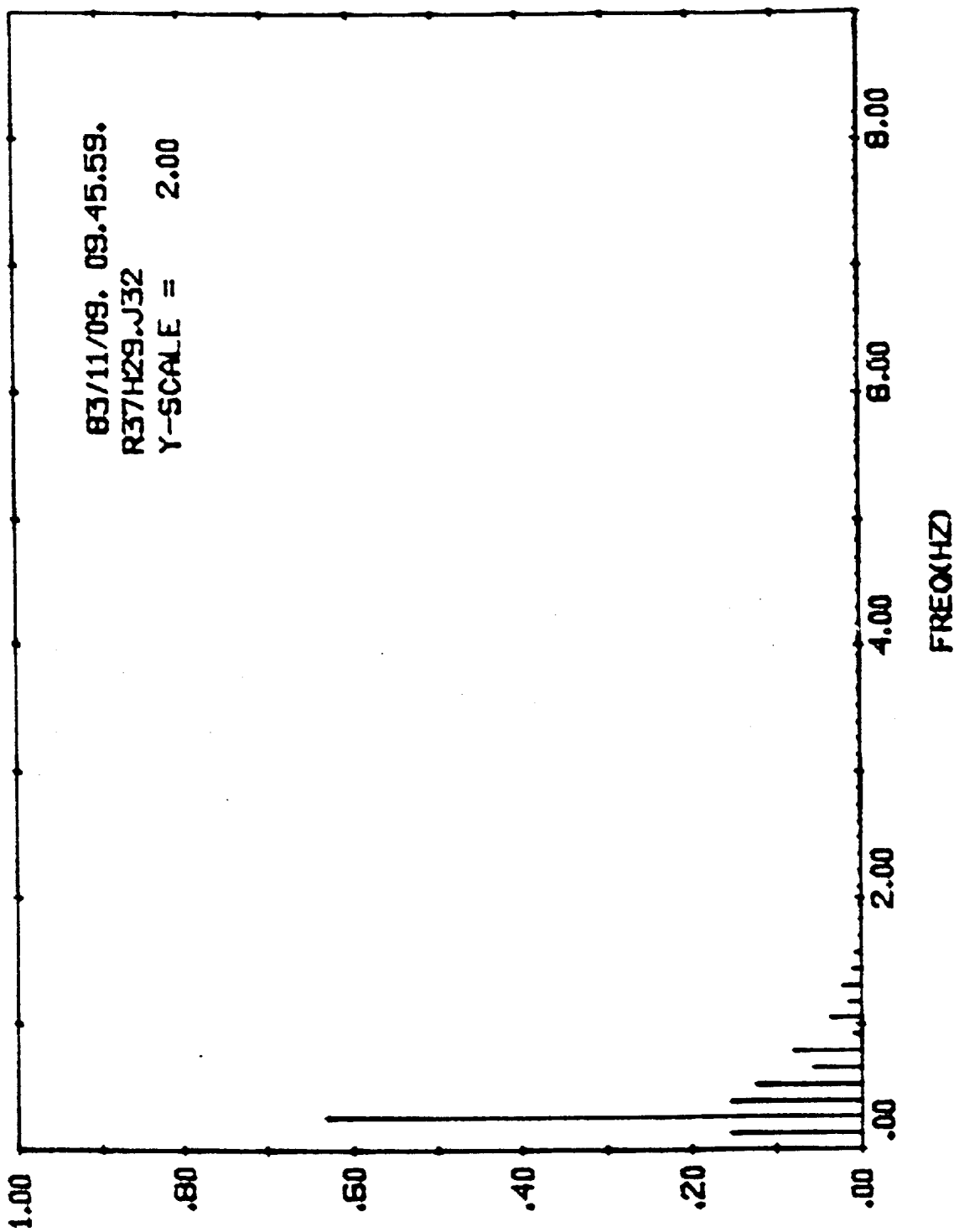



HEIGHTS = 1 52 1 99 2 51 2 69 2 01 3 56 2 70
PERIODS = 2 36 3 48 3 24 3 24 4 38 3 76 4 26
ENTER STARTING PEAK FOR THIS WAVE
? 6

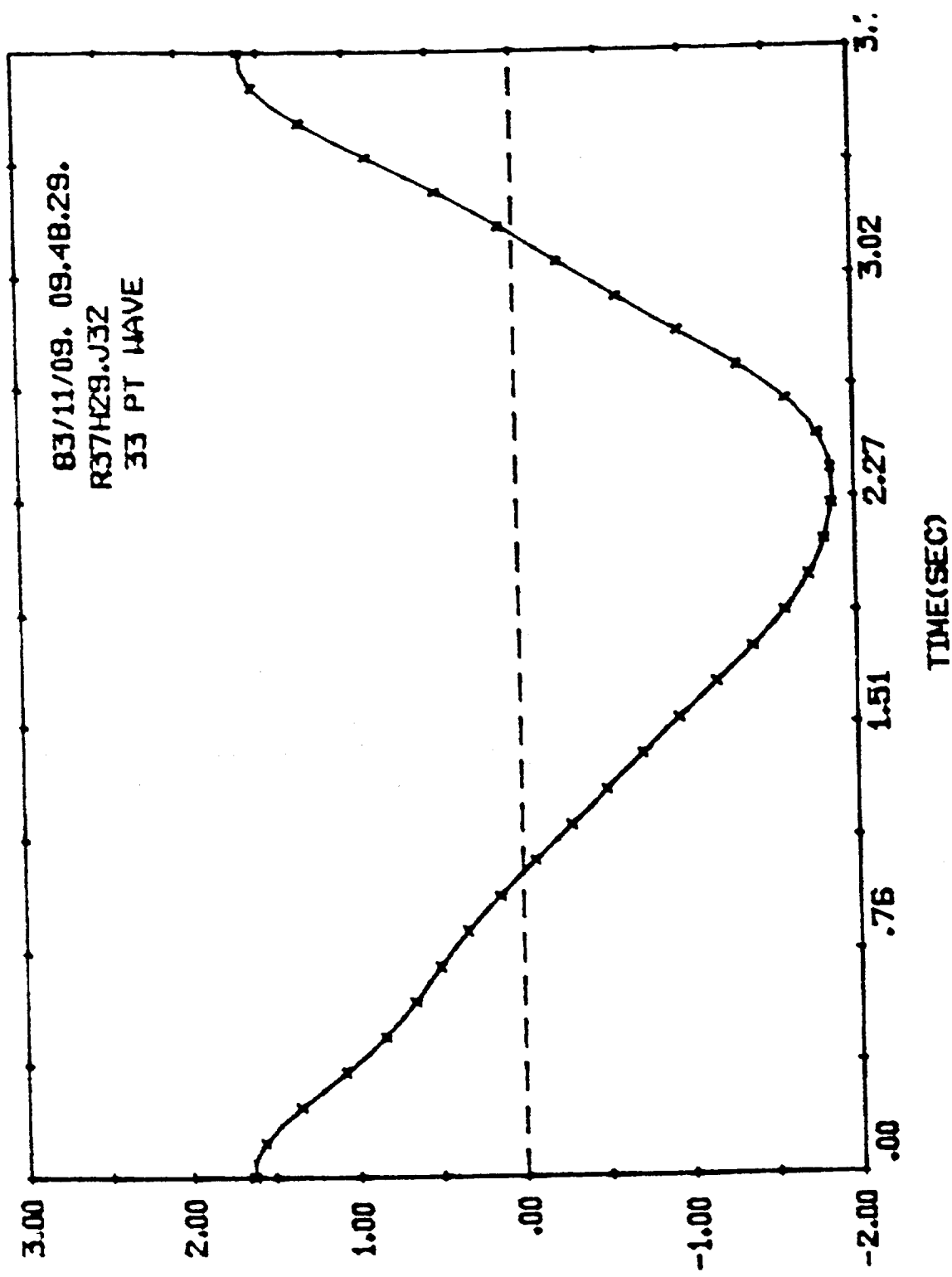
*** MEASURED WAVE HEIGHT = 3.498 FT ***







? 2.
ENTER FCUT (HZ) ... 0. IF NO CUT



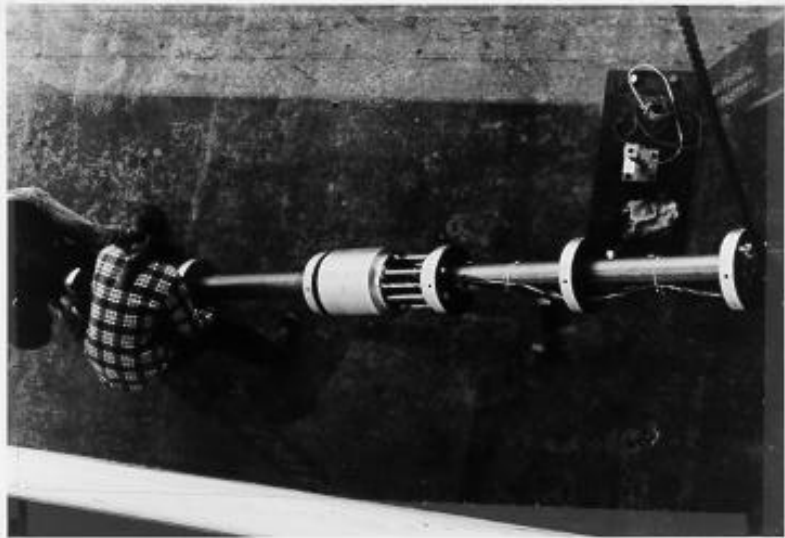


Fig. 3-3 Cylinder core during installation

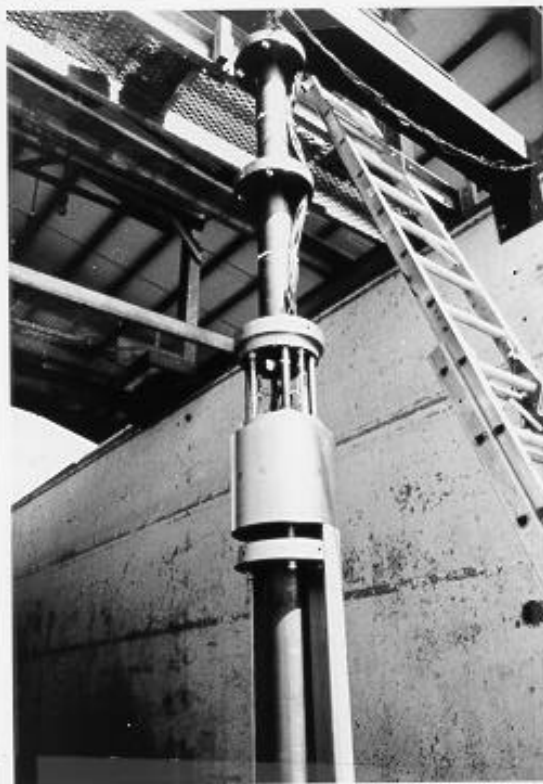


Fig. 3-4 Cylinder core in vertical position with 1/2 of lower skin in place



Fig. 3-5 Bottom (and top) support strain gaging

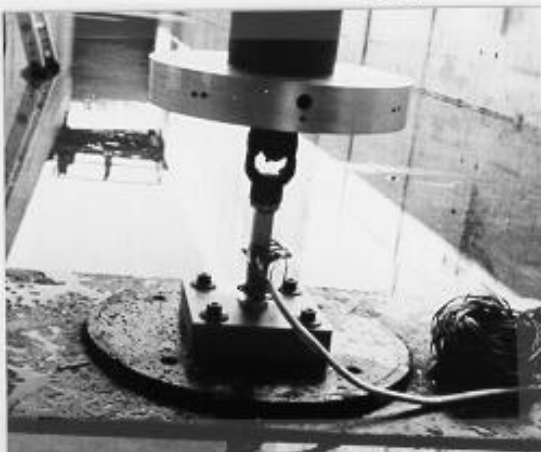


Fig. 3-6 Bottom support bolting to WRL floor



Fig. 3-7 Skin installation at bottom support

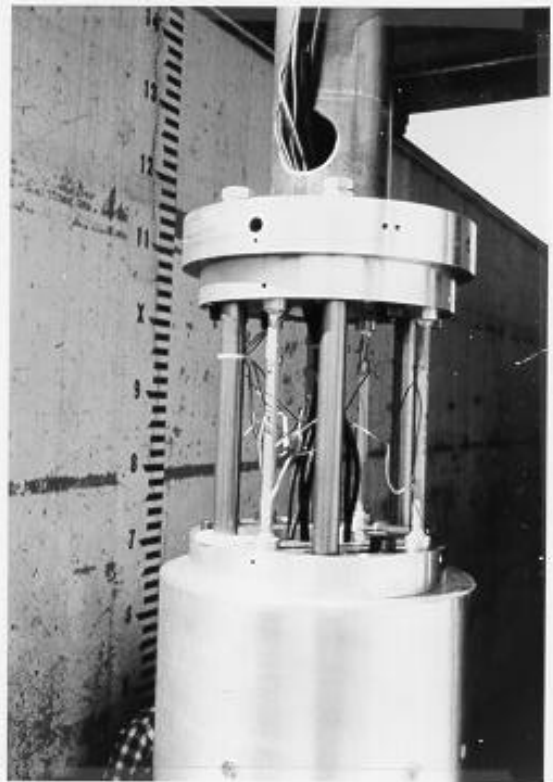


Fig. 3-10 Local force transducer strain bar support. Pressure ports shown prior to filling and sanding the immediate area around them.



Fig. 3-11 Interior of the LFT with 8 pressure transducers and 4-1" round bars which provide structural continuity for the core structure.

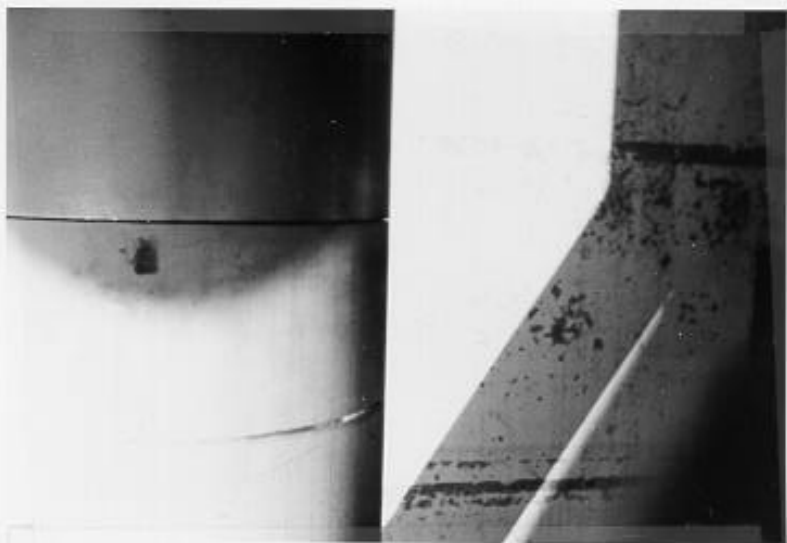


Fig. 3-12 Perfect alignment demonstrated at one azimuth position of the LFT, bottom joint

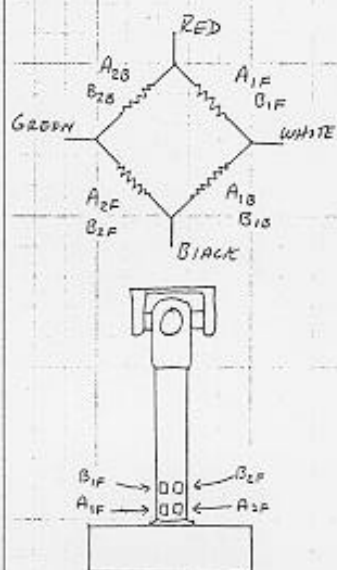


Fig. 3-13 The worst alignment for the LFT at the top joint. Offset = 1.1 mm, although it looks larger because of the sun reflection.

APRIL 19

NCEL - VERTICAL CYLINDER STRAIN GAUGE WIRING

TOP & BOTTOM FORCE BEAMS



F - FRONT, B - BACK

A - MOST SENSITIVE

- Primarily

B - LEAST SENSITIVE

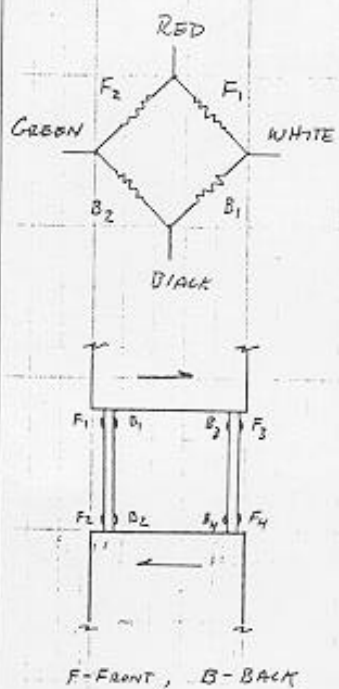
- BACKUP

TYPE	SENSITIVE DIRECTION	GAUGE #	SENSITIVITY	EXCIT. VOLTAGE	GAIN	USE	
						CALIB.	RUN
TOP	NORTH 1	1	MOST	10V.	200	X	X
	NORTH 2	2	LEAST	"	"	X	
	EAST 1	3	MOST	"	"	X	
	EAST 2	4	LEAST	"	"	X	X
BOTTOM	NORTH 1	5	MOST	"	"	X	X
	NORTH 2	6	LEAST	"	"	X	
	EAST 1	7	MOST	"	"	X	X
	EAST 2	8	LEAST	"	"	X	

Fig. 3-14 Bottom and top support strain gage wiring

APRIL 1983

NCEL - VERTICAL CYLINDER STRAIN GAGE WIRING
LOCAL FORCE BEAMS



TYPE	SENSITIVE DIRECTION	GAUGE #	SENSITIVITY	EXCIT. VOLTAGE	GAIN	USE CALIB.	RUNS
CENTER (LOCAL)	NORTH 1	9	SAME	10 V.	300	X	X
	NORTH 2	10	"	"	"	Y	X
	EAST 1	11	"	"	"	Y	X
	EAST 2	12	"	"	"	X	X

Gauge #9 was ELECTRONICALLY SUMMED WITH Gauge #10
" #11 " " " " " = 12

Fig. 3-15 Local force transducer strain gage wiring

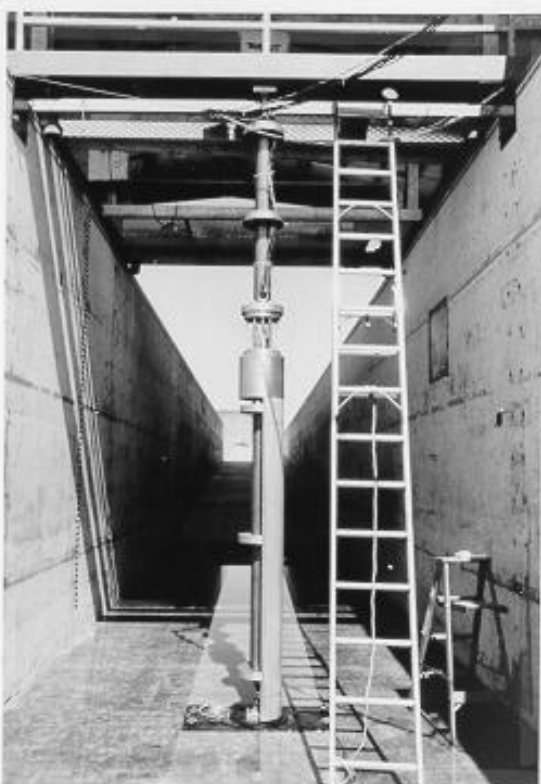


Fig. 3-17 Nearly completed installation with one of the four skins attached



Fig. 3-18 Three of the four skins bolted on. Final painting and smoothening around the pressure parts in progress.



Fig. 3-19 Final arrangement just prior to testing.
Water level is at the test level.



Fig. 3-22 XXX Calibration to the east in air



Fig. 3-23 Calibrating at position 5
with the bottom support submerged.
Also shown is the horizontal truss
used for calibrating at position 3.
The completely assembled vertical
cylinder is on the left.